Houser / Murbach, editors

Geology and Lore of Northern Anza-Borrego Desert Region

SDAG / SCGS Vol. 37 - 2010

Geology and Lore of Northern Anza-Borrego Desert Region

The Lows to Highs of Anza-Borrego Desert State Park®

South Coast Geological Society **San Diego Association of Geologists**

Editors: Monte L. Murbach **Charles E. Houser**

Geologic Time Scale

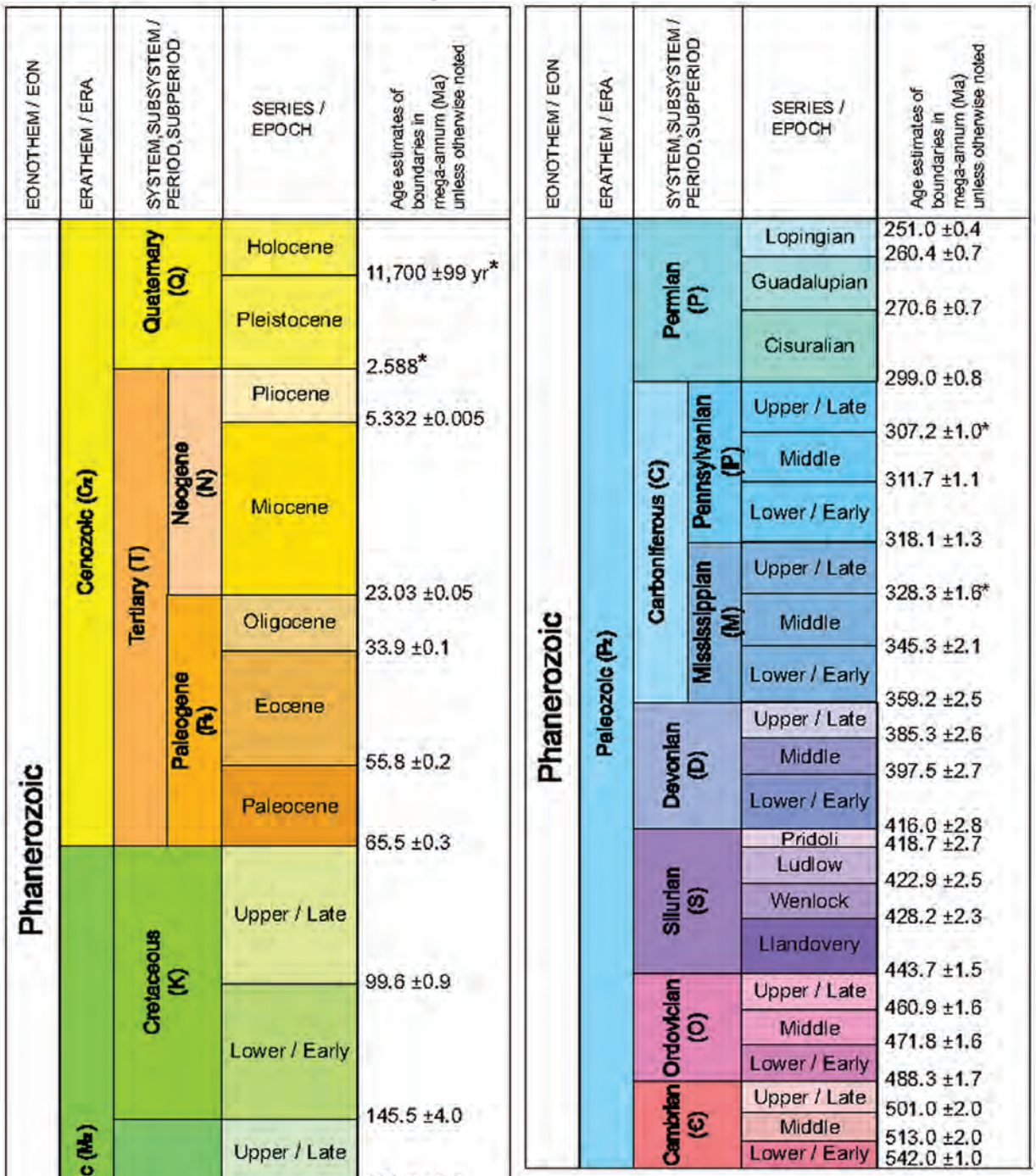

Divisions of Geologic Time approved by the U.S. Geological Survey Geologic Names Committee, 2010. The chart shows major chronostratigraphic and geochronological units. It reflects ratified unit names and boundary estimates from the International Commission on Stratigraphy (Ogg, 2009). Map symbols are in parentheses. Adapted from USGS Fact Sheet FS10-3059 (2010) by Phil Farquharson.

Geology and Lore of Northern Anza-Borrego Desert Region

The Lows to Highs of Anza-Borrego Desert State Park®

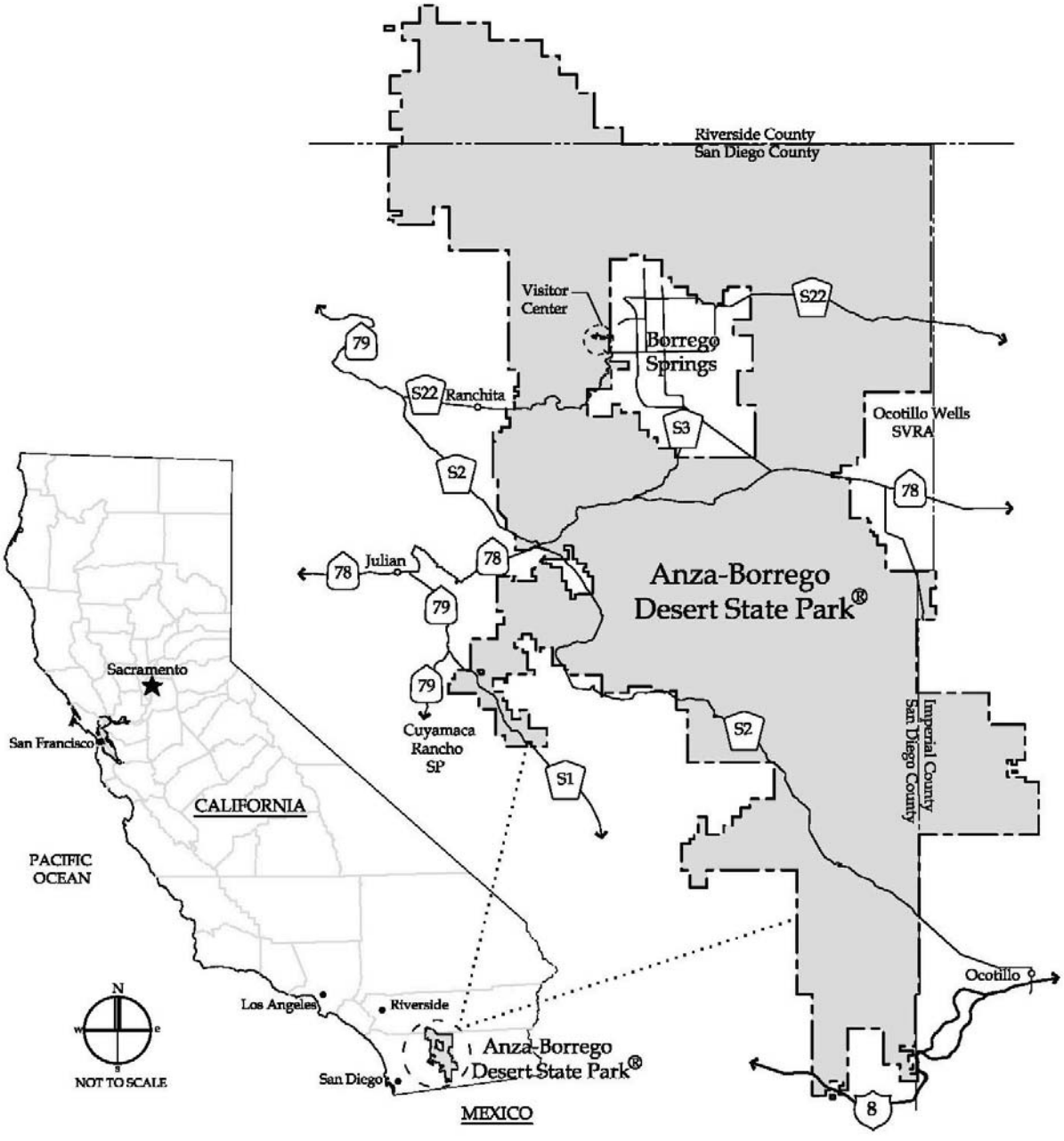

2010 SDAG/SCGS Field Trip participants, October 17th, 2010.

Photo courtesy of Dr. Prem Saint, emeritus professor, CSU-Fullerton; photo by Diana Lindsay.

Geology and Lore of Northern Anza-Borrego Desert Region

SDAG/SCGS Volume Number 37- 2010

Published in conjunction with the 2010 Field Trip:
The Lows to Highs of Anza-Borrego Desert State Park®

Editors: Charles E. Houser and Monte L. Murbach

Managing Editor: Carole L. Ziegler

San Diego Association of Geologists

Distributed by Sunbelt Publications
www.sunbeltbooks.com

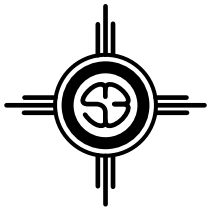

Geology and Lore of Northern Anza-Borrego Desert Region, The Lows to Highs of Anza-Borrego Desert State Park®

First edition 2010. Fifth printing 2016. Printed in the United States.

Edited by Charles E. Houser and Monte L. Murbach
Managing Editor - Carole L. Ziegler
Technical Editor – Philip T. Farquharson
Cover and Book Design by Philip T. Farquharson
Printed in the United States of America

SDAG
P.O. Box 191126
San Diego, California 92159-1126
www.sandiegogeologists.org/

SCGS
P.O. Box 10244
Santa Ana, California 92711-0244
www.southcoastgeo.org

or the distributor:

Sunbelt Publications
1250 Fayette Street
El Cajon, California 92020
(619) 258-4911, fax: (619) 258-4916
www.subeltpublications.com
19 18 17 16 8 7 6 5

Publisher's Cataloging-in-Publication Data

Houser, Charles E., 1959-
Geology and lore of northern Anza-Borrego Desert Region: San Diego association of geologists and south coast geological society 2010 field guide/Charles E. Houser, Monte L. Murbach, Carole L. Ziegler

214 p. cm.
Includes bibliographical references.
ISBN-13: 978-0-916251-16-1
1. Geology-California-San Diego County-Guidebooks. 2. History-California-San Diego County. 3. San Diego County (Calif.)-Guidebooks. I. Houser, Charles E., Murbach, Monte L., Ziegler, Carole L. III. Title.

QE90.S116 2010

Front cover photograph courtesy of:
Michael W. Hart, oblique aerial view of Borrego Valley, looking east to Coyote Mountain, Clark Dry Lake and the Santa Rosa Mountains. Charles E. Houser, pilot
Front inside – Geologic Time Scale USGS adapted from USGS Fact Sheet FS10-3059 (2010) by Philip T. Farquharson
Frontispiece – SDAG/SCGS Field Trip Participants, October 17th, 2010, courtesy of Dr. Prem Saint, emeritus professor, CSU-Fullerton; photo by Diana Lindsay
Back inside – Columbian Mammoth Sculpture by Ricardo Arroyo Breceda. Photo by Charles E. Houser
Back cover – Photo by Charles E. Houser, Anza-Borrego Desert State Park sign in the snow.

A-Z DEDICATION TO DIANA & LOWELL LINDSAY

So let us celebrate these two lives well spent, sometimes in a house, sometimes in a tent.
They taught us the geology of Anza-Borrego from A to Z; sometimes on a hike and sometimes on a bike.
They documented the desert treasures found in fossils; sometimes in a book, sometimes you had to go there to take a look.
They created Sunbelt Publications from a logo on a cocktail napkin in a Texas beer garden; sometimes providing natural history, sometimes solving the mystery.
They have shared their friendship, professionalism and their love for life and the outdoors; while always providing karma-raderie.
And when others said that there was nothing out there, nothing; they found something!

(Diane Murbach, 2010)

When the planning committee for the 2010 field trip and publication for the "Geology and Lore of Northern Anza-Borrego Desert Region: The Lows to Highs of Anza-Borrego Desert State Park" thought about whom to dedicate this volume, there was only one choice. Diana and Lowell Lindsay have been active in the geology community in the southwestern states their entire lives. Diana has presented several natural history talks to the San Diego Association of Geologists (SDAG) and a talk to the South Coast Geological Society (SCGS). Lowell Lindsay is a past president of SDAG, and is a director on the board of SDAG's non-profit parent corporation, San Diego Geological Society (SDGS). He also chairs the Publications Committee. Both Diana and Lowell have volunteered time compiling, marketing and selling publications for SDAG and SCGS at many annual geology conferences.

So what is Anza-Borrego Desert State Park? It is a desert nature reserve, primarily found within the Colorado Desert Region of eastern San Diego County but also reaches into Imperial and Riverside counties of southern California. Anza-Borrego Desert State Park® is named after 18th century Spanish explorer Juan Bautista de Anza and from the Spanish word *Borrego* meaning Bighorn Sheep. With 650,000 acres that includes one-fifth of San Diego County within its borders, Anza-Borrego is the largest State Park in the United States not including Alaska.

So who are Diana and Lowell Lindsay? Authors Diana and Lowell Lindsay envisioned a publishing and distribution company of their own. Sunbelt Publications began in 1978 as an idea drawn out on a napkin by the Lindsays at the historic Scholtz Beergarten in Austin, Texas. Today, that same logo – a sun symbol with "SB" in the middle – is found on books nationwide. The Lindsays' company, Sunbelt Publications, distributes thousands of titles and sells most of them out of a warehouse located at 1250 Fayette Street in El Cajon, California. It is open to the public. Visitors can browse through and choose from approximately 1,000 titles organized by subject area. It is a genuine mega-store for books on the natural history of southern California, USA and Baja California, Mexico.

Diana and Lowell Lindsay are still animated by the

passion for cycling and exploring the outdoors that first brought them together as undergraduates at UCLA. In 1966 Diana Lindsay went into the desert and, figuratively, never came back out. That first visit to the Anza-Borrego Desert changed her life and helped to define it. It became the subject of her master's thesis from San Diego State University, which was subsequently published as *Our Historic Desert* by Copley Books in 1973. Well-known

publications by Diana Lindsay include *Anza-Borrego A to Z: People, Places, and Things*. *Anza-Borrego A to Z* is an interesting and informative book on the Anza-Borrego Desert Region providing an overall historic summary of the area followed by an alphabetical listing of people,

places and things relevant to the Anza-Borrego Desert.

Lowell Lindsay majored in geology at UCLA and holds a MA from West Texas A&M. Besides being a past president of the San Diego Association of Geologists, Lowell is immediate past treasurer of the Association of Earth Science Editors. His books include *Geothermal Resources of the Imperial Valley* and *Geology of Anza-Borrego*.

Diana and Lowell Lindsay co-authored *The Anza-Borrego Desert Region: A Guide to the State Park and Adjacent Areas of the Western Colorado Desert* in 1978 and is now in its 5th edition. This book is the authoritative, comprehensive guide to southern California's most popular desert park, much of which is still wilderness. The publication includes a color map that is a useful guide for hikers, off-road travelers, equestrians, mountain bikers, photographers, and campers. Sunbelt's growing list of educational and interpretive books includes *Mission Memoirs*; *Anza-Borrego: A Photographic Journey*; *Fire, Chaparral and Survival*; and *Fossil Treasures of the Anza-Borrego Desert: the Last Seven Million Years*.

Thank you to Diana and Lowell Lindsay – you have changed the way we see the Anza-Borrego Desert Region, and introduced us to wonderful people and places!

Dedication by *your geology, biking and other outdoor friends!*

Happy Trails!

GEOLOGY AND LORE OF THE NORTHERN ANZA-BORREGO DESERT
LOWS TO HIGHS OF THE ANZA-BORREGO DESERT STATE PARK

TABLE OF CONTENTS

Anza-Borrego Desert State Park® is the largest State Park in the United States (except for Alaska), covering approximately 650,000 acres in two geomorphic provinces, the Peninsular Ranges and the Colorado Desert. The Park and its environs include sandy desert flatlands, rocky mountain ridges with intermountain alluvial valleys, steep canyons, and a portion of the grand Laguna Mountains. Activities available to people coming to play in the region include hiking, photography (springtime flowers in the desert are world renowned), fishing, hunting (not within the Park boundaries, of course), off-roading, and anything requiring only a beautiful desert as the prime ingredient. If one is willing to endure a moderate hike or four-wheel-drive trip far off the highway, one can see Native American rock paintings and morteros, historic homestead sites of pioneers to the region, geologically interesting mud caves, and a host of natural phenomena and man-made history enough to keep one hiking and exploring for a lifetime.

This two-day field trip takes participants from the lowest desert portions of the region to some of the highest elevations found in San Diego County. The trip covers most of the extensive stratigraphy of the region. The rocks found in this area rival those of the Grand Canyon in Arizona for the story they have to tell. In fact, many sedimentary rocks of the Anza-Borrego Desert Region have been derived from erosion of the southwest United States including the Grand Canyon! With such a vast geologic history present, these rocks also contain fossils that tell of times past when the climate of the region was much different than today. The stratigraphy and paleontology of the Anza-Borrego Desert State Park® is the focus of this trip.

For those "movers and shakers" participating in the trip, the Anza-Borrego Desert Region is home to the big three faults in the southern California desert; the Elsinore Fault, the San Jacinto Fault, and, of course, the San Andreas Fault. The San Jacinto Fault is considered the most seismically active of the three, though the El Mayor-Cucapah Earthquake of April 4, 2010, in Northern Baja showed that any of the faults found in the area may act up at any time! This trip includes several stops along the San Jacinto Fault which runs northwest-southeast through the central region of the Anza-Borrego Desert State Park®. The accompanying papers in this guidebook allow experts to share their knowledge of fault geomorphology and structure, recent fault history shaping the Colorado Desert, and current activity with future possibilities for the "Big One."

If your geological senses aren't quite full yet, the trip takes participants into the world of landslides, but with a twist. Where landslides in urban areas involve failure of soft sedimentary rock, often with a little help from man in the form of overwatering or broken water lines, landslides in the Anza-Borrego Desert Region are grand-scale failures in hard, crystalline rock, the last place one might expect to see such landforms. Visible to the participants are landmasses rotated and moved down slope, with sharp headscarps and block faulting within the slide masses. Younger landslides are seen overprinting older slides, and dry ponds occur where slide blocks rotate enough to create closed basins to capture rainwater from the intense summer thunderstorms common in the region. "Dessert" the first day of the original trip came when, after a satisfying dinner in camp, Diana Lindsay, who is so well known for presenting to groups privileged to experience the Anza-Borrego Desert Region, dished up another one of her gems: a presentation on the Galleta Meadows Sky Art.

But wait, there is more! Not all faults in the region foretell the need for man to be prepared for a modern earthquake. Some faults, no longer active, take us back to a time when the land was not sliding past itself laterally as it does today. Rather the region was extending, probably after a plate collision of the magnitude that raised the Rocky Mountains of Colorado, and crustal blocks were rotating and causing large scale normal (dip-slip) faulting in response to the great changes occurring in Earth's crust. In the southern area of Borrego Valley, these normal, or detachment, faults are visible in the slopes of Yaqui Ridge. On the way to view the detachment faults the second day of the trip, participants are also treated to a view of past life in Anza-Borrego. Roaming the valley south of town is the Galleta Meadows Sky Art which includes sculptures of mammoths and sabertooth cats, as well as other past and present animals. What an opportunity to take a picture of the largest flight-capable bird ready to consume an unsuspecting group of geologists (see this volume's frontispiece for the picture taken moments before the cataclysm!).

Finally, the trip proceeds up into the high mountains of southern California, from the lows to the highs of Anza-Borrego Desert State Park®. From the crest of the Laguna Mountains, participants are treated to a magnificent view of the Anza-Borrego Desert. The view alone is worth the drive from the city. Enjoy this view after several days of taking in and enjoying the natural, historic, and geologic wonders of the region!

In 2010, as in 2003, the field trip has come from a cooperative effort of the South Coast Geological Society and the San Diego Association of Geologists. Unlike 2003 when separate trips were run for each of the groups, only one trip with members of both organizations together was conducted. This provided a unique opportunity for members of both organizations to share their field experience and commiserate together on all things geology.

As is typical of our field trip guidebooks, this volume includes a road log and papers, both new and reprints, related to the Anza-Borrego Desert Region. Papers by Mike Hart and Tom Rockwell are included in this volume, and both of these gentlemen presented discussions at stops along the original trip. Also sharing his vast knowledge of Anza-Borrego Desert Region stratigraphy and paleontology was George Jefferson, perhaps the person most knowledgeable on the geology of the region. A special treat for this trip was Saturday's lunch, served chuckwagon-style at a remote homestead site east of Clark "Dry" Lake.

With the road log and the vast knowledge available in this guidebook, any diligent student of history and the Earth may follow the same route taken one marvelous weekend in October 2010, and may thus become a participant in yet another quality geological adventure in beautiful Anza-Borrego Desert State Park®.

ACKNOWLEDGEMENTS

The following people have contributed immeasurably to this trip.

Carole Ziegler has again performed her miracle of planning, organizing, editing, overseeing, and organizing some more, this field trip guidebook to go with this trip.

Phil Farquharson has again provided his expertise in the development of graphics, both for individual papers and for the volume in general. Phil works great in a pinch!

Mike Hart navigated for many, many pre-field trip road runs, helping to get the trip route in order. His contributions included digging snow off one of the welcome signs to the Anza-Borrego Desert State Park®, providing many photographs of the region, hand digging soil to expose faults (for the field trippers), providing geology cartoons, suggesting we get a canoe and paddle on Clark "dry" Lake after a big storm to take pictures (earlier this year), and mostly he was always available to help.

Diane Murbach provided constant support and was instrumental in coordinating the field trip by compiling the ever changing attendee list, putting instructions and maps together, working with treasurers from both geo-groups, and helping get the field trip shirt produced and ready for the trip.

Many thanks, in general, to those in the geo-groups who have helped put this trip together. Field trip stop leaders included George Jefferson, Miles Kenney, Tom Rockwell (and several of his students), Mike Hart, John Peterson, and Lowell and Diana Lindsay. Special thanks go to Jeff Miller for last-minute publication pick-up before the field trip! Thank yous also go to the Anza-Borrego Desert State Park® personnel who assisted with Park logistics and potential field trip stops, and to Paul Johnson for allowing us to use his sheep logo for the T-shirt and in this volume.

Finally, Lowell and Diana Lindsay, to whom this guidebook is dedicated, have provided an incomprehensible volume of information, knowledge, enthusiasm, ideas, guidance, and friendship throughout the process of planning this event. About two years ago when the idea for this trip was originally scribbling on a piece of lined paper it was showed to Lowell and he commented, simply, "That is a quality trip." His words have propelled that initial idea to a truly quality trip that a small group of geologists enjoyed on the 2010 joint SCGS/SDAG field trip to see the lows to highs of Anza-Borrego.

Chuck Houser
Vice President-2010
San Diego Association of Geologists

Monte Murbach
President-2010
South Coast Geological Society

SDAG SPONSORS

RUBY SPONSORS ($500)

Steve Zigan – Student Sponsor

Jim Ashby/Mission Geoscience, Inc.
(949) 955-9086
www.missiongeoscience.com

David Bloom/Tetra Tech
(619) 702-6059
www.tetratech.com

Suzie Reed/H&P Mobile Geochemistry, Inc.
(800) 834-9888
www.handpmg.com

EMERALD SPONSORS ($100)

Dr. Pat Abbott
Sally & Dennis Avery
Dr. Richard W. Berry
Curtis Burdett
Joe Corones
Greg Cranham
Eggers Environmental, Inc.
Phil Farquharson, CG-Squared Productions
Carolyn Glockhoff, Caro-Lion Enterprises
Jonas & Associates
Diana & Lowell Lindsay, Sunbelt Publications
Ninyo & Moore
Dr. Monte Marshall
Monte & Diane Murbach, Murbach Geotech
Stone Brewing Company
Dr. Anne Sturz
Sue Tanges, Southland Geotechnical Consultants
Terra Costa Consulting Group, Inc.
David & Jan Steller
Carole L. Ziegler

SCGS SPONSORS

Steve Zigan, Student Sponsor

Larry Cann, Supplies Sponsor

Albus-Keefe & Associates
(714) 630-1626
www.albus-keefe.net

ALROY Drilling Services, Inc.
(714) 779-1710
www.alroydrilling.com

Condon-Johnson & Associates, Inc.
LA (714) 826-471
San Diego (858) 530-9165
www.condonjohnson.com

Conestoga-Rovers & Associates Inc.
(949) 648-5200
www.craworld.com

Earth Consultants International
(714) 544-5321
www.earthconsultants.com

Geo-Tech Imagery, Intl.
(760)-754-8423
www.geo-tech-imagery.com

Gregg Drilling & Testing, Inc.
(562) 427-6899
www.greggdrilling.com

Ken Kupka's Precision Backhoe Service
(949) 859-9000

Layne Christensen Company
(949) 955-1122
www.laynechristensen.com

Leighton
(949) 250-1421
www.leightongeo.com

LGC Geotechnical
(949) 388-2089
www.lgcgeo.com

NMG Geotechnical, Inc.
(949) 442-2442
www.nmggeotechnical.com

Mission Geoscience, Inc.
(949) 955-9086
www.missiongeoscience.com

Test America
(949) 261-1022
www.testamericainc.com

The generosity of these sponsors allows our organizations to continue to keep membership dues low, reduce rates for students, produce monthly newsletters, purchase supplies, host the annual field trip, produce our geologic guidebooks, and provide scholarships to local geology students. To contact any of the above sponsors, please visit our websites at www.sandiegogeologists.org and www.southcoastgeo.org.

Officers 2010

SCGS

PRESIDENT – Monte Murbach,
monte@murbachgeotech.com

VICE PRESIDENT – Maria Herzberg,
mmherzberg@earthconsultants.com

SECRETARY – Stephen Jacobs,
stephenjacobs596@gmail.com

TREASURER – David Randell,
drandell001@ca.rr.com

PUBLICATIONS MANAGER – Jeff Miller,
jmiller@e2managetech.com

SDAG

PRESIDENT – Bryan Miller-Hicks,
bryanmillerhicks@gmail.com

VICE PRESIDENT – Chuck Houser,
CHouser@scsengineers.com

SECRETARY – Todd Wirth,
todd@wirths.com

TREASURER – Cari Gomes,
sdagtreas@sandiegogeologists.org

PUBLICATIONS MANAGER – Lowell Lindsay,
llindsay@sunbeltpub.com

MANAGING EDITOR – Carole L. Ziegler,
SDAGeditor@gmail.com

TECHNICAL EDITOR – Philip T. Farquharson,
geoguy@geologyguy. com

WEBMASTER – Carolyn Glockhoff,
carolyn@caro-lion.com

San Diego Geological Society (SDGS) Officers

President –	Dave Bloom	dbloom@geology.sdsu.edu
Vice President –	Mike Hart	MWHart@aol.com
Secretary –	Diane Murbach	dmurbach@aol.com
Treasurer –	Greg Cranham	gcranham@hargis.com
Publications –	Lowell Lindsay	LLindsay@SunBeltPub.com
Membership –	Monte Murbach	monte@murbachgeotech.com
2010 SDAG President –	Bryan Miller-Hicks	bryanmillerhicks@gmail.com
Scholarships –	Anne Sturz	annesturz@yahoo.com

List of Current San Diego Association of Geologists Publications

2010 – Geology and Lore of Northern Anza-Borrego Desert Region

2010 – Geology and Natural History, USMC Camp Pendleton, 2nd edition (1st ed. 1994)

2006 – Mines and Geology of the Randsburg Area, Mojave Desert, California

2005/06 – Geology and History of Southeastern San Diego County, California

2004 – Mining History and Geology of Joshua Tree National Park

2003 – Geology of the Elsinore Fault Zone, San Diego Region (co-published w/ SCGS)

2001 – Coastal Processes and Engineering Geology of San Diego, California

2000 – Geology and Enology of the Temecula Valley, Riverside County, California

1999 – Water for Southern California: Water Resources Development

1997 – Santa Cruz Island Geology

1995 – Paleontology and Geology of Anza-Borrego Desert State Park

1992 – Natural History of the Coronado Islands, Baja California, Revisited

1991 – Environmental Perils, San Diego Region

1990 – Geotechnical Engineering Case Histories in San Diego County

1989 – Seismic Risk in the San Diego Region

1988 – Landslides in Crystalline Basement Terrain — San Diego and Riverside Counties

www.sandiegogeologists.org

List of Current South Coast Geological Society Publications

2010 – Geology and Lore of Northern Anza-Borrego Desert Region

2010 – Geology and Hydrology of the East San Gabriel Mountains: A Journey Through a River of Time

2008 – Geology and Hydrogeology of the Big Bear Valley and San Bernardino Mountains, Transverse Ranges, California

2007– Geology and Tectonic Development of Western San Luis Obispo County, Southern Coast Ranges, California

2006 – Geology of the Orange County Region, Southern California

2004 – Geology and Tectonics of Santa Catalina Island and the California Continental Borderland

2003 – Geology of the Elsinore Fault Zone, San Diego Region "Hot Springs and Tourmalines of Eastern San Diego County"

2002 – Structural Geomorphology, Petroleum and Water Resources, Northwestern Transverse Ranges

2001 – Geology of the Owens Valley and Inyo Mountains Region

2000 – Geology of the Las Vegas Area

1998 – Black Canyon of the Colorado River, Arizona/Nevada and Castle Mountains Gold Mine, San Bernardino County, California

1997 – Southern San Andreas Fault-Whitewater to Bombay Beach-Salton Trough

1992 – The Regressive Pleistocene Shoreline

1991 – Southern Coast Ranges

1990 – Lower Colorado River Extensional Terrain and Whipple Mountains

1988 – Geology of the Death Valley Region

1982 – Geology and Mineral Wealth of the California Transverse Ranges

www.southcoastgeo.org

RELATED PUBLICATIONS: ANZA-BORREGO DESERT REGION, 2010

(Also see the publication lists of the San Diego Association of Geologists and the South Coast Geological Society.)

Abbott, Patrick L. and David L. Seymour, eds. (1996) Sturzstroms and Detachment Faults, Anza-Borrego Desert State Park, California. Santa Ana: South Coast Geological Society.

Abbott, Patrick L. (1999) The Rise and Fall of San Diego: 150 Million Years of History Recorded in Sedimentary Rocks. San Diego: Sunbelt Publications.

Brigandi, Phil (1991) Borrego Beginnings: Early Days in the Borrego Valley 1910-1960. Borrego Springs: Anza-Borrego Desert Natural History Association.

Cassiliano, Michael L. (2002) Revision of the Stratigraphic Nomenclature of the Plio-Pleistocene Palm Spring Group, Anza-Borrego Desert. San Diego: San Diego Natural History Museum.

Cline, Lora L. (2008) Just Before Sunset, third edition. San Diego: Sunbelt Publications.

Ellsberg, Helen (1992) Mines of Julian. Glendale: La Siesta Press.

Fetzer, Leland (2002) A Good Camp: Gold Mines of Julian and the Cuyamacas. San Diego: Sunbelt Publications.

--------. (2005) San Diego County Place Names A to Z. San Diego: Sunbelt Publications.

Jefferson, George T. and Lowell Lindsay, eds. (2006) Fossil Treasures of the Anza-Borrego Desert: The Last Seven Million Years. California State Parks and Sunbelt Publications.

Lindsay, Diana (2001) Anza-Borrego A to Z: People, Places, and Things. San Diego: Sunbelt Publications.

Lindsay, Lowell and Diana Lindsay (2009) The Anza-Borrego Desert Region: A Guide to the State Park and Adjacent Areas of the Western Colorado Desert. Berkeley: Wilderness Press, fifth edition.

Murbach, Monte L. and Michael W. Hart, eds. (2003) Geology of the Elsinore Fault Zone, San Diego Region. San Diego: San Diego Association of Geologists, and Santa Ana: South Coast Geological Society.

Pepper, Choral (1994) Desert Lore of Southern California. San Diego: Sunbelt Publications.

Reed, Lester (2004) Old Time Cattlemen and Other Pioneers of the Anza-Borrego Area. Borrego Springs: Anza-Borrego Desert Natural History Association, third edition.

Remeika, Paul, and Lowell Lindsay (1992) Geology of Anza-Borrego: Edge of Creation. San Diego: Sunbelt Publications.

Rynerson, Fred (1967) Exploring and Mining Gems and Gold in the West, Happy Camp, CA: Naturegraph Publishers, Inc.

Walawender, Michael J. (2000) The Peninsular Ranges: A Geological Guide to San Diego's Back Country. Dubuque, Iowa: Kendall/Hunt Publishing Company.

Wray, Christopher (2004) The Historic Backcountry: A Geographic Guide to the Historic Places of the San Diego County Mountains and the Colorado Desert. La Mesa: Christopher Wray.

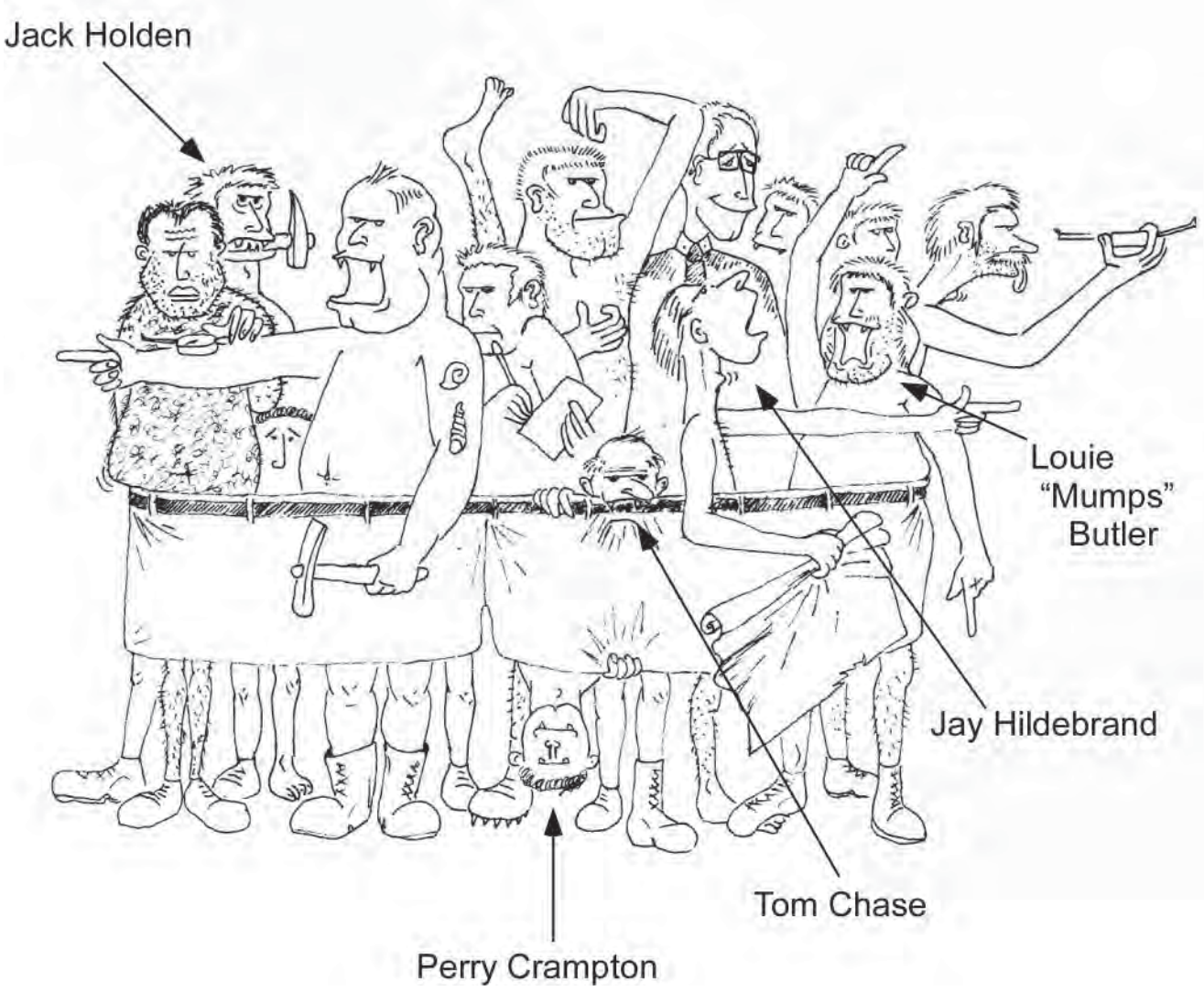

THE IDEAL FIELD CLASS (TOGETHERNESS)

Posed by members of Advanced Field Geology, Fall 1960

San Diego State College

John "Jack" Holden, Artist

Part II.

2010 Joint SCGS / SDAG Field Trip Road Log

The Lows to Highs of Anza-Borrego Desert State Park®

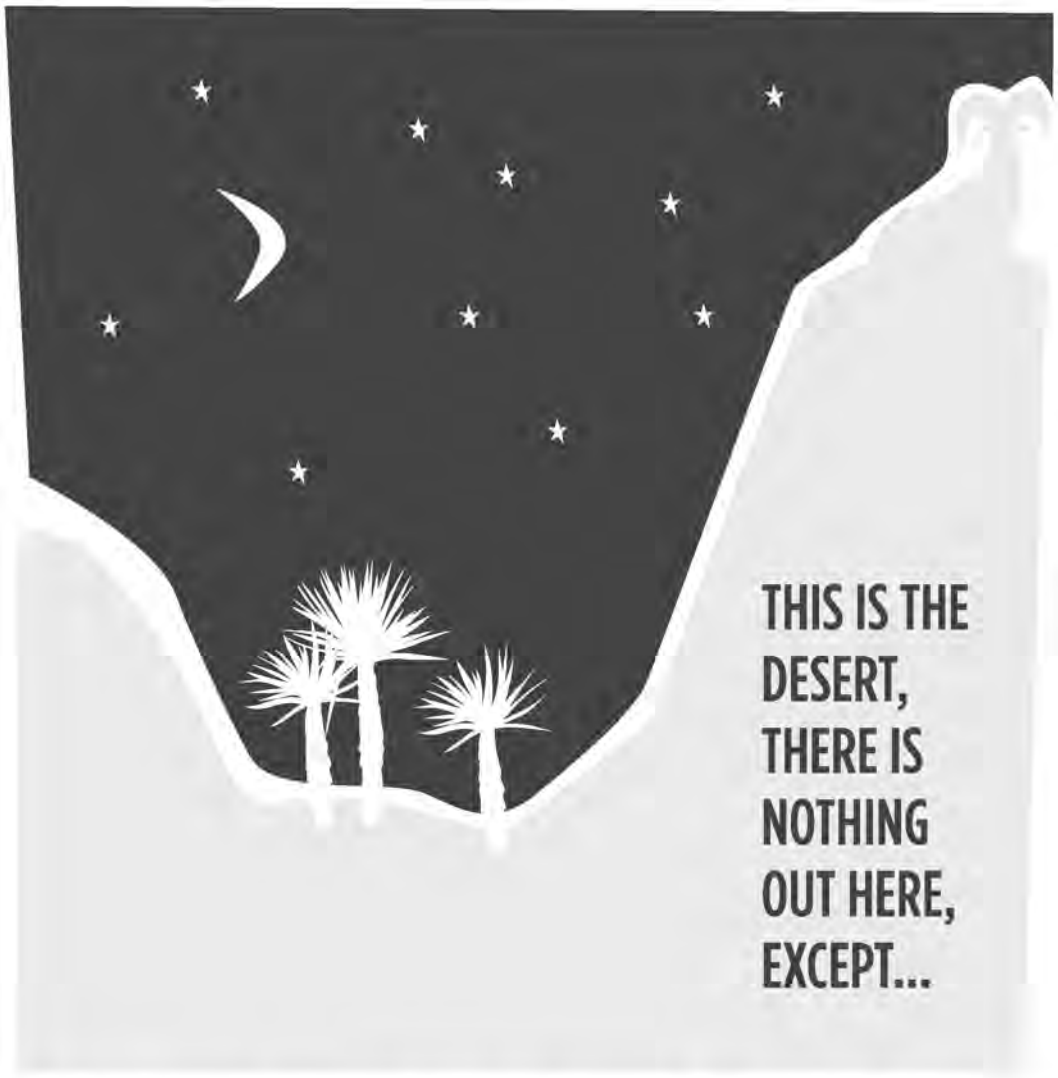

"LORES" & HIGHS ANZA-BORREGO

Idea by the Murbach's & Graphic design by Fritz Rothman.

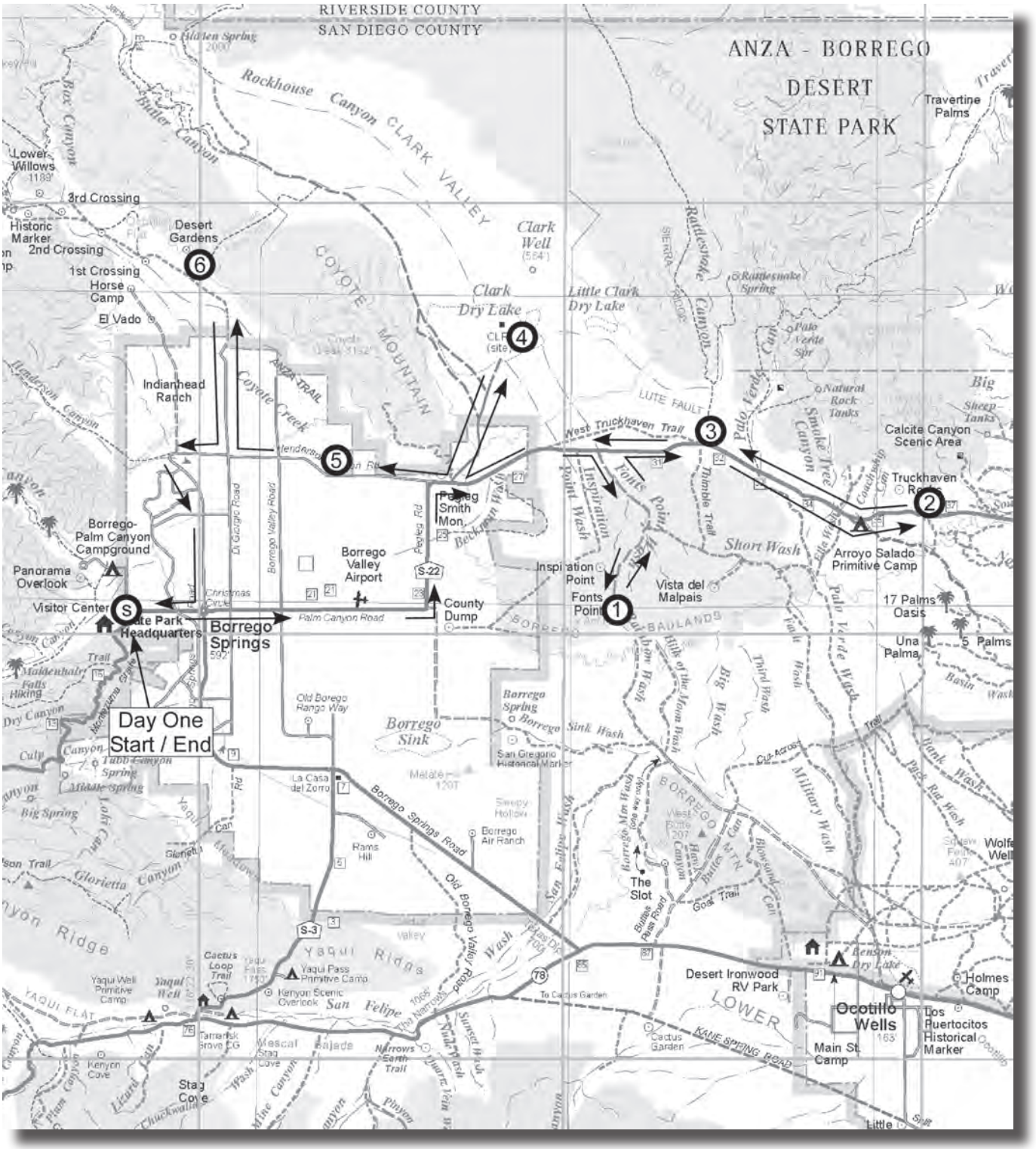

Day One Route Map

2010 Joint SCGS/SDAG Field Trip Road Log

Geology and Lore of Northern Anza-Borrego Desert Region

The Lows to Highs of Anza-Borrego Desert State Park®

Monte Murbach, Diana Lindsay

Saturday, October 16, 2010

Odometer (Trip) Mileage

Trip begins in Borrego Springs, California, at the intersection of Palm Canyon Drive, and Montezuma Valley Road. (This intersection is east of Anza-Borrego Desert State Park® Headquarters, Visitor Center, and Palm Canyon Campground.) The trip is approximately 50 miles long.

0.0 Head east on Palm Canyon Drive toward the main part of Borrego Springs, an unincorporated community developed in the late 1940s that was planned to be "another Palm Springs." Conservationists successfully fought developers to prevent a super highway from being built through Coyote Canyon in 1966 that was intended to draw tourists from the Los Angeles Basin. With no direct connection to that area, Borrego Springs has remained a slow paced, quiet community that boasts that it does not have a stop light and maintains dim lighting at night to have earned the designation as a "dark sky community." With a population of about 2,500 and completely surrounded by a state park, it is reminiscent of the Palm Springs of 75 years ago.

1.4 Enter Christmas Circle, the park-like hub of Borrego Springs with a name that has three possible origins: (1) an association with a child born on Christmas Day on the 1775-76 Anza Expedition to California; (2) where the local Kiwanis Club dressed up one of its members in a Santa suit in 1944 and gave presents to local children; or (3) named for a local cattle brand designated "xms" that the county road department interpreted as Xmas, thus naming the circle Christmas Circle.

1.6 Right turn on Palm Canyon Drive, continue east.

3.1 Stop sign at intersection with Borrego Valley Road. Proceed straight (east). The Borrego Springs Elementary School on the right is the site of the valley's first official school house with classes beginning in November 1934.

4.4 Pass entrance to Borrego Valley Airport, constructed with funds provided by the San Diego County Board of Supervisors. The May 1949 opening dedication was hosted by radio and screen star Leo Carrillo, "Pancho" of The Cisco Kid, and honorary mayor and screen star Frank Morgan of Wizard of Oz fame. There is an Italian Restaurant, Assaggio, with a great view of the runway and aircraft parking ramp.

5.7 Pass Mile Post 23. The road curves left (north) and becomes Pegleg Road. Views of Coyote Mountain (10 o'clock) and Santa Rosa Mountains with Villager Peak (2 o'clock). At 5,756 feet, Villager is the launch point for those climbing Rabbit Peak (6,666') from Borrego Valley. It is thought to have been named for the Indian village sites in the vicinity where Native Americans gathered pinyon pine nuts.

8.2 Pegleg Road curves to the right (east) and becomes Borrego-Salton Seaway (Hwy S22). The predecessor of this highway, completed in 1968, was the 28-mile long Truckhaven Trail connecting Borrego Valley with Highway 86 at the old Truckhaven Café. The original road was built at a cost of $700 during the winter of 1929-30 using a team of horses and a couple of Fresno Scrapers to level the road.

10.6 Mile Post 28 with a large sign, Welcome to Anza-Borrego Desert State Park.

11.2 Highway crosses Inspiration Wash. This wash can flood the highway, and it was flooded twice during the preparation of this road log! The wash was named by park rangers because of the view

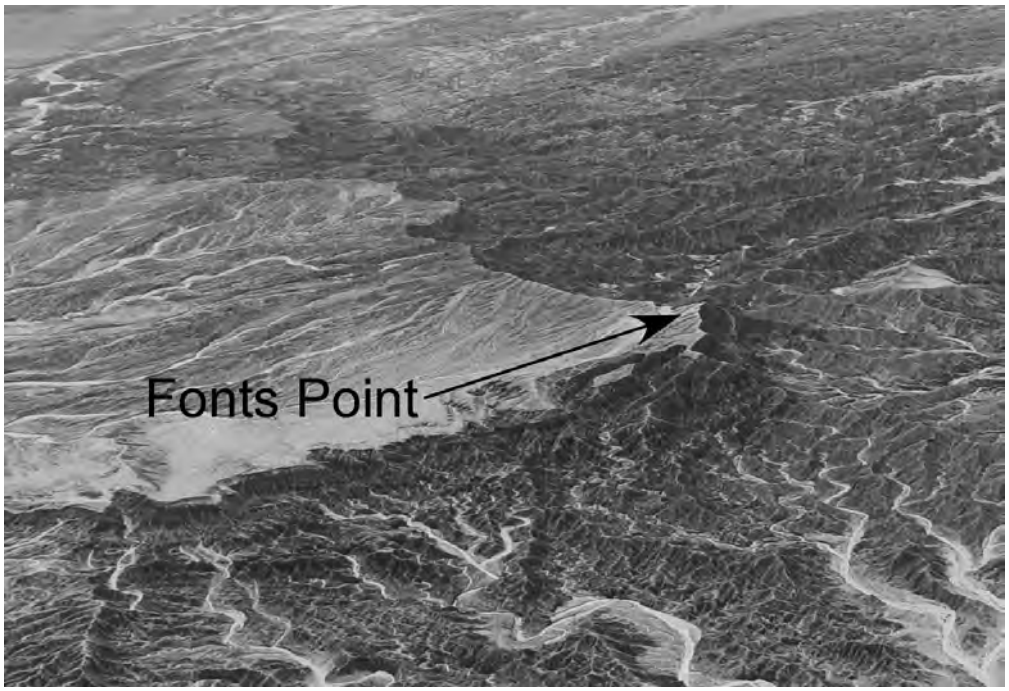

Photo of Fonts Point by Mike Hart

point at the end of the wash looking out on the ragged western portion of the Borrego Badlands and Fonts Point. This viewpoint overlooks Mammoth Cove, so named for its eponymous paleontological resource.

12.0 Stop No. 1. Pull off the highway to the right at the brown sign, "Fonts Point 4.0 Miles". The wash and point are named for Pedro Font, the priest who accompanied the second Anza Expedition to California in 1775-6, bringing colonists who would establish a pueblo in the San Francisco Bay Area. Proceed up wash and stay on the main "road" and follow signs for approximately 15 minutes travel time. Park at the end--lots of room.

Stop 1 Speaker: George Jefferson, paleontologist for the Colorado Desert District, California State Parks, discusses the geology and paleontology of the Borrego Badlands. Return to highway.

0.0 Reset odometer back at highway. Proceed east (right turn).

0.7 Pass pull-out marked by short stone walls. This pullout has great views of Santa Rosa Mountains. USGS designated these mountains as the Santa Rosas in 1901. Prior to that survey, it was called "Toro or Bull Mountain Range." The name may have its origin from the name of Santa Rosa de Lima, a canonized Indian of the New World. Santa Rosa is also the name of a Mountain Cahuilla Indian Reservation that was established in 1907 in Riverside County.

6.8 Stop No. 2. Mile Post 36. Turn left into pullout at rest/view area with the large Anza-Borrego sign noting "Truckhaven Rocks" in the background. This is a great view-stop of the Santa Rosa Mountains and the Salton Sea. Truckhaven Rocks was named by State Park naturalist Paul Johnson in the mid-1970s for its close association to the Truckhaven Trail. The rocks are massive reddish-brown sandstones derived from the Canebrake Formation. The sandstones were eroded from the rising Santa Rosa Mountains located immediately behind. The rocks were solidified and uplifted to tilt nearly 45° from horizontal. Make a U-Turn in the U-shaped driveway.

6.9 At highway, turn right, go back west on Highway S22.

11.3 Stop No. 3. Small brown sign "Pack it in, Pack it out" on north side of road in pullout area. This is a popular spot, as it is used by hikers as a trailhead to Villager Peak. Park in pullout or off highway, as room allows. This is a 15 minute, approximately ¾ mile hike (one way) up to Lute Ridge to view the Lute Fault, a strand of the Clark Fault.

Stop 3 Speakers: Dr. Miles Kenney, Barrett Salisbury, and Dr. Tom Rockwell

Lute Ridge is a fault-truncated alluvial fan named for the USGS benchmark found there. The ridge is

INTRODUCTION: A VISITOR'S PERSPECTIVE

CENTER STAGE AT FONTS POINT

In one aspect Fonts Point is a sudden place. Roads end. Carved by time. Centered in the arid Borrego Badlands, four million seasons of geology and paleontologic history band across a rawboned desertscape in richly-colored reds, browns, greens and grays. Conglomerates, sandstones, claystones and mudstones are the catalyst, chronicling the metamorphosis of differed paleoenvironments laid bare to view like so many pages of an open book. Compressed and hardened, each layer is a page recording a rock-leafed history of landscapes, fossil life forms, and climatic changes that are no longer present at Anza-Borrego.

In another aspect, Fonts Point is well named. Over 200 years ago history met geology when the Spanish explorer Juan Bautista de Anza passed this high cornice, leading a band of men, women, and mules northward to Monterey. The path he forged followed San Filipe Wash. Father Pedro Font, who served as official chaplain, diarist and observer on Anza's historic marches in 1775 and 1776, described this vantage point of the Borrego Badlands as "the sweepings of the earth".

Humbled, non-geologists verbalize about the ancient sweepings with a litany of superlatives-breath-taking, incredible, spacious and bewildering. An open window, the visual drama of the northern half of Anza-Borrego,a 360-degree view-spreads out like a map. On the southern horizon stretches the Fish Creek, Vallecito and Pinyons, guardian ramparts of the Carrizo Corridor. In the middle distance, twin buttes of Borrego Mountain, split asunder by faulting, sit as granitic ribs that came up through the sediments like a basement elevator. In front of them, is the unfenced bleakness of San Felipe Wash, Sleepy Hollow and Borrego Sink. To the east, the desert seems to have no horizon. Where the land steps downward, the placid inland pool of the Salton Sea, 235-feet below sea level, occupies the lowermost portion of the geologically young Salton Trough, down-dropped by faulting that is rafting Baja California away from mainland Mexico. To the west, the granitic bastion of the San Ysidro Mountains, abuts the Anza-Borrego desert. To the north, Clark "Dry" Lake lays in contrast to the precipitous paired mountain chains of Coyote Mountain, lesser in size, and the overwhelming 8,000 foot high dusk of the Santa Rosa Mountains. Where stone climbs into sky, monster fault lines control the mood of the land, dynamically breaking its continuity.

Old but not ancient, this upturned weathered edge may be the best place in North America to view sediments of the Pliocene and Pleistocene Epochs. But standing atop this precarious promontory and looking back into the past is no easy task. Many wonder how the sea of soft rock below came about, groping to visualize the past when water (gulf, river, delta and stream) drowned the land. Or what geological forces created this erosional masterpiece. And why? Once a wealth of muds and sands, this silent ordering of the ages is now an orchestrated tableau of ruined beds of dry-packed earth, forming a gutted and forbidding landscape. Any thought of verdant gallery forests and babbling brooks must be imaged-like a desert mirage- by its very absence. The visitor has to stretch his or her mind to visualize a landscape devoid of cacti, ocotillo and creosote bush. Think for a minute of a delta, and images of wet lowland habitats come to mind. During the Pliocene Epoch, Anza-Borrego was located south of the border as a receiving basin for the ancestral Colorado River while it carved out the Grand Canyon. Earlier, deltaic-marine waters of the northern Gulf of California were here. On a grandiose scale, marine sediments graded into deltaic facies, inaugurated by petrified wood, shellfish heaped in great abundance, and informative vertebrate trackways –such is the outcome where river meets sea. In turn, all become overlain by shallow pond, lacustrine bog and floodplain deposits as our local mountains where uplifted. Piled on top of one another, the brown earthscape is high, dry and unforgiving. Gone are shelly beaches and reefs, the Colorado River, camels, horses, cheetahs, bears and ground sloths. Many creatures are extinct. But they were here. Their story is part of our inheritance, given to us by diligent earth scientists who patiently probe the badland's history, turning back the paleontologic and geologic clock to yesteryear when the desertland was home to checks and balances of an Ice Age life system.

As the geologic story approaches our own time, acres of sedimentary rock contain enough side canyons and disoriented washes for a lifetime of adventurous exploring. Where the eventful drama of pre-

historic life once teemed, it is now, by the very nature of the area, a baked and arid rocky geography of sunken mesas and corrugated hills of dry mud. Daily, forces of erosion gently soften contour lines, evening out **highs and lows**. Ironically, the area is experiencing weathering, wind, rain and generations of flashflooding that helped in its formation. Nowhere else is this combination exactly the same. And nowhere else of equivalent size can its rocks, histories, landscapes and faunas be told. They are Anza-Borrego.

- Paul Remeika

a strike-slip pressure-ridge fault scarp that is about 2 miles long. Head back to the vehicles.

11.3 Back on highway, continue west.

13.8 Pass by "Fonts Point" sign.

16.9 Stop No. 4. Right turn on Rockhouse Canyon Road. Head north toward Clark "Dry" Lake. Stay on main road as there are many smaller splay roads. The main road forks twice; veer to the right both times. About 2 miles in there are signs that state, "Closed Area Authorized Vehicles Only." You will need to obtain permission from Anza-Borrego Desert State Park ® officials to access this area. Proceed northeast to the homestead area for lunch and an informal discussion on the history of the area. Rockhouse Canyon was named for the ruins of rock houses found at the top of the canyon. They were built by the Mountain Cahuilla Indians who once had a village there below Toro Peak. Clark "Dry" Lake and Valley were named for the Clark brothers, Fred and Frank, who used the northeast end of Clark "Dry" Lake as a cattle camp. Around 1904 they dug a well at Clark "Dry" Lake which became Borrego Valley's first well. They supposedly started digging at 10 am and by 11 pm they were watering their horses with water from 15 feet down. The Clarks ran cattle in Clark Valley until about 1915 when they moved their operations over into Coyote Canyon.

Stop 4 Speaker: Diana Lindsay

Return to highway.

0.0 Back at Highway, turn right and proceed west. Reset odometer.

0.5 Turn north (right) on Henderson Canyon Road.

0.6 Pass entrance to Pegleg Smith Monument. Here you will find a rock mound, a hand-painted sign, a desert mailbox, and a California Historical Landmark, all related to Pegleg's lost gold mine. The historical landmark commemorates Thomas L. Smith, mountain man, prospector, and "spinner of tall tales." An annual "Liar's Contest" is held here at dusk on the first Saturday night of April. All are welcome to compete, and all contestants receive a trophy and a certificate of participation. All tall tales must include Pegleg Smith, lost gold, or the desert and must not be over five minutes in length. Judges select the winners. Usually a few hundred people attend the yearly festivities, sitting around a roaring fire.

1.7 Stop No. 5. Park on right side, next to sign that says "Restricted Area". This is a short hike up hill on the existing dirt road.

Stop 5 Speaker: Mike Hart describes one of the landslides on Coyote Mountain (see paper this volume). Walk back to the vehicles. Coyote Mountain, like the canyon of the same name, derives from the Mountain Cahuilla Indians who made their home in this area. Band members were designated either "wildcat" people or "coyote" people. Those who lived in Coyote Canyon and Rockhouse Canyon were "coyote" people. Those who lived toward the ancient shoreline of Lake Cahuilla were "wildcat" people.

1.7 Back on Henderson Canyon Road, continue northwest, then west.

3.7 Cross Borrego Valley Road, continue west.

4.7 At Di Giorgio Road turn north (right).

6.5 Pavement ends. Viking Ranch is on the right with a great view of Coyote Mountain. Proceed straight on dirt road. You are entering Coyote Creek and will be heading toward the Coyote

Creek Fault segment of the San Jacinto Fault Zone. Caution! The sand can be soft and there can also be water in the creek. Be prepared. The mouth of Coyote Canyon was called "El Vado" by Juan Bautista de Anza and was a campsite during the second Anza Expedition in 1775-6. El Vado means "The Ford." The Spanish word derives from the Arabic "wadi" or desert wash, a word from the Moorish occupation of Spain. By Anza's reckoning, El Vado was about 4.5 miles below Santa Catarina Spring along Coyote Creek. Anza and Father Pedro Font referred to the mouth of Coyote Creek as the arroyo or valley of Santa Catarina, correctly believing it to be a water source for San Sebastian Marsh where they had camped several days earlier.

7.0 Pass (entering) "Anza-Borrego Desert State Park" sign.

9.6 Stop No. 6. Desert Gardens. There are picnic tables here along with a dedication sign. This desert garden was established in 1971 by the Anza-Borrego Committee of the Desert Protective Council, a predecessor of the Anza-Borrego Foundation. The Desert Gardens program began the year before to raise funds to purchase private inholdings within the Park. Title was then transferred to the State of California to become part of the Park. Some of the earliest contributors were members of the California Garden Clubs. This area also is on the Coyote Creek Fault Strand.

Stop 6 Speaker: Dr. Tom Rockwell gives an overview of regional faulting.

Take a short hike around a small hill that has been created by faulting. Return to the vehicles. Turn around and drive back to the south to the paved roads.

12.8 Back on paved northern terminus of Di Giorgio Road. The road was named for the Di Giorgio Fruit Corporation who purchased lands in the valley in the 1940s and began growing grapes – the first to mature in California and the first to reach the eastern markets. Proceed south.

13.6 Turn right on Henderson Canyon Road. Go west. The canyon to the west was named for a mining engineer who had a cabin near the canyon's mouth.

15.5 Entering Galleta Meadows Estate – The Land of Artwork. Keep an eye out for many sculpted creatures! The road curves to the south. The metal sculptures, called "Sky Art" were commissioned by Galleta Meadows Estate owner Dennis Avery who owns about three square miles of noncontiguous lands in the valley. In 2008, Avery originally asked artist Ricardo Breceda of Perris, California, to create Pleistocene-inspired animals for his lands, based on descriptions found in *Fossil Treasures of the Anza-Borrego Desert*, edited by George T. Jefferson and Lowell Lindsay. Since that time Avery has also commissioned artwork inspired by historical events and natural features of the Anza-Borrego Desert. One will also find dinosaurs, artist Breceda's specialty, although paleontologists have found no fossil evidence of creatures that date back to the Mesozoic Era in the Anza-Borrego Desert State Park®. The most recent addition to Sky Art is a World War II era Jeep.

15.7 Road becomes Borrego Springs Road. Continue to watch out for the creatures! Head south toward Christmas Circle.

18.9 Enter Circle. Turn right, then turn right immediately onto Palm Canyon Drive, head west.

20.3 Intersection with Montezuma Valley Road. Log ends here. If you are camping at Borrego Palm Canyon Campground, proceed straight and follow signs to the camp. Please stop in at the Visitor Center or enjoy a hike up Borrego Palm Canyon. The original desert park grew from acquisitions acquired here beginning in 1932. The Park's first name was Borego [one "r"] Palms Desert State Park. Diana Lindsay presents a talk on the history of the Sky Art at the camp's outdoor amphitheater.

End of Day 1.

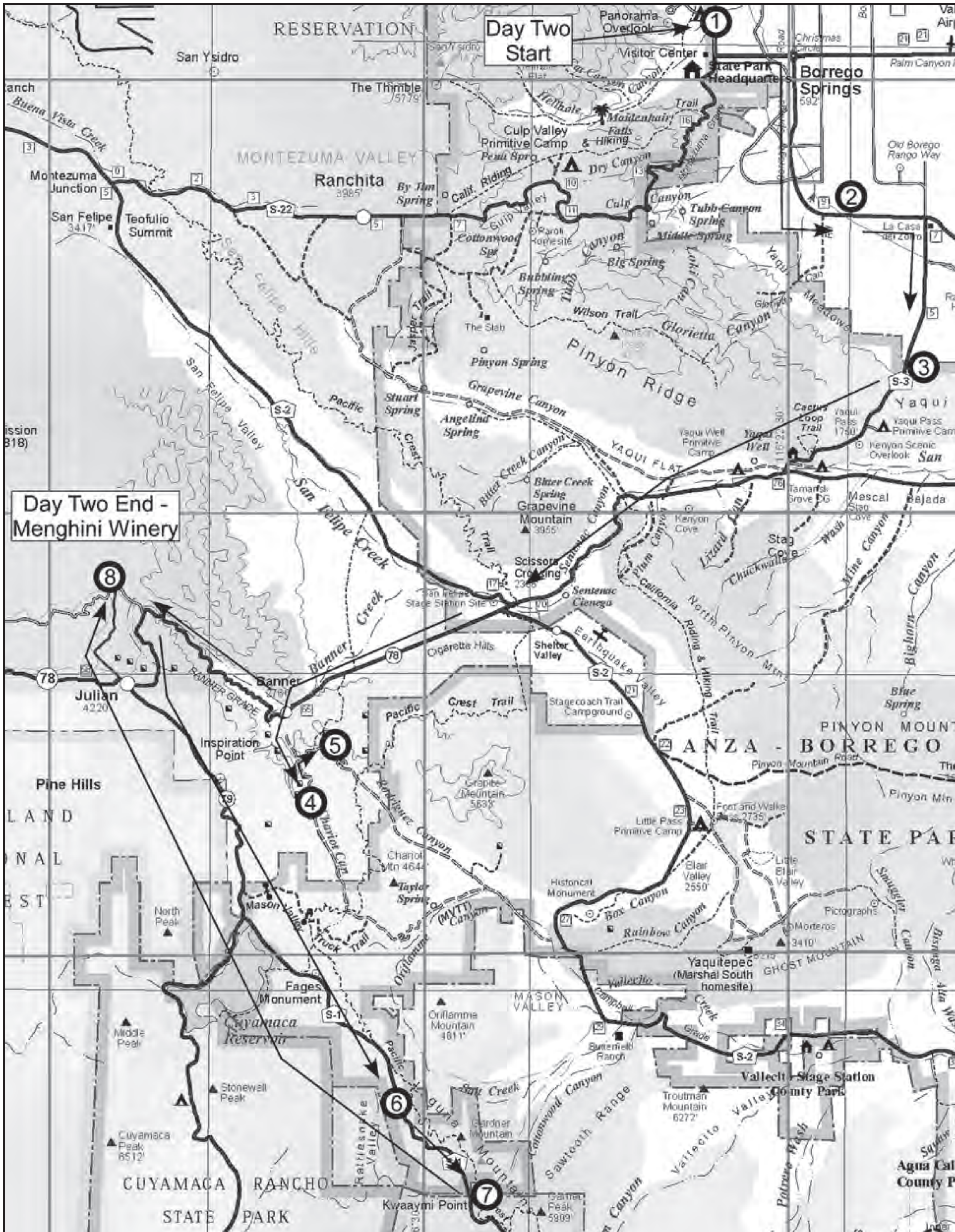

Day Two Route Map

Sunday Morning, October 17, 2010.

Stop No. 1. At Palm Canyon Campground – Group Camping Area.

Stop 1 Speaker: John Peterson, a hydrogeologist, discusses the groundwater basin that supports the people and agriculture of the Borrego Springs Valley Area. (See the not yet officially adopted Borrego Valley Groundwater Report in this volume.)

Odometer (Trip) Mileage

Road portion of the trip starts again0at the intersection of Palm Canyon Drive and Montezuma Valley Road. The trip is approximate 75 miles long.

0.0 Head east on Palm Canyon Drive toward the center of the community of Borrego Springs.

1.4 Enter Christmas Circle and bear right (south) on Borrego Springs Road. After the road curves to the east, start looking for more artwork in a couple of miles.

5.2 Stop No. 2. Aiolornis and Nest. Right turn onto dirt road and park around this large creation. The metal sculpture depicts the largest flight-capable bird in North America whose fossil remains date back to 3.5 million years ago. Aiolornis incredibilis stood four-feet tall and had a wingspan of 16-17 feet.

Stop 2 Speaker: Diana and Lowell provide additional details on the history of the artful subdivision. (See page ii for a picture of the original field trip participants before being "devoured" by Aiolornis.)

Return to vehicles and proceed to paved road.

5.4 Continue east on Borrego Springs Road. Soon veer right (south) onto Yaqui Pass Road at Mile Post 7. No Yaqui Indians lived in this area, but two Yaqui Indians from Mexico were employed by the Ball Freighter Company that worked to improve the well in San Felipe Creek known as Yaqui Well. There was also a Yaqui Indian from Sonora who married a Kumeyaay woman from Grapevine Canyon who once lived near the well in the 1880s. Today, the well, road, flat, meadows, and primitive campground all share the name "Yaqui."

9.7 Sign: "Welcome to Anza-Borrego Desert State Park."

10.5 Stop No. 3. Pull off on the right (west) side pull out next to sign "No Vehicles" and park. This pullout is between Mile Posts 3 and 3.5. Be careful walking across the highway! We will head east for a short 10 minute hike to a detachment fault.

Stop 3 Speaker: Dr. Tom Rockwell discusses the regional geologic framework of the detachment faulting. (See Schultejann paper in this volume.) Walk back to vehicles and proceed south on Yaqui Pass Road.

Note: Yaqui Pass Road was the first paved road into Borrego Valley. The initial dirt road was completed in 1934 and then later the United States Army paved it in 1942 to have better access to Camp Ensign in Borrego Valley and to Clark "Dry" Lake and the Borrego Badlands where they did their desert training preparatory to the campaign in North Africa.

11.2 Road cuts. Exposures of sandstone, and mudstones of the Mio-Pliocene Palm Spring Group.

13.4 Pass Tamarisk Grove Campground, named for the stand of athel tamarisk trees planted there. The campground was originally a San Diego County prison camp that was established in 1929 to relieve pressure from the overcrowded county jail. Inmates provided labor to build the Julian-Kane Spring Road (Highway 78). In 1933, the State Highway Commission ruled that it was illegal to use county inmates as road crews. "Borego" Valley Prison Camp ceased operations and the facility was turned over to the California State Parks to be used as a campground.

13.7 Junction with Highway 78. Turn right and proceed west toward Julian. Note the cut slopes on the left hand side. Exposed in the roadcut east and west of the intersection of Yaqui Pass

and Highway 78 are Miocene megabreccias composed of coarse-grained granitic clasts supported in a matrix composed of pulverized rock. They represent the remnants of huge Miocene landslides that slid basinward along the low-angle ramp formed by a detachment fault (Eric Frost, personal communication.)

16.6 View of Grapevine Canyon. The canyon was possibly named for the wild grapevines surrounding Stuart Spring. The Grapevine Mining District that included the mountain and the canyon was formed in 1894. By 1898, miners were actively prospecting for gold in the district. At one time an old mill was located in Grapevine Canyon and was used to refine gold.

17.2 Start heading up the narrow canyon portion of San Felipe Creek. The creek is one of the longest watercourses in the Anza-Borrego Region. The creek begins as run-off in San Felipe Valley at Teofulio Summit on Hwy S2 and flows through

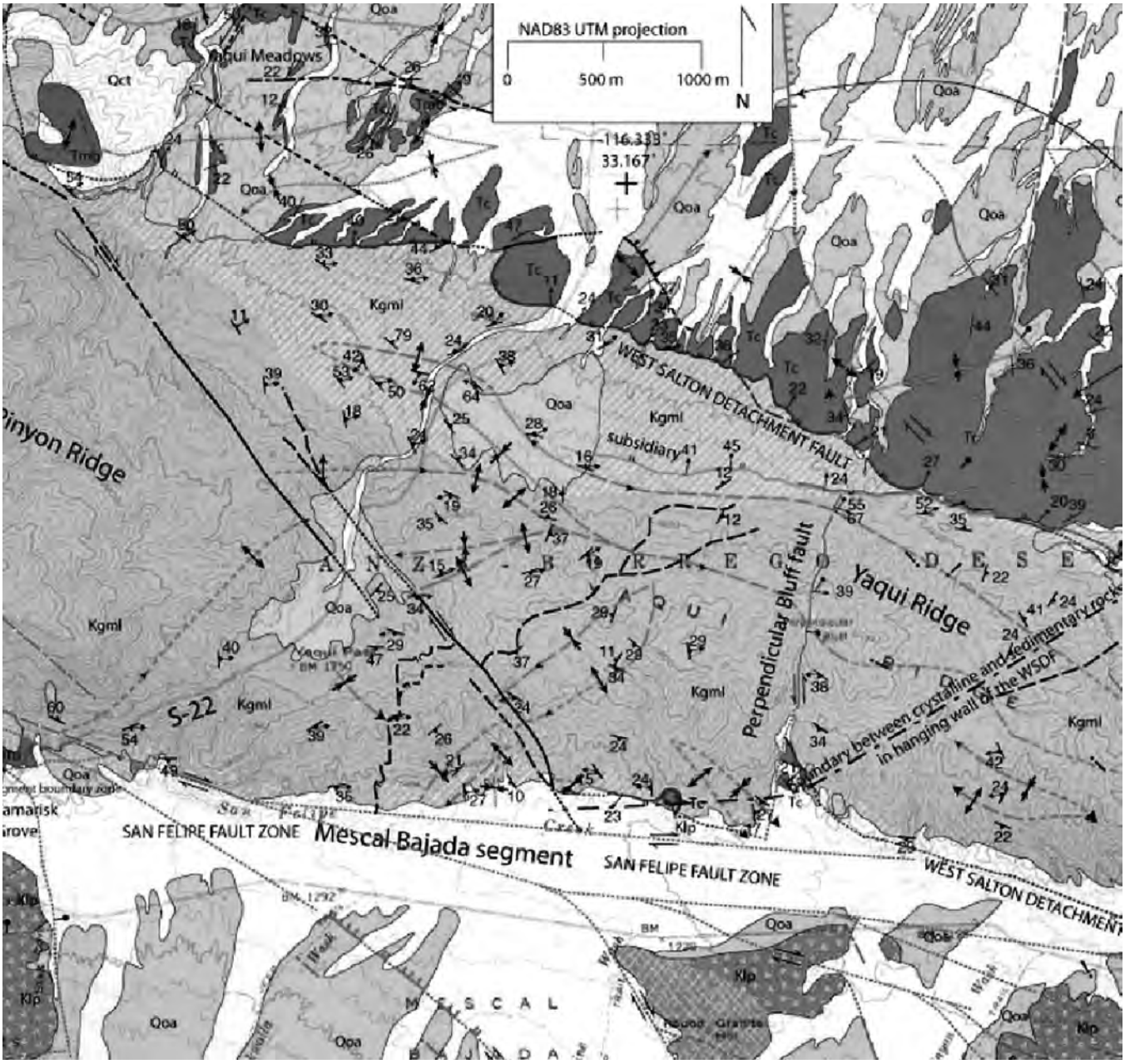

Geologic Map of the Yaqui Pass area: from Steely, A.N., Janecke, S.U., Dorsey, R.J., and Axen, G.J. (2008)
Tc: Canebrake Conglomerate; Tta: Undifferentiated Sediments of the Palm Spring Group; Kgml: Plutonic Rocks

Sentenac Canyon for a few miles before running underground. It resurfaces some 50 miles downstream where it merges with the Coyote Creek, Fish Creek, and Carrizo Creek drainages to form the San Sebastian Marsh. Ultimately, all these watersheds flow into the Salton Sea.

17.8 Cross first San Felipe Creek Bridge.

19.3 Leaving Anza-Borrego Desert State Park® (temporarily!)

20.5 Scissors Crossing. Cross Highway S2 on the north side.

20.8 Cross Highway S2 once again on the south side. In map view this intersection looks like an open pair of scissors, hence "Scissors Crossing". Continue west on Highway 78.

23.7 Pass road cuts in reddish older alluvium.

24.5 Start heading up Banner Grade. The banner for which Banner Grade, Banner Creek, Banner Recreation Ranch, Banner Queen, and long-gone Banner City are named was either the American Flag or the Confederate Flag, respectively, that marked either Louis B. Redman's claim in Chariot Canyon or Drury and James Bailey's Ready Relief Mine across the creek from Redman's mine. It depends on the source you read. Nevertheless, the discovery of gold started a rush, and soon Banner City was booming. In 1894, Banner City School had 30 students, and the graduating class equaled that of National City and exceeded Escondido. The town had a population of 600 to 1,000 and had 40 buildings, including up to seven saloons. Devastating storms that caused the creek to overflow in 1873, 1874, 1916, and again in 1926, wiped out the town each time. The town was not rebuilt after the last storm.

25.5 Pass Banner Store. Good stop for the traveler.

25.6. Stop No. 4. Left turn on dirt road. This road is unmarked. Look for a neatly built 3-foot high stone wall. Also, there is an oak tree in

Google Earth oblique view over Chariot Canyon, looking north. Black line is Elsinore Fault, white line (offset) is Chariot Canyon Fault. Image prepared by Mike Hart.

the center that you can drive around. Proceed up the hill into Chariot Canyon. You will need a high clearance vehicle for this stop. After Redman and the Baileys made their claims in the canyon, George V. King began prospecting in February 1871. He went farther up canyon discovering one of the richest veins in the Banner Area, naming it the Golden Chariot Mine. The canyon and later the mining district took its name from this mine. It was the richest strike in southern California and produced about $2 million worth of bullion.

The Chariot Canyon Fault at this location formed along the eastern boundary of the transition zone between the eastern and western zones of the Peninsular Range Batholith. The transition zone is made up of strongly deformed gneissic rocks and the Late Triassic-Early Jurassic Julian Schist. Together these rocks make up the plastically deformed Cuyamaca-Laguna Mountains Shear Zone. Rocks to the east of the zone according to Grove, et al. (2003), and Bethel-Thompson, et al. (in preparation) were originally thrust westward over western and transition zone rocks along moderately east-dipping faults: the Sunrise Highway Fault and the Chariot Canyon Fault. There is some evidence that this westward movement was reversed during the Miocene and that at least on the Chariot Canyon Fault there was significant down-to-the-east movement that accounts for the prominent escarpment along the east side of the range.

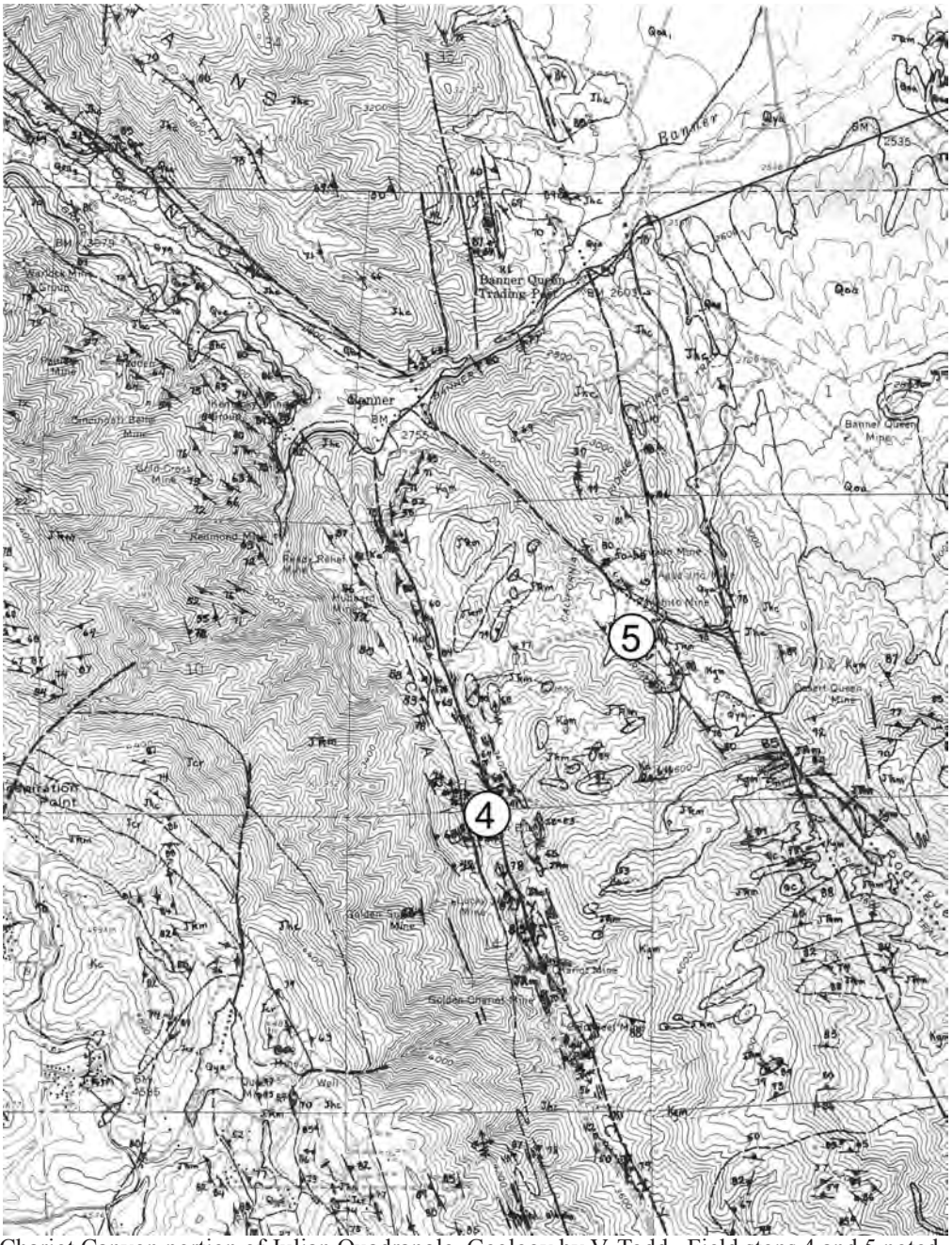

Chariot Canyon portion of Julian Quadrangle. Geology by V. Todd. Field stops 4 and 5 noted.

25.8 Closed gate. The gate is not locked; open it and pass through and close. Proceed up hill.

25.9 Great view of Banner Canyon. The Elsinore Fault Trace can be seen on the lower slopes of

the eastern side of the canyon.

26.2 Cross cattle guard.

27.0 Pass east (left) turn to Ranchito Mine in Rodriguez Canyon. Proceed straight (south).

27.3 Chariot Canyon Fault. In wide left-bending turn there is a narrow dirt road to the right. Turn onto road, veer left and park a few hundred feet down the road in the area of several wide pullouts. Take the center, more level road and walk a few hundred feet. At the second major right turn in the road is a fault contact between gneiss country rock on the left (east) and the Julian Schist on the right. This is one of the major traces of the Chariot Canyon Fault.

Stop 4 Speaker: Mike Hart

Turn around and head north on main road toward highway.

27.7 Optional Stop No. 5. At fork in road, veer right (east) and go up hill toward Ranchito Mine in Rodriguez Canyon.

28.3 Ranchito Mine tailings can be seen in the distance at 10 o'clock. The Ranchito Mine and a large five-stamp mill are among the more significant ruins found in the canyon. In 1957, this mine was owned by the family of Cave J. Couts, an Army officer who figured prominently in San Diego history during and immediately after the Mexican War. Couts was an escort with the International Boundary Commission. Couts' son, Cave J. Couts Jr., purchased the Ranchito Mine in 1895 for $5,500 cash. The Ranchito produced about 2,500 ounces of pure gold and about 100 ounces of silver between 1895 and 1948. In today's terms, this is worth several million dollars.

The Ranchito Deposit crops out low on a southwestern facing ridge slope which partially opens into a small valley. The deposit is enclosed in hybrid ("mixed") rocks which are composed of quartz diorite and schist. As the deposit lies on the northeast side of the Elsinore Fault, which extends along the base of the ridge slope, the hybrid rocks are highly sheared. The deposit consists of quartz bodies in shear zones which strike west-northwest along the fault (Weber, 1963).

28.5 Pull up to gate with sign "Right Fender Ranch"-hand lettered on a right fender. You will need permission from the property owner to access the mine. Turn around and proceed back to main road.

29.2 Veer right to main dirt road. Proceed north.

Entrance to Right Fender Ranch. Ranchito Mine works at center of picture. Photo by Monte Murbach.

30.5 Back at highway. Turn left (west) and proceed up Banner Grade on Banner Grade Road (Highway 78). This is a winding road with great views of the Elsinore Fault trace on the east canyon wall. Only non-drivers should be looking! Otherwise, there are several pull outs that can be used for parking and viewing. Note the vegetation lineaments, right laterally offset drainages, shutter ridges, etc., associated with the fault.

35.1 Pass Wynola Road. Proceed on Highway 78.

36.3 Pass Julian Historic Marker. Entering the town of Julian from the east side. Some 20 years after the 1848 discovery of gold in California, A.E. "Fred" Coleman discovered gold on what is now called Coleman Creek, and the rush to the Julian Area began in late 1869. The Coleman Mining District was created and a tent city called "Emily City" quickly grew attracting many ex-

Confederate soldiers. Among these were Drury, Frank, and James Bailey and their cousins Mike and Webb Julian. As they worked their way up the mountain looking for gold, Drew made a discovery naming it Warrior's Rest. Other miners discovered a rich ledge they named the Washington Mine. Drew also found his largest discovery in Chariot Canyon calling it the Ready Relief. After Drew's first discovery, the Julian Mining District was formed, and Mike Julian became the recorder. Drew began laying out a town on his homestead which he named Julian City for his cousin Mike. He donated land for schools, a public hall, a jail, and churches. In time, the "city" was dropped from the name of the town. Julian remains to this day a mountain community steeped in rich mining history and is a popular tourist attraction.

37.2 Left turn on Highway 79. Proceed south.

43.1 Left turn on Highway S1. Proceed south. Please note the blue "Adopt-a-Road" sign – supported by the San Diego State University Geology Alumni group. Also, watch our for road cyclists! This is a popular road for bicycling.

44.7 Pass mountain biking trailhead. Excellent mountain biking in this area.

46.3 Stop No. 6. Just south of mile post 34.5. Large cut slope on west side. This is a quick stop to look at a fault exposure of the Sunrise Highway fault, the frontal fault of the Sunrise-Highway-Oriflamme Canyon Shear Zone. The Sunrise Highway Fault truncates the western zone of foliated rocks and faults and extends along the Rattlesnake Valley Pluton as a thin proto-mylonitic rind 1m to 3m thick. The Sunrise Highway Fault merges to the north with the Chariot Canyon Fault and disappears into the Julian Schist (Bethel-Thompson, et al., in preparation).

46.4 Pass Sunrise Trailhead Parking Lot. Continue south. Highway S1 is also known as the Sunrise Highway. In San Diego County, the morning sun first lights Highway S1, hence its name. A portion of this highway is in Anza-Borrego Desert State Park®.

47.7 Pass mile post 33. Exposure of granitic ridge on the right.

50.5 Stop No. 7. Left (east) turn on Kwaaymii Point Road. Proceed to the end approximately 0.2 mile and park. This is the "highs" portion of Anza-Borrego Desert State Park®. Enjoy this overlook with Anza-Borrego and Salton Sea in the distance. The Kwaaymii were a band of Kumeyaay Indians that had their main village in the Laguna Mountains and wintered in the desert below. Most of the band members died when they shared some tainted meat. The story of the Kwaaymii can be read in Just Before Sunset, based on the reminiscences of Tom Lucas. Kwaaymii Point was part of the original highway but was vacated probably due to high road maintenance. Note the rocks on the old road and steep rock cut slope above! Also, one of the Pacific Crest Trailheads is here. Proceed back to the highway.

60.0 At the highway, turn right and proceed north toward Julian. Note the sign Anza-Borrego Desert State Park. The elevation here is approximately 6,000 feet!

67.4 At intersection with Highway 79. Turn right, head north toward Julian.

70.6 Pass Inspiration Point. Sign "Vista Point". This is an alternative viewpoint. This is the second Inspiration Point on this field trip, the first being in the Borrego Badlands just north of Fonts Point. Both offer superb and inspiring views of the "lows" to "highs" respectively of the Anza-Borrego Desert Region.

72.9 Pass the 9-acre Jess Martin County Park. This is a nice park with recreational facilities, restrooms, and picnic areas – a good place to rest!

73.4 In Julian, at the intersection with Highway 78 (Main Street). Make a left (west) turn and proceed through town. Watch out for pedestrians and Julian pies!

73.7 At stop sign intersection. (Highway 78 turns

left.) Continue north straight through – road becomes Farmer Road.

75.9 At intersection with Wynola Road. Proceed straight through intersection.

76.0 Old Dodge pickup truck on right. This truck belonged to famous geology professor, Dr. Gordon Gastil, professor emeritus, from San Diego State University.

76.2 Last Stop No. 8. Lunch at Menghini Winery. Park in parking lot or sides of roads. This is the end of the field trip. Enjoy the winery grounds, the wonderful owners, and all of the meangerie of animals.

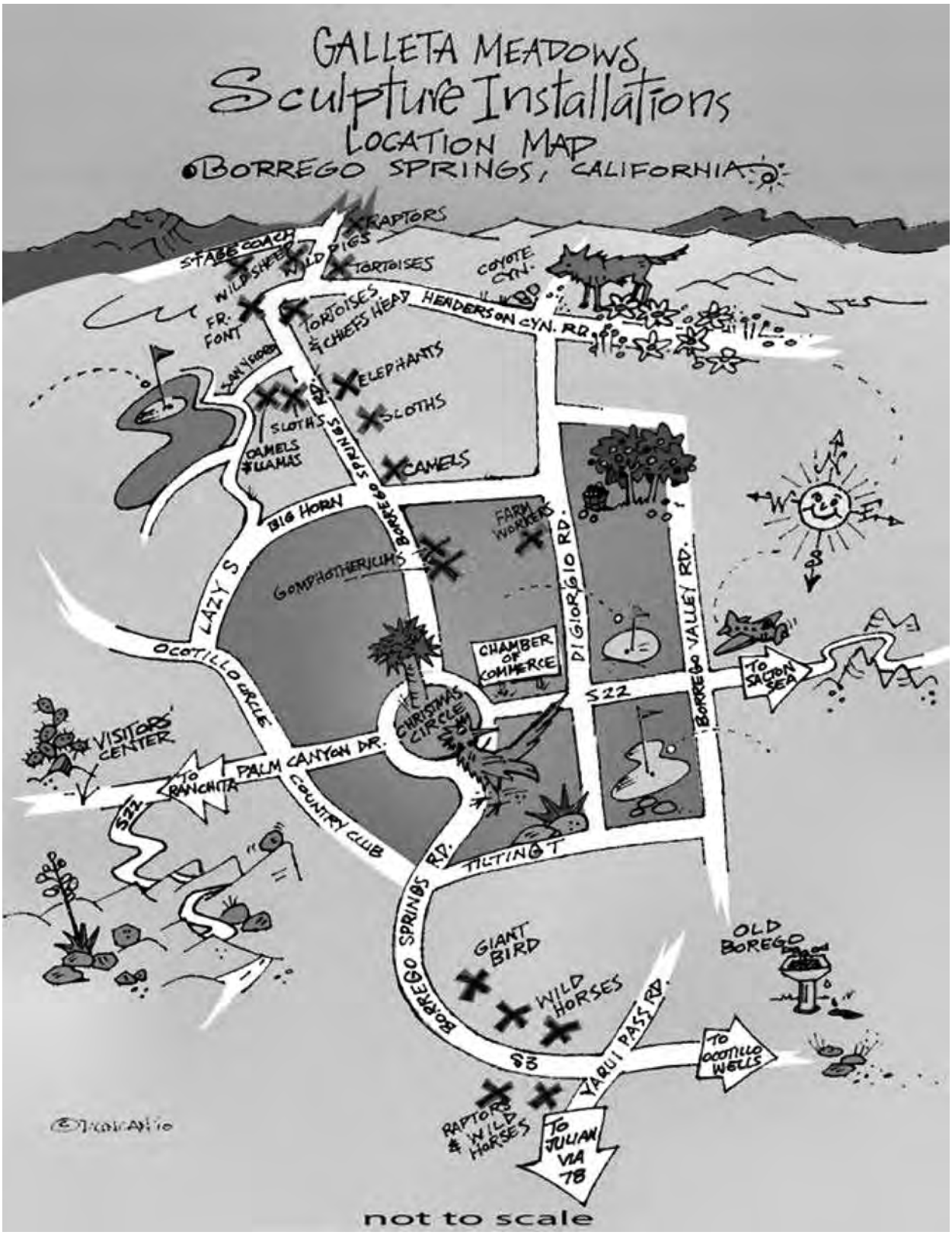

Map illustrated by: Leslie Duncan.
From the Galleta Meadows Estate website at http://www.galletameadows.com/.

Part III.

Papers

“The Borrego Trio”at Fonts Point During Rield Trip Reconnaisance, 2010. Left to right: Mike Hart, Monte Murbach and Chuck Houser. Photo by an anonymous Russian tourist.

View across Borrego Badlands, Clark Lake and Coyote Mountain to the Santa Rosa Mountains.
Photo: Phil Farquharson. Pilot: Chuck Houser.

Stratigraphy, Tectonics, and Basin Evolution in the Anza-Borrego Desert Region

Rebecca J. Dorsey, Department of Geological Sciences, University of Oregon

Southern Borrego Badlands Looking West. (Photograph by Rebecca Dorsey)

Introduction

The fossil record of past life is commonly preserved in ancient sediments and sedimentary rocks. Sediments accumulate in subsiding basins that contain different kinds of depositional environments such as rivers, lakes, deltas, and marine seaways. These environments are friendly to life, and often support assemblages of plants and animals. Through integrative studies of stratigraphy, sedimentology, and paleontology, we can reconstruct ancient life communities and the environments in which they lived.

Plate tectonic forces determine where sedimentary basins form, how long and how fast sediments accumulate, and how they may later be faulted, uplifted, and eroded at the surface. Climate also affects basins and sediments; precipitation, wind, and temperature variation affect surface processes such as erosion and soil formation. In the Salton Trough region of southern California, styles, rates, and environments of basin formation have evolved through time in response to complex changes in driving tectonic forces, fault interactions, and climate change. Because of the rich history of geologic research in Anza-Borrego Desert State Park and adjacent areas, it is impossible to summarize all of the knowledge on this subject in a few pages. This chapter presents a brief overview of existing knowledge about the regional stratigraphy, tectonic evolution, and major sedimentary basins preserved in the Park, which have supported a great diversity of plants and animals during the past ~10 million years.

(excerpted, with permission, from Chapter 5 of Jefferson and Lindsay, eds. (2006) *Fossil Treasures of the Anza-Borrego Desert*. San Diego: California State Parks and Sunbelt Publications)

Anza-Borrego Desert State Park is located within a complex zone of strike-slip faulting and oblique crustal extension and compression that defines the tectonically active boundary between the North American plate and the Pacific plate in southern California (Figures 5.1, 5.2). The southern San Andreas fault system, which includes the San Andreas, San Jacinto, and Elsinore faults, is a broad zone of past and ongoing seismic activity that separates areas belonging to the Pacific plate (Baja California and southern California) from areas located on North America (mainland Mexico and the U.S.). Long-term northwesterly movement of the Pacific plate relative to North America has resulted in progressive right-lateral fault displacements and related crustal deformation during the past ~25 to 30 million years, producing a complicated network of faults, rotating crustal blocks, mountain ranges, and sedimentary basins. The two plates are also diverging slightly in some areas, which has caused the Salton Trough and Gulf of California to open up by oblique rifting and extension during the past 10 to 15 million years. These aspects of relative plate motion and the development of geologic structures on a regional scale are known from landmark studies by Atwater (1970), Lonsdale (1989), Stock and Hodges (1989), Powell et al. (1993), DeMets (1995), Dickinson (1996), Atwater and Stock (1998), Axen and Fletcher (1998), Oskin and Stock (2003), and others.

As described below, we now know that regional subsidence related to crustal extension and transtension (a combination of strike-slip movement and oblique extension of a fault) produced a number of fault-bounded basins that filled with sediments from Miocene to Pleistocene time (Figures 5.2,

5.3, 5.4). In the recent geologic past (last 1 to 2 million years) many of these basins have been uplifted and eroded to reveal the diverse stratigraphic record of their tectonic, climatic, and paleontologic evolution. In the Salton Sea, fault-controlled subsidence has continued to the present day, accumulating a thick section of young sediments that are buried in the modern basin beneath the surface.

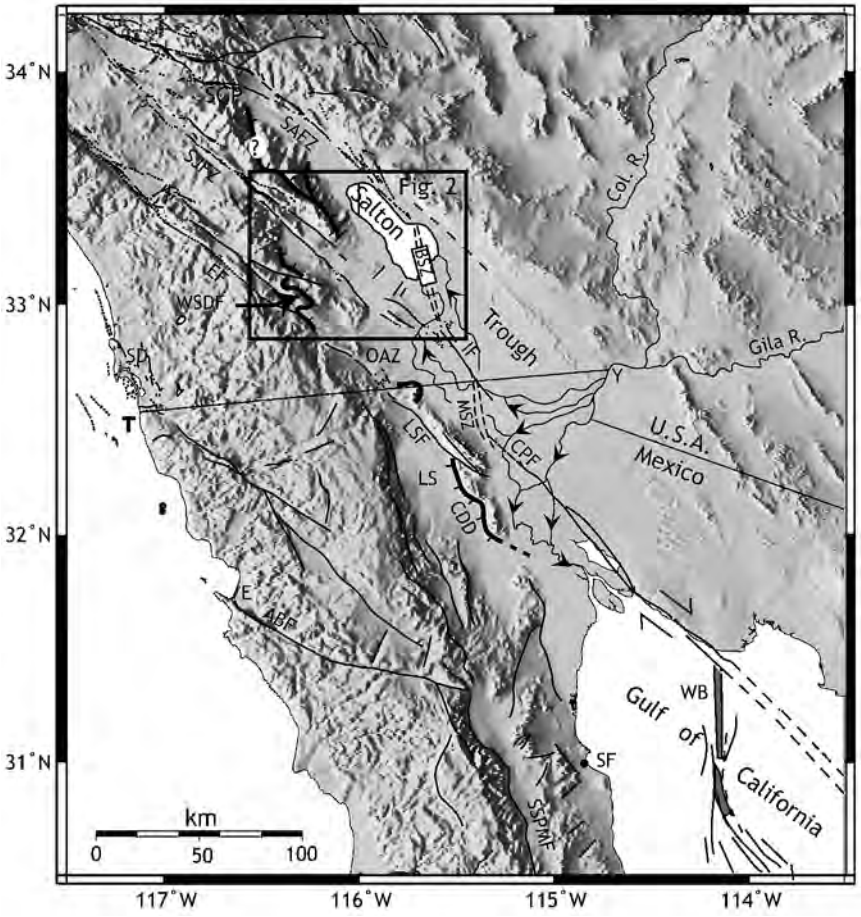

Figure 5.1 Faults and Topography of the Northern Gulf of California and Salton Trough Region. Decorated thicker lines are detachment faults, tick marks on upper plate; plain lines are high-angle normal and strike-slip faults. Explanation: ABF, Agua Blanca fault; BSZ, Brawley Spreading zone; CDD, Cañada David detachment; CPF, Cerro Prieto fault; E, Ensenada; IF, Imperial fault; SAFZ, San Andreas fault zone; SD, San Diego; SGP, San Gorgonio Pass; SF, San Felipe; SJFZ, San Jacinto fault zone; SSPMF, Sierra San Pedro Martir fault; T, Tijuana; and WB, Wagner basin. *(Shaded relief map base courtesy of H. Magistrale)*

Prior Work

Our understanding of geological events summarized below is based on decades of research by many scientists. This chapter does not present new data, it is simply an attempt to synthesize a vast body of existing knowledge and make it accessible to a broad audience. Some of the more influential studies of regional stratigraphy, basin evolution, and related structures in the western Salton Trough appear in papers and theses by: Axen and Fletcher (1998), Bartholomew (1968, 1970), Brown et al. (1991), Dean (1988, 1996), Dibblee (1954, 1984, 1996a, 1996b), Dronyk (1977), Feragen (1986), Frost et al. (1996a, 1996b), Girty and Armitage (1989), Ingle (1974), Johnson et al. (1983), Kerr (1982, 1984), Kerr and Kidwell (1991), Lough (1993, 1998), Merriam and Brady (1965), Muffler and Doe (1968), Opdyke et al. (1977), Quinn and Cronin (1984), Remeika (1995), Remeika and Beske-Diehl (1996), Schultejann (1984), Sharp (1982), Stinson (1990), Stinson and Gastil (1996), Tarbet and Holman (1944), Wells (1987), Winker (1987), Winker and Kidwell (1986, 1996), Woodard (1963, 1974). This list is only a partial sampling of many theses, papers, and abstracts that have contributed to our understanding of this fascinating region. Interested readers are encouraged to explore the original literature upon which the following summary is based.

Tectonics, Stratigraphy, and Basin Evolution

Overview

Changing patterns of faulting and subsidence in the San Andreas system have exerted a primary control on sedimentation and stratigraphy in the western Salton Trough through time. Although significant uncertainties and questions remain, the Miocene to Pleistocene tectonic evolution of this region can generally be divided into three stages: (1) early (?) to late Miocene continental sedimentation, volcanism, and formation of fault-bounded nonmarine rift basins; (2) Pliocene to early Pleistocene extension and transtension on a system of regional detachment faults (low-angle normal faults) and formation of a large basin that filled first with marine and later with terrestrial sediments; and (3) Pleistocene to modern strike-slip faulting and related folding in the San Jacinto and Elsinore fault zones, which results in uplift and erosion of the older deposits. Much of the evidence for these tectonic stages is contained in deposits that accumulated in ancient sedimentary basins. Thus, the stratigraphy can be regarded as both an integral component of the dynamic fault-basin system, and a natural record, not always easy to read, of

the tectonic processes that produced them.

The Neogene (Miocene up to Pleistocene) stratigraphy of the western Salton Trough and Imperial Valley is illustrated in Figures 5.3 and 5.4. Ages of the deposits have been determined from studies of micropaleontology, vertebrate paleontology, geochronology, and paleomagnetism (see references in figure caption). Figure 5.3 organizes the stratigraphy of the well-studied Vallecito Creek-Fish Creek area into subdivisions that reflect evolving ideas about the architecture and organization of this complex succession of strata (e.g. Winker, 1987; Kerr and Kidwell, 1991; Winker and Kidwell, 1996).

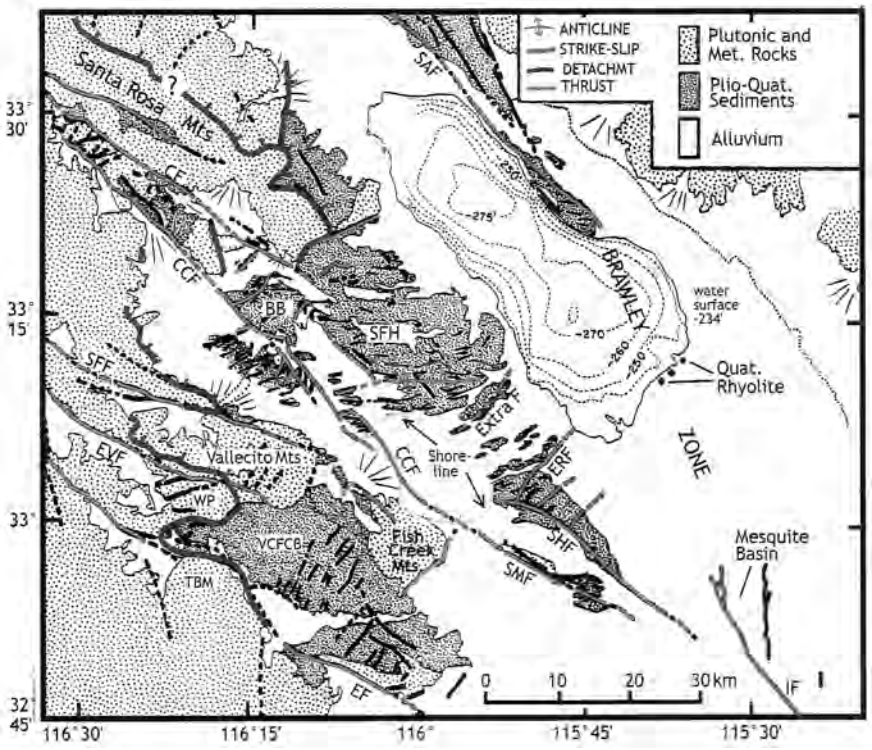

Figure 5.2 Geologic Map of the Salton Trough Region. Explanation: BB, Borrego Badlands; CF, Clark fault; CCF, Coyote Creek fault; EF, Elsinore fault; ERF, Elmore Ranch fault; EVF, Earthquake Valley fault; VCFCB, Vallecito Creek-Fish Creek basin; IF, Imperial fault; SFF, San Felipe fault; SFH, San Felipe Hills; SHF, Superstition Hills fault; SMF, Superstition Mtn fault; TBM, Tierra Blanca Mts.; and WP, Whale Peak. (Map compilation courtesy of L. Seeber)

Neogene deposits in the northwestern Salton Trough (Figure 5.4) show similarities and differences with strata in the Vallecito Creek-Fish Creek section. Upper Miocene sedimentary rocks in the northwestern Trough are sporadically exposed around the margins of the basin and typically are thinner and less complete than in Split Mountain Gorge, though they are locally abundant in the southern Santa Rosa Mountains (Hoover, 1965; Cox et al., 2002; Matti et al., 2002). The Imperial and Palm Spring Groups in the San Felipe Hills are similar to the same units in the Vallecito Creek-Fish Creek stratigraphic section, but the lacustrine (lake) Borrego Formation is much thicker than the Tapiado Formation, and the Ocotillo Conglomerate is a widespread coarse alluvial unit in the northwestern Trough that has only a limited extent in the Vallecito Creek-Fish Creek area (Figures 5.3, 5.4; Dibblee, 1954, 1984, 1996a, 1996b; Bartholomew, 1968). These similarities and differences suggest that the two areas may have occupied a single integrated basin during deposition of the Mio-Pliocene Imperial and early Palm Spring Groups, but became segregated into separate sub-basins in late Pliocene time (Dorsey et al., 2004).

Axen and Fletcher (1998) showed that the Imperial and Palm Spring Groups, and possibly the upper part of the Split Mountain Group, accumulated in a large sedimentary basin that was bounded on its western margin by the west Salton detachment fault system (tectonic stage 2, above) from late Miocene to early Pleistocene time. Detachment faults are low-angle normal faults that form in areas of strong regional extension; they are sometimes associated with high crustal heat flow and commonly produce large sedimentary basins in their upper plates (Figure 5.5; e.g. Wernicke, 1985; Friedmann and Burbank, 1995; Miller and John, 1999). The west Salton detachment fault system was recognized in prior studies and was widely believed to be early or middle Miocene age (e.g. Stinson and Gastil, 1996; Frost et al., 1996a, 1996b). The synthesis by Axen and Fletcher (1998) presented evidence that slip on the detachment system probably began in late Miocene time and continued through Pliocene into early Pleistocene time. Detachment faulting resulted in widespread crustal subsidence and accumulation of thick sedimentary deposits that are now exposed in the western Salton Trough (Figures 5.2, 5.3). In contrast to many well-known detachment fault systems, the upper-plate basin of the west Salton detachment fault was not significantly broken apart by normal faults, perhaps because slip on the detachment was terminated by initiation of strike-slip faulting (tectonic stage 3). Moreover, it experienced an oblique, partially strike-slip component of movement that is unlike orthogonal detachment faults (Steely et al., 2004a, 2004b; Axen et al., 2004). These and other aspects

of faulting and basin evolution in the Salton Trough are the subject of ongoing study by the author and her colleagues.

The three stages of tectonic evolution and basin development are briefly summarized below. The events are described from earlier to later, moving from lower to higher in the stratigraphic column. Stage 1 (Miocene) is best recorded in rocks exposed in and around Split Mountain Gorge. Stage 2 (Pliocene to early Pleistocene) is recorded in widespread deposits of the Imperial and Palm Spring Groups that are exposed extensively around the western Salton Trough region (Figure 5.2). Geomorphic, structural, and geophysical evidence for stage 3 (Pleistocene to modern) is ubiquitous in the landscape and is reflected in present-day mountain ranges and ridges, active fault scarps, alluvial fans, eroding badlands, and playa lakes.

1. Early to Late Miocene

Significant accumulation of Neogene strata began with deposition of lower Miocene continental sandstone and conglomerate of the Red Rock Formation, which occupies the lower part of the Split Mountain Group (Kerr and Kidwell, 1991; Winker and Kidwell, 1996). These deposits accumulated in rivers and eolian (wind-borne) sand dunes that filled in rugged paleotopography formed by earlier erosion of granitic and metamorphic rocks of the Peninsular Ranges batholith. In some places, they are conformably overlain by volcanic basalts, breccias, and interbedded basalt-clast conglomerates of the middle Miocene Alverson volcanics, which have been dated at approximately 22 to 14 Ma (Figure 5.3; Gjerde, 1982; Ruisaard, 1979; Kerr, 1982). Based on relationships between faulted volcanic and sedimentary rocks, Winker and Kidwell (2002) inferred that weak regional extension and slip on high-angle normal faults began during emplacement of the Alverson volcanics, prior to the late Miocene phase of strong extension and rift-basin development.

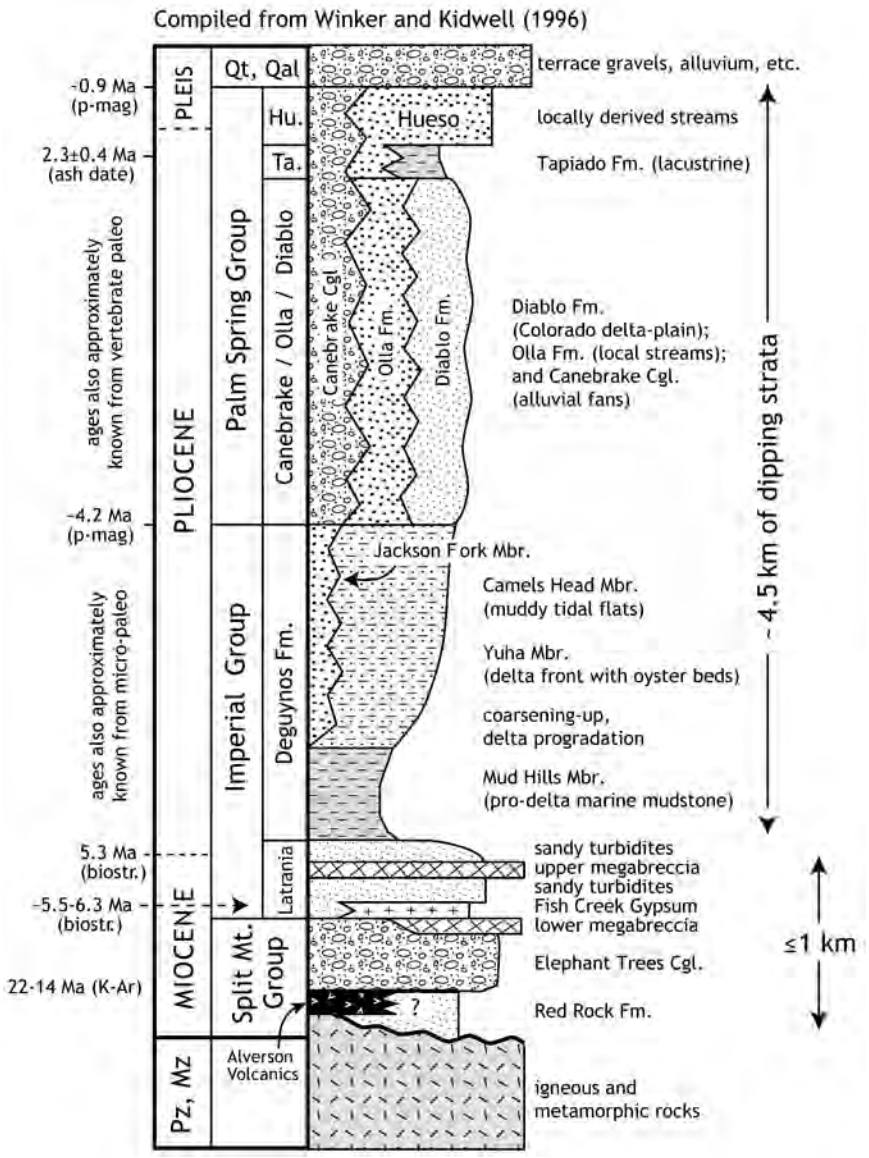

Figure 5.3 Generalized Stratigraphic Column for the Vallecito Creek-Fish Creek Stratigraphic Section.. Paleomagnetic and ash dates are from Opdyke et al. (1977) and Johnson et al. (1983). Biostratigraphic age controls are from studies of Stump (1972), Downs and White (1968), Ingle (1974), Pappajohn (1980), Dean (1988), and McDougall (personal communication, cited in Winker and Kidwell, 1996). K-Ar (potassium-argon) ages in the Alverson Volcanics are from Ruisaard (1979) and Gjerde (1982), summarized by Kerr (1982). Adapted from Winker and Kidwell (1996).

The Split Mountain Formation of earlier workers (e.g. Woodard, 1974) includes conglomerate, breccia, and sandy marine turbidites exposed in Split Mountain Gorge. Based on the conformable transition to Imperial marine strata, the upper, marine part of the Split Mountain Formation was reassigned to the lower Imperial Formation (Kerr and Kidwell, 1991), and later named the Latrania Formation of the Imperial Group (Winker and Kidwell, 1996; Remeika, 1998). The Anza, Alverson, and lower Split Mountain Formations were assigned to the Split Mountain Group in this revision (Figure 5.3; Winker and Kidwell, 1996). In

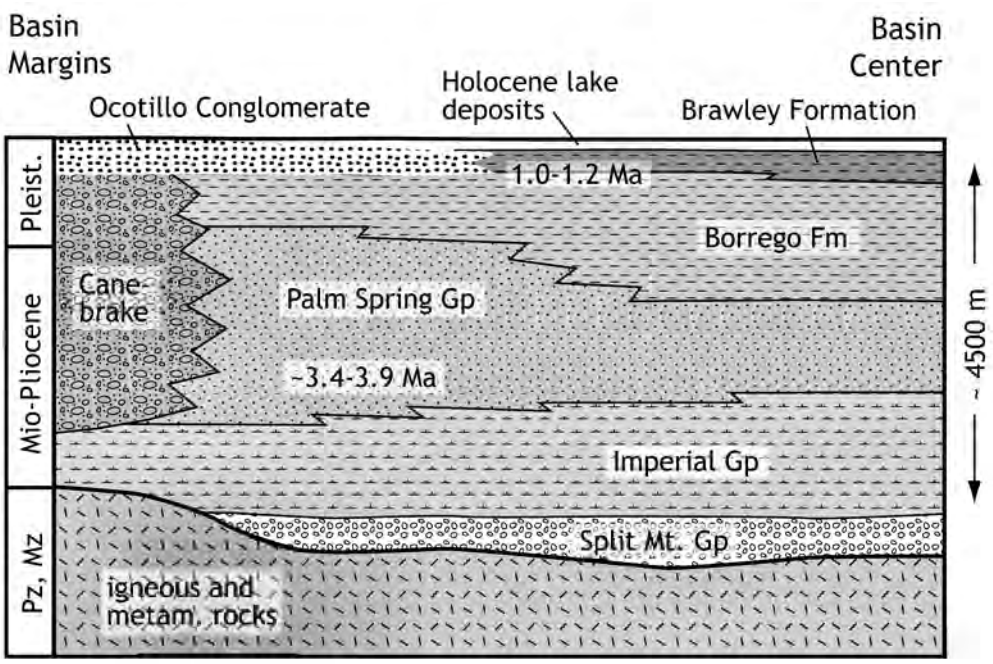

Figure 5.4 Stratigraphy of the Northwestern Salton Trough.. Age of lower Palm Spring Group is based on micropaleontologic study of Quinn and Cronin (1984); age of the base of the Ocotillo Conglomerate is based on paleomagnetic studies by Brown et al. (1991) and Remeika and Beske-Diehl (1996). Modified from Abbott (1969), Dibblee (1954) and Sharp (1982).

the Vallecito Creek-Fish Creek basin, sedimentologically variable marine deposits of the Latrania Formation are conformably overlain by regionally extensive fine-grained marine deposits of the Deguynos Formation (Winker and Kidwell, 1996; Remeika, 1998).

The stratigraphy of the Split Mountain and lower Imperial Groups is very complex, exhibiting abrupt lateral changes in facies (texture, sedimentary structures, grain size, and composition) and local thickening into the Split Mountain Gorge area (e.g. Winker, 1987). These units include two megabreccias with huge clasts (boulder to house-size rock fragments) that were emplaced catastrophically by large rock avalanches, or "sturzstroms" (Figure 5.3; Kerr and Abbott, 1996; Rightmer and Abbott, 1996; Shaller and Shaller, 1996). The Elephant Trees Conglomerate (formerly Split Mountain Formation) is an impressive unit of coarse-grained debris flow and sheet flood deposits that are superbly exposed in the walls of Split Mountain Gorge (Figure 5.6). The age of the Elephant Trees is uncertain (e.g. Kerr and Kidwell, 1991; Winker and Kidwell, 1996). Pronounced lateral thickening of the conglomerate, its conformable association with sandstone of the underlying Red Rock Formation, and the presence of normal faults overlapped by sedimentary deposits, provide evidence that this area experienced sedimentation in steep alluvial fans and flanking braided streams in an active rift basin during late Miocene extension on high-angle normal faults (Kerr, 1982, 1984; Winker, 1987; Winker and Kidwell, 1996).

The Fish Creek Gypsum is a thick, discontinuous deposit that occupies the transition from nonmarine deposits of the Split Mountain Group to marine turbidites of the lower Imperial Group (Figure 5.3; Dean, 1988; 1996; Winker and Kidwell, 1996). Neither its age nor its origins are agreed upon by geologists at this time. Index species (taxa exclusively associated with a particular time interval) of calcareous nanoplankton indicate an age of 3.4-6.3 Ma (million years) for the gypsum (Dean, 1996). This age is refined by tentative placement of the Miocene-Pliocene boundary (5.3 Ma) in the overlying Latrania Formation by Winker and Kidwell (1996), suggesting that its age is approximately 6.3 to 5.5 Ma. The environment of formation for the Fish Creek Gypsum has been variably interpreted as a marginal-marine evaporite setting (Winker, 1987), a restricted shallow-marine basin (Dean, 1988; 1996), or a marine basin with precipitation of gypsum from a hydrothermal vent system (Jefferson and Peterson, 1998). These diverse interpretations highlight the existing uncertainty about the origin of the gypsum and its relation to tectonic evolution at Split Mountain Gorge.

The Fish Creek Gypsum and laterally equivalent lower Latrania Formation record a rapid transgression of marine waters that apparently was controlled by a change in the regional tectonic regime. Onset of late Miocene rifting and high-angle normal faulting recorded in the Split Mountain Group may have been related to early movement on the west Salton detachment fault system (Axen and Fletcher, 1998), or it may represent a distinct earlier phase of extension that pre-dates detachment faulting (Dorsey and Janecke, 2002; Winker and Kidwell, 2002). In either interpretation, it appears that a major tectonic change at about 6-7 Ma produced nearly synchronous marine incursion throughout the northern Gulf of California and

Salton Trough region. This incursion flooded an area at least 400 km (250 miles) long, from San Felipe, Mexico, in the south, to San Gorgonio Pass in the north (Figure 5.1; Oskin and Stock, 2003).

Recent studies on Isla Tiburon, Mexico, have shown that marine deposits there are younger than about 6.2 Ma, contrary to previous interpretations, and that tectonic opening of the northern Gulf of California was initiated when dextral (right lateral strike-slip) plate motion stepped into the Gulf at about 6.0-6.2 Ma (Gastil et al., 1999; Oskin et al., 2001; Oskin and Stock, 2003). Oskin and Stock (2003) noted that the age of the oldest marine deposits is remarkably similar throughout the northern Gulf and Salton Trough region. Micropaleontology of diatomite near San Felipe indicates that the oldest marine deposits there accumulated between about 5.5 and 6.0 Ma (Boehm, 1984). At San Gorgonio Pass, the Imperial Group is about 6.5 to 6.3 Ma based on micropaleontologic and geochronologic data (McDougall et al., 1999; and papers cited therein). An age of about 6.3 to 5.5 Ma for the Fish Creek Gypsum in the Split Mt. area (Dean, 1988, 1996) is consistent with the timing of marine incursion in other locations around the northern Gulf and Salton Trough region. Rapid marine flooding during this short time interval probably resulted from accelerated basin subsidence and crustal thinning related to initiation of the active plate boundary in the Salton Trough at about 6 Ma (Oskin and Stock, 2003). In addition, a rapid rise in global sea level in latest Miocene time (e.g. Haq et al., 1987) may have caused flooding of an area even larger than would have resulted from tectonic forces alone.

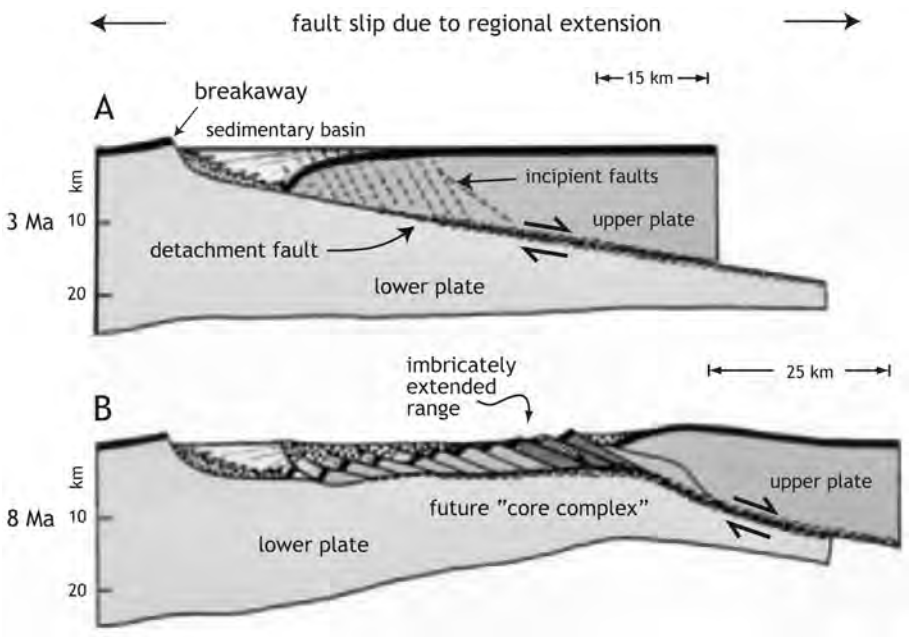

Figure 5.5 Conceptual Model for Partial Evolution of a Detachment Fault (low-angle normal fault) and Upper-plate (supradetachment) Sedimentary Basin Created by Regional Extension.

A. Early slip on the fault occurs by brittle shearing in the shallow crust and ductile deformation in the middle to lower crust. The curved, listric geometry of the breakaway produces a rollover monocline in the upper plate, which in turn produces a sedimentary basin that accumulates a thick section of syn-extensional deposits.

B. After about 8 million years of fault slip, the lower plate domes upward and the upper plate breaks apart along a series of closely spaced normal faults that disrupt sedimentation in the basin. Note that the upper plate of the west Salton detachment fault system did not experience break-up as shown in B, possibly because slip on the detachment was terminated by initiation of strike-slip faulting in late Pliocene or early Pleistocene time.

Modified from Wernicke (1985).

2. Pliocene to Early Pleistocene

The Pliocene was a time of deep basin subsidence and accumulation of thick marine and nonmarine sedimentary rocks of the Imperial and Palm Spring Groups throughout the western Salton Trough region (Figures 5.2, 5.3, 5.4). Widespread, fine-grained marine deposits of the Deguynos Formation rest on coarse-grained facies of the Split Mountain Group and Latrania Formation, and represent the culmination of the latest Miocene marine incursion (e.g. Winker and Kidwell, 1996). The tectonic setting was dominated by slip on the west Salton detachment fault system, whose bedrock and basin remains are exposed today around the western fringes of the Salton Trough (Figures 5.2, 5.3; Axen and Fletcher, 1998). The Miocene-Pliocene boundary at Split Mountain has tentatively been placed in the upper part of the Latrania Formation, above the upper megabreccia and at the base of the oldest recorded Colorado River-derived sandstones (Figure 5.3; K. McDougall, personal communication, as cited in Winker and Kidwell, 1996; Gastil et al., 1996). This stratigraphic transition is generally not exposed in the northwestern Salton Trough, but was penetrated by deep exploratory wells in the San Felipe Hills (Dibblee, 1984).

The change from locally variable, coarse-grained Latrania deposits of upper Miocene age to regionally extensive fine-grained marine deposits of the lower Pliocene Deguynos Formation may be related to rapid subsidence rates (~5 mm/yr [1/5 in.]; Johnson et al., 1983) that overwhelmed the sediment supply and submerged the Salton Trough basin during early Pliocene time. This period of rapid subsidence probably was driven by the same tectonic forces that produced the latest Miocene marine incursion: initiation or acceleration of relative plate motion in the northern Gulf-Salton Trough region and initiation or integration of the detachment fault system.

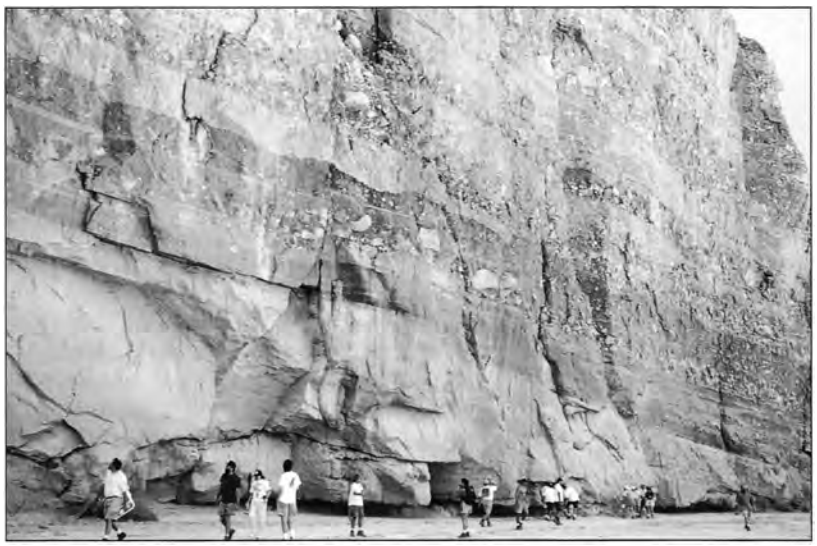

Figure 5.6 Split Mountain Group. Elephant Trees Conglomerate of the Split Mountain Group in Split Mountain Gorge, showing interbedded sandstone and boulder conglomerate that formed in an alluvial fan setting. *(Photograph by Rebecca Dorsey)*

Through a combination of tectonic controls, the Salton Trough and northern Gulf of California became a large elongate seaway in early Pliocene time that accumulated a thick succession of marine fossiliferous claystone, siltstone, sandstone, and minor limestones of the Imperial Group (Figures 5.3, 5.4, 5.7). During this time, southern California was located about 200 km (125 miles) southeast of its present location relative to North America, and the Salton Trough was part of a long marine embayment that extended a large distance to the north (Figure 5.9A; Winker, 1987; Winker and Kidwell, 1986). Shortly after the marine transgression that produced the Imperial seaway, this region became the site of a distal prodelta (outermost delta) where only very fine-grained clay and silt derived from the ancestral Colorado River were deposited by suspension settling from the marine water column. This is recorded in mudstone and silty rhythmites of the Deguynos Formation (Figure 5.3; Winker and Kidwell, 1996; 2002) and by similar deposits of the Imperial Group in the San Felipe Hills (Figure 5.4; Dibblee, 1954, 1984; Quinn and Cronin, 1984). Later, as the Pacific plate moved northwest relative to North America, fine-grained sand from the ancestral Colorado River advanced into the basin via dilute turbidity currents. This produced a coarsening-up trend in sediments of the upper Imperial Group that reflects gradual shallowing of the basin as it filled with Colorado River-derived sediments (Figures 5.3, 5.4). The youngest deposits of the Imperial Group include fossiliferous claystone disturbed by burrowing marine animals, wavy-bedded sandstone, and foraminifers (shelled protozoans) that indicate intertidal brackish water conditions; this suggests deposition in a low-energy intertidal environment similar to the broad modern tidal flats that occupy a large area of the present-day lower Colorado delta at the north end of the Gulf of California (Figure 5.1; Woodard, 1974; Quinn and Cronin, 1984; Winker, 1987; Winker and Kidwell, 1996). Marine deposits of the Imperial Group can be viewed along the sides of Fish Creek Wash, south of Split Mountain Gorge.

Shallow marine units of the upper Imperial Group are gradationally overlain by the Arroyo Diablo Formation, a thick unit of sandstone and mudstone that is exposed over much of the Salton Trough region (Figures 5.2, 5.3, 5.4). Quartzose sand of the Arroyo Diablo and Olla Formations (Figure 5.8) was eroded from the Colorado Plateau and deposited in the ancestral Colorado River delta which, at about 3.0 Ma, was located approximately 60-70 km (40 miles) southwest of the modern point of entry of the Colorado River into the Salton Trough (Figure 5.9B; Girty and Armitage, 1989; Guthrie, 1990; Winker and Kidwell, 1986). Deposition took place in a subaerial delta-plain setting that was characterized by laterally shifting distributary channels and interchannel swamps and marshes, with overall transport toward the southeast (Winker and Kidwell, 1986). The presence of fossil wood varieties including walnut, ash, and cottonwood suggests that the Pliocene climate was wetter and cooler than today (Remeika et al., 1988; Remeika and Fleming, 1995; see Remeika, this volume, Ancestral Woodlands of the Colorado River Delta Plain). The Canebrake Conglomerate, a coarse-grained lateral equivalent of the Arroyo Diablo Formation and other younger units, accumulated in alluvial fans and braided streams on the flanks of steep mountains around

Figure 5.7 Upper Imperial Group. Tan fine-grained marine mudstone capped by oyster beds in the upper Imperial Group, Vallecito Creek-Fish Creek basin; white patch in distance is Fish Creek Gypsum in the western Fish Creek Mts. *(Photograph by Rebecca Dorsey)*

the margins of the delta plain (e.g. Dibblee, 1954, 1984; Hoover, 1965; Winker, 1987).

The base of the lacustrine (lake) Tapiado and fluvial Hueso Formations (Figure 5.3) marks an abrupt end of Colorado river input in the Fish Creek area (Winker, 1987; Winker and Kidwell, 1986, 1996). This transition coincides approximately with the end of stratigraphic similarities between sediments in the Fish Creek area and the northwestern Salton Trough, and may have resulted from reorganization of the basin (Figures 5.3, 5.4; Dorsey et al., 2004). The Borrego Formation is a very thick succession of lake deposits exposed in the Borrego Badlands and San Felipe Hills that may be partially equivalent to the Tapiado Formation, but its age and stratigraphic architecture are not well known. The Borrego Formation contains abundant claystone and siltstone and rare sandstone beds with both Colorado River- and locally-derived sandstones. Our knowledge of the Borrego Formation and its paleontology, paleogeography, and Pliocene evolution in the northwestern Salton Trough is based largely on previous studies by Tarbet and Holman (1944), Morley (1963), Dibblee (1954, 1984), Hoover (1965), Merriam and Bandy (1965), Bartholomew (1968); Dronyk (1977), Feragen (1986), Wells (1987), as well as recent studies by Kirby et al., (2004a, 2004b), Steely et al. (2004a, 2004b), and Dorsey et al. (2004). Ostracodes (small crustaceans, mussel shrimp) and benthic foraminifers reflect deposition in fresh water to brackish and alkaline conditions. The Borrego Formation represents a large perennial lake basin that became isolated from the Gulf of California as it moved tectonically to the northwest past the Colorado River delta into its present position (Figure 5.1; Kirby et al., 2004a, 2004b, Dorsey et al., 2004).

The youngest deposits of the Palm Spring Group are early Pleistocene, locally derived sandstone and conglomerate of the Hueso Formation in the Vallecito Creek-Fish Creek area (Figure 5.3; Winker and Kidwell, 1996; Cassiliano, 2002) and Ocotillo Conglomerate in the Borrego and Ocotillo Badlands (Figure 5.4; Dibblee, 1954; 1984; Brown et al., 1991; Bartholomew, 1968, 1970; Lutz, 2005). These deposits accumulated in alluvial fans and ephemeral streams that drained nearby fault-bounded mountain ranges. Deposition took place in sedimentary

Figure 5.8 Lower Palm Spring Group. Channelized sandstone (tan color) and red mudstone of the Olla Formation (Palm Spring Group) that was deposited in the ancestral Colorado River delta plain. *(Photograph by Rebecca Dorsey)*

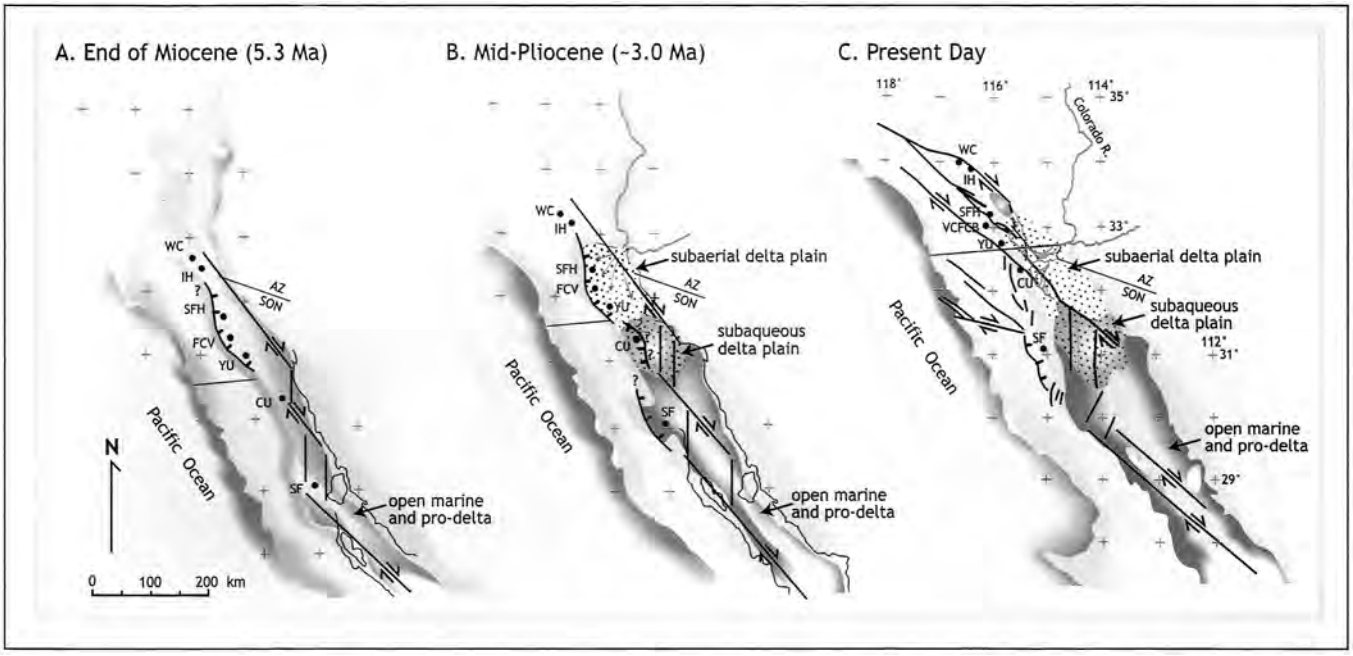

Figure 5.9 Paleogeographic Reconstructions of Sedimentary Basins and Faults in the Salton Trough and Northern Gulf of California Since the End of Miocene Time.

Southern California and northern Baja California have been moving to the northwest relative to stable North America since localization of the plate boundary in the Gulf of California at ~6.5-6.0 Ma (Oskin and Stock, 2003) or possibly earlier.

A. End of Miocene time, shortly after widespread marine incursion in the Salton Trough and northern Gulf of California.

B. Deposition of Palm Spring Group in the ancestral Colorado River delta.

C. Present-day geography, active faults, and environments. Explanation: CU, Sierra Cucapas; VCFCB, Vallecito Creek-Fish Creek basin; IH, Indio Hills; SF, San Felipe; SFH, San Felipe Hills; and WC, Whitewater Canyon. Thick lines with arrows are strike-slip faults showing relative movement; thick lines with tic marks are normal faults (low-angle detachment faults in A and B). Red arrows in B indicate inferred sediment transport directions (based on Winker and Kidwell, 1986) (see text for explanation). Redrafted from Winker (1987) with modifications from Axen (1995), Axen and Fletcher (1998), and Oskin et al. (2001).

basins that were shaped by slip on early strands of the San Jacinto fault zone (Bartholomew, 1970; Pettinga, 1991; Lutz and Dorsey, 2003; Kirby et al., 2004a, 2004b; Kirby, 2005; Lutz, 2005). The Hueso Formation is exposed in View of the Badlands Wash (Vallecito Creek-Fish Creek Badlands), and the Ocotillo Conglomerate can be seen in the cliffs directly beneath Fonts Point in the Borrego Badlands.

3. Early Pleistocene to Present

Initiation of the San Jacinto and Elsinore fault zones marks the onset of complex dextral strike-slip faulting and north-south compression in the western Salton Trough, which continues today (Figure 5.10, 5.9C). Knowledge of this stage is based on studies by Sharp (1967), Wesnousky (1986), Hudnut and Sieh (1989), Hudnut et al. (1989), Rockwell et al. (1990), Brown et al. (1991), Petersen et al. (1991), Sanders and Magistrale (1997), Heitmann (2002), Dorsey (2002), Ryter (2002), Janecke et al. (2003, 2004), Kirby et al. (2004a, 2004b), Lutz and Dorsey (2003), Lutz et al. (2004), Lutz (2005), and others. In spite of its young age, the timing and nature of the transition from transtensional detachment faulting to transpressive strike-slip faulting is poorly understood. Strike-slip faulting may have overlapped in time with movement on the detachment fault system, and the San Jacinto and Elsinore faults could have started at similar or different times. Dorsey (2002) suggested that progradation (spreading into the basin and over the top of the Borrego Formation lacustrine deposits) of the Ocotillo Conglomerate in the Borrego Badlands may have resulted from initiation of the San Jacinto fault at approximately 1.5 Ma, a date consistent with some prior estimates (e.g. Bartholomew, 1970; Morton and Matti, 1993). Other studies have inferred an earlier, Pliocene age for the San Jacinto fault zone based on total fault offset and late Pleistocene slip rates (e.g. Rockwell et al., 1990).

The Fonts Point Sandstone is a thin Pleistocene fluvial deposit with a well developed calcic paleosol (carbonate cemented ancient soil) layer. This paleosol records the end of sediment accumulation in the Borrego Badlands during slip on the Coyote Creek fault (Ryter, 2002; Lutz et al., 2004; Lutz, 2005). Based on the age of deformed sediments in the Vallecito Creek area (Johnson et al., 1983), Ocotillo Badlands (Brown et al., 1991), San Felipe Hills (Kirby et al., 2004a, 2004b), and Borrego Badlands (Remeika and Beske-Diehl, 1996; Lutz, 2005), combined with known structural relationships in the region (e.g. Dibblee, 1984; Brown et al., 1991; Janecke et al., 2003, 2004; Kirby, 2005), it is likely that the San Jacinto and Elsinore fault systems were initiated in late Pliocene or early Pleistocene time.

Early to middle Pleistocene age conglomerate, sandstone and mudstone, exposed along the northwestern San Jacinto fault zone, was informally named "Bautista beds" by Frick (1921) and later mapped and studied by Sharp (1967) and Dorsey (2002). Sharp (1967) expanded the name "Bautista beds" to include Pleistocene sedimentary rocks exposed around Clark Lake and the northern Borrego Badlands, but these deposits had already been named "Ocotillo Conglomerate" by Dibblee (1954). Recent study by Dorsey and Roering (in press) shows that the Bautista beds were deposited by west- to northwest flowing streams on the high west flank of the Peninsular Ranges during an early phase of slip in the San Jacinto fault zone. These low-gradient streams were later captured by headward erosion in steep streams flowing southeast along the modern fault zone. The Ocotillo Conglomerate in the Borrego Badlands ("Ocotillo Formation" of Remeika and Beske-Dehl, 1998; Lutz, 2005) was deposited in a low-lying basin (depocenter) at the western margin of the Salton Trough, in a physiographic setting quite different than that of the Bautista beds.

The modern phase of active faulting and seismicity has created a rugged landscape characterized by northwest-trending ridges and fault-controlled features such as Coyote Mountain, Clark Valley, and Lute Ridge (Figure 5.10). Active faults and related uplift have produced young landforms in areas such as the Borrego Badlands, Superstition Mountain, and Superstition Hills, causing older basin deposits to be eroded and reworked into young terrace deposits and modern washes (e.g. Dibblee, 1954, 1984; Ryter, 2002). The Salton Sea is a large topographic depression that exists because of ongoing oblique extension and subsidence within a releasing step-over between the Imperial and San Andreas faults, which has produced an oblique spreading center (the Brawley seismic zone) (Figure 5.1; Elders et al., 1972; Fuis et al., 1982; Fuis and Kohler, 1984; Elders and Sass, 1988). This region has repeatedly dried out and filled with waters of ancient Lake Cahuilla, a Pleistocene to Holocene lake that previously lapped against the flanks of the San Felipe Hills and Santa Rosa Mountains (Waters, 1983). These lake-level highstands created distinctive calcareous algae-derived tufa deposits that are encrusted on granitic bedrock northwest of Salton City and in the Fish Creek Mountains along the U.S. Gypsum mine railroad. Lake Cahuilla represents the most recent expression of a large ephemeral lake system that was repeatedly flooded and dried out during deposition of the Pleistocene Brawley Formation (Kirby et al., 2004a, 2004b; Kirby, 2005), but with a more restricted distribution that reflects active faulting controls on the modern depocenter.

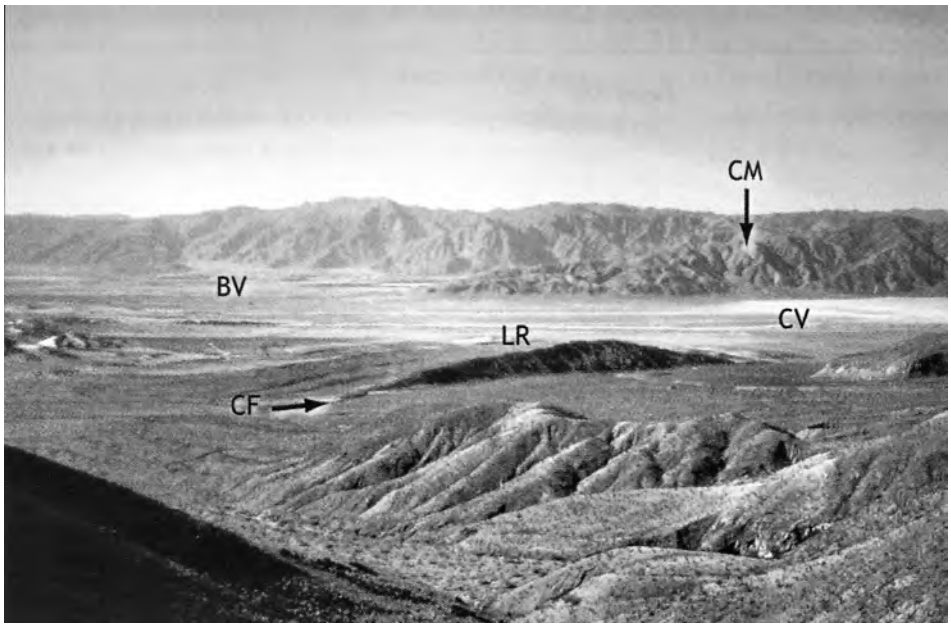

Figure 5.10 Geomorphology Along the San Jacinto Fault Zone.. View looking west across Coyote Mountain (CM), Clark Valley (CV), Borrego Valley (BV), and Lute Ridge (LR). Lute Ridge is a deposit of Pleistocene coarse alluvial gravels that have been displaced and translated by right-lateral slip on the Clark fault (CF). *(Photograph by Rebecca Dorsey)*

Conclusions

The above summary provides a brief overview of the tectonic, basinal, and sedimentary history of the western Salton Trough region. We have seen that Anza-Borrego Desert State Park lies within an active plate-boundary zone – the San Andreas fault system – which has been absorbing relative movement of the Pacific and North American plates since about 30 Ma. During Pliocene to early Pleistocene time, a large sedimentary basin associated with slip on a regional detachment fault system accumulated a thick section of marine and nonmarine sediments, recording a wide range of environments that supported the evolution and preservation of ancient plants and animals. Climate also appears to have changed during this time, shifting from a wetter and cooler climate in late Miocene time to the hyper-arid desert setting of today. The modern phase of strike-slip faulting has resulted in uplift and erosion of older sediments, creating a rich natural archive ideal for studying ancient life forms and the environments in which they lived.

References

Abbott, W.O., 1969, Salton Basin, a model for Pacific rim diastrophism. Geological Society of America Special Paper 121, p.1.

Atwater, T., 1970, Implications of plate tectonics for the Cenozoic tectonic evolution of western North America. Geological Society of America Bulletin, v. 81, p. 3513-3536.

Atwater, T., and Stock, J., 1998, Pacific-North America plate tectonics of the Neogene southwestern United States - An update. International Geology Review, v. 40, p. 375-402.

Axen, G. J., 1995, Extensional segmentation of the main Gulf escarpment, Mexico and United States. Geology, v. 23, p. 515-518.

Axen, G. J., and Fletcher, J. M., 1998, Late Miocene-Pleistocene extensional faulting, northern Gulf of California, Mexico and Salton Trough, California. International Geology Review, v. 40, p. 217-244.

Bartholomew, M.J., 1968, Geology of the northern portion of Seventeen Palms and Font's Point quadrangles, Imperial and San Diego Counties, California. Master of Science Thesis, University of Southern California, Los Angeles, 60 p.

Bartholomew, M.J., 1970, San Jacinto Fault Zone in the northern Imperial Valley. Geological Society of America Bulletin, v. 81, p. 3161-3166.

Brown, N.N., M.D. Fuller, and R.H. Sibson, 1991, Paleomagnetism of the Ocotillo Badlands, southern California, and implications for slip transfer through an antidilational fault jog. Earth and Planetary Science Letters, v. 102, p. 277-288.

Cox, B. F., Matti, J. C., King, T., and Morton, D.M., 2002, Neogene strata of southern Santa Rosa Mountains, California, and their significance for tectonic evolution of western Salton Trough. Geological Society of America Abstracts with Programs. v. 34, no. 6, p.124.

Dean, M.A., 1988, Genesis, mineralogy, and stratigraphy of the Neogene Fish Creek Gypsum, southwestern Salton Trough, California. Unpubl. M.S. Thesis, San Diego State University, CA, 150 p.

Dean, M. A., 1996, Neogene Fish Creek Gypsum and associated stratigraphy and paleontology, southwestern Salton Trough, California. In: Abbott, P. L., and Seymour, D. C., eds., Sturzstroms and Detachment Faults, Anza-Borrego Desert State Park, California. Santa Ana, California, South Coast Geological Society, p. 123-148.

DeMets, C., 1995, A reappraisal of seafloor spreading lineations in the Gulf of California: Implications for the transfer of Baja California to the Pacific plate and estimates of Pacific-North America motion. Geophysical Research Letters, v. 22, p. 3545-3548.

Dibblee, T. W., Jr., 1954, Geology of the Imperial Valley region, California, Geology of Southern California, California Division of Mines Bulletin 170, p. 21-28.

Dibblee, T.W., 1984, Stratigraphy and tectonics of the San Felipe Hills, Borrego Badlands, Superstition Hills, and vicinity. In: Rigsby, C. A. (ed.) The Imperial Basin - Tectonics, Sedimentation, and Thermal Aspects. Los Angeles, California, Pacific Section S.E.P.M., p. 31-44.

Dibblee, T. W., Jr., 1996a, Stratigraphy and tectonics of the San Felipe Hills, Borrego Badlands, Superstition Hills and vicinity. In Sturzstroms and Detachment Faults Anza-Borrego Desert State Park California, edited by P.L. Abbott and D.C. Seymour, South Coast Geological Society Annual Field Trip Guide Book Number 24, p. 45-58.

Dibblee, T. W., Jr., 1996b, Stratigraphy and tectonics of the Vallecito-Fish Creek Mountains, Vallecito Badlands, Coyote Mountains, and Yuha Desert, southwestern

Imperial Basin. In Sturzstroms and Detachment Faults Anza-Borrego Desert State Park California, edited by P.L. Abbott and D.C. Seymour, South Coast Geological Society Annual Field Trip Guide Book Number 24, p. 59-80.

Dickinson, W.R., 1996, Kinematics of transrotational tectonism in the California Transverse Ranges and its contribution to cumulative slip along the San Andreas transform fault system. Geological Society of America Special Paper 305, 46 p.

Dorsey, R.J., 2002, Stratigraphic record of Pleistocene initiation and slip on the Coyote Creek fault, lower Coyote Creek, southern California. In: Barth, A. (ed.) Contributions to Crustal Evolution of the Southwest United States: Boulder, Co. GSA Special Paper 365, p. 251-269.

Dorsey, R.J. and Janecke, S.U., 2002, Late Miocene to Pleistocene West Salton Detachment Fault System and Basin Evolution, Southern California: New Insights. Geological Society of America Abstracts with Programs, v. 34, No. 6, p. 248.

Downs, T., and White, J.A., 1968, A vertebrate faunal succession in superposed sediments from late Pliocene to middle Pleistocene in California. In Tertiary/ Quaternary Boundary, International Geological Congress 23, Prague v. 10, p. 41-47.

Dronyk, M.P., 1977, Stratigraphy, structure and seismic refraction survey of a portion of the San Felipe Hills, Imperial Valley, California. Master of Science Thesis, Department of Geological Sciences, University of California, Riverside 141 p.

Elders, W. A., Rex, R. W., Meidav, T., Robinson, P. T., and Biehler, S., 1972, Crustal Spreading in Southern California. Science v. 178, p. 15-24.

Elders, W. A., and Sass, J. H., 1988, The Salton Sea scientific drilling project. Journal of Geophysical Research, v. 93, p. 12,953-12,968.

Engel, A.E.J., and Schultejann, P.A., l984, Late Mesozoic and Cenozoic tectonic history of south central California. Tectonics v. 3, p. 659-675.

Feragen, E.S., 1986, Geology of the southeastern San Felipe Hills, Imperial Valley, California. [M.S. Thesis], San Diego State University, San Diego California, 144 p.

Friedmann, S.J., and Burbank, D.W., 1995, Rift basins and supradetachment basins: Intracontinental extensional end-members. Basin Research, v. 7, p. 109-127.

Frost, E.G., Suitt, S.C., and Fattahipour, M.J., 1996a, Emerging perspectives of the Salton Trough region with an emphasis on extensional faulting and its implications for later San Andreas deformation. In Sturzstroms and Detachment Faults Anza-Borrego Desert State Park California, edited by P.L. Abbott and D.C. Seymour, South Coast Geological Society Annual Field Trip Guide Book Number v. 24, p. 81-122.

Frost, E.G., Fattahipour, M.J., and Robinson, K.L., 1996b, Neogene detachment and strike-slip faulting in the Salton Trough region and their geometric and genetic interrelationships. In: Abbott, P.L. and Cooper, J.D., (eds.) Field Conference Guide 1996, Pacific Section AAPG, Guide Book 73, Pacific Section SEPM, Book 80, p. 263-276.

Fuis, G.S., W.D. Mooney, J.H. Healey, G.A. McMechan, and W.J. Lutter, 1982, Crustal structure of the Imperial Valley region, U. S. Geological Survey Professional Paper, 1254, 25-49.

Fuis, G. S., and Kohler, W. M., 1984, Crustal structure and tectonics of the Imperial Valley region, California. In: Rigsby, C. A., ed., The Imperial Basin - Tectonics, Sedimentation, and Thermal Aspects. Los Angeles, California, Pacific Section S. E. P. M., p. 1-13.

Gastil, R.G., Neuhaus, J., Cassidy, M., Smith, J.T., Ingle, J.C., Jr., Krummenacher, D., 1999, Geology and paleontology of southwestern Isla Tiburon, Sonora, Mexico. Revista Mexicana de Ciencias Geologicas, v. 16, no. 1, p. 1-34.

Girty, G. H., and Armitage, A., 1989, Composition of Holocene Colorado River sand; an example of mixed-provenance sand derived from multiple tectonic elements of the Cordilleran continental margin. Journal of Sedimentary Petrology v. 59, p. 597-604.

Gjerde, M.W. 1982. Petrology and geochemistry of the Alverson Formation, Imperial County, California. Master of Science Thesis, San Diego State University, California 85 p.

Guthrie, L.L., 1990, An internally standardized study of Cenozoic sand and sandstone compositions, Salton basin, southern California: Implications for rift basin evolution with emphasis on the Palm Spring and Imperial formations. Unpubl. M.S. Thesis, San Diego State University, CA, 180 p.

Haq, B.U., Hardenbol, J., Vail, P.R., 1987, Chronology

of fluctuating sea levels since the Triassic. Science, v. 235, p. 1156-1167.

Heitmann, E. A., 2002, Characteristics of the Structural Fabric Developed at the termination of a major wrench fault [M.S. thesis]: San Diego State University, 77 p.

Hoover, R.A, 1965, Areal geology and physical stratigraphy of a portion of the southern Santa Rosa Mountains, San Diego County, California. Master of Science Thesis, Department of Geological Sciences, University of California, Riverside 81 p.

Hudnut, K.W., K.E. Sieh, 1989, Behavior of the Superstition Hills Fault during the past 330 years. Seismological Society of America Bulletin v. 79, p. 304-329.

Hudnut, K. W., Seeber, L., Pacheco, J., 1989, Cross-fault triggering in the November 1987 Superstition Hills earthquakes sequence, Southern California. Geoph. Res. Letters, v. 16, p. 199-202.

Ingle, J.C. 1974. Paleobathymetric history of Neogene marine sediments, northern Gulf of California. In, Gastil, G., and Lillegraven, J. (eds.), Geology of Peninsular California. American Association of Petroleum Geologists, Pacific Section, Guidebook for Field Trips p. 121-138.

Janecke, S.U., Kirby, S.M., and Dorsey, R.J., 2003, New strand of the San Jacinto fault zone SW of the Salton Sea and a possible contractional step-over in the San Felipe Hills: A model to be tested. Geological Society of America Abstracts with Programs, v. 35, No. 4, p. 26.

Jefferson, G., and D. Peterson, 1998, Hydrothermal origin of the Fish Creek Gypsum, Imperial County, southern California. In: Geology and geothermal resources of the Imperial and Mexicali Valleys, edited by L. Lindsay, and W.G. Hample, pp. 40-51, San Diego Association of Geologists, San Diego, California.

Johnson, N. M., Officer, C. B., Opdyke, N. D., Woodard, G. D., Zeitler, P. K., and Lindsay, E. H., 1983, Rates of late Cenozoic tectonism in the Vallecito-Fish Creek basin, western Imperial Valley, California. Geology, v. 11, p. 664-667.

Kerr, D. R., 1982, Early Neogene continental sedimentation, western Salton Trough, California [M.S. thesis]. San Diego State University, San Diego, California, 138 p.

Kerr, D. R., 1984. Early Neogene continental sedimentation in the Vallecito and Fish Creek Mountains, western Salton Trough, California. Sedimentary Geology, v. 38, p. 217-246.

Kerr, D. R., and Kidwell, S. M., 1991, Late Cenozoic sedimentation and tectonics, western Salton Trough, California. In: Walawender, M. J., and Hanan, B. B., eds., Geological Excursions in Southern California and Mexico. San Diego, California, Department of Geological Sciences, San Diego State University, p. 397-416.

Lonsdale, P., 1989, Geology and tectonic history of the Gulf of California. In: Winterer, E. L., Hussong, D. M., and Decker, R. W., eds., The Eastern Pacific Ocean and Hawaii, Boulder, Colorado, Geological Society of America, p. 499-522.

Lough, C. F., 1993, Structural evolution of the Vallecitos Mountains, Colorado Desert and Salton Trough geology. San Diego, California, San Diego Association of Geologists, p. 91-109.

Lough, C. F., 1998, Detachment faulting around Borrego Valley. In: Geology and geothermal resources of the Imperial and Mexicali Valleys, edited by L. Lindsay, and W.G. Hample, pp. 40-51, San Diego Association of Geologists, San Diego, California.

Lough, C.F., and Stinson, A.L., 1991, Structural evolution of the Vallecito Mountains, southwest California. Geological Society of America Abstracts with Programs v. 23, no. 5, p. 246.

MacDougall, K.A., Poore, R.Z., Matti, J.C., 1999, Age and paleoenvironment of the Imperial Formation near San Gorgonio Pass, Southern California. Journal of Foraminiferal Research, v. 29, p. 4-25.

Matti, J.C., Cox, B.F., Morton, D.M., Sharp, R.V., and King. T., 2002, Fault-bounded Neogene sedimentary deposits in the Santa Rosa mountains, southern California: Crustal stretching or transpressional uplift? Geological Society of America Abstracts with Programs. v. 34, no. 6, p.124.

Merriam, R.H., and O.L. Bandy, 1965, Source of upper Cenozoic sediments in the Colorado delta region. Journal of Sedimentary Petrology v. 35, p. 911-916.

Morley, E.R. Jr., 1963, Geology of the Borrego Mountain quadrangle and the western portion of Shell Reef quadrangle, San Diego County, California. Master of Arts Thesis, University of Southern California, Los Angeles 138 p.

Morton, D. M., and Matti, J. C., 1993, Extension and

contraction within an evolving divergent strike-slip fault complex: the San Andreas and San Jacinto fault zones at their convergence in Southern California, in Powell, R. E., Weldon, R. J., and Matti, J. C., eds., The San Andreas fault system: displacement, palinspastic reconstruction, and geologic evolution: Geological Society of America Memoir, v. 178, p. 217-230.

Muffler, L.P.J., and B.R. Doe, 1968, Composition and mean age of detritus of the Colorado River delta in the Salton Trough, southeastern California. Journal of Sedimentary Petrology 38:384-399.

Opdyke, N.D., Lindsay, E.H., Johnson, N.M., and Downs, T., 1977, The paleomagnetism and magnetic polarity stratigraphy of the mammal-bearing section of the Anza-Borrego State Park, California, Quaternary Res., v. 7, p. 316-329.

Oskin, M.E.; Stock, J.M., and Martin-Barajas, A., 2001, Rapid localization of Pacific-North America plate motion in the Gulf of California. Geology, v. 29, p. 459-462.

Oskin, M., and Stock, J., 2003, Marine incursion synchronous with plate-boundary localization in the Gulf of California. Geology, v. 31, p. 23-26.

Pappajohn, S., 1980, Description of Neogene marine section at Split Mountain, easternmost San Diego County, California. Master of Science Thesis, San Diego State University, California 77 p.

Petersen, M. D., Seeber, L., Sykes, L. R., Nabelek, J. L., Armbruster, J. G., Paceco, J., Hudnut, K. W., 1991, Seismicity and fault interaction, southern San Jacinto fault zone and adjacent faults, Southern California; implications for seismic hazard. Tectonics, v. 10, p. 1187-1203.

Powell, R. E., Weldon, R. J., and Matti, J. C. (eds), 1993, The San Andreas fault system: Displacement, palinspastic reconstruction, and geologic evolution, Geological Society of America Memoir 178.

Quinn, H.A., and Cronin, T.M., 1984, Micropaleontology and depositional environments of the Imperial and Palm Spring formations, Imperial valley, California. In: Rigsby, C. A. (ed.) The Imperial Basin - Tectonics, Sedimentation, and Thermal Aspects. Los Angeles, California, Pacific Section S.E.P.M., p. 71-85.

Remeika, P., 1995, Basin tectonics, stratigraphy, and depositional environments of the western Salton Trough detachment: the 1995 San Diego Association of Geologist's Field Trip Guide to Anza-Borrego Desert State Park, California. In Paleontology and Geology of the Western Salton Trough Detachment, Anza-Borrego Desert State Park, California, edited by P. Remeika and A. Sturz, Field Trip Guidebook and Volume for the 1995 San Diego Association of Geologists Field Trip to Anza-Borrego Desert State Park, Volume 1:3-45.

Remeika, P., Fischbein, I.W. , and Fischbein, S.A., 1988. Lower Pliocene petrified wood from the Palm Spring Formation, Anza-Borrego Desert State Park, California. Review of Palaeobotany and Palynology 56:183-198.

Remeika, P., and Fleming R.F., 1995, Cretaceous palynoflora and Neogene angiosperm woods from Anza-Borrego Desert State Park, California: implications for Pliocene climate of the Colorado Plateau and age of the Grand Canyon. In Paleontology and Geology of the Western Salton Trough Detachment, Anza-Borrego Desert State Park, California, edited by P. Remeika and A. Sturz, Field Trip Guidebook and Volume for the 1995 San Diego Association of Geologists Field Trip to Anza-Borrego Desert State Park, Volume 1:64-81.

Remeika, P. and Beske-Diehl, S., 1996, Magnetostratigraphy of the western Borrego Badlands, Anza-Borrego Desert State Park, California: Implications for stratigraphic age control, in Abbott, P. L. and Seymour, D. C., eds., Sturzstroms and Detachment Faults, Anza-Borrego Desert State Park, California: South Coast Geological Society Annual Field Trip Guide Book, No. 24, p. 209-220.

Rightmer, D.A., and Abbott, P.L., 1996, The Pliocene Fish Creek sturzstrom, Anza-Borrego Desert State Park, southern California. In Sturzstroms and Detachment Faults Anza-Borrego Desert State Park California, edited by P.L. Abbott and D.C. Seymour, South Coast Geological Society Annual Field Trip Guide Book Number 24, p. 165-184.

Rockwell, T., Loughman, C., Merifield, P., 1990, Late Quaternary rate of slip along the San Jacinto fault zone near Anza, Southern California. Jour. Geoph. Res. B, v. 95, n. 6, p. 8593-8605.

Ruisaard, C.I. 1979. Stratigraphy of the Miocene Alverson Formation, Imperial County, California. Master of Science Thesis, San Diego State University, California 125 p.

Sanders, C. O., 1993, Interaction of the San Jacinto and San Andreas fault zones, Southern California; triggered earthquake migration and coupled recurrence intervals.

Science, v. 260, p. 973-976.

Sanders, C., and Magistrale, H., 1997, Segmentation of the northern San Jacinto fault zone, Southern California: Journal of Geophysical Research, v. 102, p. 27,453-27,467.

Schultejann, P. A., 1984, The Yaqui Ridge antiform and detachment fault: Mid-Cenozoic extensional terrane west of the San Andreas fault. Tectonics, v. 3, p. 677-691.

Sharp, R. V., 1967, San Jacinto fault zone in the Peninsular Ranges of southern California. Geological Society of America Bulletin, v. 78, p. 705-730.

Shaller, P.J., and A.S. Shaller, 1996, Review of proposed mechanisms for sturzstroms (long-runout landslides). In Sturzstroms and Detachment Faults Anza-Borrego Desert State Park California, edited by P.L. Abbott and D.C. Seymour, South Coast Geological Society Annual Field Trip Guide Book Number 24:185-202.

Sharp, R. V., 1982, Tectonic setting of the Imperial Valley region. In: The Imperial Valley, California, Earthquake of October 15, 1979. U. S. G.S. Professional Paper, P 1254, p. 5-14.

Stinson, A.L., 1990, Structural deformation within the Pinyon Mountains, San Diego County, California. Master of Science Thesis, San Diego State University, California, 133 p.

Stinson, A. L., and Gastil, R. G., 1996, Mid- to Late-Tertiary detachment faulting in the Pinyon Mountains, San Diego County, California: A setting for long-runout landslides in the Split Mountain gorge area. In: Abbott, P. L., and Seymour, D. C., eds., Sturzstroms and Detachment Faults, Anza-Borrego Desert State Park, California, Santa Ana, California, South Coast Geological Society, p. 221-244.

Stock, J. M., and Hodges, K. V., 1989, Pre-Pliocene extension around the Gulf of California and the transfer of Baja California to the Pacific plate. Tectonics, v. 8, p. 99-115.

Stump. T.E., 1972, Stratigraphy and paleoecology of the Imperial Formation in the western Colorado Desert. Master of Science Thesis, San Diego State University, California 132 p.

Tarbet, L.A., and W.H. Holman, 1944, Stratigraphy and micropaleontology of the west side of Imperial Valley. American Association of Petroleum Geologists Bulletin v. 28, p. 1781-1782.

Wells, D.L., 1987, Geology of the eastern San Felipe Hills, Imperial Valley, California: implications for wrench faulting in the southern San Jacinto fault zone [M.S. thesis]: San Diego, California, San Diego State University, 140 p.

Wernicke, B., 1985, Uniform-sense normal simple shear of the continental lithosphere. Canadian Journal of Earth Science, v. 22, p. 108-125.

Wesnousky, S. G., 1986, Earthquakes, Quaternary faults, and seismic hazard in California. Journal of Geophysical Research, v. 91, p. 12,587-12,631.

Winker, C.D., 1987, Neogene stratigraphy of the Fish Creek - Vallecito section, southern California: implications for early history of the northern Gulf of California and Colorado delta. Unpubl. Ph.D. dissertation, University of Arizona, Tucson, 494 p.

Winker, C. D., and Kidwell, S. M., 1986, Paleocurrent evidence for lateral displacement of the Colorado River delta by the San Andreas fault system, southeastern California. Geology, v. 14, p. 788-791.

Winker, C. D., and Kidwell, S. M., 1996, Stratigraphy of a marine rift basin: Neogene of the western Salton Trough, California. In: Abbott, P. L., and Cooper, J. D., eds., Field conference guidebook and volume for the annual convention, San Diego, California, May, 1996, Bakersfield, California, Pacific Section, American Association of Petroleum Geologist, p. 295-336.

Winker, C. D., and Kidwell, S. M., 2002, Stratigraphic evidence for ages of different extensional styles in the Salton Trough, southern California. Geological Society of America Abstracts with Programs, v. 34, No. 6, p. 83-84.

Winker, C. D., and Kidwell, S. M., 2003, Colorado River delta: 5 MYR-old tide-dominated, big-river delta in a tectonically evolving, oblique rift basin. Geological Society of America Abstracts with Programs, v. 35, No. 4, p. 28.

Woodard, G.D., 1974, Redefinition of Cenozoic stratigraphic column in Split Mountain Gorge, Imperial Valley, California. Am. Assoc. Petroleum Geologists Bulletin, v. 58, p. 521-539.

Woodring, W.P., 1931, Distribution and age of the marine Tertiary deposits of the Colorado Desert. Carnegie Institute of Washington Publication 418, p. 1-25.

Geomorphic Evaluation of a Late Pleistocene to Early Holocene River Meander in the Desert Cahuilla, Imperial County, California

Charles E. Houser, SCS Engineers
San Diego, California
chouser@scsengineers.com

Abstract

Geomorphic evaluation of a series of alluvial fan deposits along the southeast flank of the Santa Rosa Mountains provides insight into deposition and erosion cycles in the Desert Cahuilla. The Desert Cahuilla is approximately a 23 square mile area bounded by the Torrez-Martinez Indian Reservation on the north, Imperial-San Diego County Line on the west, Highway 22 on the south, and roughly by Highway 86 on the east. Geomorphic and paleoclimatological evidence suggests that major alluvial fan aggradational events were related to climate change during the Pleistocene. These changes were associated with glacial and interglacial transitions, and the effect of these transitions on the number and intensity of winter storm events.

The last major alluvial fan aggradation event in the Desert Cahuilla region ceased approximately 35 to 100 thousand years ago. During late-Pleistocene through mid-Holocene, alluvial fan development in the Desert Cahuilla was likely significantly influenced by climate change. A Pleistocene-Holocene climate transition involved a change from wetter and cooler to drier and warmer conditions. Resulting decreased vegetative cover and stripping of hillslope colluvium led to increased stream runoff during individual rainfall events (stream power), generally lower sediment load, and incision of alluvial fans in this region. A stream meander in the northwest Desert Cahuilla represents not only incision of the fans and fan pediments due to the change in climate, but also a stream condition of relatively low velocity and gradient, allowing development of meandering streams. Later changes, possibly due to falling base level or otherwise steepening of the stream gradient, led to higher stream velocities and development of braided and parallel drainages, cutting off the meander.

Introduction

During late 2007, I received an e-mail with the subject line, "Need a Pilot!" With a current pilots license, I responded and subsequently, on September 23, 2007, flew Phil Farquharson, Lowell Lindsay, and Diana Lindsay over an area east of Borrego Springs known as the Desert Cahuilla (Figure 1). The purpose of the flight was to conduct geologic reconnaissance in the northeast corner of the Desert Cahuilla on a parcel owned by Anza-Borrego Foundation. We photographed the area, and began evaluating the Pleistocene alluvial fan surfaces in the area.

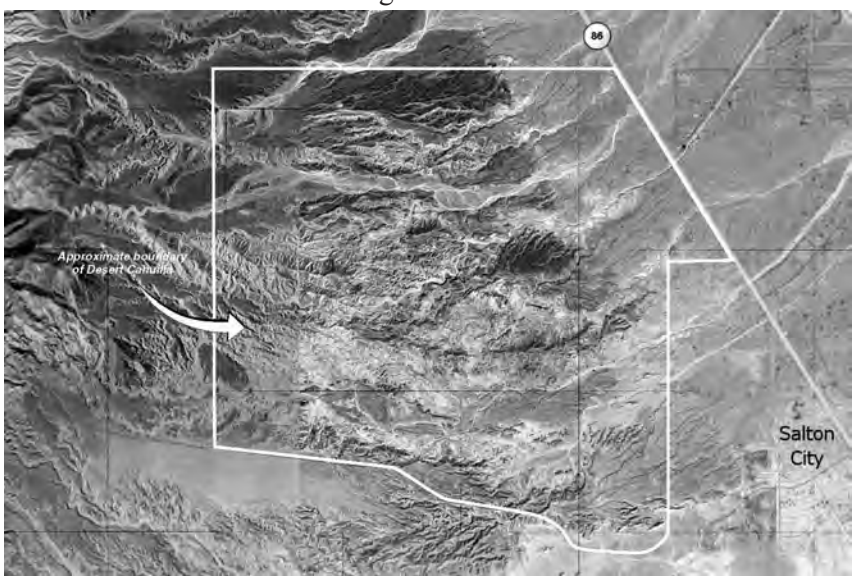

Figure 1. Desert Cahuilla Site Map.

Pleistocene alluvial fans present a fragile geologic resource that may yield information and insight into the Pleistocene and Holocene tectonic and climatic history of the region. Indeed, alluvial fans throughout the American southwest have been studied by many noted scientists. Alluvial fan surfaces provide data related to the processes involved in the formation of desert pavement and

desert varnish, calcic soils unique to arid regions like the southwestern United States, and geomorphic structures and formations shaped by time and sometimes by subtle (and occasionally, not so subtle) tectonic forces.

Between late 2007 and early 2008, I made several flights to observe the Desert Cahuilla and further evaluate these sensitive alluvial fan surfaces. On one such flight, from an altitude of approximately 4,000 feet over the northwestern corner of the Desert Cahuilla, I observed what appeared to be a quarry, an easily visible topographic feature roughly circular in shape. Upon descending for a closer look, the "quarry" turned out to be a "U"-shaped meander incised into an alluvial fan pediment along the south side of a relatively large wash. We photographed the feature (Figure 2) and continued the flight. Upon further reflection, I became convinced that this old dry river meander warranted some investigation into what it might add to the story of the geological history of the Anza-Borrego Desert Region.

Geologic Setting

The Desert Cahuilla encompasses approximately 23 square miles bounded by the Torrez-Martinez Indian Reservation on the north, Imperial-San Diego County Line on the west, Highway 22 on the south, and roughly by Highway 86 on the east (Figure 1). The project area is dominated, particularly in the northern half, by alluvial fan surfaces formed on pediments composed of Tertiary-aged sedimentary rocks along the western boundary of the Salton Trough. Dibblee (1953) mapped the units underlying the area as primarily Tertiary Palm Spring Formation with Tertiary Borrego Formation along the eastern portion of the Desert Cahuilla. Dibblee (1953) described the Palm Spring Formation as terrestrial sandstones and red clays, and the Borrego Formation as the lacustrine facies of the Palm Spring Formation composed of light gray clay and sand. Rogers (1965) mapped the area to include undivided Pliocene nonmarine sediments, Tertiary lake deposits, Quaternary nonmarine terrace deposits, and Quaternary alluvium. Morton (1966) mapped Tertiary Palm Spring Formation and Borrego Formation, along with alluvium and older alluvium, both of Quaternary-age. The Palm Spring Formation was identified by Morton as consisting of interbedded nonmarine, light gray, arkosic sandstone and reddish clay, with Borrego Formation consisting of nonmarine gray clay and interbedded sandstone of lacustrine origin.

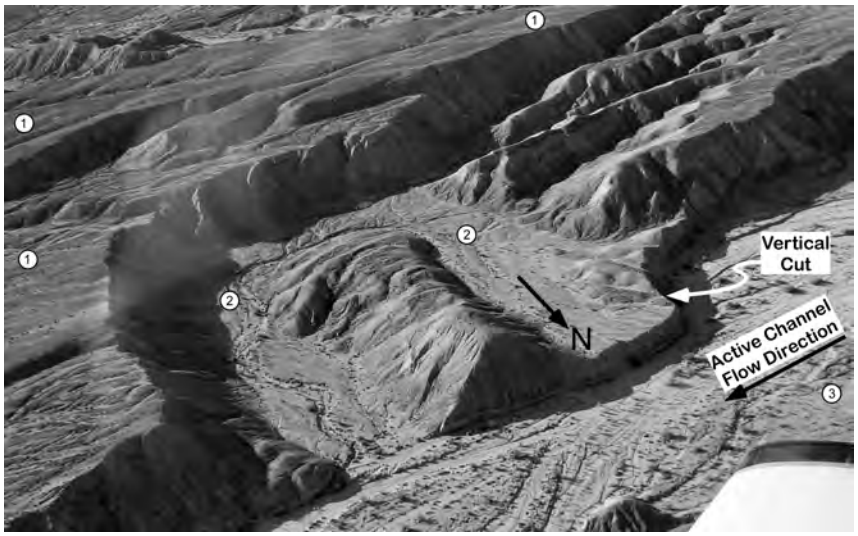

Figure 2. The "Meander." (1) Late Pleistocene Alluvial Fan Surfaces (35-100 thousand years), (2) Latest Pleistocene to middle-Holocene Alluvial Surfaces, (3) Active Channel.

According to Dorsey (2006 and this volume), the stratigraphy of the Anza-Borrego Desert Region includes the Miocene-Pliocene Imperial Group overlain by Pliocene-Pleistocene Palm Spring Group sediments. The Imperial Group rocks include the Deguynos Formation, described primarily as deltaic and tidal flats sediments. At the base of the Deguynos Formation within the Imperial Group is the Latrania Formation comprised of sandy turbidites and megabreccia. The Imperial Group rocks are marine sediments which may be partly correlative with the Bouse Formation of the lower Colorado River Valley (Dohrenwend, et. al., 1991).

The Palm Spring Group consists of delta plain and stream sediments of the Arroyo Diablo Formation overlain by lacustrine sediments of the Borrego Formation (Dorsey, 2006). Dohrenwend, et. al., (1991) described these units as two separate formations; the Palm Spring Formation comprised of fluvial and deltaic sand, silt, and clay, and the Borrego Formation comprised of fine-grained lacustrine deposits. In this paper, I am using the stratigraphic nomenclature as described by Dorsey (2006). Along the western margin of the basin, the Palm Spring Group also includes alluvial fan deposits of the Canebrake Conglomerate. Overlying the Palm Spring Group is the Pleistocene Ocotillo Conglomerate which grades into the lacustrine Brawley Formation toward the basin center. Figure 3, from Dorsey 2006, provides a summary of the general stratigraphy of the Anza-Borrego

Desert Region.

Tectonically, the study area is located between the San Jacinto Fault Zone to the west and San Andreas Fault Zone to the east. The nearest significant fault to the project area is the Clark Strand of the San Jacinto Fault Zone located approximately 3 or more miles to the southwest (Blisniuk, et. al., 2010). Although no significant faults are known to exist within the Desert Cahuilla, several lineaments suggestive of faults can be seen in the eastern portion in aerial photography. Additionally, numerous faults seen by offsets on the order of several inches to several feet are seen in Tertiary sedimentary rocks exposed below the fan pediment in the washes in the area. In many instances, offset beds can be seen constrained between beds showing no apparent offset above and below. This may be due to extensional deformation of the sediments with some extension occurring along bedding planes and not readily visible in exposures of the sediments. Figure 4 is a photograph of offset beds in one of several roughly east-west trending washes traversing the Desert Cahuilla. Unbroken sedimentary beds are seen above the offsets. In some locations, similar offsets appear as listric faults, flattening with depth into bedding plane faults exhibiting little or no offset of discrete beds.

Pleistocene-Quaternary History

The Desert Cahuilla is underlain by Miocene through Pleistocene sediments deposited in a shallow basin environment during mid-Tertiary through Quaternary extension of the region (Dohrenwend, et. al., 1991). These sediments are, in turn, overlain by alluvial fan deposits derived from the southeastern Santa Rosa Mountains to the west of the Desert Cahuilla. The fans have been deposited on a pediment dipping east toward the center of the Salton Trough. Using the discussions of Christensen and Purcell (1985), the alluvial fans in the northern portion of the Desert Cahuilla would be intermediate age fans based on the following criteria:

1. variable depth of incision on the order of 1 to 30 feet,
2. fan surfaces generally smooth and flat,
3. fan surfaces incised but well preserved,
4. desert varnish and desert pavement can be strongly developed.

The fan surfaces in the Desert Cahuilla are flat, dissected by several prominent east-west drainages, and have a strongly developed and relatively dark desert varnish. These characteristics place the age of the Desert Cahuilla alluvial fans at middle to late Pleistocene based on Dohrenwend, et. al. (1991). Desert varnish developed on the alluvial fans in the northern Desert Cahuilla have a similar or darker appearance than that developed on alluvial fans in the southern Santa Rosa Mountains approximately 5 to 8 miles west-southwest of the Desert Cahuilla. Blisniuk, et. al., (2010) assigned a date of 35 +/-7 thousand years to the fan they studied. This suggests ages for the fans in the Desert Cahuilla range from 35,000 to as old as 100,000 years.

Bull (2000) outlines three factors in alluvial fan dynamics: 1) tectonic activity, 2) climate change, and 3) internal adjustments in the alluvial fan system. Although the region of Anza-Borrego Desert State Park is quite tectonically active, the Desert Cahuilla shows relatively little, if any,

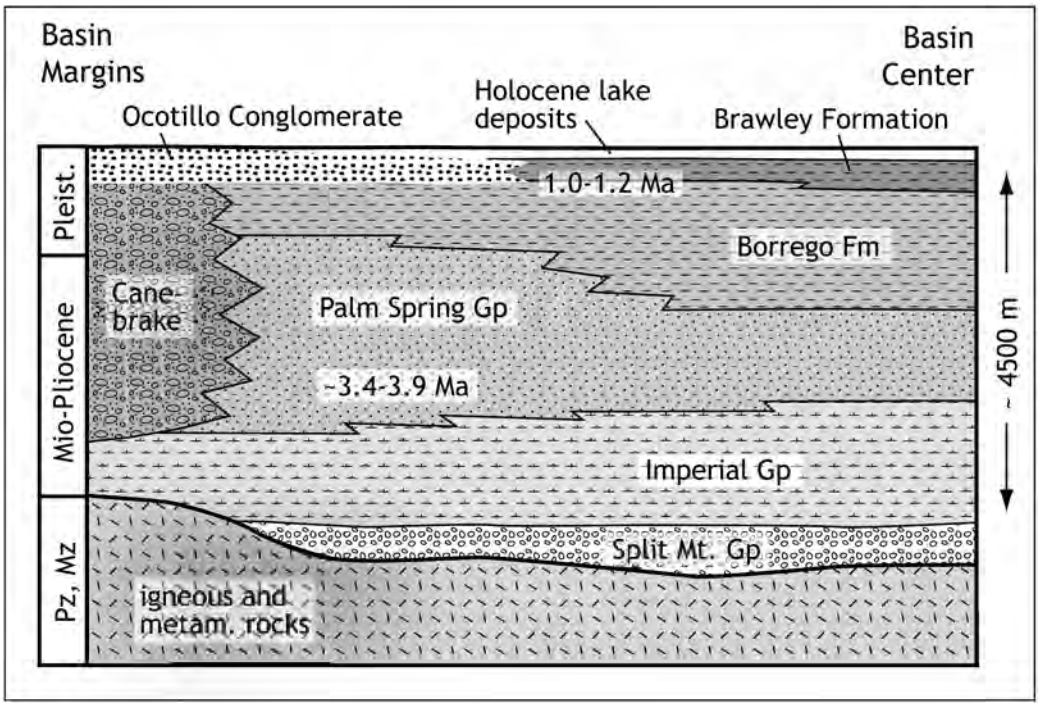

Figure 3. Stratigraphic Section. From Dorsey (2006).

notable seismicity. According to Dohrenwend, et. al. (1991), the climate south of 36ºN (roughly Las Vegas, Nevada) was cooler and wetter in the late Pleistocene, with a significant decrease in effective moisture occurring during the Pleistocene-Holocene climate transition. Bull (2000) places the Pleistocene-Holocene climate transition between 17,000 and 10,000 years ago. Coupled with changes in base level, climate changes likely were significant factors in controlling and shaping the development of late-Pleistocene and Holocene geomorphology, particularly related to alluvial fans. Harvey and Wells (2003) conclude that, in the absence of tectonic activity, climate change is the "over-riding control" of alluvial fan dynamics.

Figure 4. Offset Bedding in the Desert Cahuilla.

Stream Dynamics

Stream power (SP) is the power available to transport sediment load, and critical power (CP) is the power needed to transport sediment load (Bull, 1979). Bull (1979) defines the threshold of critical power as the point where SP/CP = 1. If this ratio is less than 1, then the stream power would be inadequate to transport the sediment load and deposition or aggradation occurs. If the stream power exceeds critical power during long time spans, vertical erosion of a V-shaped valley occurs. If a stream is close to the threshold of critical power, lateral erosion will tend to dominate. Bull (2000) describes the process by which climate change, such as occurred during the Pleistocene-Holocene climate transition, affects alluvial fan processes. As annual rainfall decreases and temperature increases, soil moisture is reduced and vegetation density decreases. This, in turn, exposes soil to erosion while increasing direct runoff. Valley floor aggradation occurs until removal of hillslope colluvium and increase in bedrock exposure causes sediment concentrations to decrease and the erosive potential of a given rainfall event increases. With the decreased sediment load, the stream power/critical power ratio increases and vertical erosion occurs. McDonald, et al. (2003) attribute channel incision and fanhead trenching to an apparent increase in summer monsoon activity in the early Holocene.

The "Meander"

The "U"-shaped meander described above is a striking feature for several reasons. This topographic feature leaves little doubt as to what geomorphic processes were involved in its evolution. It clearly represents a relatively tight, meandering turn in a fluvial drainage system. It also represents an environment in the drainage system where the flow velocity and gradient of the drainage was relatively low (SP/CP ~ 1) and thus was formed during a time when the stream was close to equilibrium. Streams with higher velocity and steeper gradients (SP/CP > 1) tend to form braided or parallel drainages. The meander is clearly incised through the surrounding alluvial fan surface down into the underlying pediment and fine-grained Tertiary sedimentary rocks. Finally, the patina developed in the bottom of the meander is obviously much lighter than the surrounding Pleistocene fan surfaces, indicating a younger age for the meander bottom. At the same time, the bottom of the meander has a noticeably darker patina than the adjacent active channel just to the north.

Several lobes of fan material within the meander can be seen in the south and southwest portions that have a patina as dark as can be seen in the meander. These observations of the meander provide a clear chronology of the order of the development of this feature in the alluvial fan system in this part of the Desert Cahuilla. The alluvial fans were deposited in the Pleistocene with aggradation ceasing between 35,000 and 100,000 years ago. As the climate became warmer and drier in the late Pleistocene transitioning into the early Holocene, runoff increased as vegetative cover decreased due to lower soil moisture. With removal of hillslope colluvium and exposure of underlying bedrock, sediment loads eventually decreased, and runoff streams began incising into the Pleistocene fan surfaces.

During incision, the position of the meander would likely have been medial to distal in the alluvial fan system, and average stream velocity and gradient would have been relatively low. Over time, possibly due to a change in base level or increase in the gradient of the drainage due to extension and lowering of the center of the Salton Trough east of the Desert Cahuilla, drainage in the location of the meander changed to braided and parallel, and the meander was cut off from the active channel by additional incision of the channel, leaving the vertical cut seen between the meander floor and active channel floor on the upstream (west) limb of the meander (Figure 2). If this occurred in latest Pleistocene to mid-Holocene time, adequate time would be available for development of the relatively weak desert varnish seen in the bottom of the meander (Dohrenwend, et. al., 1991, Helms et. al., 2003). Subsequent erosion in the meander, primarily from the southwest, incised the downstream (east) limb of the meander where it meets the active channel.

Summary

Major deposition and aggradation of Pleistocene alluvial fans in the northern portion of the Desert Cahuilla likely ended approximately 35 to 100 thousand years ago, based on fan geomorphology and well developed desert varnish on flat, smooth fan surfaces. Tectonic activity and climate change are considered two major factors in alluvial fan evolution and their relative magnitude, and thus their contribution to determining fan morphology in any particular region varies. The Desert Cahuilla, while in a region of active faulting, shows little evidence of notable tectonic activity. Therefore, climate change likely was the significant factor shaping alluvial fan geomorphology and fan processes, in particular during the Pleistocene-Holocene climate transition. Climate during this period changed from wetter to drier and warmer. Resulting increased runoff during monsoon-type storm events due to decreased vegetative soil cover, coupled with low sediment load once hillslope colluvium had been stripped, caused incision of the alluvial fans and fan pediments in the region. During latest Pleistocene to mid-Holocene in the northwest Desert Cahuilla, low stream velocity and gradient, possibly due to relatively high base level and a medial to distal position in the fan system, allowed development of a meandering drainage pattern during incision of the fans. Eventually, possibly due to falling base level or steepening of the stream gradient, drainage shifted from meandering to braided and parallel channels. One stream meander, preserved in the fan pediment, underwent soil development but was otherwise relatively undisturbed until observed in late 2007 by an unsuspecting geologist in a light aircraft at 4,000 feet over the Desert Cahuilla.

Acknowledgements

First, I'd like to thank the Anza-Borrego Foundation and Desert Protective Council for initiating the project that led to the study of the Desert Cahuilla. They facilitated the discovery and observation of the meander which is the subject of this paper. Diana Lindsay sent the e-mail initially requesting a pilot, and accompanied the author on several of the overflights of the Desert Cahuilla. Lowell Lindsay, Phil Farquharson, Mike Hart, and Monte Murbach also accompanied the author on various flights and trips to the Anza-Borrego Region, and engaged in much of the initial discussion of the meander.

Miles Kenney accompanied the author on a flight over the Desert Cahuilla and noted the rarity of the abandoned meander in an arid alluvial fan environment. Miles also assisted the author in understanding alluvial fan processes, stream processes, and Anza-Borrego Desert Region stratigraphy, and provided much "reading" material. The papers Miles provided were of immeasurable value in assisting the author to develop this paper. Tom Rockwell also provided discussion and papers aiding the author in this paper. Miles and Tom both reviewed the initial manuscript and provided valuable input.

Finally I'd like to thank my wife, Cindy, for her patience whenever I become involved in a time-consuming and sometimes frustrating project like this one.

References

Blisniuk, K., et.al., 2010, *Late Quaternary slip rate gradient defined using high-resolution topography and ^{10}Be dating of offset landforms on the southern San Jacinto Fault zone, California*, Journal of Geophysical Research, Vol. 115.

Bull, W.B., 1979, *Threshold of critical power in streams*, Geological Society of America Bulletin, Part I, Vol. 90, p. 453-464, May 1979.

Bull, W.B., 2000, *Correlation of Fluvial Aggradation Events to Times of Global Climate Change*, in Quaternary Geochronology: Methods and Applications, American Geophysical Union.

Christenson, G.E, and Purcell, C., 1985, *Correlation and age of Quaternary alluvial-fan sequences, Basin and Range province, southwestern United States*, Geological Society of America, Special Paper 203.

Diblee, T.W., 1953, *Generalized Geologic Map of Imperial Valley Region, California*, plate 2 of Chapter II, *Geology of Southern California*, California Division of Mines Bulletin 170.

Dohrenwend, J.C., Bull, W.B., McFadden, L.D., Smith, G.I., Smith, R.S.U., Wells, S.G., 1991, *Quaternary Geology of the Basin and Range Province of California*, in *Geology of North America, Vol. K-2, Quaternary Nonglacial Geology: Conterminous U.S.*, Geological Society of America.

Dorsey, R., 2006, *Stratigraphy, Tectonics, and Basin Evolution in the Anza-Borrego Desert Region*, in *Fossil Treasures of the Anza-Borrego Desert*, J.T. Jefferson and L. Lindsay, eds., Sunbelt Publications.

Harvey, A.M. and Wells, S.G., 2003, *Late Quaternary variations in alluvial fan sedimentologic and geomorphic processes, Soda Lake basin, eastern Mojave Desert, California*, Geological Society of America, Special Paper 368.

Helms, J.G., McGill, S.F., and Rockwell, T.K., 2003, *Calibrated, late Quaternary age indices using clast rubification and soil development on alluvial fan surfaces in Pilot Knob Valley, Mojave Desert, southeastern California*, Quaternary Research 60, University of Washington.

McDonald, E.V., McFadden, L.D., and Wells, S.G., 2003, *Regional response of alluvial fans to the Pleistocene-Holocene climatic transition, Mojave Desert, California*, Geological Society of America Special Paper 368.

Morton, P.K., 1966, *Geologic Map of Imperial County, California*, in *Geology and Mineral Resources of Imperial County, California*, CDMG County Report 7, 1977.

Rogers, T.H., 1965, *Geologic Map of California, Santa Ana Sheet*, CDMG Regional Geologic Map Series.

The Crew on the First Reconnaisance Flight over the Desert Cahuilla, September 23, 2007. Left to right are Phil Farquharson, Diana Lindsay, Lowell Lindsay and the author/pilot.

Late Quaternary slip rate gradient defined using high-resolution topography and ^{10}Be dating of offset landforms on the southern San Jacinto Fault zone, California

Kimberly Blisniuk,[1] Thomas Rockwell,[2] Lewis A. Owen,[3] Michael Oskin,[1] Caitlin Lippincott,[2] Marc W. Caffee,[4] and Jason Dortch[3]

Received 2 February 2009; revised 17 November 2009; accepted 1 March 2010; published 3 August 2010.

[1] Recent studies suggest the San Jacinto fault zone may be the dominant structure accommodating PA-NA relative plate motion. However, because the late Quaternary slip history of the southern San Andreas fault system is insufficiently understood, it is difficult to evaluate the partitioning of deformation across the plate boundary and its evolution. Landforms displaced by the Clark fault of the southern San Jacinto fault zone were mapped using high-resolution airborne laser-swath topography and selected offset landforms were dated using cosmogenic ^{10}Be. Beheaded channels at Rockhouse Canyon, displaced by 500 ± 70 m and 220 ± 70 m, have been dated to 47 ± 8 ka and 28 ± 9 ka, respectively. Farther south, near the southern Santa Rosa Mountains, an alluvial deposit displaced by 51 ± 9 m has been dated to 35 ± 7 ka. From these sites, the slip rate of the Clark fault is determined to diminish southward from 8.9 ± 2.0 to 1.5 ± 0.4 mm/yr. This implies a slip-rate decrease along the Clark fault from Anza southeastward to its surface termination near the Salton Trough, where slip is transferred to the Coyote Creek fault, and additional deformation is compensated by folding and thrusting in the basin. These data suggest that since ~30 to 50 ka, the slip rate along the southern San Jacinto fault zone has been lower than, or equivalent to, the rate along the southernmost San Andreas fault. Accordingly, either the slip rate of the San Jacinto fault has substantially decreased since fault initiation, or fault slip began earlier than previously suggested.

Citation: Blisniuk, K., T. Rockwell, L. A. Owen, M. Oskin, C. Lippincott, M. W. Caffee, and J. Dortch (2010), Late Quaternary slip rate gradient defined using high-resolution topography and ^{10}Be dating of offset landforms on the southern San Jacinto Fault zone, California, *J. Geophys. Res.*, *115*, B08401, doi:10.1029/2009JB006346.

1. Introduction

[2] To the south of the Big Bend at approximately 34°5′N latitude in southern California, the San Andreas fault system consists of the southern San Andreas, San Jacinto, and Elsinore fault zones (Figure 1). The southern San Andreas and the San Jacinto fault zones are the two principal structures, together accommodating ~35 mm/yr, that is ~80%, of the Pacific-North America (PA-NA) relative plate motion in this region [*King and Savage*, 1983; *DeMets and Dixon*, 1999; *Bennett et al.*, 1996; *Fialko*, 2006]. Geodetically derived slip rate estimates are on the order of 10–20 mm/yr for both of these fault zones, but only 2–6 mm/yr for the Elsinore fault zone [*Johnson et al.*, 1994; *Bennett et al.*, 1996; *Meade and Hager*, 2005; *Becker et al.*, 2005; *Fay and Humphreys*, 2005].

[3] The San Jacinto fault zone (SJFZ) has historically been more seismically active than the southern San Andreas fault zone [*Thatcher et al.*, 1975; *Richards-Dinger and Shearer*, 2000], but its longer-term slip history is controversial. Although many previous studies across the fault zone have documented well-preserved offsets of Quaternary landforms [e.g., *Sharp*, 1967, 1981; *Rockwell et al.*, 1990], fault slip rates are often more poorly defined due to the inherent difficulties of dating Quaternary deposits. Moreover, the offsets that have been dated span time scales ranging from 10^3 to 10^6 years, complicating direct comparison of slip rates over comparable periods for the San Jacinto and the San Andreas fault zones [*Sharp*, 1981; *Weldon and Sieh*, 1985; *Morton and Matti*, 1993; *Harden and Matti*, 1989; *Rockwell et al.*, 1990]. Variation in published slip rates may be resolved by a kinematic model of codependent slip histories for these fault zones [e.g., *Sharp*, 1981; *Bennett et al.*, 2004]. Alternatively, along-strike gradients in slip rate could account for the variety of slip rates measured along these fault zones without need for temporal variation.

[1]Department of Geological Sciences, University of California, Davis, California, USA.
[2]Department of Geological Sciences, San Diego State University, San Diego, California, USA.
[3]Department of Geology, University of Cincinnati, Cincinnati, Ohio, USA.
[4]Department of Physics, Purdue University, West Lafayette, Indiana, USA.

0148-0227/10/2009JB006346

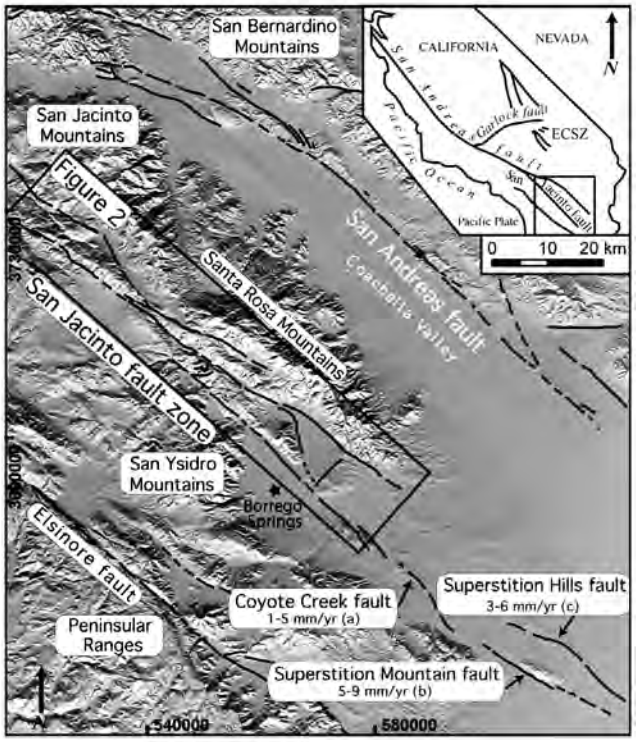

Figure 1. Location map showing the study area along the southern San Jacinto fault zone. Inset shows the index map for major faults in southern California. References are labeled as follows: a, *Clark* [1972], *Sharp* [1981], and *Pollard and Rockwell* [1995]; b, *Hudnut and Sieh* [1989]; and c, *Gurrola and Rockwell* [1996].

[4] Presently, there are no slip rate estimates from ^{10}Be exposure dating of offset landforms along the SJFZ, but the utility of this method has been demonstrated by recent work along the San Andreas fault [*Matmon et al.*, 2005; *van der Woerd et al.*, 2006]. Due to the excellent preservation of offset landforms in the arid Anza Borrego desert of southern California, the SJFZ provides an ideal location for surface exposure dating. Additionally, the availability of high resolution laser swath mapping data [*Bevis et al.*, 2005] makes the SJFZ an outstanding candidate for studying the distribution of strain within a nascent strike-slip fault system [*Oskin et al.*, 2007]. In this paper, we present the first late Quaternary slip rates from ^{10}Be dating of landforms displaced along the central and southern Clark fault segment of the SJFZ, at Rockhouse Canyon and the southern Santa Rosa Mountains, respectively (Figure 2). We integrate these newly determined slip rates with previously published slip rate estimates for the northern segment and with total bedrock displacement to make inferences on the long-term slip rate history of the SJFZ and its implication to earthquake recurrence models used in assessing seismic hazards in southern California.

2. Tectonic Setting

[5] The ~230 km long SJFZ extends from the Big Bend of the San Andreas fault southward with an average strike of ~N45°W (Figure 1). In the central and southern SJFZ, the two most active strands are the roughly parallel Coyote Creek and Clark fault, located ~10 km apart (Figure 2). Deformation is partitioned between these two strands displaying numerous active features that offset and fold Cretaceous tonalites, meta-tonalites, cataclasites, and Quaternary surfaces along the fault and adjacent to the fault (Figure 2) [*Sharp*, 1967]. Landforms along the Clark fault strand suggests that it is the dominant strand in accommodating slip of the southern SJFZ. The right-lateral strike-slip behavior of the Clark fault strand terminates southeast of the Santa Rosa Mountains into a zone of diffuse faulting and folding in the northwestern Imperial Valley [*Sharp*, 1981; *Kirby et al.*, 2007]. Quaternary features along the Clark fault strand that indicate youthful activity include folds, offset and deformed terraces, deflected channels, beheaded channels, offset surfaces, fault scarps, and linear ridges.

[6] Total bedrock displacement along the northern and central section of the SJFZ is ~22 to 24 km [*Sharp*, 1967] based on offset of the Thomas Mountain sill in contact with metamorphic rocks of the Bautista Complex (Figure 2)

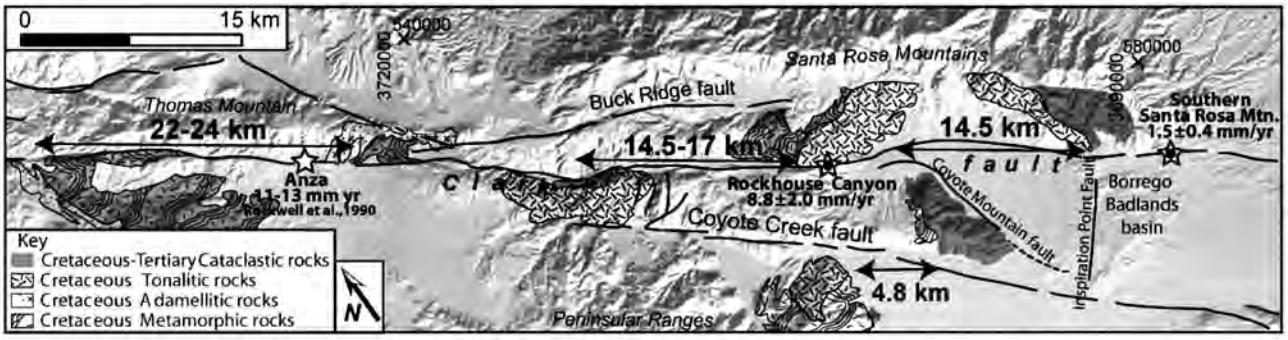

Figure 2. Geologic map of the southern San Jacinto fault zone. The black arrows show the amount of displacement of plutonic, metamorphic and cataclastic rocks mapped by *Sharp* [1967]. The white star indicates the location of a previous study along the Clark fault at Anza [*Rockwell et al.*, 1990]. The white stars with a black dot indicate the locations where we determined the slip rates reported in the present study. Total bedrock displacement at Rockhouse Canyon is based on reconstructing Cretaceous biotite-rich tonalite bodies as mapped by *Sharp* [1967] across the fault.

Table 1. Published Slip Rates for the San Jacinto Fault Zone

Time Frame	Reference	Slip Rate	Notes
Geodetic	*Bennett et al.* [1996]	9 ± 2 mm/yr	GPS & elastic block model of crustal deformation.
	Bennett et al. [2004]	8 ± 4 mm/yr	Co-dependent slip history model from published slip rates.
	Becker et al. [2005]	15 ± 1 mm/yr	GPS & stress-field orientations from earthquake focal mechanisms.
	Meade and Hager [2005]	12 ± 1 mm/yr	GPS & block model of crustal deformation.
	Fay and Humphreys [2005]	15 ± 1 mm/yr	GPS & block model of crustal deformation.
	Fialko [2006]	21 ± 1 mm/yr	InSAR & GPS.
	Lundgren et al. [2009]	12 ± 9 mm/yr (Clark strand) 12 ± 9 mm/yr (Coyote Creek strand)	InSAR, GPS & earthquake cycle.
Latest Holocene	*Sharp* [1981]	2 ± 1 mm/yr (Coyote Creek strand)	Offset of AD 1650 shoreline of Lake Cahuilla.
	Wesnousky et al. [1991]	>1.7–3.3 mm/yr	Offset channel margin and ^{14}C dating.
	Rockwell [2008]	12–15 mm/yr	5-event cluster of activity from AD 1025 to AD 1360.
Late Quaternary	*Rockwell et al.* [1990]	> 9 ± 2 mm/yr	Minimum offset along a shutter ridge since 9.5 ka from ^{14}C.
		11 $^{+9}/_{-5}$ mm/yr	Channel inset into Q3b (~14 ka soil age) terrace offset 150 ± 30 m
		12 $^{+9}/_{-5}$ mm/yr	Channel inset into Q4 (~17 ka soil age) terrace offset 210 ± 20 m
		13 $^{+10}/_{-6}$ mm/yr	Channel inset into Q5 (~50 ka soil age) terrace offset 620 ± 40 m.
	Kendrick et al. [2002]	~20 mm/yr	Dextral slip rate estimated from elastic model of uplift rates along restraining fault bend.
Mid-Quaternary	*Sharp* [1981]	10 ± 2 mm/yr	5.7 to 8.6 km offset of an alluvial fan deposit overlying the 760 ka Bishop Ash at Anza.
	Morton and Matti [1993]	16 mm/yr	Inception of faulting at 1.5 Ma and 23 ± 1 km displacement from *Sharp* [1967].
	Dorsey [2002]	10 ± 3 mm/yr (Coyote Creek strand)	Inception of faulting at 600 ka and 6 km approximate displacement.

[*Sharp*, 1967]. Farther south toward Rockhouse Canyon and the southern Santa Rosa Mountains, Cretaceous tonalite, metamorphic rocks, and the eastern Peninsular Ranges cataclastic and mylonitic zones are displaced by 14.5 to 17 km (Figure 2) [*Sharp*, 1967], and these same zones are displaced ~3.5 to 4.8 km by the adjacent Coyote Creek fault strand (Figure 2) [*Sharp*, 1967; *Janecke et al.*, 2008].

[7] Inception of the SJFZ as a major right-lateral strike slip fault zone has variably been inferred to have occurred as early as ~2.4 Ma based on a slip rate of 10 mm/yr [*Sharp*, 1981; *Rockwell et al.*, 1990] and a total offset of 24 km [*Sharp*, 1967], to 1.5 Ma [*Morton and Matti*, 1993], to as recently as ~1.1 Ma [*Lutz et al.*, 2006; *Kirby et al.*, 2007]. For the northern SJFZ, *Morton and Matti* [1993] suggest an initiation age of 1.5 Ma from sedimentologic changes in the upper San Timoteo Formation deposited adjacent to the SJFZ, dated by a rodent tooth fossil identified as *Microtus Californicus*. In the central SJFZ, using the best-estimated late Quaternary slip rate of 10–14 mm/yr [*Rockwell et al.*, 1990], one can infer an inception age of 1.7–2.4 Ma based on the 24 km of bedrock displacement, although this assumes the slip rate has been fairly constant since inception. For the southern SJFZ, a 1.05–1.07 Ma initiation age has been suggested based on dramatic changes in basin dynamics inferred from sedimentary rocks [*Lutz et al.*, 2006; *Kirby et al.*, 2007]. Based on a magnetic reversal located between two nonconformable stratigraphic units, the Ocotillo and Borrego Formations, the initial progradation of sediment beginning at ~1.1 Ma is interpreted as evidence for initiation of faults in the Salton Trough [*Lutz et al.*, 2006; *Kirby et al.*, 2007].

[8] Published mid-to-late Quaternary slip rate estimates along the SJFZ are also quite variable. Along the Clark fault strand at Anza, *Sharp* [1981] estimated a minimum mid-Quaternary to present slip rate of 8–12 mm/yr by reconstructing monolithologic alluvial fan deposits to their source (Figure 2 and Table 1). Southward, along the Coyote Creek fault strand, a mid-Quaternary to present rate of 10 ± 3 mm/yr has been suggested from clasts displaced ~6 km from their source [*Dorsey*, 2002]. However, the inferred offset by *Dorsey* [2002] 1) does not account for possible along-fault transport of these clasts, which would lower the amount of slip and 2) is greater than the total bedrock offsets of 4.8 km and 3.5 km inferred by *Sharp* [1967] and *Janecke et al.* [2008], respectively; it thus likely represents an upper limit for the mid-Quaternary slip rate of the Coyote Creek fault strand. For the late Quaternary, along the northern section of the SJFZ, in the San Timoteo badlands, a horizontal slip rate of at least 20 mm/yr was indirectly estimated from luminescence dating of uplifted terraces along a restraining bend in the fault; this estimate was obtained combining terrace uplift rates with an elastic-half-space model of deformation (Table 1) [*Kendrick et al.*, 2002]. In contrast to a fast slipping northern SJFZ, *Wesnousky et al.* [1991] used ^{14}C and an offset channel margin to determine a minimum latest Holocene rate of 1.7–3.3 mm/yr from what is considered the main strand of multiple fault strands. The only late Quaternary slip rates published on the central section of the SJFZ are from the Clark fault strand near Anza [*Rockwell et al.*, 1990]. Based on ^{14}C dating of an offset fan deposit *Rockwell et al.* [1990] obtained a slip rate of > 9 ± 2 mm/yr since 9.5 ka. Using soil development on offset alluvial deposits, they determined slip rates of 11 $^{+9}/_{-5}$ mm/yr since ~14 ka, 12 $^{+9}/_{-5}$ mm/yr since ~17 ka, and 13 $^{+10}/_{-6}$ mm/yr since ~48 ka. Additionally, a long paleoseismic record from Anza at Hog Lake shows that earthquakes recur frequently and are strongly clustered in time [*Rockwell et al.*, 2005]. Based on ^{14}C ages and paleo-

seismic investigations, *Rockwell et al.* [2005] and *Rockwell* [2008] estimate a late Holocene slip rate of 12–15 mm/yr by combining an average return period of ~230 years over the past 4000 years with surface displacement from the last two ruptures at Anza (3–4 m per event).

[9] Different geodetic models of strain accumulation across the southern SJFZ also imply a wide range of slip rate estimates. Block models of GPS data from the southern SJFZ indicate slip rates of 9–15 mm/yr (Table 1) [*Bennett et al.*, 1996; *Becker et al.*, 2005; *Meade and Hager*, 2005], which is consistent with a 14–15 mm/yr slip rate estimate inferred from elastic and viscoelastic models of crustal deformation (Table 1) [*Fay and Humphreys*, 2005]. In contrast, the results of a study by *Fialko* [2006], combining interferometric satellite synthethic aperture radar (InSAR) data with an elastic deep slipping SJFZ suggest a slip rate of 21 ± 1 mm/yr along the southern part of the fault zone, although this rate probably includes the strain accommodated by folding and NE-striking cross-faults. Similarly high rates are implied by more recent work of *Lundgren et al.* [2009], combining InSAR with geodetic data and models of the earthquake cycle to infer slip rates of 12 ± 9 mm/yr for each, the Coyote Creek and the Clark fault strands of the southern SJFZ.

[10] The ambiguity in the slip rate budget and initiation age for what might be the main plate boundary structure has implications for understanding the tectonic evolution of transform plate boundaries, and for kinematic fault models used to assess earthquake hazards in southern California. Kinematic models that attempt to explain temporal variability suggest a trade-off in slip rates between faults, implying that when one is fast the other is slow, thus the net rate should approach that of the plate boundary [*Sharp*, 1981; *Bennett et al.*, 2004]. Other kinematic fault models assume a constant slip rate along the entire length of a fault. However, mechanical models of faults show a systematic relationship between fault length and displacement with displacement decreasing toward the fault tip [*Cowie and Scholz*, 1992]. Thus, the range in slip rate estimates for the SJFZ could suggest that 1) the slip rate of the SJFZ may have decreased since its initiation, 2) faulting may have initiated earlier than 1.1 Ma [*Lutz et al.*, 2006; *Kirby et al.*, 2007], 3) a slip rate gradient may exist along the SJFZ, or 4) some previously published slip rate estimates may have been compromised by insufficiently constrained ages or displacements.

3. Methods

[11] Landforms along the Clark fault strand were mapped in the field using 1:5,000 and 1:10,000 scale contour maps constructed from high-resolution topography of the 'B4' Airborne Laser Swath Mapping (ALSM) experiment [*Bevis et al.*, 2005]. Following an initial reconnaissance survey, two sites (Rockhouse Canyon and the southern Santa Rosa Mountains) were chosen for a more detailed study, based on the following criteria: displaced landforms exhibited little post-depositional degradation, offsets were well defined, and suitable lithologies for ^{10}Be dating were present. At the northwestern site, in Rockhouse Canyon, the deflected modern channel (Channel 3) and two older beheaded channels (Channels 1 and 2) immediately SW of the fault were sampled for ^{10}Be dating. From each channel, we collected ~600 g samples from the top 1–3 cm of 7–9 quartz-bearing boulders. Samples collected from Channel 2 are from imbricated boulders lodged within relict bars that we interpret to have been deposited by debris flows. From Channel 1, due to the lack of preservation of imbricated deposits, five samples were collected from large, isolated boulders in the channel thalweg (samples Sjac 18–21 and 24) and four samples from boulders present on a relict alluvial terrace deposit ~1–2 m above the channel bottom (samples Sjac 14–17). To correct for inheritance, we collected samples from the top ~2 cm of boulder tops in the thalweg of Channel 3, with individual samples collected from boulders spaced ~100 m apart. At the southeastern site, in the southern Santa Rosa Mountains, we collected six ~500 g samples of quartz-bearing gravels and pebbles along a 2 m depth profile within an offset alluvial fan deposit. The depth profile was collected from a recently incised natural cliff exposure after removing the outer ~0.2 m of sediment.

[12] The 250 to 500 μm size fraction of the crushed and sieved samples was chemically leached in the cosmogenic dating laboratories at the University of Cincinnati and Stanford University by a minimum of four acid leaches: one aqua regia leach; two high concentration (2–5%) HF/HNO_3 leaches; and one or more low concentration (1%) HF/HNO_3 leaches. To remove acid-resistant and mafic minerals, heavy liquid separations with lithium heteropolytungstate (LST, density 2.7 g/cm^3) were used after the first 5% HF/HNO_3 leach. Low background ^{9}Be carrier (^{10}Be/^{9}Be ~1×10^{-15}) was added to the purified quartz, which was then dissolved in concentrated HF and fumed with perchloric acid. Fifteen to fifty grams of quartz was assumed for determining acid volumes used in the processing of chemical blanks. Next, the samples were passed through anion and cation exchange columns to separate the Be fractions. Ammonium hydroxide was added to the Be fractions to precipitate beryllium hydroxide gel. The beryllium hydroxide was oxidized by ignition in quartz crucibles at 750°C to produce beryllium oxide. Beryllium oxide was then mixed with niobium powder and loaded in steel targets for the measurement of the ^{10}Be/^{9}Be ratios by accelerator mass spectrometry at the CAMS at the Lawrence Livermore National Laboratory or at the PRIME Laboratory at Purdue University.

[13] All ^{10}Be model ages for sampled boulders were calculated using the CRONUS Age Calculator [*Balco et al.*, 2008; http://hess.ess.washington.edu/math/] (Table 2). No correction was made for geomagnetic field variations due to the ongoing debate regarding which, if any, correction factors are most appropriate. There also is considerable debate regarding the use of appropriate scaling models [see *Balco et al.*, 2008] and we chose to use the time independent model of *Lal* [1991] and *Stone* [2000] to calculate our ages. However, we note that the different scaling models may produce age differences of up to 11%. Uncertainties associated with the age of each sample are presented in Table 2, these uncertainties include the internal (measured AMS uncertainty based on Poisson counting statistics) [*Gosse and Phillips*, 2001] and the 1 sigma external uncertainty (which is the total uncertainty associated with the method [*Gosse and Phillips*, 2001; *Balco et al.*, 2008]).

[14] Landform exposure ages are affected by geologic factors, which include inheritance of ^{10}Be by prior exposure,

Sample Name	Thickness (cm)	Shielding Correction	Altitude (m)	Latitude (DD)	Longitude (DD)	^{10}Be Measured (10^6 atom g^{-1})	^{10}Be Age (ka) 0m/Myr	Error[b] ± (ka)	Error[c] ± (ka)	^{10}Be Age (ka) 2m/Myr	Error[c] ± (ka)	^{10}Be Age (ka) 5m/Myr	Error[c] ± (ka)
Channel 1													
Sjac-14	1	1.000	561	33.4052	−116.3708	0.4352 ± 0.0155	63.7	2.3	6.1	71.5	7.7	90.2	13.0
Sjac-15	3	1.000	561	33.4052	−116.3707	0.4734 ± 0.0163	70.6	2.5	6.7	80.3	8.8	105.4	16.3
Sjac-16	4	1.000	560	33.4051	−116.3707	0.3521 ± 0.0363	52.7	5.5	7.2	57.9	8.7	69.1	12.8
Sjac-17[d]	2	1.000	563	33.4054	−116.3708	0.5900 ± 0.0346	87.5	5.2	9.3	103.2	13.3	153.9	34.5
Sjac-18	2	1.000	564	33.4056	−116.3709	0.4002 ± 0.0137	58.9	2.0	5.6	65.5	6.9	80.4	11.0
Sjac-19	4	1.000	566	33.4058	−116.3709	0.3735 ± 0.0268	55.7	4.0	6.4	61.6	7.8	74.5	11.9
Sjac-20	2	1.000	572	33.4061	−116.3710	0.2727 ± 0.0406	39.7	6.0	6.9	42.6	8.0	48.0	10.3
Sjac-21	5	1.000	589	33.4066	−116.3712	0.3130 ± 0.0143	46.2	2.1	4.6	50.1	5.4	58.0	7.4
Sjac-24	5	1.000	614	33.4076	−116.3710	0.3639 ± 0.0106	52.8	1.6	4.9	58.0	5.9	69.1	8.7
Weighted mean of sample ages ± error[e]							54.4 ± 7.5			59.4 ± 8.9		69.1 ± 10.4	
Inheritance corrected sample ages ± error[e]							47.3 ± 7.7			52.3 ± 9.3		62.1 ± 13.0	
Channel 2													
Sjac-33	3	0.977	587	33.4061	−116.3657	0.3169 ± 0.0222	47.6	3.4	5.4	51.8	6.4	60.3	8.9
Sjac-34	3	0.979	577	33.4053	−116.3656	0.1930 ± 0.0048	29.0	0.7	2.6	30.5	2.9	33.1	3.5
Sjac-35	4	0.985	573	33.4046	−116.3644	0.2523 ± 0.0059	38.2	0.9	3.5	40.9	4.0	45.9	5.1
Sjac-36	3	0.988	567	33.4039	−116.3640	0.3433 ± 0.0078	51.8	1.2	4.7	56.8	5.7	67.5	8.3
Sjac-37	3	0.989	561	33.4033	−116.3635	0.2884 ± 0.0052	43.5	0.8	3.9	46.9	4.6	53.7	6.1
Sjac-38	5	0.975	545	33.4025	−116.3631	0.2867 ± 0.0067	45.3	1.1	4.1	49.0	4.8	56.5	6.6
Sjac-39	2	0.976	546	33.4017	−116.3630	0.1871 ± 0.0049	28.7	0.8	2.6	30.1	2.9	32.7	3.4
Sjac-40	2	0.977	527	33.4039	−116.3664	0.1435 ± 0.0039	22.3	0.6	2.0	23.1	2.2	24.6	2.5
Weighted mean of sample ages ± error[e]							32.3 ± 8.5			36.6 ± 9.5		41.1 ± 10.7	
Inheritance corrected sample ages ± error[e]							27.8 ± 8.8			29.3 ± 9.9		31.4 ± 11.9	
Channel 3													
Sjac-25	4	1.000	587	33.4067	−116.3681	0.0333 ± 0.0039	4.9	0.6	1.3				
Sjac-27	3	1.000	577	33.4063	−116.3680	0.0715 ± 0.0044	10.5	0.6	1.8				
Sjac-28	3	1.000	573	33.4060	−116.3679	0.0370 ± 0.0049	5.5	0.7	1.6				
Sjac-29	3	1.000	567	33.4055	−116.3675	0.0893 ± 0.0055	13.6	0.8	2.3				
Sjac-30	4	1.000	561	33.4055	−116.3675	0.0486 ± 0.0038	7.5	0.6	1.5				
Sjac-31	4	1.000	545	33.4046	−116.3666	0.0991 ± 0.0067	15.6	1.1	2.8				
Sjac-32	1	1.000	546	33.4048	−116.3667	0.0397 ± 0.0036	6.2	0.6	1.3				
Weighted mean of sample ages ± error[e]							7.3 ± 3.0						

Sample Name	Depth (cm)	Shielding Correction	Altitude (m)	Latitude (DD)	Longitude (DD)	^{10}Be Measured (10^6 atom g^{-1})	^{10}Be Age (ka) 0m/Myr
SJF-P1	0	1.000	314	33.2967	−116.1677	0.2437 ± 0.0104	
SJF-P2	20	1.000	314	33.2967	−116.1677	0.1967 ± 0.0080	
SJF-P3	50	1.000	314	33.2967	−116.1677	0.1456 ± 0.0030	
SJF-P4	83	1.000	314	33.2967	−116.1677	0.1272 ± 0.0029	
SJF-P5	136	1.000	314	33.2967	−116.1677	0.1006 ± 0.0020	
SJF-P6	175	1.000	314	33.2967	−116.1677	0.0667 ± 0.0001	
Model age ± error							34.5 ± 6.6

[a]The ^{10}Be model ages calculated using the CRONUS calculator at Rockhouse Canyon (see Figures 2, 3, and 6 for sample locations). Abbreviations: DD is decimal degrees.
[b]Internal error associated with AMS measurement.
[c]External error associated with ^{10}Be model exposure ages.
[d]Boulder samples that are not used in the calculation of the weighted mean age. See text for details.
[e]95% confidence interval of the 2-sigma external error associated with ^{10}Be model exposure ages.

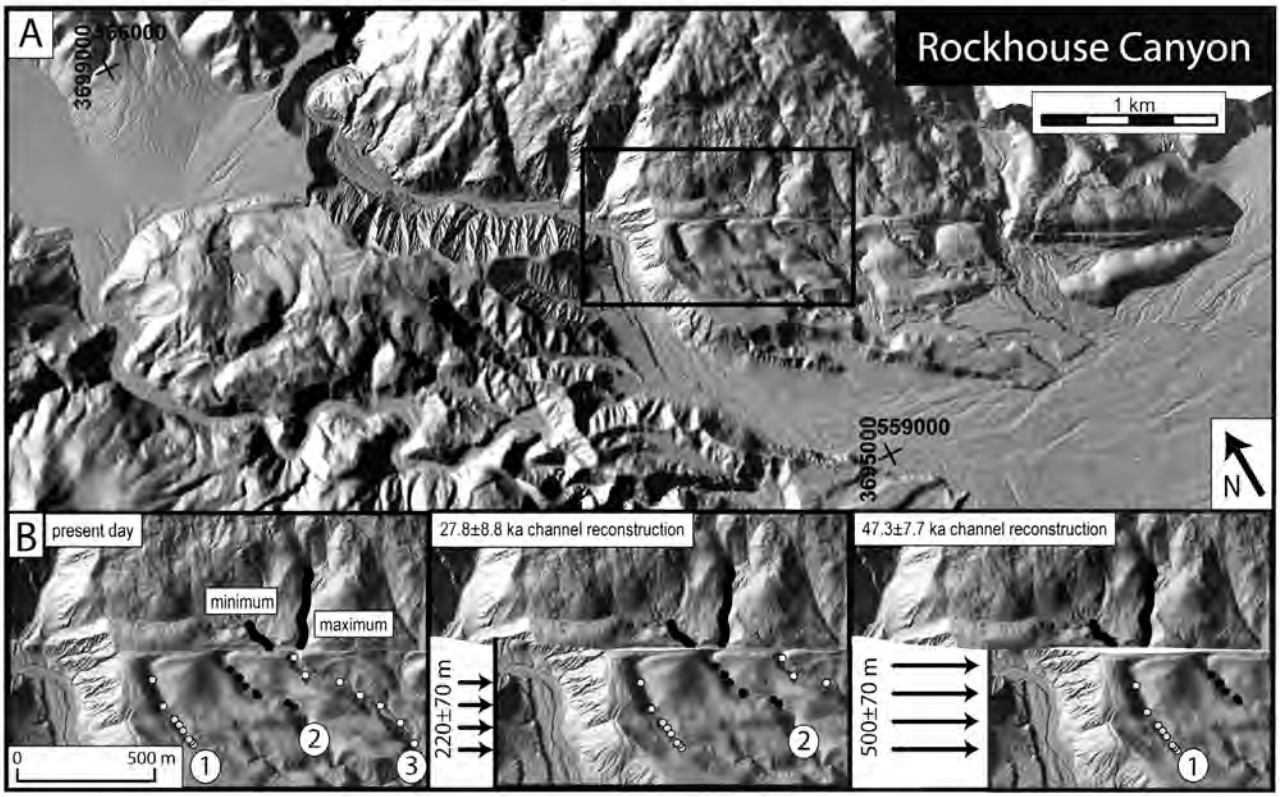

Figure 3. (a) ALSM image of the Rockhouse Canyon site. Frame shows the location of Figure 3b. (b) Location of beheaded and deflected channels at Rockhouse Canyon: (left) the present-day configuration of Channels 1, 2 and 3; (middle) the reconstruction for Channel 2; and (right) the reconstruction for Channel 1. The black solid lines indicate the maximum and minimum displacements from the source drainage(s) for offset channels. The dots in Figure 3b indicate the location of boulder samples collected for ^{10}Be exposure dating. See Figure 2 for location.

toppling and exhumation of boulders, and weathering of boulders and alluvial fan surfaces. To estimate inheritance of ^{10}Be from hillslope residence and transport we collected 7 samples from boulders in the active channel 3. Not accounting for such inheritance would result in incorrectly old ages and lower slip rates. We assume that the sampled boulders have been exposed at least since the time the channels were abandoned. Our field observations suggest little to no exhumation of boulders by winnowing of surrounding finer deposits. We also assume that streams from a source area northeast of the Clark fault strand transported all the boulders that were sampled and that none of the sampled boulders originated from more recent collapse of hillslopes adjacent to the sample sites. To explore the potential effects of boulder weathering, we also calculated ^{10}Be exposure ages that account for 2m/Myr and 5m/Myr of surface attrition. These rates of erosion, if present, would result in modestly decreased slip rates as compared to the case of no boulder surface erosion.

4. Results

4.1. Rockhouse Canyon

[15] The Rockhouse Canyon site is located along the western range front of the Santa Rosa Mountains at the northernmost end of Clark Valley in the Anza Borrego desert (Figure 2). At Rockhouse Canyon, strike-slip fault activity is mostly localized onto a single strand displaying channels in various stages of capture (Figure 3). Two channels (Channel 1 and Channel 2) are completely beheaded from their source and no longer transporting large boulders (Figure 3 and auxiliary material).[1] Contained within these channels are boulder bar deposits, fan deposits, and isolated boulders, which could only have originated from the present-day drainage areas located to the northeast of the fault (Figure 3). Realignment of Channel 1 and Channel 2 indicates displacement of 500 ± 70 m and 220 ± 70 m, respectively (Figure 3b). To realign the beheaded channels along the fault, we used contour maps derived from high-resolution topography to assess the maximum and minimum displacement from two drainage areas that could supply large boulders into the channel (Figure 3b). The midpoint between the maximum and minimum distance is then used for the offset and the uncertainties associated with the displacement are based on the maximum and minimum distance permitted to realign the channels to their source (Figure 3).

[1] Auxiliary materials are available in the HTML. doi:10.1029/2009JB006346.

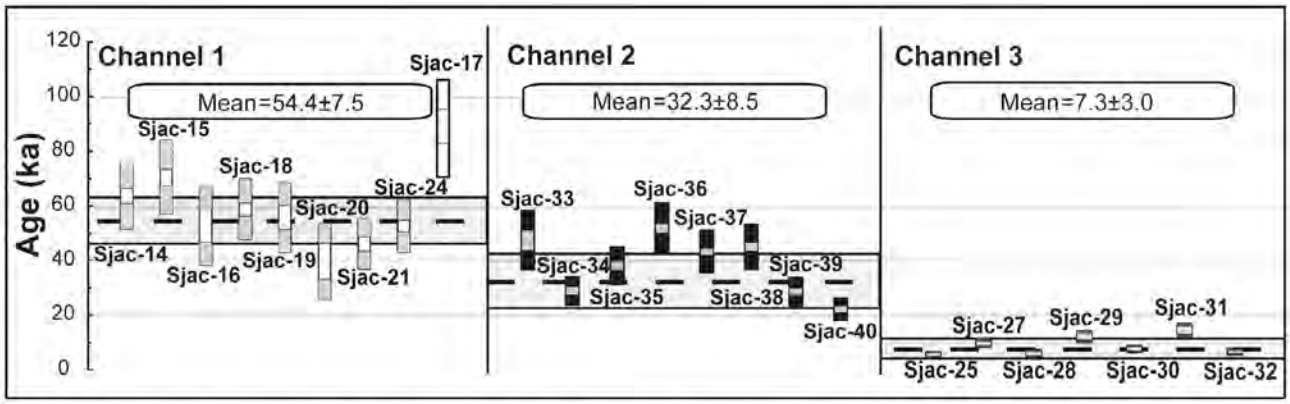

Figure 4. Chart showing the error-weighted mean age of Channel 1, Channel 2 and Channel 3. ^{10}Be surface exposure ages of boulders from Channel 1 and Channel 2 do not include inheritance from Channel 3. The gray and black vertical bars are ages of individual boulder samples used in calculating the age of each channel. The inset shaded box within each vertical bar is the ^{10}Be model age and associated internal uncertainty with the AMS measurement. The white vertical bar is an outlier that is outside the 95% confidence interval of the remaining 8 samples from Channel 1. Please see text and Table 2 for details.

[16] To define the ages of these displacements, we determined ^{10}Be exposure ages of 8 to 9 boulders in each of the beheaded channels, and of 7 boulders in the active channel; the resulting 24 sample ages are presented in Table 2 and Figure 4. The error-weighted mean of the individual boulder ages from the active channel, 7.3 ± 3.0 ka, was used to infer the inheritance of ^{10}Be produced during exposure and transport prior to boulder deposition in each channel. We note that this inheritance only defines prior exposure of ^{10}Be from the larger source area. The age of abandonment for each of the two beheaded channels is the error-weighted mean age of the individual boulder ages from the channel minus the 7.3 ± 3.0 ka inheritance age obtained from the active channel. This yields ages of 47 ± 8 ka for Channel 1, and 28 ± 9 ka for Channel 2 (age uncertainties given as the 95% confidence interval based on the 2-sigma external error associated with ^{10}Be model ages (Table 2)). The age of one sample from Channel 1 (Sjac-17) was discarded because it is outside the 95% confidence interval of the average calculated from the remaining 8 exposure ages determined for this channel (Table 2 and Figure 4). The clustering of modeled ^{10}Be ages from individual boulders in each channel, combined with the dichotomy of ages between channels, gives us confidence that the boulders were likely transported and deposited in discrete subsequent episodes by one or both of the potential source streams (Table 2 and Figures 3 and 4).

[17] Fitting a single slip rate through both channel offsets versus their age yields an average late Quaternary to present slip rate of 8.9 ± 2.0 mm/yr for the Clark fault strand at Rockhouse Canyon. This rate is the error-weighted linear least squares fit of both the displacement and age, with uncertainty calculated at the 95% confidence interval. Because minor erosion of the boulder surface is permissible from field observations, we also calculated ages assuming 2 m/Myr and 5 m/Myr of boulder surface erosion, yielding lower slip rates of 7.8 ± 1.8 mm/yr, and 6.1 ± 1.4 mm/yr, respectively. Differencing the raw mean boulder ages (with no erosion) and displacements of Channel 1 from Channel 2 yields a significantly faster slip rate of 14.4 ± 3.4 mm/yr over the time interval from ~30–50 ka, followed by a slower rate of 7.7 ± 3.6 since ~30 ka. These two slip rates from the same site could indicate temporal variation of the slip rate on the Clark fault strand over the latest Quaternary. However, at this time we cannot discriminate this apparent temporal variation from a constant slip rate with confidence.

4.2. Southern Santa Rosa Mountains

[18] The southern Santa Rosa Mountains site of the Clark fault strand is located at the mouth of Rattlesnake Canyon on the southwestern range front of the Santa Rosa Mountains. Just to the southeast of this locality, the dextral Clark fault strand bends to the south into a set of normal-fault (horsetail) splays (Figure 5). Alluvial fans emplaced across the Clark fault strand originate from the Santa Rosa Mountains plutonic and cataclastic zones, which are predominately comprised of tonalite, marble, and mylonitic gneiss [*Dibblee*, 1954; *Sharp*, 1967]. Using the nomenclature of *Bull* [1991] we map a Q2c alluvial fan surface that has been cut by dextral Clark fault slip. The alluvial fan surface at this site exhibits muted bar and swale microtopography, moderate desert pavement, and a slightly undulating surface morphology. Clasts on the surface display moderate to strong desert varnish development and strong rubification on their undersides. The Av soil horizon of the Q2c surface is ~1 cm thick and overlies a relic A horizon, that presumably formed before the Holocene, as the site is now in a hyper arid soil moisture regime. These observations imply that there has been minimal denudation or aggradation of the surface during the extremely arid local climate of the past 8–12 ka.

[19] The fan surface is cut by multiple fault strands, but only one of these shows significant dextral offset. The displacement along this strand is estimated as 51 ± 9 m (Figure 5 and auxiliary material), using a beheaded channel (Channel 1) and two deflected channels (Channels 2 and 3) as piercing lines (Figure 5). To reconstruct this offset, we

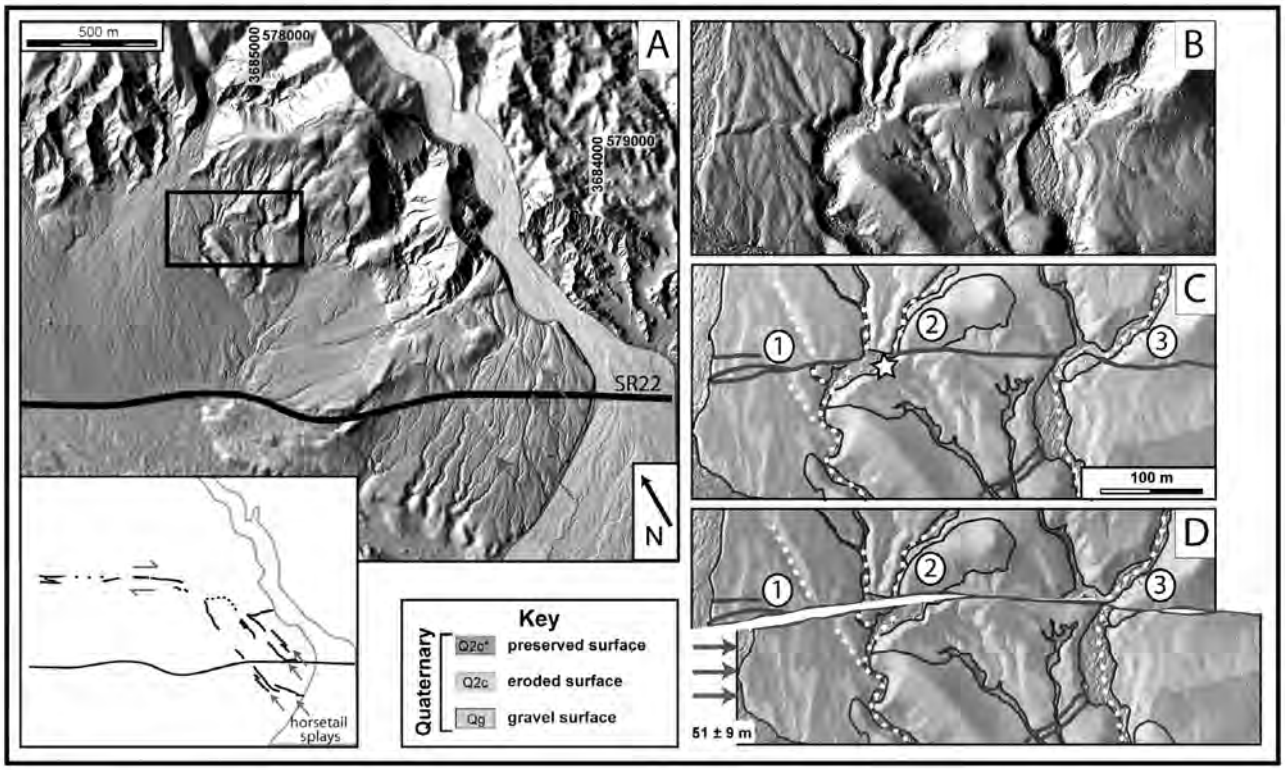

Figure 5. ALSM image of the southern Santa Rosa Mountains site. (a) The present-day configuration of 3 channels incised into the Q2c surface. Inset is a fault map showing traces of the Clark fault in Figure 5a. (b and c) The present-day configuration of beheaded and deflected channels incised into the Q2c fan deposit. The white star in Figure 5c is the location of the 2 m deep depth profile sampled for ^{10}Be surface exposure age dating. (d) The reconstruction of a beheaded channel (Channel 1) and two deflected (Channels 2 and 3) for 35 ± 7 kyr ago. Please see text and Table 2 for details.

used contour maps derived from high-resolution topography and field measurements to assess the maximum and minimum distance that would permit all three channels to align. We note that Channel 3 has two potential upstream piercing lines northeast of the fault (Figure 5). However, we choose to realign Channel 3 with the more eastern drainage area and not the midpoint of the two northeast sources because doing so would cause mis-alignment of Channels 2 and 3. The uncertainty associated with the offset is based on the maximum and minimum distance permitted to realign all three channels. This distance is minimized by lining up the thalweg and wall (9 m width) of beheaded Channel 1 on both sides of the fault (Figure 5).

[20] To determine the slip rate, we dated the fan surface using ^{10}Be concentrations from a 2 m-deep vertical stream-cut exposure. The age was determined from the slope of a linear least squares fit of ^{10}Be concentration versus exp(-z/z*), where z is depth and z* is the depth where ^{10}Be production declines by 1/e (Figure 6). The intercept of this line with zero (i.e., infinite depth) yields an estimate of the ^{10}Be inheritance of the sediment. This implies a ^{10}Be depth profile age of 35 ± 7 ka (95% confidence) for the displaced fan surface, yielding a slip rate of 1.5 ± 0.4 mm/yr (Table 2 and Figure 6). The uncertainty associated with the slip rate is the root mean squared error for both age and offset. Although a robust method to deduce the ^{10}Be surface concentration [*Anderson et al.*, 1996; *Repka et al.*, 1997], ages determined from the depth profile may be subject to erosion that will reduce the apparent surface age. However, soil characteristics from the displaced Q2c surface imply that minimal

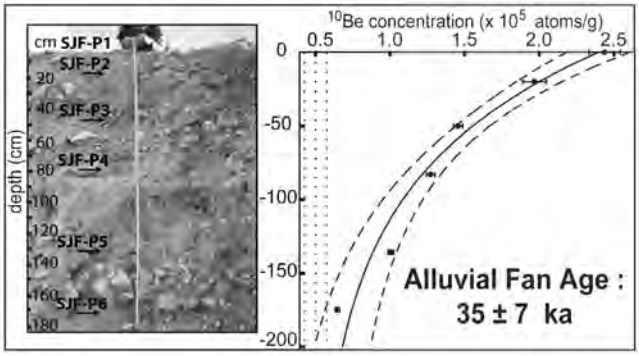

Figure 6. Field photo and graph of the exponential decrease in the concentration of ^{10}Be with depth from an alluvial surface cut by the Clark fault at the southern Santa Rosa Mountain locality. The dashed black lines indicate the 95% confidence interval around the black regression line. Vertical dotted lines represent the inheritance and its associated errors. The regression line indicates a surface age of 35 ± 7 ka.

surface lowering has occurred since 8–12 ka, giving us confidence that our modeled age is reliable and has not been modified by major surface lowering, at least during the Holocene.

5. Discussion

[21] Our new data allow us to compare slip rate estimates over the same time interval (30–50 ka) along the Clark fault strand of the SJFZ from Anza to the southern Santa Rosa Mountains. Since ~30–50 ka, our results show a pronounced southward slip rate decrease along the Clark fault strand. The ~13 mm/yr late Quaternary rate at Anza [*Rockwell et al.*, 1990] decreases southeastward to 8.9 ± 2.0 mm/yr at Rockhouse Canyon and to 1.5 ± 0.4 mm/yr at the southern Santa Rosa Mountains (Figure 2). This southward gradient in slip rate along the Clark fault strand is consistent with a similar decrease in slip per event for the past several events, as documented from small channel offsets [*Middleton*, 2006; W. B. Bull, personal communication, 2008]. This decrease is also consistent with the decrease in total bedrock displacement [*Sharp*, 1967] from Anza (22–24 km) to Rockhouse Canyon (14.5 to 17 km) (Figure 2). Farther southeast, toward the southern Santa Rosa Mountains, the total bedrock displacement has been estimated to be similar to that at Rockhouse Canyon (~14.5 km) [*Sharp*, 1967], but because the offset cataclasite marker is as much as 5 km away from the main fault strand (Figure 2) this estimate is less well constrained. The consistent decrease in total bedrock offset and slip rate between Anza and Rockhouse Canyon can be attributed to a transfer of slip onto the adjacent Coyote Creek fault strand (Figure 2) [*Sharp*, 1967]. A plausible explanation for the more dramatic decrease in slip rate from Rockhouse Canyon to the Santa Rosa Mountains is that much of the deformation has been absorbed by young and active distributed deformation in the Borrego Badlands basin, where slip has juxtaposed thick sediments of the Salton Trough against bedrock of the Santa Rosa Mountains (Figure 2) [*Belgarde and Janecke*, 2006], and some displacement may also be taken up by the Coyote Mountain and Inspiration Point faults (Figure 2). Overall, the Clark fault strand exemplifies how slip rates are not maintained along the entire length of faults and that considerable strain may be accommodated in a distributed manner, especially near the fault tip [*Cowie and Scholz*, 1992]. Gradients in slip rate appear to be especially dramatic where faulting juxtaposes sedimentary rocks [*Cowie and Scholz*, 1992].

[22] The strong correlation between total bedrock displacement and our late Quaternary slip rates along the Clark fault strand between Anza and Rockhouse Canyon leads to interesting speculations on fault system behavior. Assuming that fault slip rates have been constant since fault inception, our rates are slower than required by the ca. ~1.1 Ma inception of dextral faulting proposed for the Salton Trough by *Lutz et al.* [2006] and *Kirby et al.* [2007]. Conversely, if we combine bedrock displacements and slip rates at Anza (22–24 km and ~12–15 mm/yr, respectively) and Rockhouse Canyon (14.5 to 17 km and 8.9 ± 2.0 mm/yr, respectively), we would estimate the age of fault initiation at both sites as 1.8 ± 0.5 Ma. This earlier onset, which is consistent with constraints from the San Timoteo badlands [*Morton and Matti*, 1993] could also be permitted in the Salton Trough if some slip on the Clark fault accrued prior to the dramatic stratigraphic transition documented by *Lutz et al.* [2006] and *Kirby et al.* [2007]. A 1.8 ± 0.5 Ma initiation age of the SJFZ is also consistent with thermochronologic studies from the San Bernardino Mountains at Yucaipa Ridge, which are thought to have uplifted contemporaneously with initiation of the SJFZ [*Morton and Matti*, 1993; *Spotila et al.*, 2001] and show rapid exhumation since ~1.8 Ma (U-Th/He apatite age) [*Spotila et al.*, 2001]. Alternatively, slip rates at both Anza and Rockhouse Canyon may have decreased together in the late Quaternary. This would suggest that the mechanism responsible for the trade-off in slip from the Clark fault strand to the Coyote Creek fault strand acts independently of the rate of strain accumulation across the entire southern SJFZ.

[23] The slip rate estimates presented in this study support a consistent overall rate of strain accumulation across the southern SJFZ of 10 to 14 mm/yr over the late Quaternary. Taking our late Quaternary rate from Rockhouse Canyon (8.9 ± 2.0 mm/yr) as representative of the current slip rate of the southern Clark fault strand, and combining this with previously published Holocene slip rates for the Coyote Creek fault strand (~1–5 mm/yr [*Clark*, 1972; *Sharp*, 1981; *Pollard and Rockwell*, 1995]), suggests that the southern SJFZ accommodates ~10 to 14 mm/yr of plate boundary motion. This rate is similar to the combined slip rates of the Superstition Mountain fault (5–9 mm/yr [*Gurrola and Rockwell*, 1996]) and Superstition Hills fault (3–6 mm/yr [*Hudnut and Sieh*, 1989]) as well as the slip rate near Anza where the Clark fault is essentially the single strand of the SJFZ [*Sharp*, 1981; *Rockwell et al.*, 1990; *Rockwell*, 2008]. Combining slip rates across a transect from the southern Santa Rosa Mountains locality (1.5 ± 0.4 mm/yr) with previously determined Holocene slip rates for the Coyote Creek fault (~1–5 mm/yr) implies a southward slip rate decrease across the southern SJFZ, from ~10–14 mm/yr in its central portion to ~2–7 mm/yr near the fault at the latitude of the Borrego and Fish Creek badlands (Figures 1 and 2); however, the residual strain in this region is presumably accommodated through folding and thrusting in the adjacent Borrego Badlands basin [*Belgarde and Janecke*, 2006]. Farther south, the entire 8–15 mm/yr may be accommodated by slip along the Superstition Hills and Superstition Mountain faults [*Gurrola and Rockwell*, 1996; *Hudnut and Sieh*, 1989], at least in the Holocene. Comparing these results with the 15.9 ± 3.4 mm/yr slip rate determined over the same late Quaternary time interval for the Indio segment of the San Andreas fault [*van der Woerd et al.*, 2006] suggests that the SJFZ is probably subordinate to the southern San Andreas fault zone, although it is also possible (within uncertainties) that deformation is partitioned fairly evenly between the two. The remaining plate boundary strain in this region is likely taken up by the Elsinore fault, the Eastern California Shear Zone, NE-striking cross-faulting, and locally distributed folding and thrusting.

[24] Our slip rate estimates for the Clark fault strand show pronounced spatial variability, and possible temporal variability of fault slip rates along the southern San Andreas fault system during the late Quaternary. This, in turn, suggests a complex kinematic evolution, which may explain apparent discrepancies between slip rate estimates obtained from geologic and geodetic data. Our results are at odds

with combined InSAR and GPS data, which suggest much higher slip rates for the southern SJFZ [*Fialko*, 2006; *Lundgren et al.*, 2009], but consistent with GPS block models, as well as elastic and viscoelastic models of crustal deformation in this region [*Bennett et al.*, 1996; *Meade and Hager*, 2005; *Becker et al.*, 2005; *Fay and Humphreys*, 2005]; the large differences of these geodetically derived slip rates may result from differences in modeling approaches, or temporal and spatial coverage of the geodetic data. Seismic hazard studies commonly rely on long-term Quaternary rates to infer short-term hazard. Our observations suggest that information at many different localities along a fault and over multiple time frames is needed to adequately construct kinematic models and to better assess earthquake hazards along evolving plate margins.

6. Conclusion

[25] The Clark fault strand of the southern SJFZ displays a pronounced southeastward decrease in late Quaternary slip rate. ^{10}Be exposure ages of 47 ± 8 ka and 28 ± 9 ka for two beheaded channels and 35 ± 7 ka for a displaced alluvial deposit imply slip rates of 8.9 ± 2.0 mm/yr at Rockhouse Canyon and 1.5 ± 0.4 mm/yr for the southern Santa Rosa Mountains. This gradient in slip rate must be largely accommodated by distributed deformation within the Salton Trough and the transfer of slip to the Coyote Creek fault strand. Our results show that, at least for the past ~30–50 kyr, the SJFZ may have been equivalent, but more likely was subordinate, to the southern San Andreas fault in accommodating plate margin strain. This suggests that either the slip rate of the San Jacinto fault has decreased since its initiation or faulting began earlier than 1.1 Ma.

[26] **Acknowledgments.** This research was supported by the Southern California Earthquake Center (SCEC). SCEC is funded by NSF Cooperative Agreement EAR-0529922 and USGS Cooperative Agreement 07HQAG0008. The SCEC contribution number for this paper is 1295. This research was also supported by NEHRP grant G00006871. Special thanks to Alana Wilson and Eitan Shelef for field assistance, George Hilley for use of the cosmogenic nuclide extraction laboratory at Stanford University, George Jefferson and all the Rangers and volunteers (especially the Shuguns and Keeleys) at the Anza Borrego State Park for their help throughout the field work and the 2008 FOP participants for their lively discussions and comments. We also thank Robert Finkel and Dylan Rood for AMS measurements at the Lawrence Livermore National Laboratory. We would also like to express our sincere thanks to Richard Lease and an anonymous reviewer and editor who provided insightful and constructive reviews, and C. Prentice and R. Dorsey for comments on an earlier version of the manuscript.

References

Anderson, R. S., J. L. Repka, and G. S. Dick (1996), Explicit treatment of inheritance in dating depositional surfaces using in situ ^{10}Be and ^{26}Al, *Geology*, *24*, 47–51, doi:10.1130/0091-7613(1996)024<0047:ETOIID>2.3.CO;2.

Balco, G., J. O. Stone, N. A. Lifton, and T. J. Dunai (2008), A complete and easily accessible means of calculating surface exposure ages or erosion rates from ^{10}Be and ^{26}Al measurements, *Quat. Geochronol.*, *3*, 174–195, doi:10.1016/j.quageo.2007.12.001.

Becker, T., J. Hardebeck, and G. Anderson (2005), Constraints on fault slip rates of the southern California plate boundary from GPS velocity and stress inversions, *Geophys. J. Int.*, *160*, 634–650, doi:10.1111/j.1365-246X.2004.02528.x.

Belgarde, E., and S. U. Janecke (2006), Structural characterization and microseismicity near the SE end of the Clark fault of the San Jacinto fault in the southwestern Salton Trough, paper presented at Annual Meeting, South. Calif. Earthquake Cent., Palm Springs, Calif.

Bennett, R. A., W. Rodi, and R. E. Reilinger (1996), Global Positioning System constraints on fault slip rates in southern California and northern Baja, Mexico, *J. Geophys. Res.*, *101*(21), 21,943–21,960, doi:10.1029/96JB02488.

Bennett, R., A. Friedrich, and K. Furlong (2004), Codependent histories of the San Andreas and San Jacinto fault zones from inversion of fault displacement rates, *Geology*, *32*, 961–965, doi:10.1130/G20806.1.

Bevis, M., et al. (2005), The B4 Project: Scanning the San Andreas and San Jacinto Fault Zones, *Eos Trans. AGU*, *86*(52), Fall Meet. Suppl., Abstract H34B-01.

Bull, W. B. (1991), *Geomorphic Responses to Climatic Change*, Oxford Univ. Press, New York.

Clark, M. M. (1972), Surface rupture along the Coyote Creek Fault, *U.S. Geol. Surv. Prof. Pap.*, *787*, 55–86.

Cowie, P. A., and C. H. Scholz (1992), Physical explanation for the displacement-length relationship of faults using a post-yield fracture mechanics model, *J. Struct. Geol.*, *14*, 1133–1148, doi:10.1016/0191-8141(92)90065-5.

DeMets, C., and T. H. Dixon (1999), New kinematic models for Pacific-North America motion from 3 Ma to present, I: Evidence for steady state motion and biases in the NUVEL-1A model, *Geophys. Res. Lett.*, *26*, 1921–1924, doi:10.1029/1999GL900405.

Dibblee, T. W. (1954), Geology of the Imperial Valley region, in *Geology of Southern California*, *Bull. 170*, edited by R. H. Jahns, pp. 21–28, Calif. Div. of Mines, San Francisco.

Dorsey, R. J. (2002), Stratigraphic record of Pleistocene initiation and slip on the Coyote Creek fault, lower Coyote Creek, southern California, in *Contributions to Crustal Evolution of the Southwestern United States*, *Spec. Pap. Geol. Soc. Am.*, 365, 251–269.

Fay, N., and G. Humphreys (2005), Fault slip rates, effects of elastic heterogeneity on geodetic data, and the strength of the lower crust in the Salton Trough region, southern California, *J. Geophys. Res.*, *110*, B09401, doi:10.1029/2004JB003548.

Fialko, Y. (2006), Interseismic strain accumulation and the earthquake potential on the southern San Andreas fault system, *Nature*, *441*, 968–971, doi:10.1038/nature04797.

Gosse, J. C., and F. M. Phillips (2001), Terrestrial in-situ cosmogenic nuclides: Theory and applications, *Quat. Sci. Rev.*, *20*, 1475–1560, doi:10.1016/S0277-3791(00)00171-2.

Gurrola, L. D., and T. K. Rockwell (1996), Timing and slip for prehistoric earthquakes on the Superstition Mountain fault, Imperial Valley, southern California, *J. Geophys. Res.*, *101*, 5977–5985, doi:10.1029/95JB03061.

Harden, J. W., and J. C. Matti (1989), Holocene and late Pleistocene slip rates on the San Andreas fault in Yucaipa, California, using displaced alluvial-fan deposits and soil chronology, *Geol. Soc. Am. Bull.*, *101*, 1107–1117, doi:10.1130/0016-7606(1989)101.

Hudnut, K., and K. Sieh (1989), Behavior of the Superstition Hills fault during the past 330 years, *Bull. Seismol. Soc. Am.*, *79*, 304–329.

Janecke, S. U., R. J. Dorsey, A. N. Steely, S. M. Kirby, A. Lutz, B. A. Housen, B. Belgarde, V. Langenheim, T. Rittenour, and D. Forand (2008), High geologic slip rates since Early Pleistocene initiation of the San Jacinto and San Felipe Fault zones in the San Andreas fault system, paper presented at Annual Meeting, South. Calif. Earthquake Cent., Palm Springs, Calif.

Johnson, H. O., D. C. Agnew, and F. K. Wyatt (1994), Present-day crustal deformation in southern California, *J. Geophys. Res.*, *99*, 23,951–23,974, doi:10.1029/94JB01902.

Kendrick, K. J., D. M. Morton, S. G. Wells, and R. W. Simpson (2002), Spatial and temporal deformation along the northern San Jacinto fault, southern California: Implications for slip rates, *Bull. Seismol. Soc. Am.*, *92*, 2782–2802, doi:10.1785-/0120000615.

King, N. E., and J. C. Savage (1983), Strain-rate profile across the Elsinore, San Jacinto, and San Andreas faults near Palm Springs, California, 1973–1981, *Geophys. Res. Lett.*, *10*, 55–57, doi:10.1029/GL010i001p00055.

Kirby, S. M., S. U. Janecke, and R. J. Dorsey (2007), Pleistocene Brawley and Ocotillo formations: Evidence for initial strike-slip deformation along the San Felipe and San Jacinto fault zones, southern California, *J. Geol.*, *115*, 43–62, doi:10.1086/509248.

Lal, D. (1991), Cosmic ray labeling of erosion surfaces-In situ nuclide production rates and erosion models, *Earth Planet. Sci. Lett.*, *104*, 424–439, doi:10.1016/0012-821X(91)90220-C.

Lundgren, P., E. A. Hetland, Z. Liu, and E. J. Fielding (2009), Southern San Andreas-San Jacinto fault system slip rates estimated from earthquake cycle models constrained by GPS and interferometric synthetic aperture radar observations, *J. Geophys. Res.*, *114*, B02403, doi:10.1029/2008JB005996.

Lutz, A. T., R. J. Dorsey, B. A. Housen, and S. U. Janecke (2006), Stratigraphic record of Pleistocene faulting and basin evolution in the Borrego

Badlands, San Jacinto fault, southern California, *Geol. Soc. Am. Bull.*, *118*, 1377–1397, doi:10.1130/B25946.1.

Matmon, A., D. Schwartz, R. Finkel, S. Clemmens, and T. Hanks (2005), Dating offset fans along the Mojave section of the San Andreas fault using cosmogenic ^{26}Al and ^{10}Be, *Geol. Soc. Am. Bull.*, *117*, 795–807, doi:10.1130/B25590.1.

Meade, B. J., and B. H. Hager (2005), Block models of crustal motion in southern California constrained by GPS measurements, *J. Geophys. Res.*, *110*, B03403, doi:10.1029/2004JB003209.

Middleton, T. (2006), Tectonic geomorphology of the southern Clark Fault from Anza southeast to the San Felipe Hills: Implications of slip distribution for recent past earthquakes, M.S. thesis, 95 pp., San Diego State Univ., San Diego, Calif.

Morton, D. M., and J. C. Matti (1993), Extension and contraction within an evolving divergent strike-slip fault complex: The San Jacinto fault zones at their convergence in Southern California, in *The San Andreas Fault System: Displacement, Mem. Geol. Soc. Am.*, *178*, 107–159.

Oskin, M. E., K. Le, and M. D. Strane (2007), Quantifying fault-zone activity in arid environments with high-resolution topography, *Geophys. Res. Lett.*, *34*, L23S05, doi:10.1029/2007GL031295.

Pollard, W., and T. Rockwell (1995), Late Holocene slip rate for the Coyote Creek fault, Imperial County, California, *Geol. Soc. Am. Abstr. Programs*, *27*, 72.

Repka, J. L., R. S. Anderson, and R. Finkel (1997), Cosmogenic dating of fluvial terraces, Fremont River, Utah, *Earth Planet. Sci. Lett.*, *152*, 59–73, doi:10.1016/S0012-821X(97)00149-0.

Richards-Dinger, K. B., and P. M. Shearer (2000), Earthquake locations in southern California obtained using source-specific station terms, *J. Geophys. Res.*, *105*, 10,939–10,960, doi:10.1029/2000JB9000014.

Rockwell, T. K. (2008), Observations of mode-switching from long paleoseismic records of earthquakes on the San Jacinto and San Andreas faults: Implications for making hazard estimates from short paleoseismic records, paper presented at International Geological Congress, Int. Union of Geol. Sci., Oslo.

Rockwell, T. K., C. Loughman, and P. Merifield (1990), Late Quaternary rate of slip along the San Jacinto fault zone near Anza, southern California, *J. Geophys. Res.*, *95*, 8593–8605, doi:10.1029/JB095iB06p08593.

Rockwell, T. K., G. Seitz, D. E. Ragona, T. E. Dawson, G. Faneros, D. M. Verdugo, and O. Altangerwel (2005), Investigation of segment controls on the rupture history of the southern San Jacinto fault, *Seismol. Res. Lett.*, *76*(2), 254.

Sharp, R. V. (1967), San Jacinto fault zone in the Peninsular Ranges of southern California, *Geol. Soc. Am. Bull.*, *78*, 705–730, doi:10.1130/0016-7606(1967)78[705:SJFZIT]2.0.CO;2.

Sharp, R. V. (1981), Variable rates of late Quaternary strike slip on the San Jacinto fault zone, southern California, *J. Geophys. Res.*, *86*, 1754–1762, doi:10.1029/JB086iB03p01754.

Spotila, J. A., K. A. Farley, J. D. Yule, and P. W. Reiners (2001), Near-field transpressive deformation along the San Andreas fault zone in southern California, based exhumation constrained by (U-Th)/He dating, *J. Geophys. Res.*, *106*(30), 909–930, doi:10.1029/2001JB000348.

Stone, J. O. (2000), Air pressure and cosmogenic isotope production, *J. Geophys. Res.*, *105*, 23,753–23,759, doi:10.1029/2000JB90081.

Thatcher, W., J. A. Hileman, and T. Hanks (1975), Seismic slip distribution along the San Jacinto fault zone, southern California, and its implications, *Geol. Soc. Am. Bull.*, *86*, 1140–1146, doi:10.1130/0016-7606(1975)86<1140:SSDATS>2.0.CO;2.

van der Woerd, J., Y. Klinger, K. Sieh, P. Tapponnier, F. J. Ryerson, and A. Meriaux (2006), Long-term slip rate of the southern San Andreas Fault from ^{10}Be-^{26}Al surface exposure dating of an offset alluvial fan, *J. Geophys. Res.*, *111*, B04407, doi:10.1029/2004JB003559.

Weldon, R. J., and K. E. Sieh (1985), Holocene rate of slip and tentative recurrence interval for large earthquakes on the San Andreas fault, Cajon Pass, southern California, *Geol. Soc. Am. Bull.*, *96*, 793–812, doi:10.1130/0016-7606(1985)96<793:HROSAT>2.0.CO;2.

Wesnousky, S. G., C. S. Prentice, and K. Sieh (1991), An offset Holocene stream channel and the rate of slip along the northern reach of the San Jacinto fault zone, San Bernardino Valley, *Geol. Soc. Am. Bull.*, *103*, 700–709, doi:10.1130/0016-7606(1991)103.

K. Blisniuk and M. Oskin, Department of Geological Sciences, University of California, Davis, CA 95616, USA. (kimle@geology.ucdavis.edu)

M. W. Caffee, Department of Physics, Purdue University, West Lafayette, IN 47906, USA.

J. Dortch and L. A. Owen, Department of Geology, University of Cincinnati, Cincinnati, OH 45221, USA.

C. Lippincott and T. Rockwell, Department of Geological Sciences, San Diego State University, San Diego, CA 92182, USA.

The “Borrego Trio” in Flight. Left to right: Mike Hart, Monte Murbach and Chuck Hart.

Structural and Geomorphic Characteristics of Landslides at Coyote Mountain, Anza-Borrego Desert State Park, California

MICHAEL W. HART

Consultant, P.O. Box 261227, San Diego, CA 92196

Key Terms: ***Landslide, Structure, Geomorphology***

ABSTRACT

Coyote Mountain is an 8-mi-long (13 km) elongate fault block made up of granitic and metamorphic rocks in northeastern San Diego County, California. A series of landslides, most of which have distinct morphology and failure mechanisms, occurs in the tonalite and gneiss underlying the steep southwest slope of the mountain. The southernmost landslide area is the Peg Leg Smith landslide complex, which is composed of several translational slides and a unique remnant of a long-runout rock avalanche. In the central portion of the mountain, two distinct landslide types underlie the slopes near Coyote Peak. The first is represented by a pair of rock-block landslides, the Coyote Peak landslides, which failed along foliation planes in metamorphic rock. The second is the Coyote Ridge landslide, a 2-mi-wide (3.2 km) area of incipient landsliding in highly fractured tonalite. The Alcoholic Pass landslides, located at the northwestern end of the mountain block, are situated in tonalite. This complex consists of two juxtaposed landslides that failed at nearly right angles to each other. The base of the northernmost landslide is not exposed, and the failure mechanism is postulated to have been block sliding along a well-developed fracture system. The basal rupture zone of the southern landslide is composed of coarse, matrix-rich breccia. The southern flank of the slide grades into linear scarps which define the head of the Coyote Ridge landslide. The Alcoholic Pass landslides are concluded to be rare examples of fully developed translational failure resulting from formation of a through-going rupture surface created by incremental movement along interconnecting fractures.

INTRODUCTION

The purpose of this study is to: (1) identify the factors that lead to large-scale landsliding in granitic and metamorphic terranes, and (2) to describe how failure mechanisms are determined from landslide structural and geomorphic characteristics. Coyote Mountain is located in Anza-Borrego Desert State Park in the northeast corner of San Diego County, California (Figure 1). Coyote Mountain, an 8-mi-long (13 km), northwest-trending fault block that juts out abruptly into Borrego Valley from the north, is made up principally of Cretaceous granitic rocks, pre-batholithic metasediments, and gneiss. It is bounded on the west by the Coyote Creek fault and on the east by the Coyote Mountain fault, a northwest-trending splay of the San Jacinto fault (Figure 2). The western slope of the mountain is a steep fault scarp (Sharp, 1967) that rises from the surrounding valleys to an elevation of 3,192 ft (973 m).

The southwest-facing slope of the mountain extends from Alcoholic Pass on the north to the Peg Leg Smith monument at the south end of the mountain block, a distance of approximately 6 mi (10 km). This mountain front is occupied by a series of deep-seated landslides or landslide complexes, each of which has been assigned informal names for ease of discussion, beginning with the Peg Leg Smith landslide complex in the south and ending with the Alcoholic Pass landslides in the north (Figure 2). The landslide structure (basal rupture zones and rupture surfaces, internal slip surfaces, and stratification of landslide debris), as well as landslide morphology, suggests a variety of failure mechanisms, including slumping, rock-block failure, rock avalanche, and a newly proposed variety of incremental landsliding that is similar to sackung but results from seismic activity instead of gravitational stress. Identification of the landslides that make up the Peg Leg Smith landslide complex, as well as the Coyote Peak landslides in the central part of the range, was difficult because of erosional modification of headscarps and lack of quality field exposures.

GEOLOGIC SETTING

Coyote Mountain is situated in the eastern part of the Peninsular Ranges Geomorphic Province between the San Jacinto fault on the east and the Coyote

Figure 1. Location map.

Creek fault on the west. Coyote Mountain is a northwest-trending ridge dominated by 3,200-ft (973 m) high Coyote Peak after which the ridge is named. The bedrock that makes up the Coyote Mountain block has been divided by Theodore and Sharp (1975) into 15 mappable rock units, including two Quaternary sedimentary formations, several types of Cretaceous granitic rocks, and pre-batholithic metamorphic rocks consisting of gneiss, schist, and marble.

The southern part of Coyote Mountain, from Coyote Peak to the Peg Leg Smith historical marker at the southern end of the block, makes up the Coyote Mountain cataclastic zone (Sharp, 1967), in which both the plutonic and pre-batholithic rocks have been subjected to deep-seated plastic deformation that has created a generally east-dipping shear foliation. The northern half of the area is underlain by pervasively fractured and sheared hornblende-biotite tonalite.

The Pleistocene Ocotillo Conglomerate overlies the tonalite in the northern and central portions of the mountain block and occupies a prominent broad depression in the ridge north of Coyote Peak. At its southern limit, the Ocotillo Conglomerate lies in fault contact with tonalite and metamorphic bedrock. These deposits consist of poorly consolidated terrestrial sands and conglomerates that accumulated primarily under fluvial conditions in coalescing basins and fan environments (Sharp, 1967).

GEOLOGIC STRUCTURE

Outcrops of granitic rocks undisturbed by landsliding can be observed only in a few limited areas on the western slopes of Coyote Mountain, primarily in the central part just west of Coyote Peak. Here, the rocks exhibit intense fracturing and shearing resulting from gravitational stress, as well as tectonic stresses resulting from displacement along the nearby Coyote Creek and San Jacinto faults.

Sharp (1967) and Theodore and Sharp (1975) have indicated that motion on the Coyote Creek fault is primarily dip slip, based on the presence of the steep western slope of Coyote Mountain, which abruptly rises from the floor of Borrego Valley. It seems more probable, given the strike-slip tectonic environment in which the mountain block is situated, that the Coyote Creek fault also has a strong component of right slip and that this motion accounts for the fact that Coyote Mountain block is separated from the range front approximately 8 mi (13 km) to the north. The Alcoholic Pass landslides in the northern part of the mountain block have relatively young geomorphic features, such as well-defined headscarps and, in one location, a very young scarp in alluvium, while the landslides of the Peg Leg Smith landslide complex at the southern tip of Coyote Mountain have erosionally modified and much subdued scarps with basal rupture surfaces buried by alluvium of Coyote Creek. Based on the apparent age difference between the northern and southern landsides, described more fully later in this discussion, it is tempting to conclude that the mountain block has been separated from the ranges to the north primarily by right-lateral motion along the Coyote Creek fault, and, as a result, the older landslides occupy the southern parts of the block.

Low-angle shears with dips parallel to foliation of 10 to 25 degrees are accompanied by thick breccia zones and occur outside of areas underlain by landslides. One such area lies adjacent to the south flank of the Coyote Peak landslides. A prominent shear zone at this location was observed dipping into the mountain front at inclinations of 18 to 25 degrees. The complete lack of any geomorphic feature even remotely resembling a landslide upslope from the shear zone indicates that the shearing is tectonic in origin. Fractures, at least where they can be observed in the near surface in stream cuts, are primarily vertical and strike essentially parallel to slopes. In some areas, the fracturing is very intense, and there is a significant amount of silty matrix or breccia-like material separating the blocks.

Rocks within the plastically deformed Coyote Mountain cataclastic zone exhibit a generally eastward-dipping shear foliation and a pronounced, roughly eastward-plunging lineation in the foliation due to streaked-out alternating concentrations of light and dark minerals Sharp (1967). The texture and coherence of the rocks within the cataclastic zone indicate deformation at considerable depth in the crust. In outcrop, the gneissic rocks are hard,

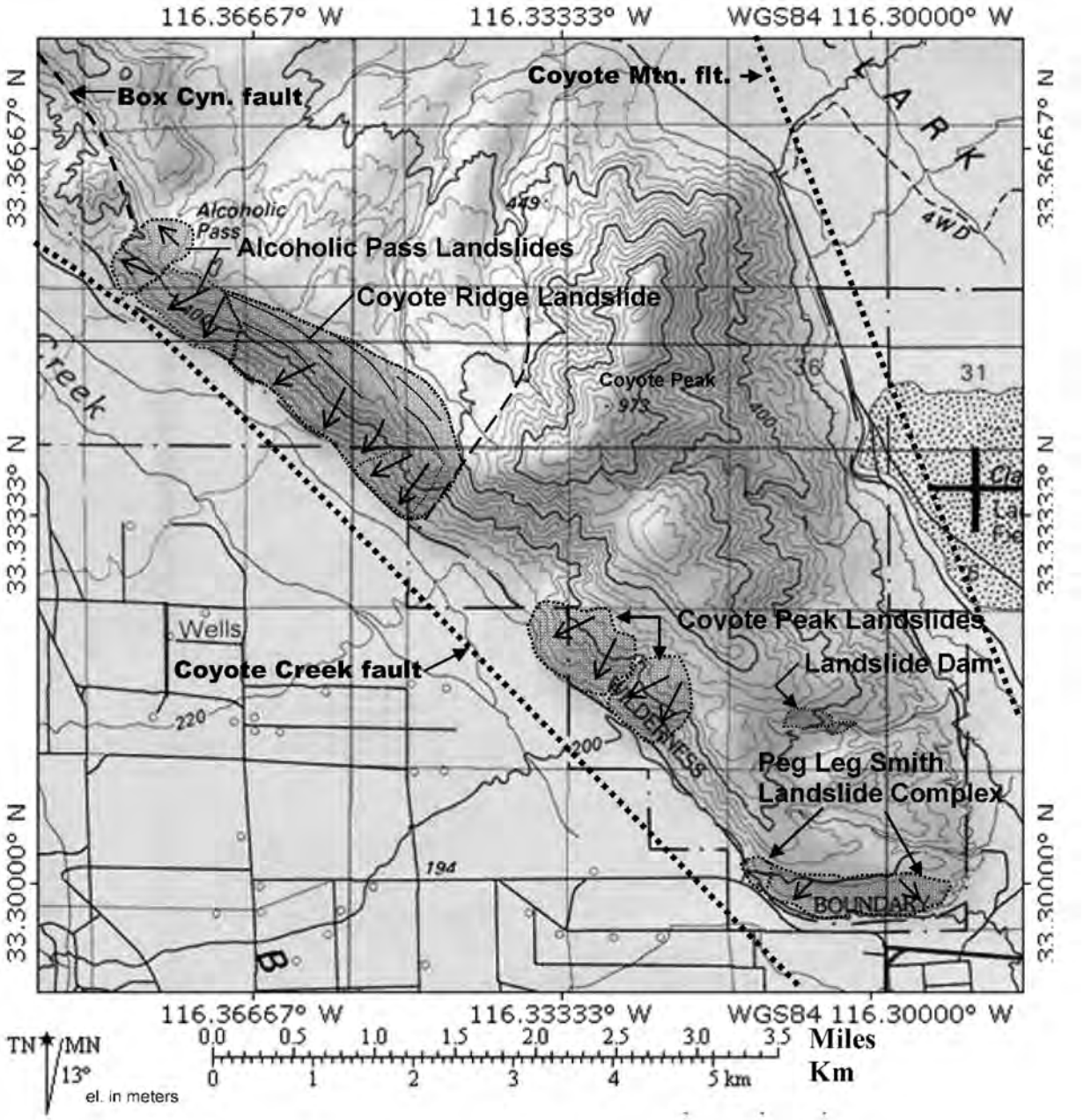

Figure 2. Topographic map of Coyote Mountain showing location of features discussed in text.

relatively fresh, and are poorly to thinly foliated with platy cleavage.

THE PEG LEG SMITH LANDSLIDE COMPLEX

The Peg Leg Smith landslide complex is named after a nearby monument honoring the mountain man, prospector, and teller of tall tales of the early 1800's who claimed to have found a rich gold strike in the Borrego area but unfortunately could not remember the location of the mine. Legends concerning its location abound and have enticed many unsuccessful amateur prospectors into the surrounding hills. The landslide complex consists of a 1.5-mi-long (2.4 km) series of coalescing and superposed landslides located at the southern terminus of the Coyote Mountain block (Figure 2).

Seven landslides occur within the Peg Leg Smith landslide complex, ranging in width from 600 ft (190 m) to over 3,200 ft (975 m). The westernmost of the landslides is a remnant of a possible rock avalanche, the more distal portions of which are buried by alluvium. The remaining six landslides and four landslides north of the complex on the east side of Coyote Mountain are large, essentially intact rock masses that failed along foliation planes. Accordingly,

Figure 3. Southern terminus of Coyote Mountain showing the western end of the Peg Leg Smith landslide complex. View is toward the northeast. Santa Rosa Mountains are on horizon. Point A = location of Figure 4; B = location of Figure 5.

they are classified as rock-block slides after the classification of Varnes (1978). All the landslides occur within the Coyote Mountain cataclastic zone, which is made up predominantly of well-foliated gneiss and metasediments.

The westernmost landslide is well-exposed along an old mining road that traverses the central portion of the slide mass and along two deeply incised gullies near its southern flank (Figure 3). The landslide extends from an elevation of approximately 1,000 ft (305 m) at the head to an elevation of 600 ft (183 m) along the valley floor, where the base of the slide is buried by alluvium and talus. The precise location of the southern flank of the landslide is not known because of insufficient outcrop. Although the base of the landslide is buried beneath alluvium and talus at its northern flank, the base of the landslide is well-exposed near its southern flank in the walls of a gulley just south of the mining road, approximately 30 ft (9 m) above the valley floor (Figure 4).

Several observations indicate that the landslide is an erosional remnant of what was a much larger landslide. First, the upper portion of the north flank of the slide mass lying above Coyote Creek has a slope that exceeds 45 degrees. The absence of talus at the base of slope at this location suggests that Coyote Creek is actively cutting into the slide mass and that much of the medial and distal portions of the landslide have been removed by stream erosion and buried by alluvium. Secondly, the crude stratification of the slide debris visible along the mining road is diagnostic of the proximal portion of rock avalanche deposits. Zones of pulverized slide debris and matrix-rich breccia observed in the road cut lie in near-horizontal contact with overlying fractured rock containing little or no matrix (Figure 5). Well-stratified slide debris with distinct vertical zones or facies, which vary from a slurry-like mixture of sand, silt, and clay at the base to a matrix-poor middle facies to an upper crackle breccia (megaclasts are parted along planes of weakness but show little or no displacement or rotation relative to one another), is characteristic of medial and distal portions of long-runout landslides. The more proximal portions of such landslides show little or no stratification (Yarnold and Lombard, 1989). While this evidence

Figure 4. Basal shear zone of the westernmost landslide, Peg Leg Smith complex. See Point A, Figure 3 for location of photograph.

Figure 5. View to northwest along old mining road of crude stratigraphy in the western landslide, Peg Leg Smith landslide complex. Arrows delineate matrix-rich breccia and thin pulverized zone at base.

suggests that this landslide could be classified as a rock avalanche, the diagnostic medial and distal portions of the slide that would allow such a determination to be made with certainty are no longer present.

An exposure of the slide base occurs in a narrow gulley approximately 30 ft (9 m) in elevation above the valley floor (Figure 4). Here, the basal rupture zone consists of matrix-rich breccia that dips subhorizontally and parallel to the foliation in the underlying gneiss. A true slip surface typical of translational landslides is not present at this location, and the light brown, fine-grained material at the base of the slide mass has the consistency of fine silty sand with only slight plasticity. The elevated position of the basal shear above the valley floor indicates that the slide has a very irregular slip-surface geometry, since several hundred feet to the north, the basal shear zone lies much lower in elevation where it is buried by alluvium.

A group of six coalescing and superposed rock-block landslides, which occur over a distance of approximately 2 mi (3.3 km), makes up the remainder of the Peg Leg Smith landslide complex (Figures 6 and 7). Evidence of landsliding within this slide complex varies from very strong to weak and required consideration of a combination of structural and geomorphic evidence in order to have a high degree of confidence that landsliding was the responsible process. Geomorphic evidence of landsliding, such as the presence of scarps and ponded alluvium in side-hill benches, even in conjunction with what may be interpreted as structural evidence (chiefly shear zones and matrix-rich breccia), is strong but not necessarily conclusive proof of landsliding in an environment of active faulting. Some of the more important hypotheses to consider are: (1) the structure and landslide-like geomorphic features are a result of landsliding; (2) the features are the result of faulting; (3) the features are the result of faulting overprinted by later landsliding; or (4) the features are purely erosional in nature and are not related to any of the above.

The ability to positively identify landslides is directly related to the age of the slide and the quality of the exposures. A complication in landslide identification is the presence of landslide pseudomorphs, or landslide imposters, which are formed as products of differentially eroding rock types and preferential erosion along fractures and faults. In the case of the landslides in the Peg Leg Smith landslide complex, the availability and quality of structural and geomorphic evidence of sliding vary from slide to slide. When a single line of conclusive evidence was lacking, such as the presence of young diagnostic geomorphic features or a basal rupture surface, several lines of evidence tabulated next were utilized to obtain a high degree of confidence that the features in the Peg Leg Smith landslide complex were the result of massive landsliding.

Geomorphic Evidence

1. Rectilinear to somewhat sinuous scarps. The heads of the landslide "candidates" are delineated by eroded scarps, below which there occur topographic benches followed by valley-ward convex slopes. The fact that the scarps are discontinuous is further evidence that they were not caused by faulting.

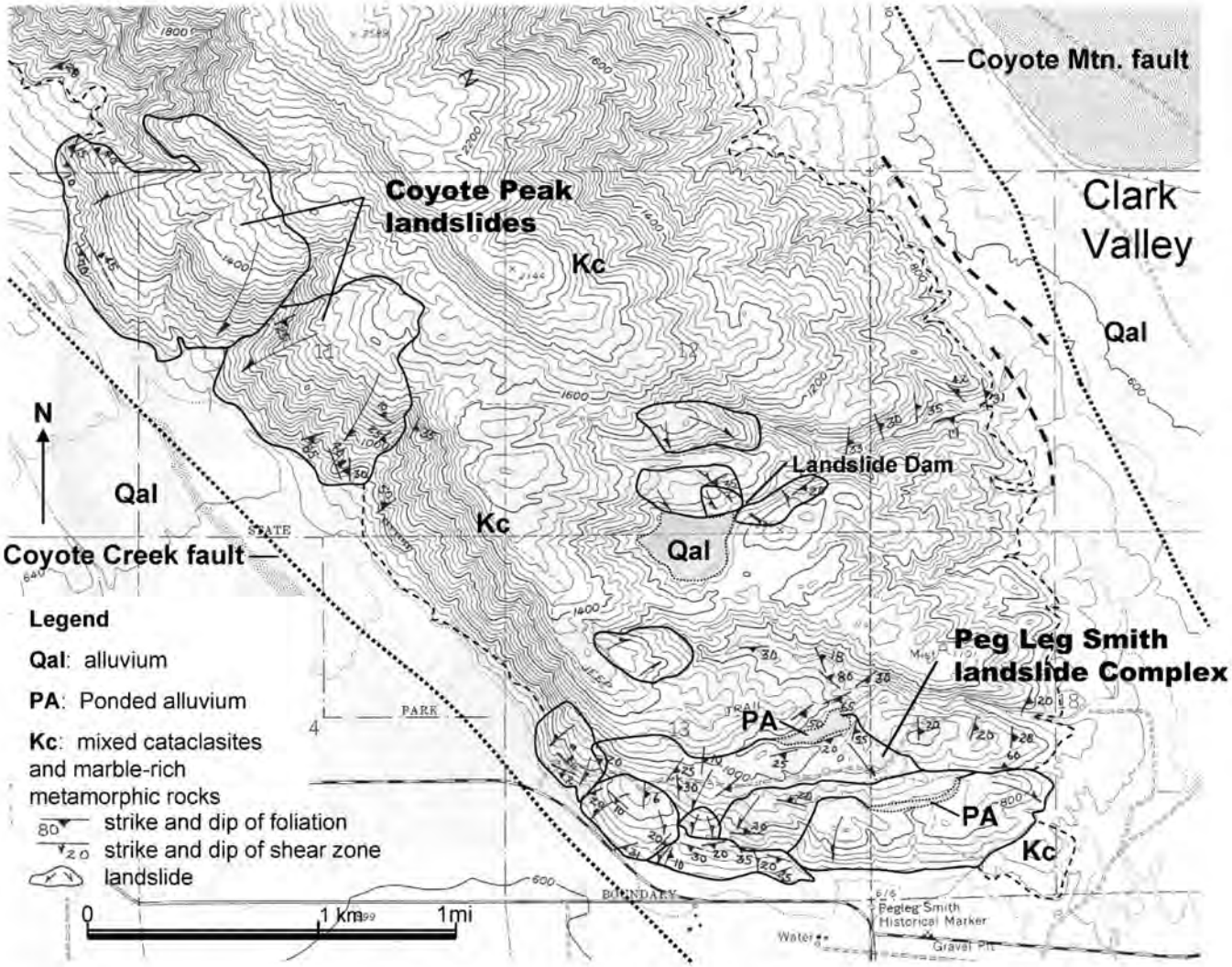

Figure 6. Map of Peg Leg Smith landslide complex and Coyote Peak landslides.

2. Ponded alluvium. Ponded alluvium, or anomalously large areas of alluvium with rock-floored outlets located in side-hill valleys below scarps, is a common characteristic of the Peg Leg Smith landslide complex (Figure 6). A short distance north of the complex (Figures 6, 7, and 8), there is a landslide dam that has ponded an estimated 150 ft (47 m) of alluvium. The ephemeral lake that once occupied the valley behind the dam is now completely filled with alluvium, and drainage now flows unimpeded toward the east into Clark Valley.

3. The head of the principal, or largest, of the landslide features is denoted by a long, essentially linear valley marked in some localities by ponded alluvium. The scarp is fully developed to where it intersects an opposite-facing descending slope at its upstream terminus. This type of abrupt termination is reminiscent of features created by stream piracy. In this case, it is evidence of a non-erosional origin of the canyon.

4. Arcuate drainage systems that in map view join to form the classic outline of the flanks and head of a landslide.

Structural Evidence

1. Near-horizontal shear surfaces overlain by pulverized rock debris or matrix-rich breccia.

2. Stream cuts located below possible headscarps that contain nearly continuous exposures of matrix-supported breccia consistent with the type of material expected to occur above a landslide's basal rupture surface.

3. Textures that are diagnostic of rock avalanche deposits, such as crackle breccia and matrix-supported breccia in several localities (Figure 9).

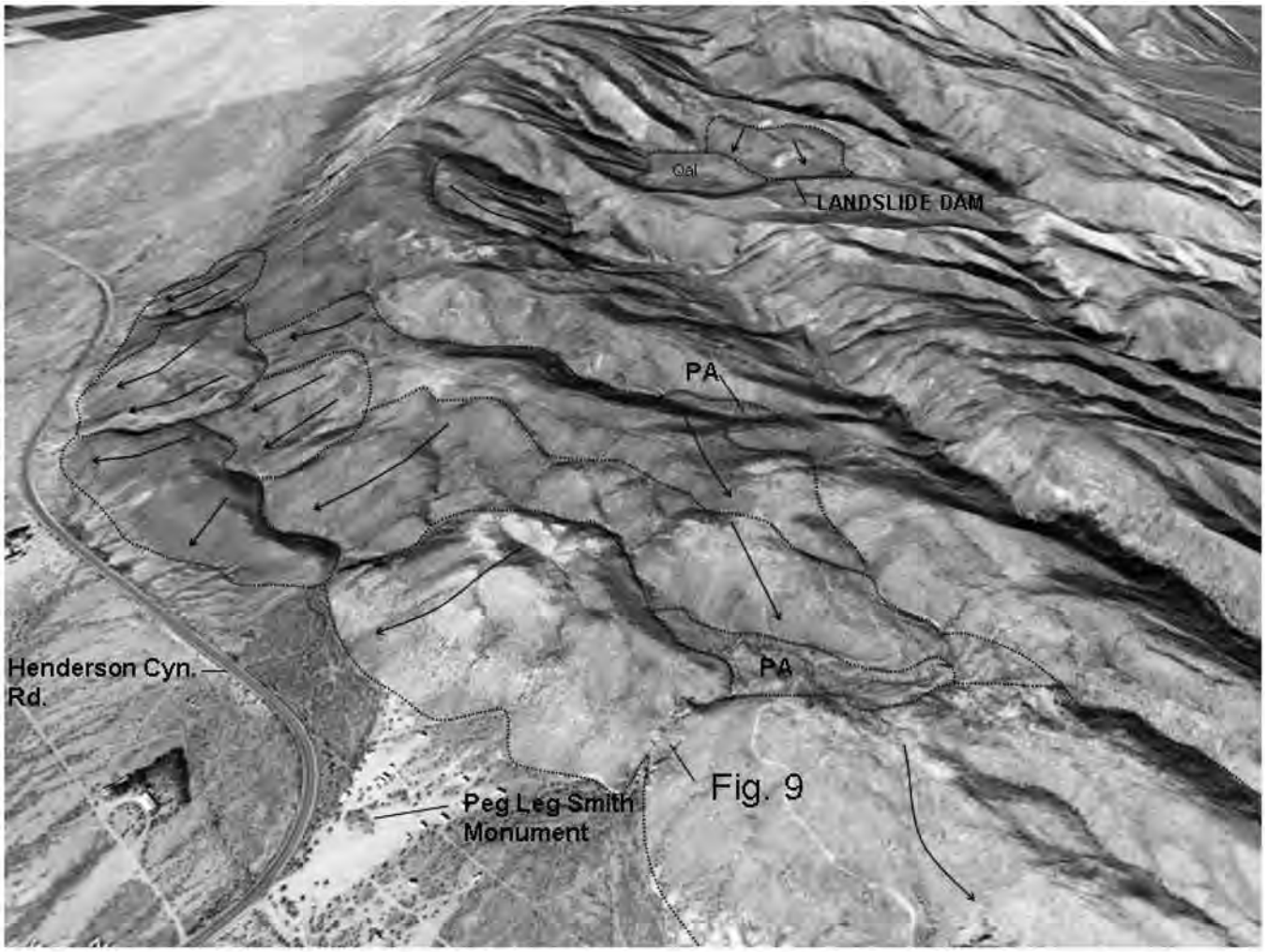

Figure 7. Annotated aerial view of Peg Leg Smith landslide complex showing areas of ponded alluvium and location of Figure 9.

4. Near-vertical "faults" exposed below and parallel to postulated headscarps. The occurrence of any one of these features is consistent with but not conclusive evidence of landsliding. When several lines of geomorphic and structural evidence are considered together, the evidence for landsliding is strong, even without exposure of the basal failure surface.

In the only location where a basal failure surface can be observed near the southern flank of the westernmost landslide, the material that makes up the shear zone is cemented with calcium carbonate and consists of what could be described, if it were wet, as a slurry composed of a mixture of rock fragments, sand, and silt with little clay. The appearance of the mud-like slurry observed near the base of several of the slides indicates that they likely occurred at a time when the slide mass was fully or nearly saturated. The lack of clay gouge along the rupture surfaces would seemingly require that failure occurred along foliation planes already weakened by tectonic slip, similar to flexural-slip faulting common in folded sedimentary rocks.

COYOTE PEAK LANDSLIDES

The Coyote Peak landslides are located on the west side of Coyote Mountain approximately 1 mi (1.6 km) north of the Peg Leg Smith landslide complex. Together, these landslides are 1.25 mi (2 km) wide and extend from the valley floor to an elevation of 1,640 ft (512 m) on the west side of Coyote Peak. The most striking geomorphic characteristic of the landslides is the drainage texture, which is dissimilar to that which occurs on the much steeper adjacent terrain. The landslide slopes are smoother and more rounded as a consequence of there being fewer and less-well-developed drainages within the slide mass. In addition, slopes in the medial and distal

Figure 8. Landslide dam north of the Peg Leg Smith landslide complex. See Figure 6 for location. Trapped alluvium in valley is estimated to be 150 ft (47 m) thick.

Figure 9. View to east of brecciated landslide debris in Peg Leg Smith landslide complex. See Figure 7 for location.

portions of the landslides are much gentler than slopes that make up the west side of the mountain front to the north and south.

The relatively subtle headscarps of the Coyote Peak landslides occur to the west of a more obvious, longer, and much higher scarp (Figure 10), which at first glance appears to be a headscarp of a larger landslide. A closer evaluation, however, reveals that the scarp continues further south than the landslide terrain and eventually terminates in an area removed from any evidence of landsliding. Although it is tempting to attribute the origin of the scarp to landsliding, outcrops of in-place metamorphic rocks in the deep canyon at the northern terminus indicate an erosional or perhaps fault origin. Shallow rockfall debris estimated to be approximately 20 to 30 ft (6 to 9 m) thick occurs on the bench below the scarp. Evidence for landsliding consists of the subtle head-

Figure 10. Heavily eroded north slide and portion of south slide, Coyote Peak landslides, showing location of Figures 12, 13, and 14. Short arrows point to top of headscarps. View is to east from Borrego Valley.

scarps (Figures 10 and 11), the presence of matrix-rich landslide debris, and low- to high-angle shear zones exposed in several deeply incised canyons.

The northernmost of the two landslides has an approximately 200-ft-high (60 m) headscarp partly separated from the body of the slide by a deep, northwesterly draining canyon. Erosion has removed most of the landslide debris from the head of the slide and has exposed the underlying gneissic bedrock. Remnants of landslide debris below the steep headscarp can be seen from the canyon bottom, where the basal shear zone truncates a steeply dipping mafic dike within well-foliated migmatite country rock approximately 200 ft (60 m) above the canyon floor. The base of the slide can also be observed high on the canyon wall just west of the headscarp, and it is manifested by a zone of shearing and a disaggregated sub-horizontal dike. The metamorphic bedrock at this location is highly shattered and contains numerous high- to low-angle shear zones that parallel the foliation, making precise determination of the limits of landsliding difficult.

An approximately 300-ft-long (90 m) and up to 15-ft-high (4.5 m) exposure in a stream cut at the northern edge of the landslide reveals classic landslide debris. At this location, highly fractured, sheared, and, most significantly, contorted metamorphic and gneissic rocks are terminated by a low-angle shear zone composed of several feet of pulverized metasediments. The contact between the thoroughly pulverized materials in the shear zone and the overlying brecciated rocks is formed by ¼-inch-thick (5 mm) clayey gouge that dips 20 degrees to the northeast. Further to the west, along the fringe of the alluvial fan, erosion has exposed matrix-rich breccia that consists of a mixture of angular gneissic and metasedimentary clasts with a distinctly chaotic structure typical of material expected near the toe of a landslide (Figure 12). To the east of this exposure, there are outcrops of undisturbed, lightly fractured

Figure 11. Coyote Peak landslides. View is to east of the south slide.

metamorphic rocks with foliation dipping gently to the southwest. The eastern limit of the landslide cannot be directly observed at this locality but is inferred between the well-exposed slide debris in the stream cut and the in-place migmatite observed in the steep walls of the adjacent canyon. Minor drainages along the toe of the slide include numerous outcrops of moderately dipping shear zones and matrix-rich breccias. The reentrant southerly draining canyon, the mouth of which is located along the south flank of the slide, exhibits good exposures of thin, white dikes that are so thoroughly sheared that they are now best described as white breccia zones consisting of clasts rotated along the planes of the dikes during shearing and translation (Figures 13 and 14).

The southernmost of the two landslides has a highly eroded arcuate headscarp that varies from 80 to 160 ft (24 to 50 m) high (Figure 11). Smaller, secondary scarps are located at the head of the slide, and there is a low uphill-facing scarp near the toe. Structural evidence of landsliding is present in several small canyons along the toe of the slide, where thin zones of shearing and breccia can be observed. The basal shear zone of this slide is buried beneath the

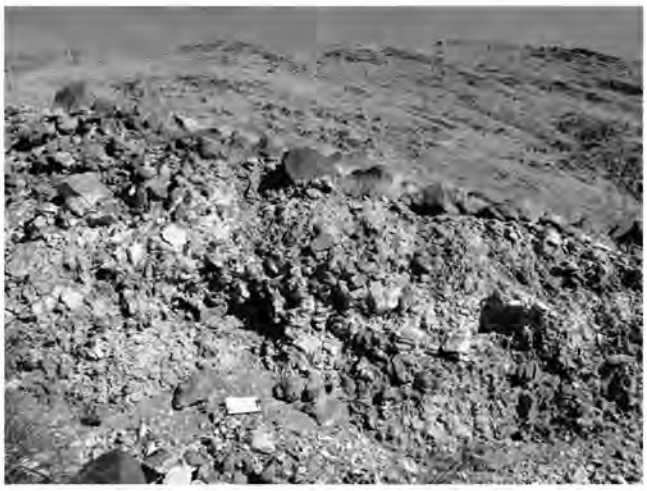

Figure 12. Coyote Peak landslides. Landslide debris can be seen at the toe of the north slide. Clipboard at base of stream cut is shown for scale.

alluvium of Coyote Creek. The north wall of the canyon located along the southern flank of the slide exhibits good evidence of landsliding, such as steeply dipping shear zones, as well as matrix- and clast-supported breccia. As previously discussed in the section on the Peg Leg Smith landslide complex, the presence of shear zones and breccia is not conclusive evidence of landsliding; however, the combination of this structural evidence with geomorphic evidence (the presence of a well-defined headscarp) allows a high degree of confidence in a landslide interpretation.

The steep, highly dissected slopes directly south of the Coyote Peak landslides also exhibit thick zones of brecciated rock and shear zones dipping up to 20

Figure 13. Coyote Peak landslides. Landslide breccia on west side of the canyon near the toe of the north slide shows location of rotated clasts comprising disrupted low-angle dike in Figure 14.

Figure 14. Rotated clasts of white dike material near toe of north slide. Largest clasts have maximum dimension of approximately 1 ft (0.3 m).

degrees into the mountain front. Low scarps estimated to be 20 ft (6 m) in height occur at the crest of the west-facing slopes south of the landslide complex. There is also a 15-ft-high (4.5 m) uphill-facing scarp near the foot of the slope. A shallow stream cut across the northern terminus of the scarp exposes a steeply east-dipping shear zone which trends parallel to the slope and is manifested by brecciated and sheared metamorphic rocks. The discontinuous nature of the scarp, which extends only a few hundred feet, suggests that it is not the result of faulting. Foliation planes measured in the canyon along the southern flank of the slide area have a strong out-of-slope dip component that varies between 25 and 45 degrees to the southwest. Because this portion of the slope exhibits no geomorphic evidence of large-scale landsliding, these features are most likely the result of small incremental movements triggered by local earthquakes, the same mechanism ascribed to the Coyote Ridge landslide described next.

COYOTE RIDGE LANDSLIDE

For the purposes of this discussion, Coyote Ridge is that low-lying area located about midway between Coyote Peak on the south and Alcoholic Pass on the north (Figure 2). Coyote Ridge, as a consequence of uplift along the Coyote Canyon fault, has an asymmetrical profile, and the western side is very steep and difficult to climb because of its steep inclination and the presence of loose bouldery slope debris. The eastern slope is a gentle, deeply dissected dip-slope that has an average gradient of 6 degrees toward Clark Valley on the east side of Coyote Mountain.

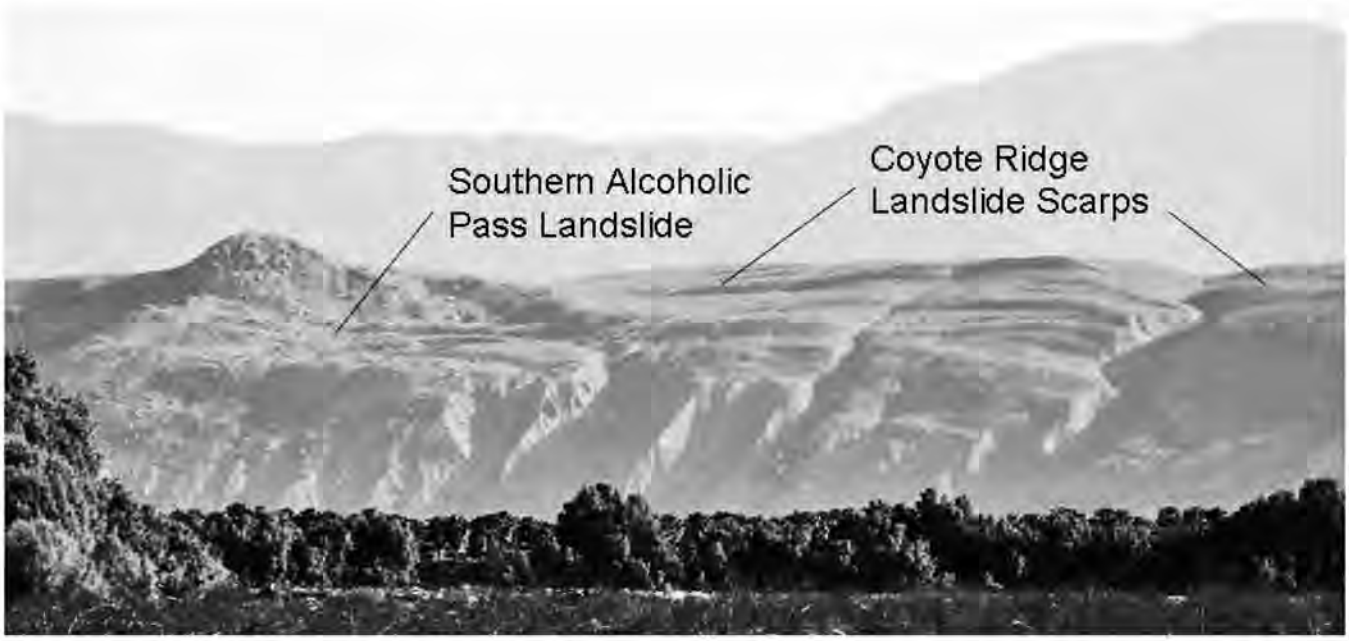

Figure 15. View to northeast of Coyote Ridge landslide scarps. Santa Rosa Mountains are on horizon.

The ridge is capped by a variable thickness of Pleistocene gravels correlated with the Pleistocene Ocotillo Conglomerate. Just south of the Alcoholic Pass landslides, the conglomerate attains an estimated thickness of 100 ft (30 m), while at the northern foot of Coyote Peak, this unit is over 800 ft (245 m) thick where it has been down-faulted against granitic and metamorphic bedrock. Underlying the relatively thin cap of Ocotillo Conglomerate, there are pre-batholithic metamorphic rocks and tonalite that make up the bulk of the landslide mass. Nearly the entire face of the steep western slope is veneered with talus resulting from numerous rockfalls and small slumps composed of granitic and conglomeratic debris. Since loose debris derived from the Ocotillo Conglomerate covers much of the lower portions of the slope, nearly the entire face of the ridge was previously mapped by Sharp (1967) and Theodore and Sharp (1975) as Ocotillo Conglomerate.

The Coyote Ridge landslide is manifested by a 1.75-mi-long (2.8 km) zone of scarps, some of which are 30 ft (9 m) in height, and intervening grabens filled with alluvium. The scarps occur in a 2,000-ft-wide (610 m) zone and descend as a group of en-echelon and sub-parallel features (Figure 15) from the high point of the ridge to the sharp break in slope at the face of the mountain front. Evidence of any bulging that might have been present near the base of the slope is not present because of erosion by Coyote Creek and the masking effect of smaller landslides, rockfalls, and talus. These surficial features also obscure any basal rupture surface that might be present near the base of the slope.

The tonalite underlying Coyote Ridge is homogeneous, and although low-angle detachment faults have been utilized as basal rupture surfaces of very large landslides in other areas of the Imperial Valley and Anza-Borrego State Park (Baldwin, 1986; Hart, 1991), there is no indication that such features are present on Coyote Mountain. Since the shear strength of the unfractured rock is very high, it is suggested that movement occurs along interconnecting fracture systems in step-like fashion as a result of high transient shear stresses produced during earthquakes along the nearby Coyote Creek and San Jacinto faults.

The San Jacinto fault, located only 3 mi (4.8 km) to the east, is one of the most active faults in California. This fault is capable of producing earthquakes of M 6.8 and peak ground accelerations (neglecting possible topographic amplification) at Coyote Mountain of approximately 0.6 *g*. The Coyote Creek fault that lies buried beneath alluvium at the western foot of Coyote Mountain has similar seismic potential. Shakal and others (1994) showed that unusually high accelerations are possible near the crest of hills near the seismic source. During the Northridge, California, earthquake of 1994, for example, amplification values of horizontal accelerations were measured on a hilltop that were twice those observed at other sites with similar epicentral distances.

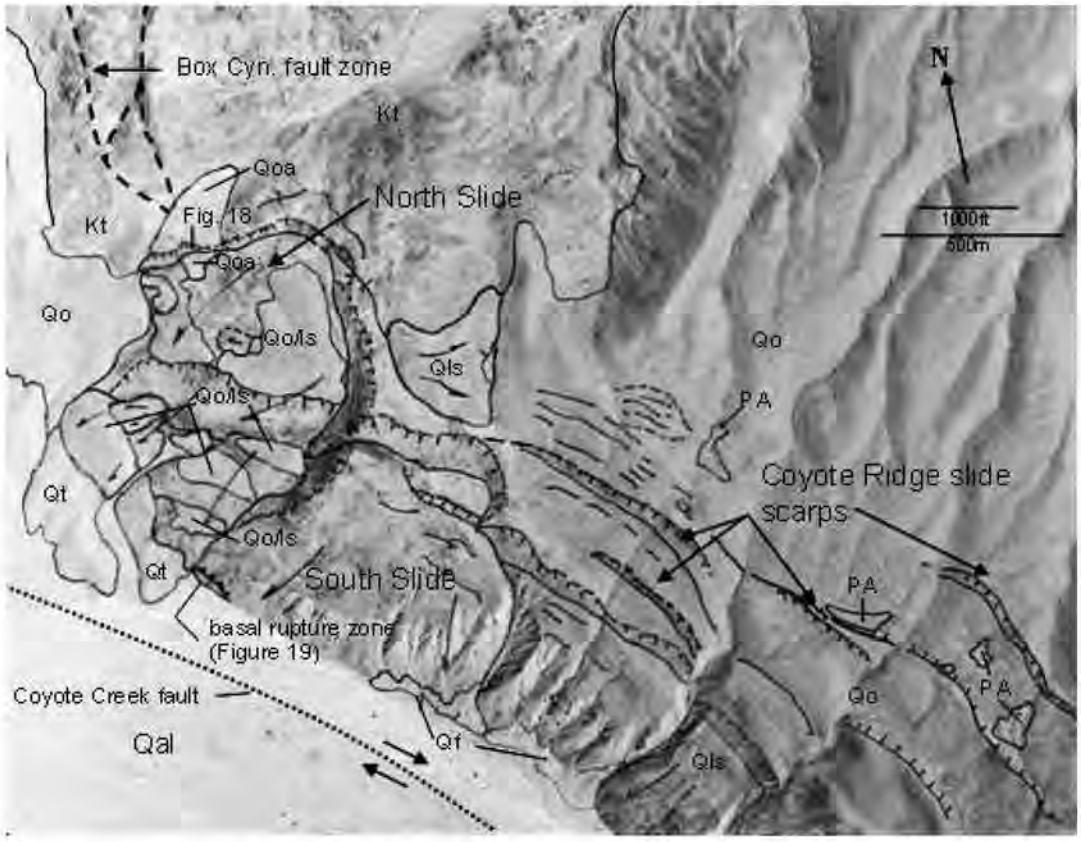

Figure 16. Annotated vertical aerial photograph of Alcoholic Pass landslides and adjacent Coyote Ridge landslide scarps. Qoa = older alluvium; Qal = alluvium; Qt = stream-terrace deposits; Qls = landslide; Qo = Ocotillo Conglomerate; Qo/ls = Ocotillo Conglomerate displaced by landsliding; Kt = tonalite; PA = ponded alluvium.

This type of failure mechanism is similar in some respects to rock creep as described by Bisci and others (1996). The driving mechanism for rock creep, however, is gravity working on extremely high and steep mountain fronts (Radbruch-Hall, 1978; Dramis and Sorriso-Valvo, 1994). The difference in elevation between the valley floor at the base of Coyote Ridge and the ridge crest is approximately 1,000 ft (312 m); this height is not likely to result in the type of rock creep or sackung phenomena described by Bisci and others (1996).

ALCOHOLIC PASS LANDSLIDES

The two Alcoholic Pass landslides are located near the northern terminus of the Coyote Mountain block and are contiguous with northern flank of the Coyote Ridge landslide (Figures 2 and 16). These moderately sized landslides, the headscarps of which intersect at approximately 90 degrees, occurred in massive, hornblende biotite tonalite overlain by the Ocotillo Conglomerate. The south slide (Figures 16 and 17) is approximately 3,700 ft (1130 m) wide and extends from an elevation of 800 ft (244 m) near Coyote Creek to an elevation of 1,980 ft (604 m) at the top of the headscarp. There are several smaller and younger landslides superposed on the landslide manifested by a series of westward-descending topographic benches capped by Ocotillo Conglomerate. Movement of the much smaller secondary slides occurred after primary failure of both landslides and buried stream terrace deposits on the east side of Coyote Creek.

The approximately 100-ft-high (30 m) headscarp of the north slide has offset Ocotillo Conglomerate beds as well as younger alluvial deposits at the top of Alcoholic Pass, producing a prominent 20-ft-high (6 m) scarp in alluvium (Figure 18). The arcuate headscarp suggests that the landslide is a complex slide characterized by rotational movement at the head combined with primarily translational movement along fracture surfaces in the medial and distal portions of the landslide. The south landslide has a more linear headscarp and becomes slightly more arcuate near the southern flank. The linearity of the scarp suggests primarily translational movement with little or no rotation at the head. The Alcoholic Pass landslides appear from their geomorphic expression (well-defined geomorphic features and headscarp in

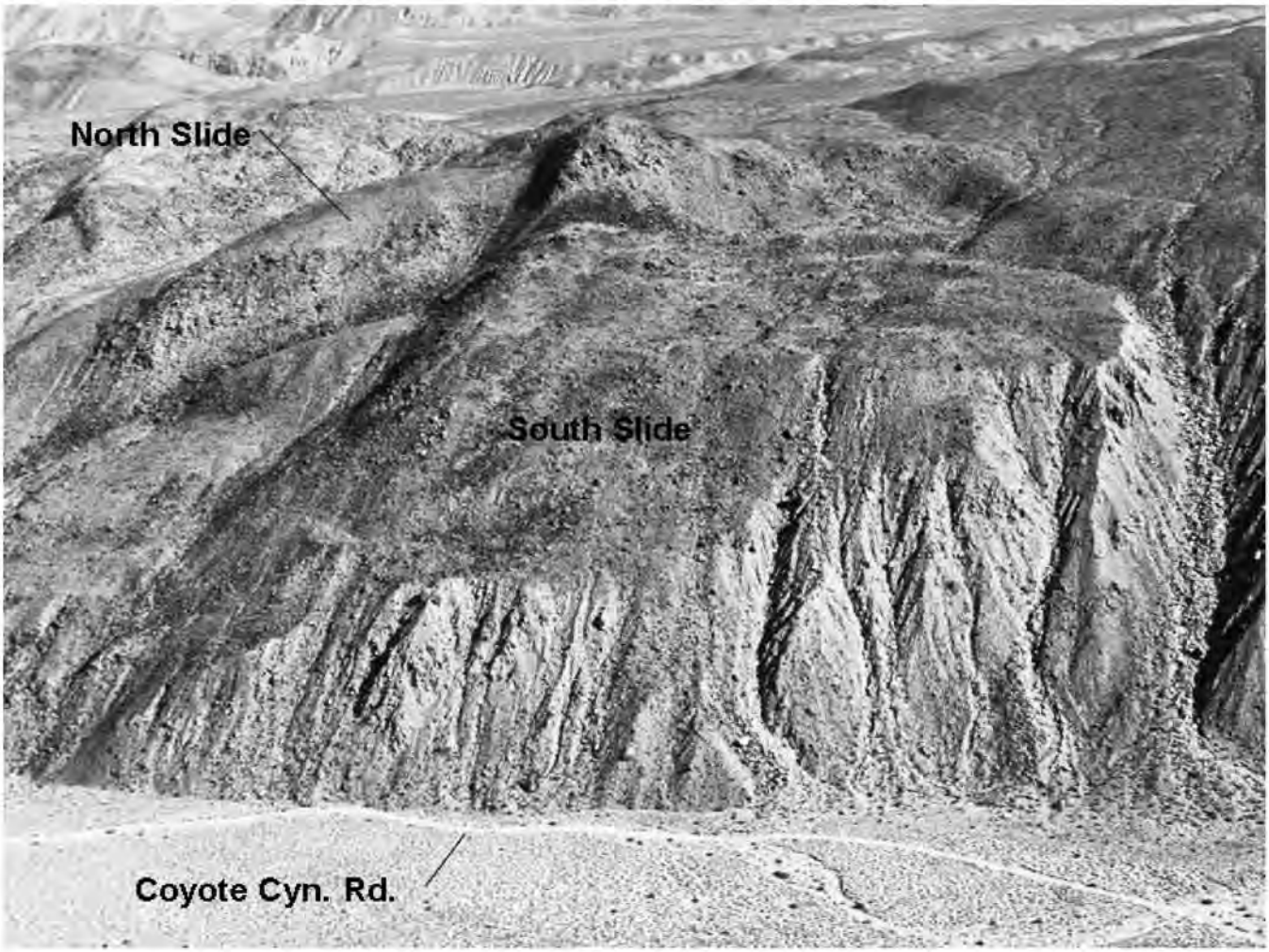

Figure 17. Alcoholic Pass landslides. View is to northeast from over Borrego Valley.

alluvium) to be the youngest of the larger landslides that have occurred on the western slopes of Coyote Mountain.

The most interesting aspect of these landslides is their failure mechanism. As is often the case, the basal rupture surface is not well exposed, and failure mechanisms must be inferred from the geologic and geomorphic characteristics of the slide. The failure surface of the north slide is not exposed, and there is only one poor exposure of the base of the south slide near Coyote Creek. At this location, approximately 30 ft (9 m) above the valley floor (Figures 16 and 19), the fractured rock that makes up the landslide debris overlies a sedimentary breccia that contains highly angular, cobble-sized, metamorphic and granitic clasts grading downward over a vertical distance of approximately 25 ft (7.6 m) to sandy, well-rounded cobble conglomerate resembling adjacent stream-terrace deposits. The outcrop does not expose that portion of the failure surface developed on bedrock.

Because of the high strength of homogeneous granitic rocks, large translational landslides often utilize existing low-strength planes of weakness in the rock, such as low-angle detachment faults, as basal rupture surfaces. This is not the case at Coyote Mountain, since the Coyote Creek and the Box Canyon faults either lie outside the zone of landsliding or have been demonstrated to dip nearly vertically in the vicinity of the landslides (Theodore and Sharp, 1975). Therefore, another mechanism must be responsible for the formation of the basal rupture surface. Several prominent scarps formed during incremental movement of the Coyote Ridge landslide are coincident with the headscarp and a prominent secondary scarp of the southern Alcoholic Pass landslide. This suggests that the landslides are related and have similar failure mechanisms.

It is here proposed that the Alcoholic Pass landslides are examples of translational landslides that developed from seismically induced incremental movement in highly fractured, massive granitic rocks.

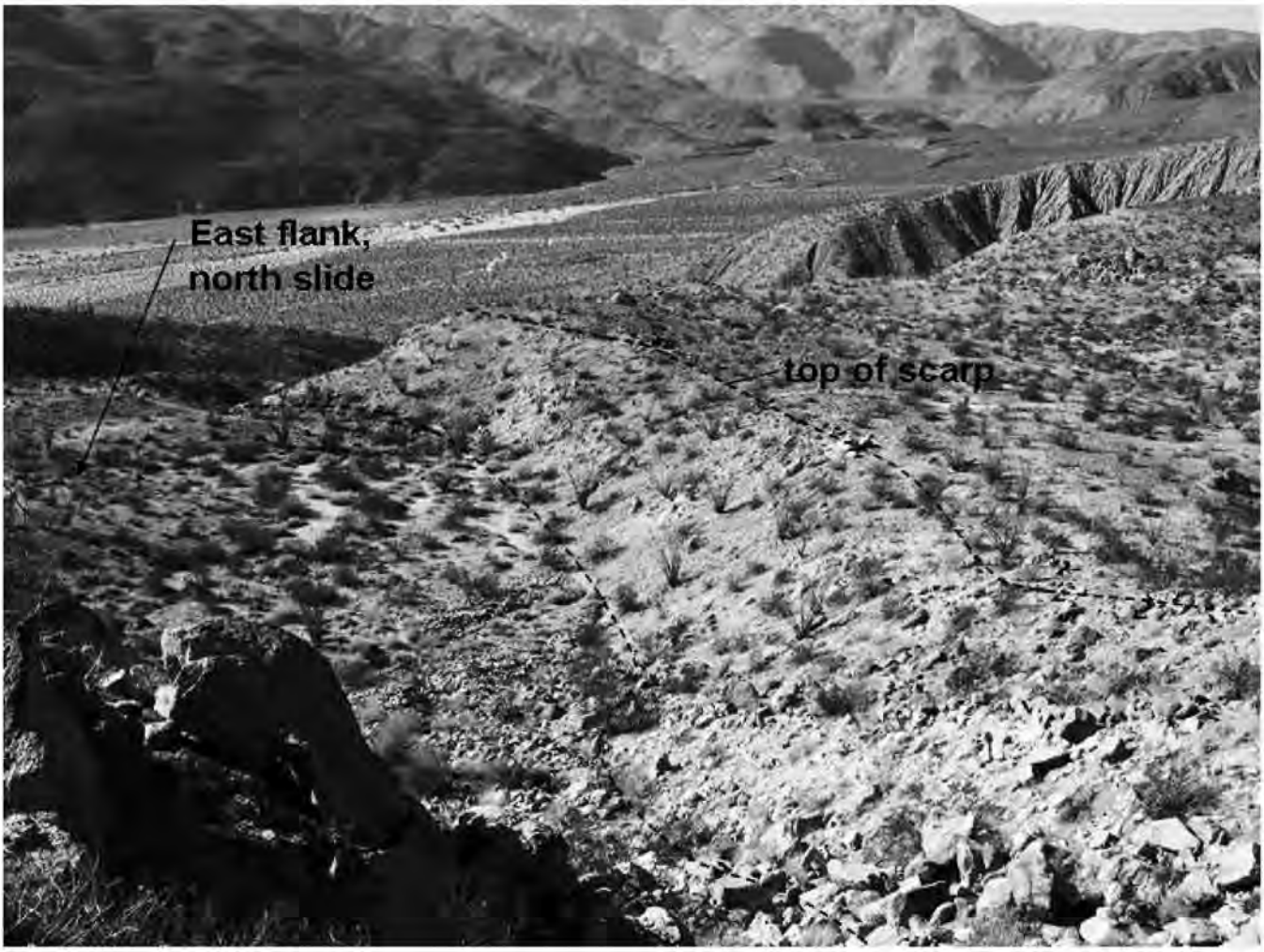

Figure 18. Northern Alcoholic Pass landslide and scarp in older alluvium on the eastern flank. Mouth of Coyote Canyon can be seen in the distance.

Since significant translational movement is necessary to produce the observed scarp heights and runout indicated by the exposure of the landslide debris overlying the alluvium shown in Figure 19, the landslides must have a continuous basal rupture surface. The most likely mechanism for the formation of such a surface is the joining of randomly oriented fracture surfaces through relatively small incremental movements. After sufficient movement has occurred, there would be high potential for a continuous slip surface to form. Once a slip surface has formed, the overall shear strength and resistance to fully developed translational movement would be greatly reduced.

CONCLUSIONS

Positive identification of very old and erosionally subdued landslides in granitic and metamorphic terrain in mountainous areas can be made by careful observation of stream cuts and other exposures. Certainty of identification depends on several factors, the most important of which are the age of last significant movement, the tectonic history of the host rock, and the quality of the outcrops. For relatively young landslides, identification can be made with certainty on the basis of classic landslide morphology alone. As the landforms become more subdued by erosion, differentiation of fracturing and shearing caused by active faulting and rock creep from that resulting from landsliding becomes increasingly more difficult and important. In the Peg Leg Smith landslide complex, evidence such as ponded alluvium in drainages located at head of the landslides and discontinuous arcuate and linear headscarps in combination with extensive zones of brecciation and sub-horizontal shearing combines to allow a high degree of certainty that landsliding is the responsible process. Because landslide-like geomorphic features are common in granitic and metamorphic rocks, there

Figure 19. Basal rupture zone exposed at the toe of the southern Alcoholic Pass landslide. Note how matrix-supported angular breccia clasts grade upward to clast-supported breccia.

should be a combination of structural and geomorphic evidence in order to have a high degree of certainty of landslide identification.

The south flank of the fully developed southern Alcoholic Pass landslide grades into a zone of incipient landsliding in massive tonalite. For this reason, it is postulated that the southern Alcoholic Pass landslide is an example of a fully developed translational landslide that developed from incremental movement in highly fractured, massive granitic rocks.

ACKNOWLEDGMENTS

The author thanks the reviewers, William Cotton and Robert L. Schuster, whose comments greatly improved the manuscript. Thanks also to Rupert Adams who assisted on several occasions in the field. A special thanks to Chuck Houser, geologist and pilot, for the photographic flights over Coyote Mountain.

REFERENCES

Baldwin, J., 1986, Martinez Mountain rock avalanche. In Guptill, P. D.; Ruff, R. W.; and Gath, E. M. (Editors), *Geology of the Imperial Valley, California*: Guidebook of the South Coast Geological Society, Santa Ana, California, pp. 37–48.

Bisci, C.; Dramis, F.; and Sorriso-Valvo, M., 1996, Rock flow (sackung). In Dikau, R.; Brunsden, D.; Schrott, L.; and Ibsen, M. (Editors), *Landslide Recognition*: Report 1 of the European Commission Environment Programme, Contract No. EV5V-CT94-0454, John Wiley & Sons Ltd., Chichester, UK, pp. 150–160.

Dramis, F. and Sorriso-Valvo, M., 1994, Deep-seated gravitational slope deformation, related landslides, and tectonics: *Engineering Geology*, Vol. 38, pp. 231–243.

Hart, M. W., 1991, Landslides in the Peninsular Ranges, southern California. In Walawender, M. J. and Hanan, B. B. (Editors), *Geological Excursions in Southern California and Mexico*: Geologic Society of America Guidebook for the 1991 Annual Meeting, Geological Society of America, Boulder, CO, pp. 349–365.

Radbruch-Hall, D., 1978, Gravitational creep of rock masses on slopes. In Voigt, B. (Editor), *Rockslides and Avalanches*, Vol. I: Elsevier Scientific, Amsterdam, pp. 607–657.

Shakal, A. F.; Huang, M. J.; and Darragh, R. B., 1994, Some implications of strong-motion records from the 1994 Northridge earthquake. In SMIP94: Proceedings of the Seminar on Seismological and Engineering Implications of Recorded Strong Motion Data, California Div. Mines & Geology.

Sharp, R. V., 1967, San Jacinto fault zone in the Peninsular Ranges of Southern California: *Bulletin Geological Society America*, Vol. 78, No. 6, pp. 705–730.

Theodore, T. G. and Sharp, R. V., 1975, *Geologic Map of the Clark Lake Quadrangle, San Diego County, California*: U.S. Geological Survey Map MF 644. Scale 1:24,000.

Varnes, D. J., 1978, Slope movement types and processes. In Schuster, R. L. and Krizek, R. J. (Editors), *Landslides Analysis and Control*: Special Report 176, Transportation Research Board Commission on Sociotechnical Systems, National Research Council, Washington, D.C., pp. 11–33.

Yarnold, J. C. and Lombard, J. P., 1989, A facies model for large rock-avalanche deposits found in dry climates. In Colburn, I. P.; Abbott, P.; and Minch, J. (Editors), *Conglomerates in Basin Analysis: A Symposium Dedicated to A. O. Woodward*, Vol. 62: Pacific Section, Society of Economic Paleontologists and Mineralogists, Book 62, pp. 9–32.

Environmental & Engineering Geoscience, Vol. XIV, No. 2, May 2008, pp. 81–96.
Reprinted by permssion.

OUR TREMBLING EARTH

PAUL REMEIKA
Anza-Borrego Foundation and Institute,
P.O. Box 2001, Borrego Springs, California 92004

Fig. 1. Quake Damage in Calexico's Red-Tagged Hotel de Anza. *All photos by Paul Remeika.*

"Earthquakes Shake Valley," "Quakes Jar Wide Area," "Quake Biggest Known in Desert," "Twin Quakes Jolt Area," "Aftershocks Keep Desert on Edge," "5.6 earthquake rattles region," "Desert Quakes Shake up the World of Geology," "Earthquake centered on active, dangerous fault," "7.2 quake rocks region." Harrowing newspaper headlines only scratch the surface. In the geological maelstrom of the Salton Basin, the magnitude (M) 6.6 Imperial Valley Quake of 1979, the M6.4 Westmorland Quake of 1981, the double-whammy M6.2 Elmore Ranch Quake on November 23rd followed by the M6.6 Superstition Hills Quake the next morning, and the recent Easter Sunday M7.2 El Mayor-Cucapah shaker along the Laguna Salada on April 4, 2010, were no more than passing yawns compared to some of the real whoppers of yesteryear, or the portending "Big One" expected to uncoil along the San Andreas Fault Zone between Bombay Beach and San Bernardino sometime within the next 30 years. As a product of fault movement, these earthquakes provide restless, bone-shaking evidence that a divergent tectonic plate boundary, separating the Pacific Plate from the North American Plate, is at work beneath the crust of the Salton Basin, of which the seismically-active Imperial-Mexicali Valley is its prominent southern half.

On a scale worthy of Genesis, a zigzag pattern of en echelon strike-slip faults, such as the Cerro Prieto, Imperial, and San Andreas, tears the land horizontally in a northwest right-lateral sense, offsetting in opposite directions the northernmost sea-floor spreading centers that have migrated up the Gulf of California. Like the seams on a baseball they define pull-apart basins along a plate boundary as Alta and Baja California rift and raft obliquely away from mainland Mexico opening up a new seaway filled by the Sea of Cortez. In doing so, new crust is generated beneath these basins at Cerro Prieto, Brawley Seismic Zone, and at the Salton Buttes.

Other dynamic faults, such as the brutally-powerful San Jacinto, Elsinore, Laguna Salada, and Sierra Juarez, stretch and thin the crust through dip-slip (vertical) motion with subordinate strike-slipping. They control elongated northwest-trending desert mountain ranges like the fault-bounded Sierra Cucapá, with its asymmetric sedimentary basin (Laguna Salada), both canted into the depths of the Salton Basin incompletely buried in a vast arena of sand and sea. These faults are responsible for uplifting the Peninsular Ranges, and widening of the valley making it one of the lowest and driest places on the North American continent.

As a daily consequence of faulting, or indigestion, earthquakes are dangerous natural hazards that annually

assault the troubled belly of the Salton Basin. Through a density of geologic time, this restlessness has triggered at least 34 legendarily-strong earthquakes (greater than M6.0) since 1850 within the basin. That is an onslaught of about one earthquake of M6.0+ every 4.6 years. Since 1954, the area has experienced 50 shakers measuring M5.0 or greater, and thousands of lesser events in one of the most geologically-intense places on Earth. Up until April 4, 2010, it had been 23 years since the last large temblor occurred within the basin (M6.6 Superstition Hills Earthquake on November 24, 1987).

DANCING WITH DEMONS

The Salton Basin is indeed restless, as quake-jittery residents of Brawley, El Centro, and Mexicali can attest to. The most recent swaying of the ground began between February 8 and 21, 2008, a swarm of 500 temblors rattled the ground beneath Guadalupe Victoria and the Cerro Prieto Volcano. The largest measured M5.4 on February 8th, and was powerful enough to knock-out electricity and cell phone service to over half-a-million people in Mexicali. This initial wake-up call was shortly followed by two modest aftershocks registering M5.1 and M5.0 on February 11th. More rumbles occurred on February 27th when six earthquakes measuring between M3.0 and M4.1 hit along the Imperial Fault. With good reason, these harbingers raised the blood pressure of the scientific community who sponsored a "Great Southern California Shakeout" drill on November 13, 2008, simulating a mock M7.8 temblor with a hypothetical epicenter beneath Bombay Beach along the eastern shore of the Salton Sea.

Fig. 2. Larry McCaffery straddles a crack on Mexico Route 2 south of Cerro el Centinela. Phillip Carskadan on right.

Ironically, four months later, between March 21 and 24, 2009, a handful of medium-sized M3.1-M3.3 quakes and several hundred smaller aftershocks rattled the Salton Buttes. In an on-going dance of crustal extension, one stretch recorded a shock every hour for 48 hours. In the middle of all this mayhem an M4.8 (March 24) thumper in the early morning hours followed later by an M3.5 (April 8) bump in the afternoon punched in where the San Andreas Fault meets up with the spreading center beneath Bombay Beach. The swarm continued for two more weeks triggering an unprecedented 400 micro quakes.

Any appreciable quietude south of the border did not last long as more shaking abruptly jolted Guadalupe Victoria and Cerro Prieto on March 29th (M4.2), April 11th (M4.2), April 12th (M4.3), and June 2nd (M3.0). Between November 1 and 3, 2009, the area of Heber and Calexico also got exciting when low-level seismic swarms along the Imperial Fault registering between M3.0-M4.1 gave residents a renewed appreciation for the power of nature. They were followed by a wrenching M5.8 quake on December 30th near Cerro Prieto and the Imperial Fault. Within minutes, this quake was felt as far away as Kern County, California. Most of the shaking occurred in and around Mexicali where 90,000 people lost power for half-an-hour. On January 9, 2010, March 31st, and April 4th, the peace and quiet of the same general area (Guadalupe Victoria) was shattered again at the M4.1, M4.2, and M4.3 levels, respectively. Hence, ominous warning signs that not only indicate a volcanically restless magma chamber beneath Cerro Prieto is set on medium-high but the stove itself is about to move.

EL MAYOR-CUCAPAH EARTHQUAKE

All preceding seismic activity in the Salton Basin pales in comparison to the Easter Sunday monster juggernaut M7.2 El Mayor-Cucapah Earthquake which stopped the clocks at 3:40 p.m. on the afternoon of April 4, 2010. This powerful temblor, sent seismograph needles jumping

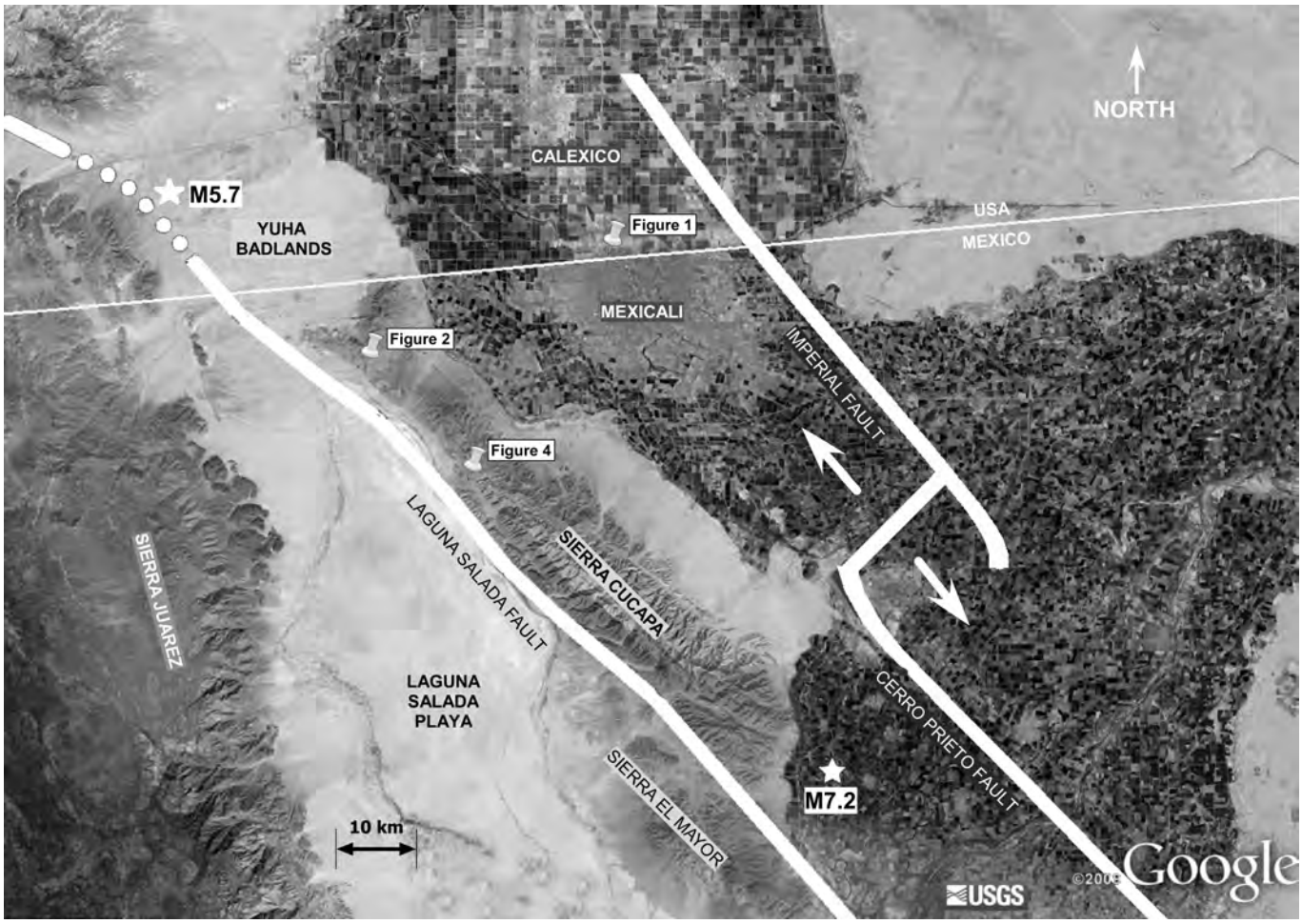

Fig. 3. Locations of faults, earthquakes, and photos discussed in the text. Graphic by Larry McCaffery and Paul Remeika.

nervously up and down on rolling graphs, as surface rupture scarred a swath of destruction 43 miles long, initially lifting parts of the Sierra El Mayor and Sierra Cucapá mountain ranges a record-setting 8 feet or more along the periphery of the Laguna Salada playa. This shaker was Baja and Alta California's largest earthquake in 18 years (since the M7.3 Landers Earthquake on June 28, 1992), was three times stronger than the M6.9 1940 El Centro Quake on the Imperial Fault, nearly twice as strong as the M7.1 1934 Mexicali Quake on the Cerro Prieto Fault, and the worst natural disaster felt in the Salton Basin since the M7.2 1892 blaster which incidentally occurred in the same general vicinity.

Within seconds the peace and quietude of the Imperial-Mexicali Valley was shattered. The main shock epicenter was shallow-seated, located on the southeastern end of the Laguna Salada Fault, only 11 miles west of the sparsely populated agricultural community of Guadalupe Victoria, and 29 miles south from Mexicali. In the maelstrom of the moment, ground motion, building in intensity and traveling at speeds of two miles per second, shook and shook and shook the Salton Basin for about 40 seconds, mercilessly jarring the entire region like a bowl full of Jell-O. So much energy was released that it transferred pent-up strain and stress onto nearby fault lines, triggering "aftershock" activity on the Imperial, Cerro Praetor, Elsinore, and the San Jacinto, which are overdue for a catastrophic rupture themselves. Incredibly, the enormous fury was felt by over 20 million people throughout the southland, swaying high rise buildings from Las Vegas to Santa Barbara, and from Phoenix to Ensenada. In Los Angeles and San Diego, popular amusement parks temporarily shut down as a precautionary measure. Understandably, the Governor's Office of Emergency Services and the San Diego and Imperial County Offices of Disaster Preparedness issued a formal "earthquake alert" for more damaging earthquakes to come within the Salton Basin.

In its aftermath extensive damage was reported in heavily-populated border communities. Quake-riddled Mexicali was hardest hit, suffering buckled and severed roadways, highways and railroad lines, broken gas and water pipelines, communication gridlock, fires, flooding,

and over one million people were without electrical power. Thousands of homes and businesses were destroyed or damaged leaving behind at least 35,000 people homeless. Making matters worse, 34% of the valley's agricultural crops were made unsuitable due to extensive leakage from broken canal levees, aqueduct spillage, liquefaction, or ironically, a lack of running water. Due to the intensity of ground shaking, many frightened residents moved into the streets surviving in tents and vehicles. By the next morning, 100 rumbling aftershocks in the M3.0-M4.5 range had occurred fraying everyone's nerves. 48 hours later, the total had climbed to 700. Two weeks later, the ground continued to nervously quiver from over 3,000 aftershocks. Structural damage, including property, business, and agricultural throughout Mexicali and surrounding communities was estimated at over $300 million. Incredibly, the earthquake only injured about 200 people and contributed to two deaths. By April 27th, over 6,000 aftershocks had been recorded making seismologists nervous since this seemed to be a higher rate than normal.

Fig. 4. Large fault scarp clearly visible east of the Laguna Salada playa. Phillip Carskaddan (left) and Larry McCaffery shown for scale.

North of the border, the entire downtown district of Calexico was declared off-limits due to tons of falling wreckage from collapsed ceilings, stucco walls, cladding, broken glass panes, retaining walls, and roofing tiles. Two story buildings sustained more structural distress than single story structures. Many were red-flagged, including the aging Hotel de Anza which suffered irreparable damage (Figure 1). The town's infrastructure also experienced problems as its main water clarifier was thrashed including 120 miles of broken waterline and sewage. Many mobile homes were knocked off their foundations, there were widespread power and telephone service outages, the Imperial airport terminal was put out of commission, and westbound lanes of Interstate 8 were temporarily closed due to cracking of the pavement. Property damage alone exceeded $91 million. By May 1st, schools continued to remain closed.

The El Mayor-Cocopah Earthquake is a breakaway margin event. Typical faulting is where rocks below the fault surface (the footwall block) drop or rise relative to rocks hanging over the fault surface (the hanging wall block), parallel to the dip of the fault surface. Canted up-and-down vertical orientation, or tilt-blocking, whereby a mountain block tends to lean to the east or to the west, such as the Sierra Cicada, is the hallmark of a breakaway margin, and attests to a stressed-out terrain that is literally ripping itself apart. Repetitive faulting with tilt-block rotation of elevated footwalls, evidence of highly varied, asymmetric dimension both vertically and laterally with growing accommodation of 15 feet or more , are not uncommon to the edge of a divergent rift boundary, such as along the western side of the Imperial-Mexicali Valley.

On June 14th, a M5.7 aftershock whipsawed the desert 5 miles south of the tiny community of Ocotillo. It was centered in a large cluster of aftershock sequencing at the northern terminus of the fault rupture west of Cerro el Centinel, bunching up along the eastern side of the Jacumba Wilderness Area north of the border. This post-quake dirge of activity is commonly associated with crustal stretching. In Ocotillo, the temblor shattered windows and cracked walls, broke pipes, and topped book cases. In San Diego, it briefly interrupted the Padres baseball game at Petco Park.

When rocks suddenly break along a fault and a massive temblor is unleashed, it can be a harrowing experience. Geologic aficionados can visit the fault scarp without much effort. The easiest place (Figure 2) is located along old Mexico Highway 2 in the saddle south of Cerro el Centinela (Signal Mountain), about 15 miles west of Mexicali. Here fresh cracks in the asphalt can be examined and traced northward across the California-Mexican border into the Yuha Badlands. It is here that clearly disturbed ground along the Borrego strand of the Laguna Salada

Fault reveals cumulative vertical displacements of about 2 feet, with lateral offsets even more. Two months after the main event, Highway 2 is still under repair as the ground continues to adjust. Another location is about 10 miles south along the eastern side of the Laguna Salada playa (Figure 4). If the lakebed is dry, it is worth the effort. After a 1 mile hike up an unnamed soft sandy wash, the 8-foot-high fault scarp is located on the Borrego Fault controlling a small strike valley where the Sierra Cucapá splits into west and east mountain ranges. Everywhere the ground is extensively cracked with rupture lines cutting crystalline basement as well as unconsolidated gravel veneers and arroyo bottoms. At the fault scarp, the land east of the fault has dramatically dropped down, while the west side has risen up, physically blocking all drainage channels in the arroyos. This is a spectacular example of a shutter ridge, since older arroyos are shingled one on top of the other, altered from similar past activity along the fault. Stay tuned for more shaking!

Note: As if to underscore Paul Remeika's last sentence in this piece, the Salton Basin landscape jolted again as we went press. A M5.4 earthquake occurred in Southern California at 4:53 pm (PDT) on July 7, its epicenter 13 miles north-northwest of Borrego Springs. The earthquake, triggered by the M7.2 El Mayor-Cucupah Earthquake, occurred on the Coyote Creek segment of the San Jacinto Fault. The earthquake exhibited sideways horizontal motion to the northwest, consistent with slip on the San Jacinto Fault. It was followed by more than 60 aftershocks of M1.3 and greater during the first hour. Seismologists expect continued aftershock activity.

Paul Remeika is a retired California State Park Ranger, and is an expert on the paleontology and geology of the Anza-Borrego Desert. He authored the best-selling book Edge of Creation: the Geology of Anza-Borrego Desert State Park®. He spends time as a Field Program Instructor and Guide for the Anza-Borrego Foundation and Institute. His field trips are very popular and include his special Desert Hostel visits onto the Colorado Plateau which are usually booked months in advance. He is currently completing freelance research on fossil footprints from the Colorado Desert.

Adapted with permission from: Remeika, Paul, 2010. Our Trembling Earth, Educational Bulletin #10-2, a publication of the Desert Protective Council, www.dpcinc.org

EARTHQUAKE ALMANAC

DATE	LOCATION	MAGNITUDE	FAULT OR FAULT ZONE
unknown date	Canebrake	M7.0+	Elsinore
December 26, 1775	Terwilliger Valley	M5.2	San Jacinto
November 29, 1852	Volcano Lake	M6.5	Cerro Prieto
December 16, 1858	San Bernardino	M6.0	San Jacinto
November 15, 1875	Imperial Valley	M7.0	Imperial
February 9, 1891	San Jacinto	M6.3	San Jacinto
July 30, 1891	Colorado River Delta	M7.0	Cerro Prieto
February 23, 1892	Laguna Salada	M7.2*	Laguna Salada
May 28, 1892	Hemet	M6.3	San Jacinto
October 23, 1894	Julian	M5.6	Elsinore
July 22, 1899	Cajon Pass	M6.5	San Andreas
December 25, 1899	San Jacinto	M6.8	San Jacinto
January 23, 1903	Colorado River Delta	M7.0	Cerro Prieto
April 19, 1906	Imperial Valley	M6.0	Imperial
September 20, 1907	San Bernardino	M6.0	San Jacinto
June 22, 1915	El Centro	M6.1	Imperial
June 22, 1915	El Centro	M6.3	Imperial
November 20, 1915	Cerro Prieto	M7.1	Cerro Prieto
April 21, 1918	San Jacinto	M7.2	San Jacinto
July 23, 1923	San Bernardino	M6.2	San Jacinto
December 31, 1934	Mexicali	M7.1	Cerro Prieto
March 25, 1937	Terwilliger Valley	M6.0	San Jacinto
May 18, 1940	El Centro	M6.9	Imperial
April 9, 1941	Northern Gulf of California	M6.0	Cerro Prieto
October 21, 1942	Fish Creek Mountains	M6.5	Superstition Hills
December 4, 1948	Desert Hot Springs	M6.5	San Andreas (Mission Creek)
November 4, 1949	Northern Baja California	M5.7	Sierra Juarez
June 13, 1953	Imperial Valley	M5.5	Imperial
March 19, 1954	Arroyo Salado	M6.4	San Jacinto (Clark)
November 12, 1954	Northern Baja California	M6.3	Sierra Juarez
February 9, 1956	El Alamo, Baja California	M6.8	Cerro Prieto
April 9, 1968	Borrego Mountain	M6.5	San Jacinto (Coyote Creek)
April 28, 1969	Borrego Valley	M5.8	San Jacinto (Coyote Creek)
October 15, 1979	Imperial Valley	M6.6	Imperial
April 26, 1981	Westmorland	M6.4	Imperial
July 8, 1986	North Palm Springs	M5.9	San Andreas (Banning)
November 23, 1987	Elmore Ranch	M6.2	Elmore Ranch
November 24, 1987	Superstition Mountain	M6.6	Superstition Hills
January 25, 1988	Sierra Juarez	M5.1	Sierra Juarez
April 22, 1992	Desert Hot Springs	M4.6	San Andreas (Mission Creek)
April 22, 1992	Joshua Tree National Park	M6.1	Eureka Peak
June 28, 1992	Landers	M7.3**	Landers and related strands
June 28, 1992	Big Bear	M6.6	unknown transcurrent fault
February 8, 2008	Sierra Cucapa, Baja	M5.4	Laguna Salada
February 11, 2008	Cerro Prieto, Baja	M5.1, M5.0	Imperial
February 19, 2008	Sierra Cucapá, Baja	M5.0	Laguna Salada
December 30, 2009	Guadalupe Victoria, Baja	M5.8	Laguna Salada
April 4, 2010	El Mayor-Cucapah, Baja	M7.2*	Laguna Salada
May 8, 2010	El Mayor-Cucapah	M4.8	Laguna Salada-Elsinore
June 12, 2010	Coyote Canyon	M4.9, M4.5	San Jacinto (Coyote Creek)
June 14, 2010	El Mayor-Cucapah	M5.7	Laguna Salada-Elsinore

* Salton Basin's strongest earthquakes
**Outside Salton Basin but too close to ignore

A Preliminary Pseudostatic Analysis of a Large Rockslide near the San Jacinto Fault, Southern California

Nissa Morton
Department of Geological Sciences
San Diego State University

ABSTRACT

Seismically-induced landslides are a common occurrence in steep terrains near active fault zones. Geomorphic evidence suggests the presence of multiple large-scale (5-6 km^2) landslides along the southwestern side of the Santa Rosa Mountains and adjacent to the Clark Strand of the San Jacinto Fault. These landslides occur in Cretaceous-age granite and may be analyzed for ground motion characteristics at failure through pseudostatic slope stability analysis. A selected rockslide was reconstructed and analyzed for failure along a polygonal slip surface. Critical seismic accelerations (kc) of between 0.18g and 0.30g were determined depending on the angle of basal slip, and are to be considered the *minimum* acceleration due to default parameters used in the analysis. Correlative magnitudes for the estimated volume of the rockslide indicate an event of M_W 7.2-7.6 for the triggering earthquake, which has not been observed historically on the San Jacinto Fault.

INTRODUCTION

It is a common occurrence for steep or unstable slopes to reach threshold conditions during an earthquake and become landslides. Formal study of the relationships between earthquakes and landslides dates to the 1783 earthquake near Calabria, Italy, which caused widespread landsliding, including several exceptionally large slides (Keefer, 2002). Study of such relationships is essential as landsliding can be a significant cause of damage and casualties associated with earthquakes. It has been shown that earthquakes of a threshold magnitude of Mw 4.3±0.4 will trigger landslides (Malamud et al., 2004). As such, analyses of slope stability are an important part of mitigating this hazard in seismically active areas. Three common approaches to analyze slope stability during an earthquake are: (1) numerical methods that use stress-strain relationships to calculate expected displacements, (2) Newmark's method of equation integration to evaluate displacement of rigid-block displacement, and (3) pseudostatic analysis of slope stability at different seismic accelerations to determine the factor of safety (Bojorque and De Roeck, 2007). For the purposes of this study, the pseudostatic approach will be used. As described by Hack, et al. (2007), the factor of safety (Fs) under pseudostatic conditions is expressed by the following equation:

$$Fs = \text{resisting stresses/driving stresses} = \frac{coh + ((W-\beta W)\cos\theta - \alpha W\sin\theta - u)*\tan\phi}{(W-\beta W)\sin\theta + \alpha W\cos\theta + v\cos\theta}$$

where coh=cohesion or respective friction along discontinuity, ; ϕ=angle of internal shear; ɵ=slope of discontinuity; W=weight of block; u and v are the water pressures in the discontinuities; αW and ßW are horizontal and vertical acceleration due to an earthquake. Failure occurs at Fs = 1.

Back analysis of landslides induced by earthquakes can provide insight into the characteristics of ground motion at the time of failure. Such studies have proven useful for analysis of rotational slides within weak materials such as tufa (Luo et al., 2005), translational slides within materials exhibiting moderate strength such as shale and sandstone (Chen et al., 2003), and rockslides within granite (Havenith, et al., 2002). Here we present an analysis of a large rockslide within granitic rock, located adjacent to an active fault in southern California (Figure 1).

Figure 1: Map View of Project Area

GEOLOGIC AND TECTONIC SETTING

The Santa Rosa Mountains block is a member of the Peninsular Ranges of southern California, and is comprised of various Cretaceous granitic and metamorphic rocks. The physiography of these mountains has effectively been altered by the San Jacinto Fault Zone, a complex system of

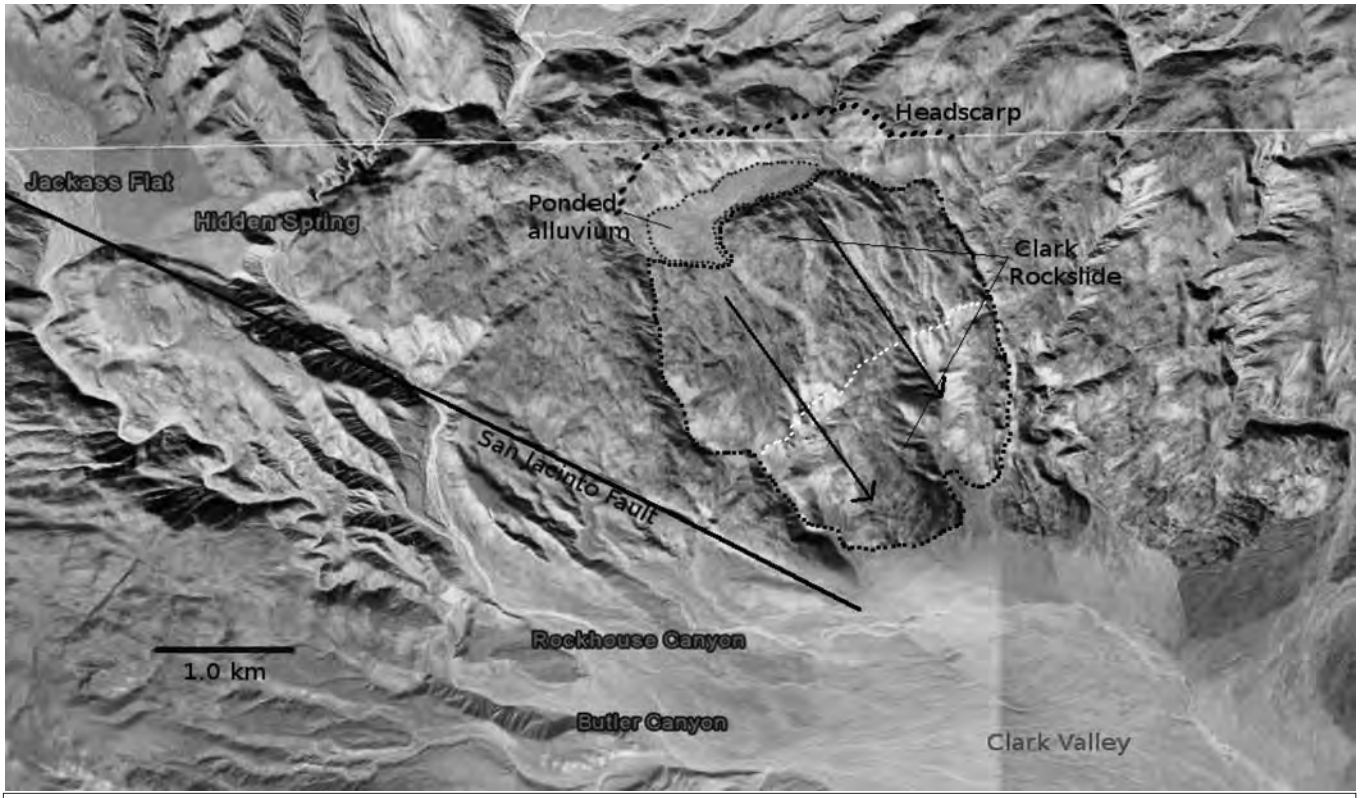

Figure 2: Aerial Photograph of Project Area Showing Key Features. Clark Rockslide outlined by black dots, headscarp-dashed black lines, minor scarp-dashed white lines, ponded alluvium-outlined gray hashes, San Jacinto Fault (approx.)-black line

young and active strike-slip fault segments (Sharp, 1967). Faulting activity has resulted in distinct morphologic features within the fault zone, including landslides (Dorsey and Roering, 2006). Along the southwest side of the Santa Rosa Mountains, the Clark segment of the San Jacinto Fault trends southeast into Clark Valley, where it becomes buried in alluvium. Within Clark Valley, Sharp (1967) has mapped several large granitic masses outcropping in this alluvium as "probable landslide blocks". The source bedrock for these blocks is medium-grained, hornblende-biotite tonalite. On the opposite side of Clark Valley, landslides have also been mapped within the granitic and metamorphic rock along Coyote Mountain (Hart, 2008). Considering the high strength of the source bedrock of these slides, failure was likely induced along fractures by intense seismic shaking during rupture of the San Jacinto Fault. The earthquake magnitude required for such events is as yet unknown. Historically, the San Jacinto Fault Zone has produced earthquakes with moment magnitudes ranging from 5.6 to 6.8; it has been postulated however, that a multiple segment rupture could produce a Mw 7.5 or greater (Sanders and Magistrale, 1997).

GEOMORPHIC EVIDENCE

In addition to the "probable landslide blocks" mapped by Sharp (1967), other probable landslide blocks are found within the granitic rock along the southwestern side of the Santa Rosa Mountains. The best expressed of these is the Clark Rockslide (Figure 2).

The Clark Rockslide covers an area of approximately 5-6km2. The headscarp is somewhat sinuous and reaches a maximum height of 150 meters. The total height of the rockslide from toe to crown is about 685 meters, and total length is approximately 3.75 km. Immediately below the headscarp is a benched area with ponded alluvium that has been mapped by Sharp (1967) as terrace deposits. The margins of the slide are here inferred as arcuate drainages that drain the head of the rockslide. The steep slopes of these drainages indicates incision within weak or possibly sheared rock. A minor scarp is delineated by a moderately eroded bench in the middle-portion of the slide mass. As depicted in Figure 2, the Clark segment of the San Jacinto fault is less than 2 kilometers from the center of the Clark Rockslide.

Preliminary field reconnaissance of the slide mass has not found structural evidence of landsliding similar to that exposed on Coyote Mountain and described by Hart (2008). It may be that such evidence is buried and not exposed in available stream cuts. However, stream cut exposures did reveal continuous high angle fractures (60°-85°) and a variety of often discontinuous low angle fractures, the

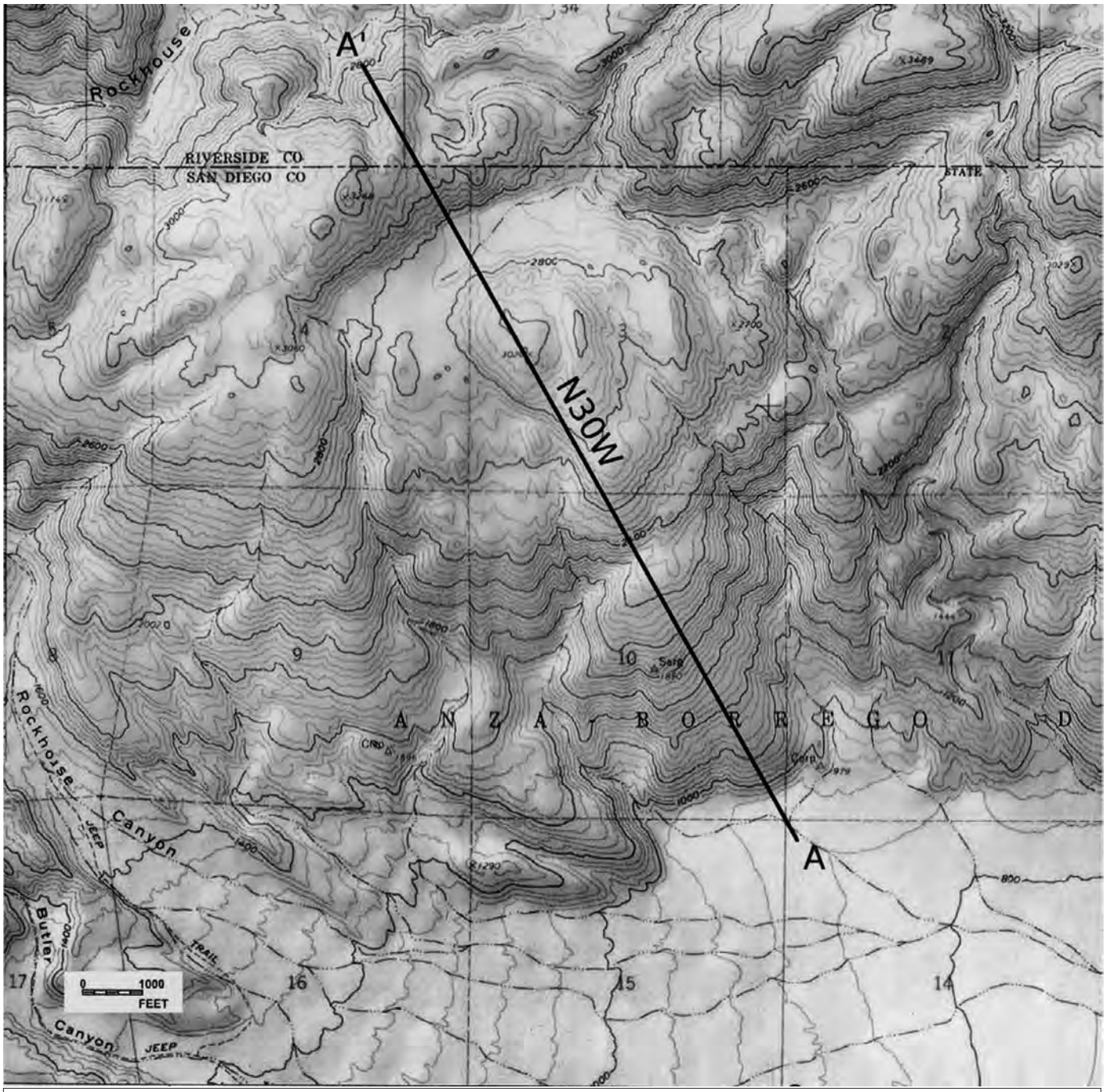

Figure 3: Map View of Clark Rockslide Showing Location of Cross-Section Used in Analysis.

presence of which is considered indicative of potential failure surfaces at depth.

SLOPE STABILITY MODELING

A cross-section was constructed from composite USGS 7.5' quads for the project area (Figure 3). Section A-A' was drawn through the center of the slide mass and extends beyond the prominent headscarp previously described. The current slope configuration is presented as Figure 4a. In order to conduct a back analysis of the Clark Rockslide, the original slope was reconstructed in cross section by closure of the head and minor scarp and lateral recession of the toe. The reconstruction resulted in an increase of average slope angle from approximately 10.5° to 16° and a toe recession of 1210 meters. The reconstructed slope configuration is presented as Figure 4b.

The reconstructed slope was analyzed for failure using the demo version GEO5 Rock Stability program. The failure surface was defined as polygonal, consisting of two planes

along low and high angle fractures within the granite, as supported by field evidence. Three inclinations of a low-angle basal slide plane were analyzed (5°, 10° and 15°), each using a 75° bounding tension crack for the upper block slide plane (Figure 4c). Rock parameters included rock density of 160 pcf, cohesion of 200 psf, and an angle of internal shear of 30°. Pore pressure was not considered in this analysis as the projected slide planes reach a depth and pressure such that water is anticipated to have a negligible effect on slide conditions.

Initial stability analysis of the reconstructed slope during static conditions produces a safety factor range of 2.17-3.69, indicating that the rockslide could only fail with the influence of seismic activity. The reconstructed slope was then analyzed using different seismic accelerations to determine the acceleration condition at failure (Fs=1.0), also known as the critical seismic acceleration (kc). Identical vertical (kv) and horizontal (kh) accelerations were used for each analysis as a means of consistency. The results of these analyses are presented in Figure 5 and indicate increasing critical seismic accelerations for decreasing angles of basal slip plane.

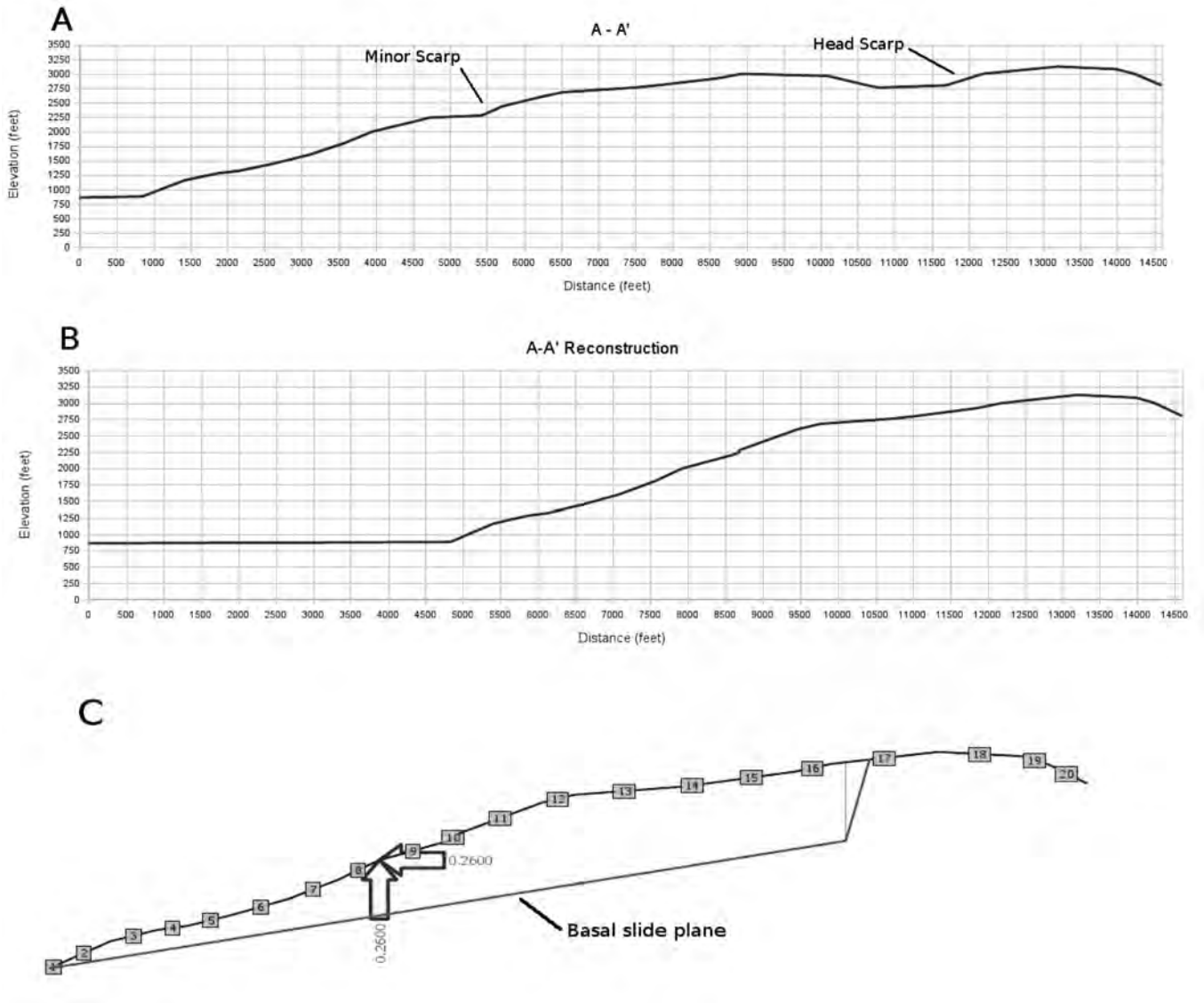

Figure 4: (a) Current Configuration of Clark Rockslide in Cross Section Showing Headscarp and Subscarp Locations.
(b) Reconstructed Configuration of the Slope.
(c) Example Configuration of Slope Stability Analysis. The basal slide plane has an inclination of 10°, arrows show direction of seismic acceleration.

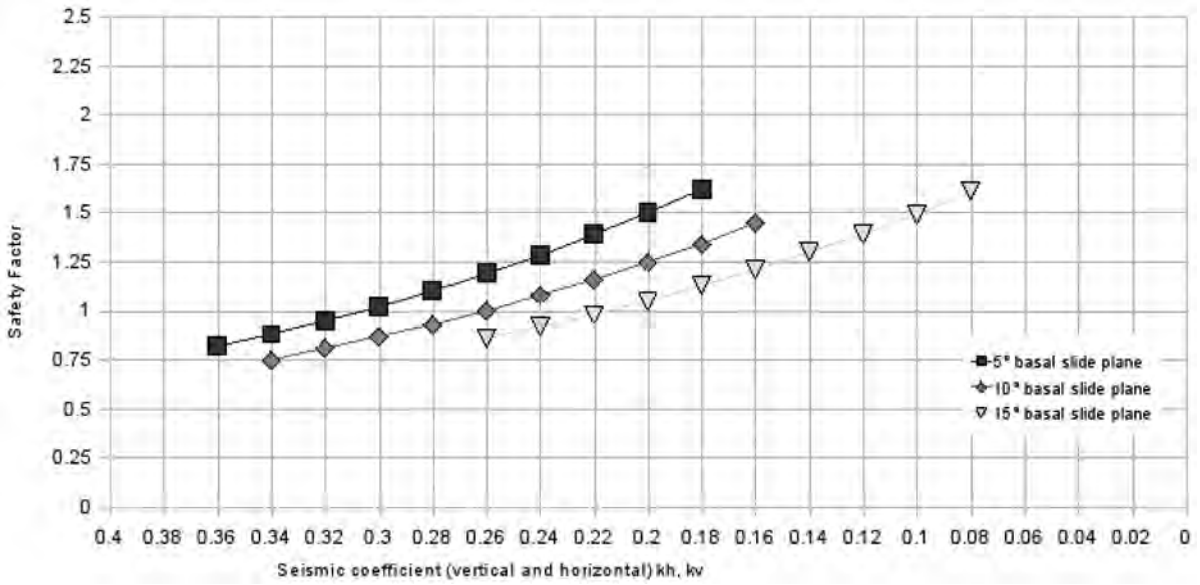

Figure 5: Results of Pseudostatic Geo5 Rock Stability Analysis.
(kc) values for basal slip plane: ~0.30g(5°); ~0.26g(10°); ~0.22g (15°)

DISCUSSION

It must be noted that the critical seismic acceleration range produced in this analysis is expected to reflect a minimum value. The default parameters provided by Geo5 and used in this analysis—cohesion (C) 200 psf and angle of internal shear (ϕ) 30°--make a significant underestimation of the strength of the granite. Weathered granite has been shown to have such high strength parameters as C=6500 psf and ϕ=55.5° (Baynes and Dearman, 1978). As slip is anticipated to have occurred along fractures, the actual C and ϕ for the fractured granite are anticipated to be much closer to that of weathered granite than the default parameters. The results of the analysis should thus be treated as minimum values for critical seismic acceleration.

Seismic ground motions are understood to be a function of specific source, path, and site characteristics. The critical seismic acceleration for the presented analysis is determined to be between 0.22 and 0.30g. Because the Clark Rockslide is situated adjacent to the San Jacinto fault, accelerations during rupture are expected to be at or near peak values. Seismic accelerations may also be especially high at this location due to topographic amplification.

The critical seismic acceleration results are consistent with the ground motion hazard model developed for the region by Cao et al. (1996) based on a magnitude 6.5 event or smaller. According to their study of recorded seismicity patterns in southern California, peak ground accelerations (PGA) in the vicinity of the Clark segment of the San Jacinto Fault are anticipated to be between 0.30 and 0.35g. As our highest (kc) result is equivocal to the lowest anticipated PGA for a magnitude 6.5 event, the rockslide triggering event may be inferred to be of magnitude 6.5 or less. However, as previously described, our (kc) results are to be considered minima and a magnitude greater than 6.5 should be expected for the triggering event of the Clark Rockslide. Additionally, as two recorded earthquakes in vicinity of the Clark Rockslide—a 1937 event of Mw 5.6 and a 1954 event of Mw 6.3 (Sanders and Magistrale, 1997)--did not result in significant landslide events, the triggering event is furthermore expected to be of greater magnitude.

Another method of analysis that may be used to estimate the magnitude of a triggeringevent does not require back-analyzed seismic acceleration. Based on sixteen historic landslides triggered by earthquakes, Malamud et al. (2004) have determined a power law dependence of total landslide volume (VLT) on earthquake moment magnitude (M) (Figure 6). This correlation is expressed as

$$\log V_{LT} = 1.42M - 11.26\ (\pm 0.52)$$

Based on the predicted configurations of slope failure analyzed here, the volume of the Clark Rockslide is estimated to be between 0.08km3 and 0.32km3. This corresponds to a triggering moment magnitude event of between 7.2 and 7.5. While such an event has not happened historically, it has been postulated that a multiple segment rupture could produce a Mw 7.5 or greater (Sanders and Magistrale, 1997). Analysis suggests that the event that triggered the Clark Rockslide may be the result of such an event.

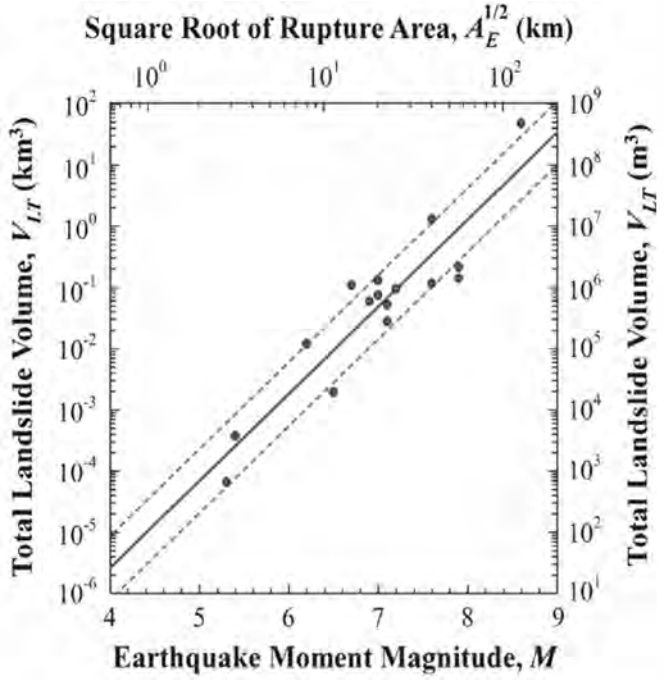

Figure 6: Total Landslide Volume as a Function of Earthquake Moment Magnitude. Solid line represents least-square best-fit line to data (From Malamud et al., 2004)

The Clark Rockslide provides strong geomorphic evidence for bedrock landsliding induced by a large earthquake on the Clark segment of the San Jacinto Fault. In order to properly back analyze the critical seismic acceleration, appropriate strength parameters need to be considered. Additional stability analysis may include other methods than the polygonal slip surface configuration used here, such as three-dimensional modeling, rotational failure or Newmark's integration method. Given the numerous landslides expressed in the landscape adjacent to the San Jacinto fault, a back-analysis model may provide yet another tool for the study of large earthquakes beyond historical records.

REFERENCES

Baynes, F.J., and Dearman, W.R., 1978, *The relationship between the microfabric and the engineering properties of weathered granite*; Bulletin of the International Association of Engineering Geology, No 18, p.191-197.

Bojorque, J., and De Roeck, G., 2007, *Determination of the critical seismic acceleration coefficient in slope stability analysis using finite element methods*, Structural Mechanics, Katholieke Universiteit Leuven, p.8.

Chen, Tien-Chien; Lin, Meei-Ling, and Hung, Ju-Jiang, 2003, *Pseudostatic analysis of Tsao-Ling rockslide caused by Chi-Chi earthquake*; Engineering Geology, Vol 71, p.31-47.

Cao, T, Petersen, M.D., and Reichle, M.S., 1996, *Seismic Hazard Estimate from Background Seismicity in Southern California*; Bulletin of the Seismological Society of America, Vol 86, No.5, p.1372-1381. October ..

Dorsey, R.J., and Roering, J.J., 2006, *Quaternary landscape evolution in the San Jacinto fault zone, Peninsular Ranges of Southern California: Transient response to strike-slip fault initiation*; Geomorphology Vol 73, p.16-32.

GEO5 Geotechnical Analysis Software, Rock Stability, demonstration version; gINT Geotechnical and Geoenvironmental Software. *User's Guide* p.634-635.

Hack, R., Alkema, D., Kruse, G.A.M., Leenders, N., and Luzi, L., 2007, *Influence of earthquakes on the stability of slopes*; Engineering Geology Vol 91, p.4-15.

Hart, M.W., 2008, *Structural and geomorphic characteristics of landslides at Coyote Mountain, Anza-Borrego Desert State Park, California*; Environmental and Engineering Geoscience, Vol XIV, No.2, p.81-96.

Havenith, H-B, Jongmans, D., Faccioli, E., Abdrakhmatov, K., and Bard, P-Y., 2002, *Site effect analysis around the seismically induced Ananevo Rockslide, Kyrgystan*; Bulletin of the Seismological Society of America, Vol 92, No. 8, pp.3190-3209, December .

Keefer, David K., 2002, *Investigating landslides caused by earthquakes—a historic review*; Surveys in Geophysics, Vol 23, p.473-510.

Luo, H.Y., Zhou, W., Huang, S.L., and Chen, G., 2004, *Earthquake-Induced Landslide Stability Analysis of the Las Colinas Landslide in El Salvador*; Int. J. Rock Mech. Min. Sci. , Vol 41, No. 3., Paper 2B 26.

Malamud, B.D., Turcotte, D.L., Guzzetti, F., and Reichenbach, P., 2004, *Landslides, earthquakes, and erosion*; Earth and Planetary Science Letters, Vol 229, p.45-59.

Sanders, Christopher, and Magistrale, Harold, 1997, *Segmentation of the northern San Jacinto fault zone, southern California*; Journal of Geophysical Research, Vol 102, No.B12, p.27,453-27,467, December 10, 1997.

Sharp, R.V., 1967, *San Jacinto Fault Zone in the Peninsular Ranges of Southern California*; Geological Society of America Bulletin, Vol 78, p.705-730, 7figs., 3 pls., June.

Large Landslide North of Clark Lake.

Large Landslides North of Clark Lake

Charles F. Lough

At the north edge of Clark Valley there is a group of very large landslides composed largely of granitic rock. The landslide mass is approximately 11 x 4 km (7 x 2 ½ miles), with individual slides up to 1.6 km (1 mile) wide. Many of the slides are cut by secondary slides. They show extremely well on aerial photographs, fairly well on a shaded relief topographic map, and poorly on Google Earth. An attempt was made on the accompanying map to show individual slides by shading.

I mapped these slides in the 1990's as part of a series of geological hazard maps covering all of San Diego County. Copies of the original map were sent to Rebecca Dorsey at the University of Oregon and Bret Cox at the United States Geological Survey, both of whom are mapping in the Santa Rosa Mountains. I supplemented my original mapping, which only extended as far north as the Riverside County Line; with maps by Dorsey (2002) (SW corner), Sharp (1967) (Riverside County), and Ryter (2002) (SE corner). More recently, Nissa Morton (2009) did a stability analysis on a portion of the landslide mass.

Interpretation and Origin

In attempting to compile a map from various sources, problems were revealed. The first is that interpretation and contacts do not match. For instance, Sharp's map does not show the landslides at all, but it does show considerable detail at the head of the slide. No previous report attempts an explanation of the cause of the landsliding. Rather than laying out the answer for the origin of the landslides, I will just present some alternatives for your consideration.

Off of the Santa Rosa Mountains Scarp

A likely appearing source for the landslides is the steep west-facing scarp of the Santa Rosa Mountains. Failure most likely would have been along a fault plane. A high-angle normal fault would be the usual explanation for such a steep mountain front. Paul Remeika believes there is a major high-angle normal fault along the toe of the mountains. Derek Ryter sketched in a Santa Rosa Fault in the NW corner of his map. Robert Sharp shows the Buck Ridge Fault heading toward the base of the mountains. However, I do not believe that the structure along the scarp of the Santa Rosa Mountains has yet been adequately explained. Speculation about the structure along the mountain front should, for the time being, remain just that—speculation. Access is difficult; but someone carrying plenty of water, but no preconceived ideas, needs to carefully map the base of the Santa Rosas.

Arguments against the landslides coming from the scarp of the Santa Rosa Mountains are twofold: First, the outcrop patterns on the scarp and at the head of the slides do not match. On the scarp, granitic rock is above schist; but at the head of the slides (area mapped by Sharp) schist occurs north of the granitic rock. Second, the schist appears to be continuous from Buck Ridge across Rockhouse Canyon. Furthermore, these large landslides do not appear to have traveled far. They are definitely not long-runout landslides. They have traveled just far enough to develop the characteristic shapes typical of landslides. Nissa Morton assumed that the Clark Rockslide was locally derived and moved 0.8 to 1.1 km (based on her cross sections).

Off of Detachment Fault

Another possibility is that the large landslide came off of the southwesterly dipping limb of a detachment fault. Douglas English (1985) proposed that the detachment fault clearly exposed on the east side of the Santa Rosa Mountains "arches up and over the crest of the range." His report includes a map and cross sections that show the Santa Rosa and San Jacinto Mountains as a very large dome. Neither English nor anyone else has followed up on this idea by careful field mapping, which would support **or disprove this idea.**

It is conceivable that the faults mapped by Sharp across the head of the large landslides are actually part of the back folded limb of a folded detachment fault. If this is so, the large landslides at the head of Clark Valley would be analogous to those mapped by Mike Hart (1991) on the south side of Whale Peak. Those slides seem clearly to have come off of the south dipping limb of the folded detachment fault that arches over Whale Peak.

Off of Buck Ridge Fault

A third possibility is that the large landslides came off of the Buck Ridge Fault. This fault can be clearly traced for 25 km to the head of Rockhouse Valley and, with a lesser degree of confidence, for another 12 km to the base of the Santa Rosa Mountains at the NE corner of the landslides. Sharp (1967) shows the fault buried beneath the alluvium of the valley, and reappearing near the head of the large landslide. He shows faults cutting what I believe to be landslides on the west end and south sides of Mojave Valley.

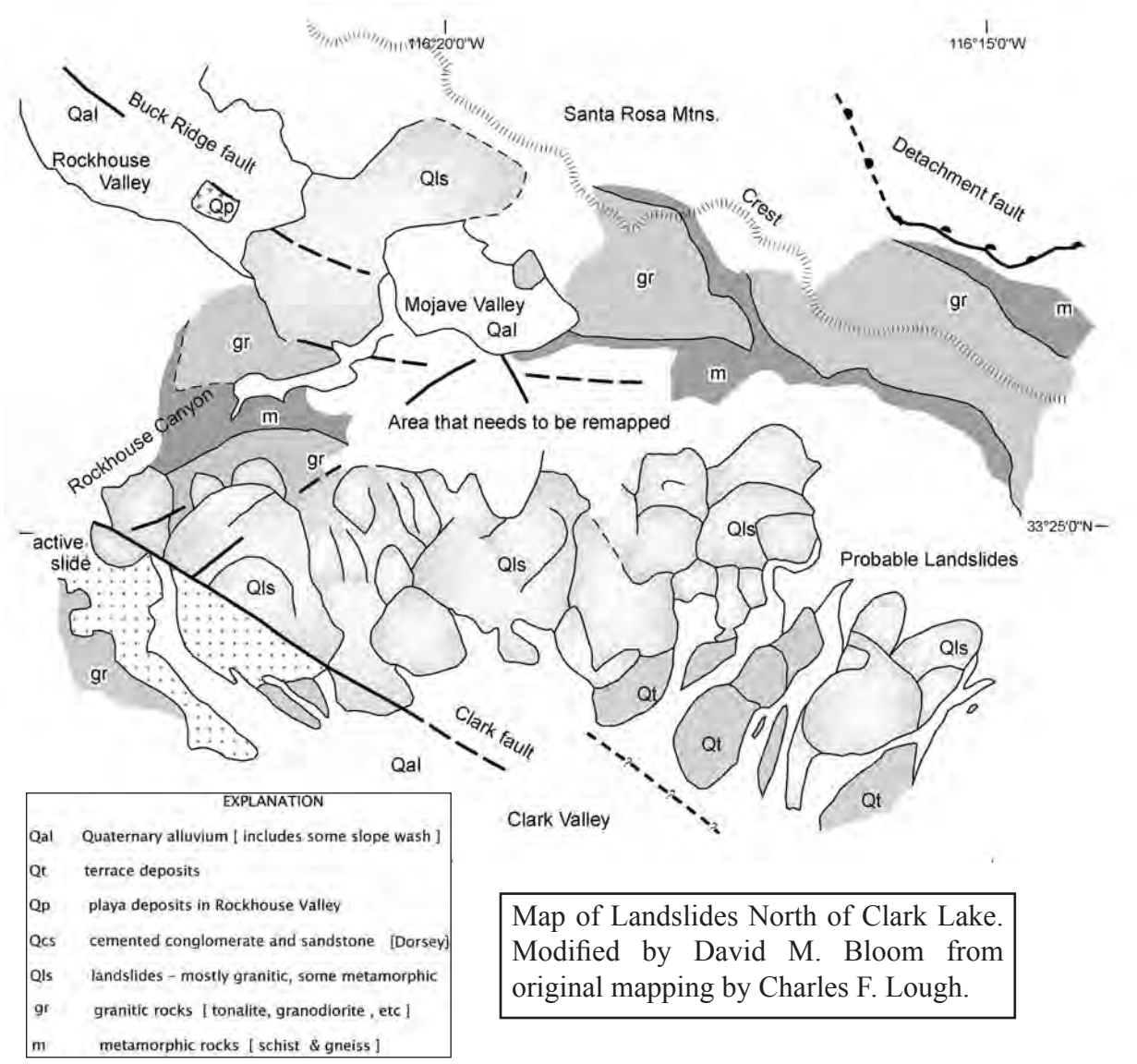

Map of Landslides North of Clark Lake. Modified by David M. Bloom from original mapping by Charles F. Lough.

But, these "faults" are not necessarily part of the Buck Ridge Fault. They may be landslide scarps, fault planes displaced by landslides, contacts, or part of a detachment fault. In other words, I don't understand this structure at the head of the large landslides found immediately north of the Riverside County Line. I believe that area needs to be carefully remapped, keeping all options in mind.

Off of Older Structures

Yet another possibility is that the large landslides resulted from failure on a plane of weakness that predates the strike-slip fault system. Perhaps they failed along the contact between metamorphic rocks (schist and gneiss) and granitic rocks. (A short hike up Rockhouse Canyon takes you to excellent exposures of metamorphics at Hidden Spring.) And/or failure could have occurred faults that predated the strike slip faults. A vertical view (aerial photographs or Google Earth) of the NW corner of the landslides reveals several small NE trending faults or fractures.

The Event

Whatever the exact origin of the landslides, they most likely came from a zone of damaged rock at the intersection of Buck Ridge and other faults. Motion on the Clark Fault probably both allowed and caused these landslides. Right-lateral motion on the Clark Fault would have removed lateral support from the fractured rock to the NE, allowing the landslides to occur. A major earthquake on the Clark or Coyote Canyon faults likely caused the collapse.

Origin of Rockhouse Canyon

There is another interesting problem to solve in the

immediate vicinity of the large landslides. At the NW corner of the slides, Rockhouse Canyon cuts across bedrock in the nose of Buck Ridge. There is no obvious plane of weakness along the canyon, such as a fault to explain the presence of a canyon.

For an answer, I would suggest something like this: The hills between Rockhouse Valley and Mojave Valley are a landslide that came off the Santa Rosa Mountains scarp, blocking the original drainage toward Clark Valley. Rockhouse Valley gradually filled with alluvial fans and some playa sediments. (A small patch of fine-grained sediments remains near the former site of Cottonwood Spring.) When Rockhouse Valley was filled to the level of the present rim of Rockhouse Canyon, drainage could flow across the nose of Buck Ridge, cutting the canyon. Subsequently, drainage from Mojave Valley was captured.

References

Calzia, J.P., Madden-McGuire, D.J., Oliver, H.W., and Schreiner, R.A., 1998, *Mineral resources of the Santa Rosa Mountain Wilderness Study Area, Riverside County, California*: U.S. Geological Survey Bulletin, v. 1710, p. D1 – D14.

Dorsey, R.J., 2002, *Stratigraphic record of Pleistocene initiation and slip on the Coyote Creek fault, lower Coyote Creek, Southern California*. In: Barth, A. (Ed.), *Contributions to Crustal Evolution of the Southwest United States*, Special Paper 365, Geological Society of America, Boulder, CO, pp. 251 – 269.

English, D.J. 1985, *Regional structural analysis of the Santa Rosa Mountains, San Diego and Riverside Counties, California: Implications for the geologic history of southern California* (M.S. thesis), San Diego State University, California, 170 p.

Hart, M.W., 1991, *Landslides in The Peninsular Ranges, Southern California* in Walawender, M.J., and Hanan, B.B. eds., *Geological Excursions in Southern California and Mexico*, Geological Society of America, pp. 349-365.

Lough, C.F., 1991, Unpublished geological hazards maps of San Diego County.

Morton, Nissa, 2009, *A preliminary pseudostatic analysis of a large rockslide near the San Jacinto fault*, Southern California: Department of Geological Sciences, San Diego State University.

Ryter, D.W., 2002, *Late Pleistocene Kinematics of the Central San Jacinto Fault Zone, Southern California*, Doctoral Dissertation, University of Oregon.

Sharp, R.V., 1967, *San Jacinto Fault Zone in the Peninsular Ranges of Southern California*: Geological Society of America Bulletin, v. 78, p. 705-730.

Wise, J., 1991, *Structural geometries of the Santa Rosa Mountains detachment terrane along the western margin of the Salton Trough*, senior thesis, San Diego State University.

County of San Diego

General Plan Update Groundwater Study

Appendix A

Evaluation of Groundwater Conditions in Borrego Valley (*Draft**)

***This document is not yet officially adopted by the County of San Diego.**

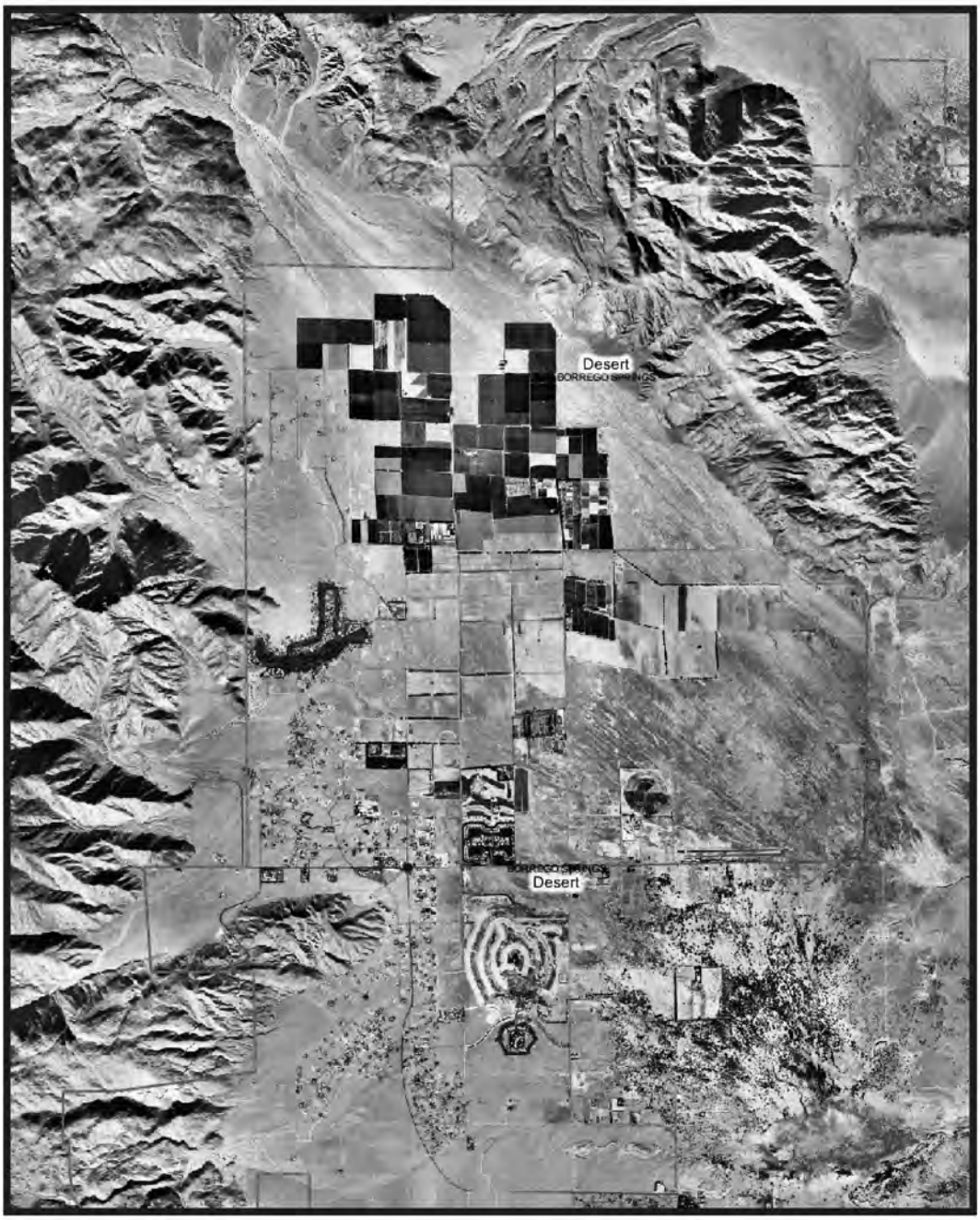

April 2010

TABLE OF CONTENTS

FIGURES

A.1 INTRODUCTION

The objectives of this report are (1) to provide a basic understanding of the groundwater overdraft condition in Borrego Valley, and (2) provide mitigation and alternatives to reduce or minimize predicted significant unavoidable impacts to groundwater resources.

Desert basins account for approximately 14% of the unincorporated area of the County and are located in the extreme eastern portions of the County as shown on Figure 1. Desert basins are characterized by extremely limited groundwater recharge, but typically large storage capacities. Based on these characteristics, groundwater pumping that exceeds the rate of recharge results in a groundwater overdraft condition, which is not sustainable for long-term groundwater use.

The Borrego Valley aquifer (Figure 2), which is completely groundwater dependent, has a well documented groundwater overdraft condition where year after year groundwater extraction exceeds the amount of groundwater that is recharged back into the aquifer. Groundwater extraction exceeds 20,000 acre-feet per year whereas average groundwater recharge is estimated at approximately 5,000 acre-feet per year. The aquifer holds a large amount of groundwater in storage, estimated to be approximately 1.6-million acre-feet of useable groundwater. Water levels have been declining for decades as a result of the overdraft condition and groundwater production at current rates is not sustainable.

Plans to import water from the Colorado River are currently improbable based on the cost and competition from other jurisdictions; and importation of saline groundwater from nearby basins would require a local desalination plant which is likely to be cost prohibitive. Therefore, the County of San Diego assumes, for long-term planning, that development in Borrego Valley will not have access to supplemental imported water, and therefore must prove long-term groundwater adequacy independent of imported water.

A.2 EXISTING CONDITIONS

A.2.1 Topographic Setting

Borrego Valley covers an area of approximately 110 square miles and ranges in elevation from approximately 1,100 to 1,200 ft MSL around the margins of the aquifer to approximately 450 ft MSL within the vicinity of Borrego Sink (see Figure 2). Approximately 400 square miles of tributary watershed from multiple intermittent creeks and streams drain from the mountains into Borrego Valley, which provide the primary source of groundwater recharge to the Borrego Valley aquifer. The largest surface water inflow occurs along the Coyote Creek drainage entering into the northern portion of Borrego Valley, and another important drainage is Borrego Palm Canyon, where surface water enters into the western portion of the valley.

A.2.2 Climate

Borrego Valley has an arid climate with precipitation averaging approximately 3 to 6 inches in the center of the valley and 6 to 9 inches along the western margins of the valley. Precipitation in the mountainous regions located west of Borrego Valley average from 15 to over 21 inches annually. On average, over 75 percent of the annual precipitation occurs between November and May, and less than 25 percent of the annual precipitation occurs from summer rain and thunderstorms that typically occur from July through September. Temperatures are very hot during the summers with average high temperatures exceeding 105 degrees F, and winters are cool with average lows below 40 degrees F.

Monthly reference evapotranspiration (ETo), which is a measure of potential evapotranspiration (PET) from a known surface such as grass or alfalfa, has been estimated for Borrego Valley to be approximately 71.6 inches per year (DWR, 1999). The ETo rates are highest in July at 9.6 inches, and are lowest in December at 2.2 inches.

A.2.3 Land Use

The land uses in Borrego Valley primarily include residential, agricultural, recreational, and commercial uses. Most of the land is owned by private individuals or corporations. The majority of agricultural lands are located in the northern portion of Borrego Valley. The Anza Borrego Desert State Park and other parkland cover some of the margins of Borrego Valley and the mountain regions above Borrego Valley. Borrego Springs is completely surrounded and encompassed by State park land which also includes Indian, private, and National forest land.

Existing Residential Land Use: As of 2005, there were roughly 2,500 existing residential units in Borrego Valley. From January 2001 through June 2008, the County processed 318 residential building permits for manufactured homes and stick built homes (both custom and mass produced). During that time, an average of 42 residential building permits was processed per year. As of January 2007, there were approximately 3,725 existing, private unbuilt parcels in Borrego Valley. Of these, roughly 85% (approximately 3,166 parcels) are

estimated to have legal lot status (County of San Diego, 1999). Having a legally created lot which meets Zoning requirements still may not be buildable due to a number of factors such as floodplain issues, having legal access to roadways, having access to sewer or water, etc. Building permits are granted on a case-by-case basis by the County, and it is not possible to accurately estimate the number of legally buildable parcels in Borrego Valley. However, the significant inventory of existing unbuilt lots could possibly provide up to an additional 3,000+ future residential units without any additional subdivision.

Current GP and GP Update Residential Land Use: Below is a table which provides the maximum allowable additional residential units permitted by the current GP as well as those proposed by the GP Update Referral Map and Environmentally Superior Map:

Current GP Map	GP Update Referral Map	GP Update Environmentally Superior Map
19,466	8,689	6,515

A.2.4 Hydrogeologic Units

The United States Geological Survey (USGS) estimates that Borrego Valley is underlain with up to 2,400 feet of consolidated to unconsolidated sediments resting on basement granitic rocks. In 1982, the USGS estimated at steady-state groundwater conditions (in the year 1945), the Borrego Valley groundwater basin contained approximately 5.5 million acre-feet of water in storage. Further, the USGS identified three Hydrogeologic units: an upper, middle, and lower aquifer (Moyle and others, 1982; Mitten and others, 1988). In 1988, the USGS prepared a numerical model of the aquifer. The results of the model suggest that the specific yield of the upper, middle, and lower aquifers are 14%, 7%, and 3%, respectively.

Based upon subsequent study by Dr. David Huntley, the majority of readily available water to existing well users in the Borrego Valley exists in the upper and middle aquifer. The amount of groundwater within these two aquifers was estimated to be approximately 2,131,000 acre-feet in 1945 and 1,900,500 acre-feet in 1979 (Huntley, 1993). The remaining water located within the lower aquifer is more difficult and costly to extract due to its low specific yield (estimated to be approximately 3%), its depth, and low specific capacity (estimated to be 5 gallons per minute/foot of drawdown or less). The Borrego Water District estimated that in 1999 the water remaining in the upper and middle aquifers was approximately 1,685,000 acre-feet (BWD, 2001).

The USGS is conducting a new phase of groundwater investigative work in Borrego Valley projected to be completed in 2010. The objective is to refine their 1980s groundwater flow model to take advantage of flow modeling tools not available in their 1988 numerical model. The model will be used as a predictive tool to estimate the amount of time left before the groundwater table drops below the pump intake in production wells currently being used in Borrego Valley. This should provide a more specific estimation of future groundwater impacts than previous studies conducted.

A.2.5 Water Quality

In general, water quality has historically been good within Borrego Water District's wells with total dissolved solids at concentrations of less than 500 mg/L (BWD, 2001). Historical nitrate impacts have been noted as evidenced by wells taken out of production including Borrego Water District ID-4 wells 1 & 4, and the Roadrunner Mobile Home Park well.

High salinity, poor quality connate water is thought to occur in deeper formational materials of the aquifer as well as shallow groundwater in the vicinity of the Borrego Sink in the southern portion of the Borrego Valley. Since there have been no comprehensive studies of water quality within Borrego Valley, it is difficult to assess the amount of potable groundwater still available in Borrego Valley. Water quality impacts may occur as decreased water levels may induce flow of poor quality water found in deeper formational materials of the aquifer. This may eventually necessitate additional expensive treatment of groundwater to make the water suitable as a drinking water supply.

Drilling of a dual screened monitoring well by DWR in the southern portion of Borrego Valley (northeast of Borrego Sink) provides confirmation of poor water quality in shallow groundwater and deteriorating with depth (DWR, 2007). Water analyzed from the upper completion (45 to 155 feet below ground surface) indicated total dissolved solids (TDS) of 1,300 mg/L. Water analyzed from the lower completion (200 to 345 feet below ground surface) indicated TDS of 2,300 mg/L. The high TDS content in both screened intervals of this well (as well as high sulfate content) make the water unsuitable for a drinking water supply without expensive treatment.

A.2.6 Groundwater Recharge

Estimated Recharge

Estimated annual recharge to the Borrego Valley aquifer was initially estimated by the USGS to be approximately 4,800 acre-feet per year (Mitten and others, 1988). The source of recharge was estimated to come primarily from three major drainages: Coyote Creek (approximately 65%), Borrego Palm Canyon and San Felipe Creek (approximately 35% combined). Little recharge, if any from San Felipe Creek benefits users in Borrego Springs as the majority exits Borrego Valley and flows toward Ocotillo Wells.

In a thesis by Netto in 2001, it was estimated that from 1945 to 2000, recharge from groundwater underflow, stream recharge, and bedrock recharge is approximately on average 5,670 acre-feet per year. In a thesis by Henderson in 2001, it was estimated that recharge from 1945 to 2000 averaged approximately 6,170 acre-feet per year. Both estimates showed that recharge had a very large range due to the extremes in rainfall, from very little during dry years to recharge above 50,000 acre-feet in the wettest year.

Age of Groundwater from Borrego Water District Wells

The Borrego Water District in 2001 obtained the age of the water being pumped in two of their pumping wells, well ID 4-11 and well ID 4-18. Analytical results from water sampled from well ID 4-11 indicated the water to be 873 years old (+- 42 years), and results from

water sampled from well ID 4-18 indicated the water to be 1,982 years old (+- 54 years). The results indicate that water in these wells was from not from recent groundwater recharge, but rather from water that percolated and was recharged many hundreds of years ago.

A.2.7 Groundwater Demand

The Borrego Water District has estimated the amount of water used within Borrego Valley from 1950 to 2007. While groundwater demand more than doubled from 1978 to 1999, it appears that overall water usage may have leveled off between 1999 and 2007.

Year	Municipal (AFY)	Agricultural (AFY)	Golf Course and Landscape (AFY)	Total (AFY)
1950	170	11,435	190	11,795
1958	225	22,455	790	23,470
1962	265	13,455	1,725	15,820
1968	475	7,260	1,720	9,455
1972	530	5,320	2,270	8,120
1978	600	5,705	2,050	8,355
1980	430	10,600	2,100	13,130
1999	2,272	15,590	4,435	22,297
2007	1,920	14,650	5,240	21,810

AFY – Acre-feet per Year

A.2.8 Groundwater Levels

Groundwater levels in Borrego Valley were originally monitored by the USGS as far back as the 1940s. The County of San Diego has been collecting groundwater level data since the early 1980s. Water levels in Borrego Valley have been declining since 1945, indicating a long-term overdraft condition. Between 1945 and 1980, water levels declined by as much as 100 feet, due to more water being extracted than was being replenished (USGS, 1982). To provide an understanding of water level trends since the 1980s, water levels from eight wells monitored by the County are summarized in the table below (Figure 3).

Well	Period of Monitoring	Cumulative Drawdown (feet)	Average Change in Water Levels (feet per year)		
			1980s	1990 to 1997	Since 1998
BOR-10	1983-2002	30.6	-1.1	-1.7	-2.3
BOR-36	1987-2006	47.2	-1.5	-2.3	-3.2
BOR-37	1983-2006	55.6	-0.6	-3.4	-3.1
BOR-42	1986-2005	38.9	-1.0	-2.2	-2.4
BOR-54	1987-2006	49.8	-2.4	-2.2	-3.3
BOR-56	1985-2006	26.7	-1.2	-0.5	-2.1
BOR-57	1984-2006	24.0	-1.3	-0.5	-2.1
BOR-58	1983-2001	15.3	-0.9	-0.7	-1.1
AVERAGE OF ALL WELLS			**-1.2**	**-1.7**	**-2.4**

Since the 1980s, water level declines in the 8 wells have ranged from 15.3 feet (BOR-58 well) to 55.6 feet (BOR-37 well). From 1998 to 2006, water level declines have averaged 2.4 feet per year, which is roughly twice the rate of decline measured in the 1980s. This is likely due to the increased extraction rates that are occurring compared to extraction in the 1980s.

It has been estimated that the volume of groundwater in storage decreases with depth in Borrego Valley. Therefore, it is estimated that basin-wide rates of water level decline will increase with ongoing groundwater mining, even without any change in the deficit between groundwater extraction and recharge.

A.2.9 Groundwater Overdraft Condition

Since 1945, water levels in Borrego Valley have continually declined in some cases by as much as over 150 feet. Groundwater has and is continuing to be extracted at rates that exceed recharge, which has caused an apparent long-term overdraft condition, also known as groundwater mining. In the past 20 years, rates of decline have increased sharply likely in response to new development and additional groundwater extraction. Dr. Tim Ross of the California Department of Water Resources has estimated the overall rate of overdraft in the aquifer through time as follows:

1980-1989: -4,200 acre-feet per year
1989-2000: -9,100 acre-feet per year
1998-2005: -14,300 acre-feet year
It was estimated that a total of 550,000 acre-feet of water was permanently removed from the aquifer from 1945 to 2005 (Ross, 2006).

The Borrego Water District estimated that in 1999 the water remaining in the upper and middle aquifers was approximately 1,685,000 acre-feet (Borrego Water District, 2001). Based upon this estimation of groundwater storage in 1999, if the overdraft condition continues at the estimated rate of 14,300 acre-feet of water per year, the upper and middle aquifers may be 50% depleted in approximately 50 years, and may be completely depleted in approximately 100 years. These numbers, however, should be used with extreme caution, as there are a number of factors that are not fully known regarding the Borrego Valley aquifer. Groundwater pumping has more than tripled since the 1980s, and continued development without groundwater mitigation measures in Borrego Valley will exacerbate the existing overdraft conditions estimated by Dr. Ross.

It should be understood that groundwater impacts from the overdraft condition are already occurring and will continue to worsen as mining of groundwater continues. Current impacts include dry wells, decreased well efficiency and increased pumping costs as water levels continue to decline. This will continue and more wells will need to be replaced as water levels drop below perforated levels. Also, water quality impacts may occur as decreased water levels may induce flow of high salinity, poor quality connate water found in deeper formational materials of the aquifer. This may eventually necessitate additional expensive treatment of groundwater to make the water suitable as a drinking water supply.

The General Plan Update Referral Map (project) would allow for up to 8,689 additional residential units which would be anticipated to use approximately 8255 acre-feet of groundwater per year (0.95 acre-feet per residential unit). Without mitigation, this would increase the overdraft condition to over 22,000 acre-feet per year and the aquifer would be depleted in far less time compared to existing conditions groundwater use. However, based on recent development trends, buildout in the 21st century is unlikely, unless development trends in Borrego Valley change drastically. Between January 2001 and June 2008, approximately 42 residential building permits were processed per year by the County. At this rate of development, it would take approximately 200 years for buildout of the project to occur.

A.2.10 Groundwater Dependent Habitat

The mesquite bosque, a rare and sensitive groundwater-dependent habitat, is believed by many experts to be desiccating in portions of Borrego Valley, even though their taproots can reach down to 150 feet for water. The habitat covers an approximate four-square mile area (Figure 4). Recent groundwater levels from wells adjacent to the main mapped habitat range from approximately 55 to 134 feet below the ground surface. With the exception of the southernmost mapped habitat where recent groundwater levels have been relatively static, groundwater levels been declining at a rate of approximately 1 to nearly 3 feet per year. It is likely that as groundwater levels continue to drop, portions of the mesquite bosque will not be able to adequately adapt and habitat will be permanently lost. Potential secondary affects could also negatively impact local residents, plants, and wildlife from dust storms resulting from topsoil that is left exposed when plants die off.

A.3 GROUNDWATER MANAGEMENT IN BORREGO VALLEY

There are three basic methods available for managing local groundwater resources in California, which include: 1) local water agencies, 2) local groundwater ordinances, and 3) basin adjudication, in which a court determines allocation of groundwater resources (CDWR, 2003). No law requires that any specific form of management be applied to a particular basin. Groundwater in Borrego Valley is currently managed through local water agencies (the Borrego Water District and the Borrego Springs Park Community Services District), and the County Groundwater Ordinance (as well as application of CEQA for land use discretionary applications). In the case of Borrego Valley, the basin has not been adjudicated. Therefore, individual well users are not limited in the amount of groundwater they can extract.

A.3.1 Local Water Agencies

In 1962, the Borrego Water District (BWD) was formed as a landowner-voter district under the provisions of the California Water District Act to protect the water rights in Borrego Valley. However, the District was inactive until 1979 when the San Diego Local Agency Formation Commission (LAFCO) sanctioned the District to exercise its latent water authority. The BWD now provides approximately 4,100 acre-feet of groundwater annually to nearly 2,000 residential and commercial customers from 11 wells tapping the Borrego Valley aquifer. The water district service area is approximately 6,130 acres, and excludes the area served by the Borrego Springs Park Community Services District (BSPCSD). The BSPCSD is much smaller than the BWD and serves less than 200 customers within a 1,200-acre service area. The BSPCSD is in process of a merger to become part of the BWD.

While the majority of residences and commercial entities in Borrego Valley receive their water from the BWD, there are private property owners within the BWD service area that utilize private wells. The vast majority of the water supplied to agricultural users within Borrego Valley comes from privately owned wells within the BWD service area. The BWD has water rights under some residential areas within its service area.

A.3.1.1 Groundwater Management Plan (GMP)

In 2002, the BWD adopted a GMP which allowed the District to become the groundwater management agency for the Borrego Valley aquifer as allowed under State Statute AB 3030. The adoption of the GMP thus placed the BWD as the responsible agency for the stewardship of the aquifer and resolution of the overdraft. The GMP contained a summary of the Borrego overdraft condition, projections of future groundwater demand, and identification of potential groundwater overdraft mitigation measures. Specifically, it set out goals to achieve including: (1) development of programs to assist in stabilizing the overdraft of the aquifer, (2) seek programs to provide a long-term supply of water for the valley, (3) continue to expand the knowledge of the water resources of the aquifer, (4) development and implementation of conservation programs, (5) work with state and county agencies to try to minimize any adverse impact new land uses would have on groundwater resources, (6) develop the ability to obtain funding for acquisition of actively irrigated agricultural land, and (7) evaluate the feasibility of acquiring land in adjacent basins and exploring for such water to be transported for use in Borrego Valley.

A.3.1.2Groundwater Replenishment District

As part of the groundwater management plan that was adopted in 2002, the BWD obtained the authority as a groundwater replenishment district, which provides BWD specific groundwater management authority including: (1) the ability to buy and sell water, (2) exchange water, (3) distribute water in exchange for ceasing or reducing groundwater extraction, (4) recharge the basin, and (5) build necessary works to achieve groundwater replenishment.

A.3.1.3Integrated Water Resources Management Plan

The State has initiated funding of projects as a result of Proposition 50 (and subsequently Proposition 84) such as a proposed importation water pipeline, but it requires that any agencies wishing to benefit from funding participate in an Integrated Water Resources Management Plan (IWRMP). This plan requires that an agency develop a water management plan for incorporation in a regional process to integrate its plan with other agencies having responsibilities for water management. The BWD is in the process of preparing an IWRMP which is meant to provide an update on the BWD efforts to mitigate the overdraft condition of the Borrego aquifer, and to present alternatives for the BWD to further evaluate as it strives to provide a sustainable water supply for its customers (BWD, 2008).

As outlined in the draft IWRMP, a number of programs have since been implemented to achieve the goals contained within the GMP including:

1. Groundwater Preservation Fee: By resolution, the BWD implemented a groundwater mitigation program that requires all new development in Borrego Valley that proposes to utilize water from the BWD to implement mitigation measures which would "retire existing demands on a 2:1 basis." The BWD will accept an in-lieu payment for the required reduction of demand in which fees could be used for various overdraft mitigation programs including: (1) purchase actively irrigated agricultural land for fallowing, (2) construction of artificial recharge basins for capturing storm events, (3) development of groundwater extraction and conveyance systems to convey water to Borrego Valley from nearby areas.

2. Irrigated Agricultural Land Purchase: In 2007 and 2008, the BWD concluded the purchase of water easements over approximately 46 acres of farmland, which resulted in the permanent fallowing of approximately 175 acre-feet per year of water use.

3. Conservation Management Program (Tiered Water Rates): In June 2008, the BWD adopted tiered water rates, which encourages water conservation and penalizes high water use. Funds received from higher tiers of water use are intended to be earmarked for a rebate program to encourage customers to purchase water conserving devices such as low-flow toilets, low-flow washing machines, turf removal, and water-efficient irrigation systems.

4. Water Recycling: Water recycling has been proposed for irrigation of the golf course at Rams Hill (now known as Montesoro). The wastewater treatment system for the development was designed to meet California Department of Public Health Services

requirements for landscape irrigation. Current sewage flows into the treatment plant have been insufficient to provide a supply for the golf course and are primarily lost to evaporation. The BWD has applied for grant funding under Proposition 50 to conduct a feasibility study for connecting all residences to a central collection and conveyance system to send the wastewater to the existing wastewater treatment plant. Treated effluent flows could then be used for landscape irrigation at the golf course.

5. Artificial Recharge: In 1984, DWR conducted a brief study of constructing artificial recharge facilities to capture and recharge storm waters emanating from the Coastal range mountains on the west side of the Borrego aquifer. Dike systems were envisioned at the terminus of several canyons including Borrego Palm Canyon, Henderson, and Coyote canyons. DWR estimated that an additional 300 to 500 afy might be expected through catchment basins in exceptionally wet years. A planned residential development, known as the Viking Ranch, is proposing the first such project by proposing to incorporate channels within the development which would recharge Coyote Creek storm water. Additionally, the De Anza Country Club excavated a storm water detention basin located immediately up-stream of their development which has since become filled with sediment. This sediment has hindered its ability to provide flood protection. The BWD is interested in investigating the potential for a cooperative use of the storm water detention basin as both a flood retarding and water conservation basin.

6. Defining the Reliability of Groundwater Supply: As summarized below, the BWD has a number of ongoing data-gathering projects which will provide tools to further the understanding of the Borrego Valley aquifer:

   USGS Numerical Model: The amount of usable groundwater in storage is not well defined and therefore the amount of time the aquifer can continue to supply groundwater users in Borrego Valley is not fully known. The BWD has recently requested that the USGS develop a working numerical model of the basin based on more-current data collected in the basin by DWR and others. The model will provide estimations regarding future impacts on the basin from various development and extraction scenarios. This model will be useful in defining impacts in order to develop a timeline for alternative water management strategies for the basin.

   DWR Local Assistance Program: In 2004, DWR began assisting the BWD with groundwater assessment. DWR constructed groundwater elevation maps for several years, and providing estimations of changes of groundwater in storage with time for several periods. Currently, DWR is preparing to perform a well inventory and to obtain and analyze groundwater samples from selected pumping wells. The work is being coordinated with the USGS for use in their numerical model.

   Construction of Monitoring Wells: Recognizing that the data collected on the characterization of the groundwater basin were obtained solely from well completion reports submitted by drillers, the BWD obtained funding for construction of four

monitoring wells in 2003 and 2005. The wells were professionally logged by DWR geologists.

Geographical Information System (GIS): The BWD is in the process of developing a GIS system to incorporate all available groundwater data such as historical water levels, water quality, groundwater contour maps, land use, water extractions, groundwater recharge, etc. The system is a necessary component for the USGS numeric model.

Depth Dependent Aquifer Data: There is a concern of possible upwelling of poor-quality water from deeper portions of the Borrego aquifer as water levels continue to fall. The BWD is pursuing grant funding for construction of a 'nested' well (four small diameter wells within the same borehole) that could provide data on potential water quality differences with depth at a strategic location.

Ongoing Water Level Monitoring: The BWD, DWR, and County continue a collective effort to monitor water levels from a series of wells in Borrego Valley. Monitoring by the County began in 1981, and the monitoring well network provides long-term data to assess the downward trends in water levels in various areas within Borrego Valley.

As outlined in the draft IWRMP, there are several non-local water supply opportunities that the BWD is exploring as summarized below:

1. Importation of Groundwater from Nearby Basins: Three groundwater sources near Borrego Valley were investigated to determine if additional water from these basins could be imported for use by the BWD. This included the Clark Dry Lake basin, the Dr. Nel property (located southeast of Borrego Valley along San Felipe Creek), and the Allegretti Farms (located southeast of Ocotillo Wells). Rough estimations based on very limited hydrogeological information indicate that potential groundwater production for the three projects range from 2,000 acre-feet per year each from the Clark Dry Lake and Dr. Nel property, and upwards of 6,000 acre-feet per year for the Allegretti Farms property. Both Clark Dry Lake and Allegretti farms have high TDS that may require treatment if it is to be used for domestic purposes. Costs in the IRWMP indicate it may require grant money and/or an increased base of BWD customers.

2. Importation Pipeline Projects from Imperial Irrigation District (IID) or Coachella Valley Water District (CVWD): Since the quantity and quality of water that may be available from nearby groundwater basins is not well defined due to the lack of hydrogeologic data, the BWD included the potential of obtaining a source of water from the Colorado River, State Water Project, or other sources. Costs associated are likely currently prohibitive but may become feasible as Borrego Springs continues to grow and grant money could augment other funds available to the BWD.

3. Groundwater Storage and Recovery Project: The Borrego Valley aquifer may be a good candidate as an aquifer storage and recovery (ASR) project, which involves

injecting imported water into the aquifer through wells or by surface spreading and infiltration and then pumping it out when needed. The aquifer essentially functions as a water bank. Deposits are made in times of surplus, and withdrawals occur when available water falls short of demand. As water agencies throughout the State continue to diversify their water portfolios, ASR is becoming an increasingly viable alternative to surface water reservoirs to increase water storage capacity for use during extended droughts. The IID or CVWD would be the two most likely water agencies that could potentially utilize the Borrego Valley aquifer for ASR. It is estimated that more than 500,000 acre-feet of groundwater have been removed from storage from Borrego Valley since the 1940s. As water levels continue to decline, nearly 15,000 acre-feet of groundwater is continuing to be removed each year. This continues to create additional storage space within the aquifer. The draft IRWMP does not include a feasibility study and cost benefit analysis but indicates that all costs associated would be requested from the partnering agency.

A.3.2 County Groundwater Ordinance and CEQA

The County of San Diego has regulatory control over proposed land uses but does not actively manage groundwater resources in Borrego Valley. All management of groundwater resources in Borrego Valley is the responsibility of the BWD, other entities, and individual well owners who utilize groundwater. However, the County does have regulations to review anticipated future groundwater demand through the County Groundwater Ordinance (Ordinance #9826, N.S.) and application of CEQA to proposed discretionary permits. The Groundwater Ordinance does not limit the number of wells or the amount of groundwater extraction by existing landowners. However, the Groundwater Ordinance has a specific section for Borrego Valley (Section 67.720) which imposes requirements on projects of more than 100 acres, projects requiring a General Plan Amendment, and projects with an annual demand of more than 20 acre-feet of water. In any of these cases, the Groundwater Ordinance requires that a finding be made that groundwater resources are adequate to meet the groundwater demands of the project.

Proposed discretionary permits proposing the use of groundwater in Borrego are also subject to the DPLU Policy Regarding CEQA Cumulative Analyses for Borrego Valley Groundwater Use, which is included as an attachment to this document. The policy which first went into effect in 2004 requires evaluation of potential cumulative impacts to groundwater resources in Borrego Valley which is guided by the following principles:

1. Applicants for projects using groundwater resources in Borrego Valley are encouraged to include with their projects, offsetting groundwater use reduction measures which will make up for the project's proposed groundwater use and result in "no net gain" in the overall rate or amount of extraction of groundwater.

2. For projects where offsetting groundwater use reduction measures are not proposed as part of the project, except as provided in sections 3 and 4 below, an EIR will generally be required to be prepared, to analyze the significance of cumulative impacts to

groundwater resources, to propose mitigation measures, and to consider project alternatives.

3. For projects with previously approved environmental documents, the project must be assessed per the requirements of Section 15162 of the State CEQA Guidelines (summarized at paragraph A.2.b above). If the project proposes to use more groundwater than initially proposed, then offsetting groundwater use reduction measures may be proposed and included in this analysis. If such measures are not included, the Section 15162 analysis may lead to a requirement to prepare a supplemental or subsequent EIR.

4. Proponents of some small projects may be able to demonstrate that potential cumulative impacts to groundwater resources are not significant, because the project's incremental additional groundwater demand is not "cumulatively considerable."

Mitigation is typically achieved by a project (e.g., a tentative map or other discretionary permit) by recording an easement on off-site land that has been continuously used for agriculture or golf course purposes for at least the past five years and is being irrigated with at least the same amount of groundwater annually of which the project will consume. The easement is then granted to the County of San Diego and it prohibits the use, extraction, storage, distribution, or diversion of water from the Borrego Valley aquifer on the land subject to the easement. Recording easements has proven to be an effective, albeit cumbersome, process and the County is now coordinating with the BWD to create a water credits program. The water credits program would allow farmers or any other owners of water intensive uses in Borrego Valley to permanently fallow their land and in turn the BWD would issue “water entitlement certificates” in standard increments. The certificates could then potentially be applied towards meeting both BWD and County requirements for groundwater mitigation.

A.3.3 Basin Adjudication

When the demand for groundwater exceeds its supply, landowners can turn to the courts to determine how much groundwater each user can rightfully extract. There are 19 court adjudications for groundwater basins in California. This court-directed process can be lengthy and costly, with the longest adjudication taking 24 years (DWR, 2003). Currently, groundwater users in Borrego Valley have an adequate water supply to meet their current needs and there has been no action to bring about court adjudication of the Borrego Valley aquifer. As the overdraft condition continues there may come a time when court adjudication becomes necessary. Since the County does not actively manage groundwater resources in Borrego Valley, it is not in the position to initiate a court adjudication of the basin. Thus, the BWD and/or other groundwater users in Borrego Valley would be plaintiffs or litigants to initiate an adjudication of the basin.

A.4 GROUNDWATER IMPACT ANALYSIS

This section evaluates impacts of the proposed GP Update land uses in Borrego Valley on groundwater quantity. The following question listed in the CEQA Guidelines, Appendix G., VIII. Hydrology and Water Quality must be considered:

Would the proposed project substantially deplete groundwater supplies or interfere substantially with groundwater recharge such that there would be a net deficit in aquifer volume or a lowering of the local groundwater table level (e.g., the production rate of pre-existing nearby wells would drop to a level which would not support existing land uses or planned uses for which permits are granted)?

A.4.1 Impacts Prior to Mitigation

The Borrego Valley aquifer has a well documented groundwater overdraft condition, where year after year groundwater extraction exceeds the amount of groundwater that is recharged back into the aquifer. In the long-term, this situation is not sustainable. It is the cumulative impact of all users that has resulted in the overdraft condition and additional groundwater extraction to support new development will further contribute to this cumulative impact. Any additional development requiring groundwater in Borrego Valley without mitigation would have a potentially significant impact to groundwater resources.

Current impacts include dry wells, decreased well efficiency and increased pumping costs as water levels continue to decline. This will continue and more wells will need to be replaced as water levels drop below perforated intervals. Also, water quality impacts may occur as decreased water levels may induce flow of high salinity, poor quality connate water found in deeper formational materials of the aquifer. This may eventually necessitate additional expensive treatment of groundwater to make the water suitable as a drinking water supply.

A.4.2 Potential Mitigation Measures

Below is a discussion of potential mitigation measures and alternatives which could reduce or minimize potentially significant impacts to groundwater resources as the result of implementation of the General Plan Update. At the present time, there is an adequate groundwater supply to meet current groundwater demand in Borrego Valley. As the groundwater overdraft condition continues increasingly aggressive mitigation measures will likely be required to assure a long-term water supply for Borrego Valley. Unfortunately, there is no single answer or approach to take to mitigate the effects of the groundwater overdraft. The County has no active groundwater management authority in Borrego Valley beyond its land use authority. The primary groundwater management agency for the Borrego Valley aquifer is the BWD. The BWD has developed a comprehensive multi-faceted approach to address the groundwater overdraft situation in Borrego Valley as outlined in Section 3.1. The following mitigation measures could be implemented by the County using its land use authority versus measures that the BWD is currently or potentially could implement using its groundwater management authority:

A.4.2.1 County of San Diego

1. Groundwater Offsetting Measures: As discussed in Section 3.2, new discretionary projects which are proposing the use of groundwater in Borrego Valley are strongly encouraged to include with their projects, offsetting groundwater use reduction measures which will make up for the project's proposed groundwater use and result in "no net gain" in the overall amount of extraction of groundwater. As one example of such a measure, land could be purchased or an easement could be placed over the land which currently has groundwater use associated with it. If the water use on this land were reduced by an amount equivalent to the water demand of the proposed project, then there would be "no net gain" in the amount of water extracted from the aquifer, and thus the overdraft condition would not be made worse by the proposed project. The applicant would have to propose a legally enforceable mechanism to the satisfaction of the County for achieving the reduction on the other land. An example would be taking agricultural or golf course land permanently out of production. For tentative maps or tentative parcel maps, the County requires the mitigation to be implemented prior to approval of the final map. This mitigation measure is feasible and is currently being implemented by DPLU.

The County's CEQA policy for Borrego Valley does not apply to pre-existing legally buildable lots or for projects with previously approved environmental documents (unless the given project is proposing more groundwater than was initially proposed). Currently, in these cases no mitigation is required. While not required under CEQA, the County could adopt measures through the Groundwater Ordinance to require groundwater offsetting measures for all potential water uses which would include ministerial permits such as a building permit or projects with previously approved environmental documents.

The County could potentially implement a mitigation ratio higher than 1:1. The BWD has implemented a groundwater mitigation policy which has a mitigation ratio of 2:1. To illustrate the effectiveness of implementation of higher mitigation ratios, two scenarios have been analyzed in the following table assuming a baseline overdraft condition of 14,300 acre-feet per year in the year 2008, and 1,685,000 acre-feet of groundwater in storage as of 1999. This assumes that all new development in Borrego Valley is required to mitigate its groundwater use at the prescribed ratios.

Scenario	Additional Residential Units in Next 30 Years	Rough Estimate of Years Until Upper and Middle Aquifers are 50% Depleted		
		No Mitigation	1:1	2:1
1. Building Moratorium, No Change in Overdraft	0	50	50	50
2. Development at Current Rate of Construction (42 residential units per year)	1260	47	50	54
3. Accelerated Development at Double Current Rate of Construction (84 residential units per year)	2520	44	50	60
4. Accelerated Development at Triple Current Rate of Construction (126 residential units per year)	4780	39	50	71

As of November 2008, there were 11 subdivisions in Borrego Valley in process with the County which are proposing a combined total of nearly 1,000 acre-feet of water use per year. If all of these projects are approved by the County, this would result in offsetting groundwater measures to occur prior to finalization of each map. So, until the last parcel is built out, the mitigation ratio is higher than 1:1. At a current development rate of approximately 42 residential units per year, these new developments could take 50 to 100 years before being built out. Therefore, if 1,000 acre-feet of overdraft was removed from the aquifer right now, this would give the aquifer more time than what is indicated in the table above.

2. Landscape Conservation: Having recognized the large impact that landscape irrigation has on water supplies and wanting to further reduce waste of water, recent legislation has mandated that the California Department of Water Resources (DWR) update its Model Water Efficient Landscape Ordinance (MWELO) on January 1, 2009. All local agencies, including the County of San Diego, are required to adopt the updated Model Ordinance or adopt their own local landscape ordinance that is at least as effective as the updated Model Ordinance by January 1, 2010. The updated MWELO would be mandated to reflect improvements in landscape and irrigation design plans, irrigation technologies, and water management with the goal of achievable water savings.

   The estimated average groundwater use per single-family residence in Borrego Valley is approximately 0.95 acre-feet per year based on analysis of four years of water use data from over 1,300 homes in Borrego Valley (BWD, 2006). The average water use of a single-family residence within the CWA is approximately 0.5 acre-feet per year (CWA, 2006). The relatively high water demand per residence in Borrego Valley can be attributed to the high evapotranspiration rates associated with outdoor landscaping. By reducing or eliminating water intensive landscaping such as lawns and tropical landscaping and replacing those with xeriscape/desert landscaping could significantly reduce the overall water demand per residence in Borrego Valley. The updated MWELO

could be the mechanism for implementation of stringent landscape conservation measures in Borrego Valley to achieve needed water savings.

3. Environmentally Superior Alternative: The GP Update Environmentally Superior Alternative could be selected to reduce future development potential in Borrego Valley. The Environmentally Superior Alternative would result in a reduction at buildout of over 2,000 residential units when compared with the Referral Map (project) alternative. This is a feasible mitigation measure. However, the Environmentally Superior Alternative proposes significant reductions in densities over actively irrigated agricultural land. Potential conversion of intensely irrigated agricultural land to residential lands would be discouraged by selecting the Environmentally Superior Alternative, which could be counter to reducing water use in Borrego Valley.

4. Building Moratorium: A moratorium on building permits and development applications by the County could be proposed. This would effectively result in no increase in the amount of groundwater extracted from the Borrego Valley aquifer. There are obvious socioeconomic impacts that would occur as the result of a building moratorium in Borrego Valley. There is no conclusive scientific data available that indicates an imminent groundwater supply shortage for Borrego Valley within the next 20 to 30 years. As such, a moratorium against new development appears unwarranted.

A.4.2.2 Borrego Water District

1. Groundwater Preservation Fee: The BWD has implemented a groundwater mitigation program in which all new development in Borrego Valley that proposes to utilize water from the BWD must implement mitigation measures which would retire existing water demands on a 2:1 basis. A Groundwater Preservation Fee is accepted by the BWD as an in-lieu payment for the required reduction of demand which could then be used for various overdraft mitigation programs including:

    i. Irrigated Agricultural Land Purchase: BWD has permanently fallowed approximately 175 acre-feet per year of water use and additional lands are intended to be purchased as funds become available through groundwater preservation fee collection.

    ii. Importation of Groundwater from Nearby Basins: The BWD is evaluating three groundwater sources near Borrego Valley that could potentially be imported for use by the BWD.

    iii. Importation Pipeline Projects from Imperial Irrigation District (IID) or Coachella Valley Water District (CVWD): The BWD is evaluating potentially obtaining a source of water from the Colorado River, State Water Project, or other sources through an importation pipeline project from the IID or CVWD into

Borrego Valley. This is likely infeasible at this time due to the costs associated.

iv. Artificial Recharge: The BWD is interested in investigating the potential for a cooperative use of a storm water detention basin as both a flood retarding and water conservation basin.

2. Conservation Management Program (Tiered Water Rates): BWD adopted tiered water rates in an effort to encourage water conservation and penalize high water use. Additional fees received will be applied to a rebate program to encourage customers to purchase low-flush toilets, low-water-use washing machines, turf removal, and water-efficient irrigation systems.

3. Water Recycling: The BWD could potentially connect all residences sewage to an existing wastewater treatment plant at Rams Hill (now known as Montesoro) golf course for re-use as landscape irrigation.

4. Groundwater Storage and Recovery Project: The Borrego Valley aquifer may be a good candidate as an aquifer storage and recovery (ASR) project, which involves injecting imported water into the aquifer through wells or by surface spreading and infiltration and then pumping it out when needed. The IID or CVWD would be the two most likely water agencies that could potentially utilize the Borrego Valley aquifer for ASR.

5. Basin Adjudication: When the demand for groundwater exceeds its supply, landowners can turn to the courts to determine how much groundwater each user can rightfully extract. There are 19 court adjudications for groundwater basins in California. This court-directed process can be lengthy and costly, with the longest adjudication taking 24 years (DWR, 2003). Currently, groundwater users in Borrego Valley have an adequate water supply to meet their current needs and there has been no action to bring about court adjudication of the Borrego Valley aquifer. However, the overextraction is not sustainable and as the overdraft condition continues there may come a time when court adjudication becomes necessary. Since the County does not actively manage groundwater resources in Borrego Valley, it is not in the position to initiate a court adjudication of the basin. Thus, the BWD and/or other groundwater users in Borrego Valley would be responsible parties to initiate an adjudication of the basin.

6. Projects Outside of the BWD: For projects which do not choose to receive water from the BWD, they could drill private domestic wells or form a County or State-regulated water system in which public supply wells would provide water to the project. In such cases, these projects would not provide any economic benefit to the BWD in its efforts to secure a long-term water supply through its various overdraft mitigation programs. As possible mitigation, these projects could be required to pay a groundwater preservation fee to the BWD in addition to providing groundwater offsetting measures. The County would need

to initiate such an action and the money would need to be earmarked specifically towards BWD mitigation programs that the County would consider to be legally enforceable if used for purposes of CEQA mitigation.

A.5 LIMITATIONS

The information in this report was prepared based on best available information from groundwater investigations conducted by the USGS, DWR, and others. Future hydrogeological investigations conducted in Borrego Valley (such as the current USGS investigation) may result in revisions to previous estimates made of the estimated groundwater remaining in storage and the overall rate of overdraft occurring. At the current rate of overdraft estimated by DWR and especially if overdraft conditions increase as it has within the past 25 years, the decline in water levels will continue to result in increasing costs to pump water and dry wells. It is possible that impacts including, but not limited to, dry wells and potential water quality degradation from high salinity water within deeper formational deposits may occur in Borrego Valley within the next 20 to 30 years.

This document is not yet officially adopted by the County of San Diego.

A.6 REFERENCES

Borrego Water District (BWD), 2002. Borrego Water District Groundwater Management Plan, September 25, 2002

BWD, 2006. Groundwater Use Data from 1,328 Single-Family Homes, August 2002 through July 2006.

BWD, 2008. Borrego Water District Integrated Water Resources Management Plan, Draft No.4, October, 2008.

California Department of Water Resources (DWR), Water Use Efficiency Office, 1999. California Irrigation Management Information System (CIMIS) Reference Evapotranspiration Map.

DWR, 2003, Bulletin 118, California's Groundwater, Update 2003.

County of San Diego, 1999. Legal Lot Study of Various Areas in San Diego County, General Plan Update Research Study, April 1999.

County of San Diego, 2007. DPLU Policy Regarding CEQA Cumulative Impact Analyses for Borrego Valley Groundwater Use, revised January 2007.

Henderson, T.W., 2001. Hydrogeology and Numerical Modeling of the Borrego Valley Aquifer System. Masters Thesis, San Diego State University, Fall 2001.

Huntley, David, 1993. Letter to DPLU Regarding Groundwater Situation in Borrego Valley, San Diego State University, January 26, 1993.

Mitten, H.t., G.C. Lines, C. Berenbrock, and T.J. Durbvin, 1988. Water Resources of Borrego Valley and Vicinity, San Diego County, California: Phase 2--Development of a Groundwater-Water Model. U.S. Geological Survey Water-Resources Investigations Report 87-4199.

Moyle, Jr., W.R., 1982. Water Resources of Borrego Valley and Vicinity, Phase 1-- Definition of Geologic and Hydrologic Characteristics of Basin, U.S. Geological Survey Open-File Report 82-855.

Netto, S.P., 2001. Water Resources of Borrego Valley San Diego County, California. Masters Thesis, San Diego State University, Fall 2001.

Ross, Timothy, 2006. Characterizing Water Resources of Borrego Valley Groundwater Basin Presentation, California Department of Water Resources, September 2006.

San Diego County Water Authority (CWA), 2006. Drought Management Plan, prepared by the CWA Water Resources Department, March 23, 2006.

San Diego County. Groundwater Monitoring Program Data. Department of Planning and Land Use. Data from 1980 through 2006.

San Diego County Groundwater Ordinance (#9826, N.S.).

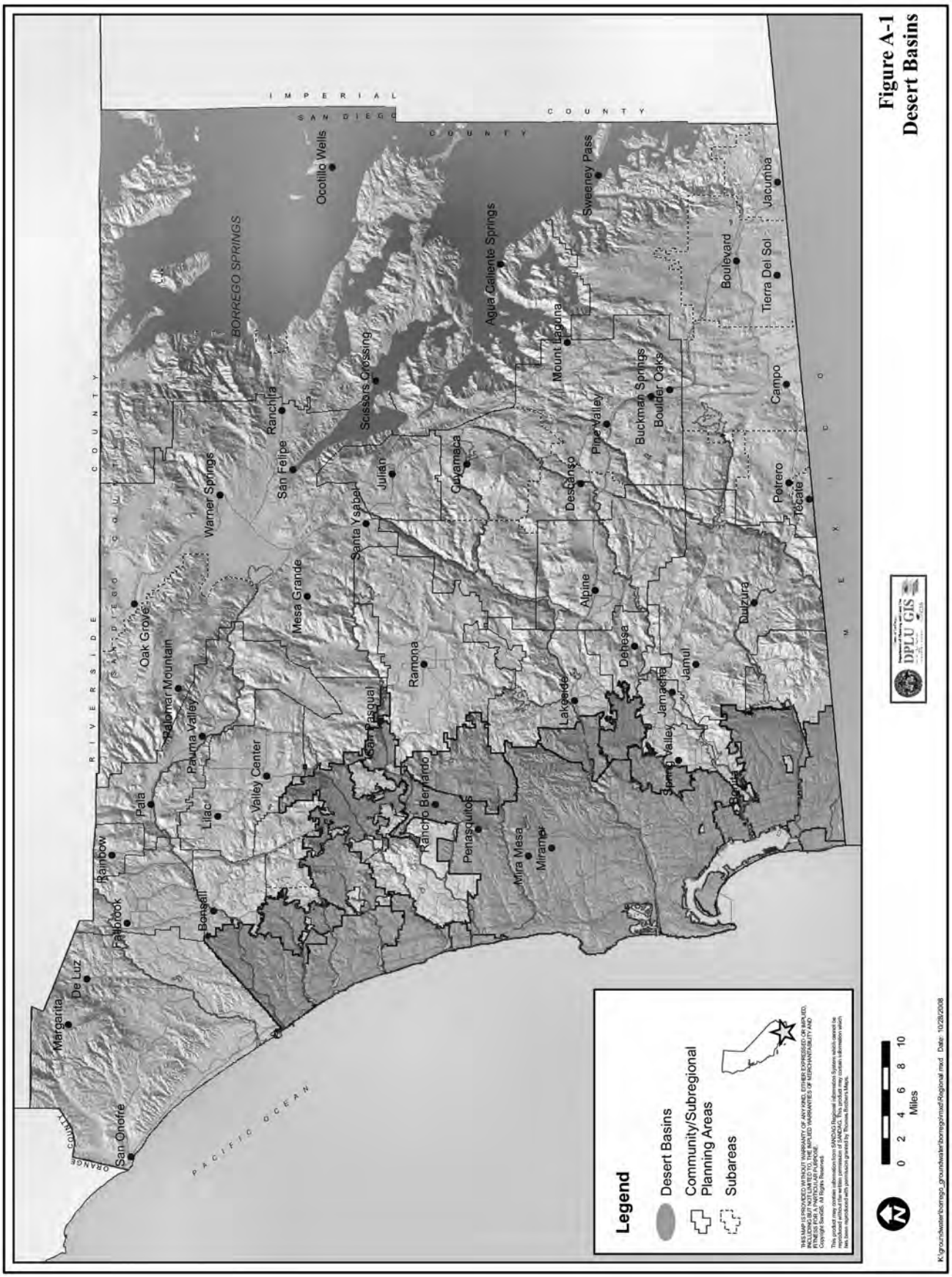

Figure A-1
Desert Basins

Figure A-2
Borrego Valley Aquifer

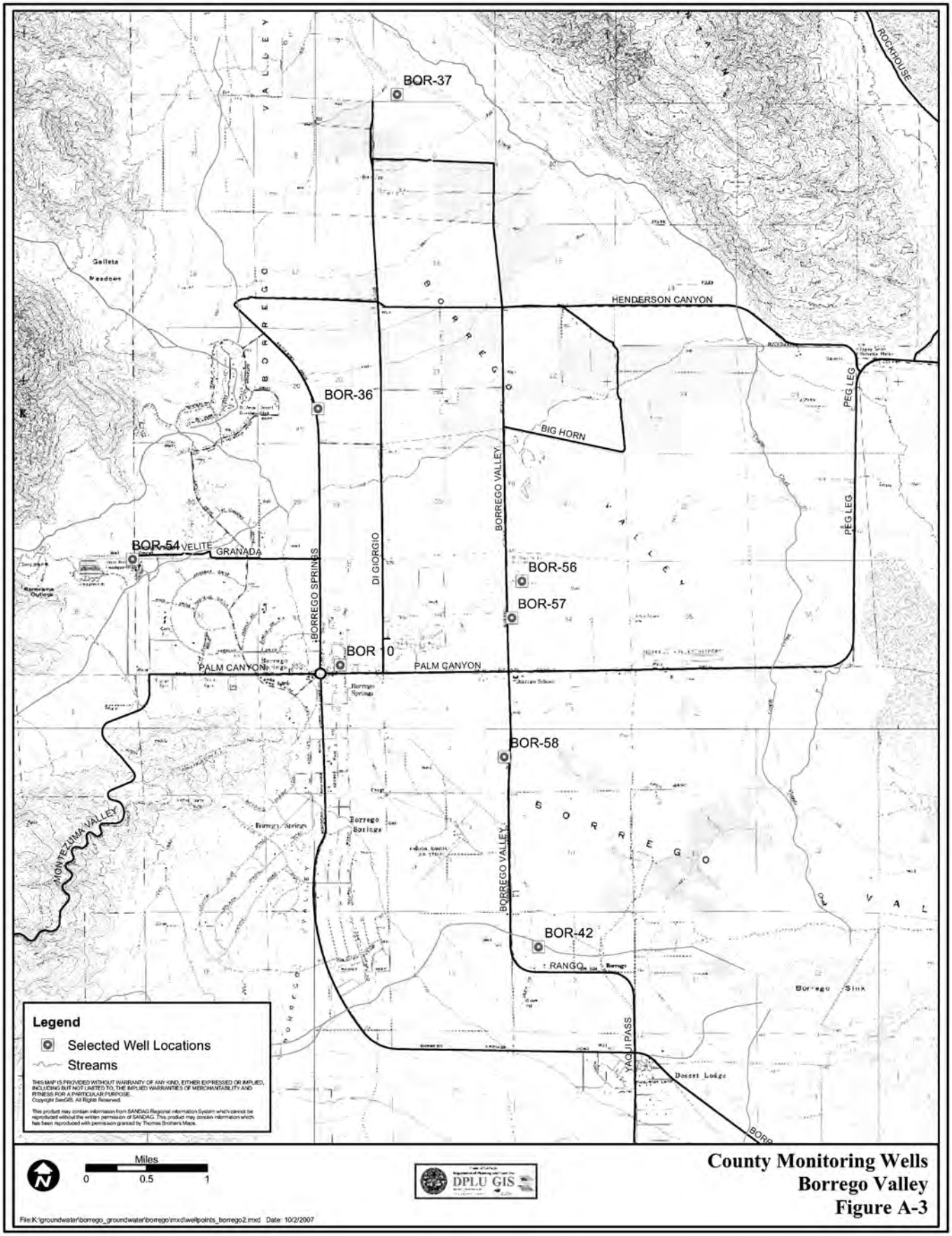
BOR-37
BOR-36
BOR-54
BOR-56
BOR-57
BOR-58
BOR-42
HENDERSON CANYON
BIG HORN
PEG LEG
PEG LEG
BORREGO VALLEY
BORREGO VALLEY
BORREGO SPRINGS
DI GIORGIO
VELITE
GRANADA
PALM CANYON
PALM CANYON
MONTEZUMA VALLEY
ROCKHOUSE
Galleta Meadows
Borrego Springs
Borrego Springs
RANGO
YAQUI PASS
Desert Lodge
Borrego Sink
Legend
Selected Well Locations
Streams
Miles
0
0.5
1
DPLU GIS
County Monitoring Wells
Borrego Valley
Figure A-3

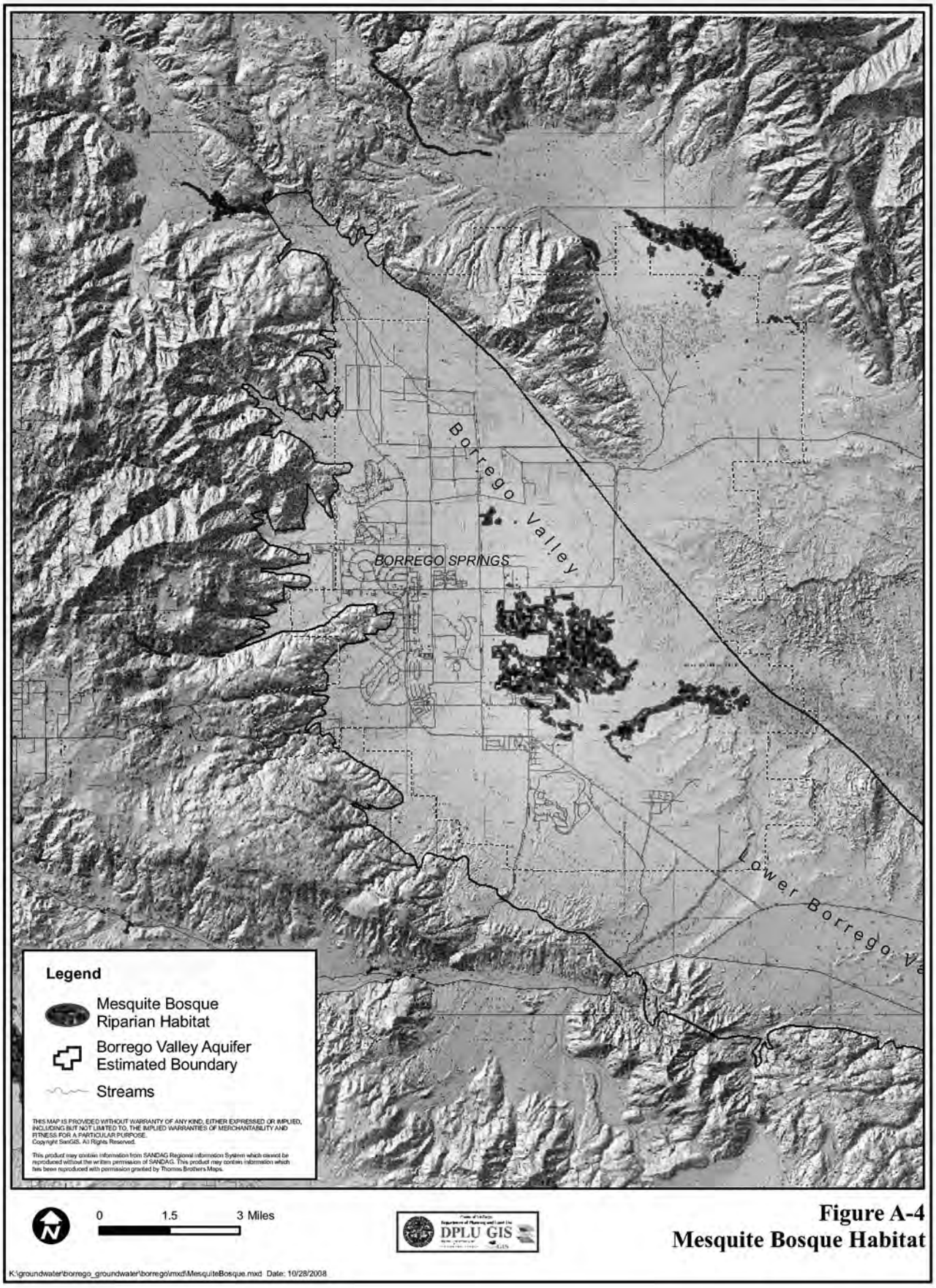

Figure A-4
Mesquite Bosque Habitat

Geologic Time Scale

ERA	PERIOD		EPOCH	START DATE (mya)
Cenozoic "Age of Mammals"	Quaternary		Holocene	0.01
			Pleistocene	2.5
	Tertiary	Neogene	Pliocene	5
			Miocene	24
		Paleogene	Oligocene	34
			Eocene	55
			Paleocene	65
Mesozoic "Age of Reptiles"	Cretaceous			144
	Jurassic			208
	Triassic			245
Paleozoic				570

Source: *Fossil Treasures of the Anza-Borrego Desert* (2006)

Adapted by Diana E. Lindsay per correspondence with George T. Jefferson (2010)

(See also stratigraphy.org/upload/ISChart2009.pdf)

Sky Art: HN-4 1951 Willys Jeep (CJ-3A)

GALLETA MEADOWS SKY ART

INSPIRED BY SCIENCE, HISTORY, NATURE, AND WHIM

A Catalog and Guide to Sky Art Assemblages in Borrego Springs, California,
With Accompanying Text Detailing the Inspiration for the Metal Sculptures

Compiled by Diana E. Lindsay, Trustee, Anza-Borrego Foundation

On Saturday morning, April 10, 2008, the small desert community of Borrego Springs, situated in the middle of Anza-Borrego Desert State Park, stepped back in deep time. A family of metal *Gomphotherium* standing in a field just off Borrego Springs Road startled passersby. The 12-foot tall, 800- to 1000-pound Neogene sculptures were placed in position that day by artist Ricardo Arroyo Breceda and property owner-benefactor Dennis Avery [Brancheau, April 2008]. The last living gomphotheres had roamed this land some 3.7 million years ago, and they had returned.

Since that day more than 125 life-size metal sculptures, all commissioned by Avery, have been placed in the Borrego Valley, scattered over 3 miles of non-contiguous private property that Avery purchased in the mid-1990s in the wake of the savings-and-loan crash. Avery calls the undeveloped land "Galleta Meadows," named for the tough native grass (*Hilaria rigida*) found in the Borrego Valley western canyons. Galleta Meadows is open to the public for their enjoyment. One will find no interpretive signs, roadway signs, bathrooms, or drinking water. It is not a public exhibition of art. It is just "pure, expressive art" that has avoided county regulators and is, according to Avery, an expression of First Amendment rights to free expression.

The metal sculptures were originally inspired by the 2006 publication of *Fossil Treasures of the Anza-Borrego Desert*, edited by George T. Jefferson and Lowell Lindsay. Avery was a major sponsor of the publication of this book, funding the artwork by Pat Ortega, an award-winning scientific illustrator, and John Francis, a renowned landscape artist whose illustrations are now the background paleolandscapes at the Park Visitor Center.

Fossil Treasures is a landmark publication featuring the comprehensive work of 23 leading paleontologists and experts from key scientific institutions across the United States. Their work provides an in-depth examination of fossil plants, extinct animals, and changing environments that opens a window into this region's long-vanished past. And, within this window is found one of the richest fossil records of its time in the western hemisphere – a continuous history of life for most of the last 7 million years. Through this same window came the inspiration to bring the past to the present for the enjoyment, delight, and perhaps consternation for all who have viewed the Sky Art sculptures.

Avery calls the sculptures "Sky Art." The sculptures, like the living forms of the past, have evolved with time. Avery's original goal was "to inspire visitors and residents, especially young people, to learn more about the fossil history of Anza-Borrego." He saw the idea of fossil sculptures as perhaps not "completely rational, but it is pretty amazing. Especially if you're 8 years old." Avery explained in an interview in April 2008 that he felt he was "awakening interest" by erecting fossil animals that have been buried in the desert for 7 million years. "OK," he said, "there are bones here. But now they're coming out of the ground and are three-dimensional" [Brancheau, April 2008].

The actual idea to create fossil metal sculptures came about during one of Avery's regular visits to the University of Redlands where two of his children were students. While driving back and forth on I-215, he noticed large metal sculptures towering on the edge of the freeway behind a fence that read "Perris Jurassic Park." A giant *Tyrannosaurus rex* with gaping mouth greeted daily commuters. One day his curiosity got to him. Avery took the nearest exit and worked his way back to Perris Jurassic Park where he found a welding shop, a sculpture garden, and its proprietor, Ricardo Breceda.

Breceda, who originally came to California from Durango, Mexico, was living his dream of creating metal dinosaurs, literally by accident. A back injury caused by a fall from a two-story building in the 1990s prevented him from working in his regular construction job of carpentry and welding. After his injury he took up the hobby of metal sculpting and gradually began selling his sculptures [McKinnon 2008]. His dinosaurs are his best sellers. His creations are made from sheet and scrap metal, wire, and re-bar pounded with various sized hammers to create

texture and then welded together.

When Avery asked Breceda if he could create other things besides dinosaurs, Breceda told him he only needed a photograph. And so, the first Galleta Meadows Sky Art sculptures – the gomphotheres – were commissioned. Then quickly followed gracile sabertooth cats, giant tortoises, camelids, and ground sloths. There was never a master plan in creating the sculptures – they just grew, evolved, and morphed into different things. For Breceda, the project has been a dream come true, including adding his beloved dinosaurs to the landscape. His vision parallels that of Avery's. He sees his work as finding "A Place in the Heart & Sight of Children of Any Age" [*Borrego Sun* 2008].

As a whole, the Galleta Meadows "Sky Art" now falls into three general categories: (1) Fossil inspired sculptures based on the research presented in *Fossil Treasures of the Anza-Borrego Desert*; (2) Historical Event or Natural Feature inspired sculptures based on the Anza-Borrego desert; and (3) sculptures inspired by a long-ago past – Jurassic and Triassic periods – that grab the imagination but have no historical or known fossil connection to this desert.

All of the sculptures, especially the latter group, are for "fun and whim," according to Avery. It is an art form with Breceda the artist, and Borrego Valley his palette. "It is fun, foible, science and (Ricardo's) imagination…. His natural talents and creations from ready materials, distinguish his expressions…born of fantasy and…fact."

Galleta Meadows Sky Arts, according to Avery,

> …are not projecting accurately either history or science – intentionally. The Sky Arts are lyrical invites to visual confrontation with the myth of it all as well as "fact." It is this Whim, the careless presentation, the incomplete explanations which have been so accurately comprehended by the public. In flows the adoration, and importantly, participation. They want a treasure hunt of their own and now find it here. [Avery e-mail 8/23/10]

For Avery, Sky Arts have something for everyone, a "cornucopia of visions, observations, and sciences. One can have all, none, or one it seems, and [it] is the fun in it." Even the controversial dinosaurs have managed to meet one of Avery's goals regarding children:

> It is interesting, so many of the children call all now extinct vertebrates dinosaurs. They see the mastodons and say, "Mom Mom look, more dinosaurs." Not very scientific, yet very revealing of children who perhaps enjoy all the "dinosaurs" the most. Fantasy, purely to some. It might lead children to the hard sciences though. [Avery e-mail 8/25/10]

The addition of dinosaurs and the "last" Sky Art sculpture – a 1951 Willys Jeep – have and will continue to stir much interest and many comments that may be viewed in the "guestbook" at www.galletameadows.com.

"Sky Art," and more recently appearing as "SkyArt," is a term coined by Avery to describe a particular art form. Other southern California examples include the Los Angeles Watts Tower built by Italian immigrant construction worker Sabato "Sam" Rodia in his spare time over a period of 33 years, from 1921 to 1954. Also included are the environmental art work of Christo and Jeanne-Claude: the 1,760 "Yellow Umbrellas" placed on the Tejon Ranch in 1991, the wrapping of the Reichstag in Berlin in 1995, the "Running Fence" in Sonoma and Marin counties in 1976, and many others. Their art was temporary and was appreciated for the experience.

Still another example is Stanley March 3's Ant Farm art group that created the now famous Cadillac Ranch in Amarillo, Texas, in which are found five buried Cadillacs. He also founded a group called the "Dynamite Museum" that consists of young men who paint whimsical traffic signs and post them around town and in yards with the owner's permission. And, he has a giant phantom pool table that can only be seen from the air and is moved about his ranch – always a surprise to come across as one never knows where it will be. All are whimsical and many would call them folly.

British philosopher Richard Wollheim distinguishes three different approaches to the aesthetic value of art: the realist, the objectivist, and the relativist [Wollheim 1980]. Sky Art falls into the relativist category. According to Wollheim, art in the relativist category does not have an absolute value – it depends on and varies with the human experience. The art may have an intention or not, but it will be a vehicle to express emotions and ideas and a means for exploration.

As the project comes to a close, Avery muses about it, and leaves it for the critics to decide – "fantasy, foible, fact… fun, folly, and turmoil. Finite. Eventually a pile of rust. Everyone senses that, the life, the death of it."

That being said, perhaps the sane thing to do is to just sit and enjoy the art, but for those pragmatic realists out there, here are the links of inspiration that have led to all this whimsy, grouped into the three categories.

SKY ART GALLETA MEADOWS -- SORTED BY INSPIRATIONAL SOURCES FOR SCULPTURES
(Sites Numerically Ordered Generally North to South within Categories)
Some Sites Have Multiple Assemblages

Inspiration Sources	Map Site Symbol	Assemblage	Scientific Name	Units Installed	Date Installed	Location
Fossil Treasures (FT)	FT-1	peccary family	*Platygonus* sp.	6	9/28/2008	W side Galleta Pkwy at Stagecoach, Indian Head Ranch
	FT-2	giant tortoises	*Hesperotestudo* sp.	2	7/11/2009	E side Galleta Pkwy at Stagecoach, Indian Head Ranch
	FT-3	Merriam's tapir	*Tapirus merriami*	7	3/25/2010	E side Galleta Pkwy between velociraptors & saberthooth cats
	FT-4	sabertooth cats	*Smilodon gracilis*	2	5/10/2008	immediately inside Indian Head Ranch gate E side
	FT-5	giant tortoises	*Hesperotestudo* sp.	5	5/10/2008	Henderson Cyn Rd across from Indian Head Ranch gate
	FT-6	African elephants	*Loxodonta africana*	2	5/10/2008	E side Bor Sprs Rd, N of Santa Rosa
	FT-7	llamas	*Hemiauchenia* sp.	3	5/17/2008	S side San Ysidro Dr, E of Catarina Dr
	"	*Camelops*	*Camelops* sp.	2	5/17/2008	S side San Ysidro Dr, E of Catarina Dr
	FT-8	Shasta ground sloths	*Nothrotheriops shastensis*	2	5/17/2008	W side Bor Sprs Rd, S of San Ysidro Dr
	FT-9	*Camelops*	*Camelops* sp.	2	6/15/2008	E side Bor Sprs Rd, N of Big Horn Rd
	"	Harlan's ground sloths	*Paramylodon harlani*	2	6/15/2008	E side Bor Sprs Rd, N of Big Horn Rd
	"	Harlan's ground sloth	*Paramylodon harlani*	1	7/12/2008	E side Bor Sprs Rd, N of Big Horn Rd
	FT-10	gomphotheres	*Gomphotherium*	3	4/10/2008	E side Bor Sprs Rd, S of Big Horn Rd
	"	*Camelops*	*Camelops* sp.	2	7/12/2008	E side Bor Sprs Rd, S of Big Horn Rd
	FT-11	sabertooth cats	*Smilodon gracilis*	6	9/28/2008	3.8m S of Xmas Circle on S3, S side
	"	extinct horses	*Equus* sp.	4	9/28/2008	3.8m S of Xmas Circle on S3, S side
	FT-12	*Aiolornis* in nest	*Aiolornis incredibilis*	4	11/15/2008	N side of S3, across from horses & sabertooth cats
	FT-13	extinct horses	*Equus* sp.	9	9/28/2008	N side S3, E of *Aiolornis* , W of mammoths
	FT-14	mammoth family	*mammuthus columbi*	3	8/23/2008	N side S3, E of horses, NW of Anzio Dr
	FT-15	*Aiolornis* with prey	*Aiolornis incredibilis*	2	11/17/2008	.2m S on Anzio Dr off S3
History/Nature (H/N)	H/N-1	Peninsular bighorn sheep	*Ovis canadensis cremnobates*	12	4/9/2009	S side Stagecoach, .2m W Galleta Pkwy, Indian Head Ranch
	"	miner & mule		2	7/10/2010	S side Stagecoach, .2m W Galleta Pkwy, Indian Head Ranch
	H/N-2	Indian head		1	12/30/2008	Henderson Cyn Rd across from Indian Head Ranch gate
	H/N-3	padre and dog		2	12/30/2008	N on dirt road past intersection Bor Sprs Rd/Henderson Cyn Rd
	"	saguaro	*Carnegiea gigantea*	1	9/18/2009	W of padre on dirt road
	H/N-4	1951 Willys Jeep (CJ-3A)		1	10/30/2010	W of Indian head on Borrego Springs Rd
	H/N-5	Farm Workers		23	9/18/2009 1/20/2010	(11/21/09 some units removed & replaced in January) SW corner of Big Horn Rd & Di Giorgio Rd
	H/N-6	Anza on horse		2	6/25/2010	in front of BS Chamber of Commerce, Palm Cyn Dr
Dinosaurs (D)	D-1	*Velociraptor*	*Velociraptor*	2	4/9/2009	E side Galleta Pkway between tapirs and tortoises
	D-2	*Spinosaurus*	*Spinosaurus*	4	5/28/2009	S of S3 on dirt rd between Anzio extension & Glorietta Cyn Rd
	D-3	fighting dinosaurs	*Carnotaurus & Allosaurus*	2	7/11/2009	S of S3 on dirt rd between Anzio extension & Glorietta Cyn Rd
	D-4	*Utahraptor*	*Utahraptor*	3	7/11/2009	S of S3 on dirt rd between Anzio extension & Glorietta Cyn Rd
	D-5	*Tyrannosaurus rex*	*Tyrannosaurus rex*	4	5/29/2009	S of S3 on dirt rd between Anzio extension & Glorietta Cyn Rd

SKY ART GALLETA MEADOWS -- SITES LISTED GENERALLY NORTH TO SOUTH

Generalized Groupings	Total Units in Group	Assemblage	Scientific Name	Map Site Symbol	Location
Indian Head - Stagecoach Way Grp	14	Peninsular bighorn sheep	*Ovis canadensis cremnobates*	H/N-1	S side Stagecoach, .2m W Galleta Pkwy, Indian Head Ranch
		miner & mule		"	S side Stagecoach, .2m W Galleta Pkwy, Indian Head Ranch
Indian Head - Galleta Prkwy Grp	19	peccary family	*Platygonus* sp.	FT-1	W side Galleta Pkwy at Stagecoach, Indian Head Ranch
		giant tortoises	*Hesperotestudo* sp.	FT-2	E side Galleta Pkwy at Stagecoach, Indian Head Ranch
		Velociraptor	*Velociraptor*	D-1	E side Galleta Pkwy between tapirs and tortoises
		Merriam's tapir	*Tapirus merriami*	FT-3	E side Galleta Pkwy between velociraptors & saberthooth cats
		sabertooth cats	*Smilodon gracilis*	FT-4	immediately inside Indian Head Ranch gate, E side
Indian Head Entrance Gate Grp	6	giant tortoises	*Hesperotestudo* sp.	FT-5	Henderson Cyn Rd across from Indian Head Ranch gate
		Indian head		H/N-2	Henderson Cyn Rd across from Indian Head Ranch gate
Henderson Cyn Grp	4	padre and dog		H/N-3	N on dirt road past intersection Bor Sprs Rd/Henderson Cyn Rd
		saguaro	*Carnegiea gigantea*	"	W of padre on dirt road
		1951 Willys Jeep (CJ-3A)		H/N-4	W of Indian head on Borrego Springs Rd
Galleta Meadows Sign & Monument	2	African elephants	*Loxodonta africana*	FT-6	E side Bor Sprs Rd, N of Santa Rosa
Camelid Grp	5	llamas	*Hemiauchenia* sp.	FT-7	S side San Ysidro Dr, E of Catarina Dr
		Camelops	*Camelops* sp.		S side San Ysidro Dr, E of Catarina Dr
Borrego Springs Rd Grp	12	Shasta ground sloths	*Nothrotheriops shastensis*	FT-8	W side Bor Sprs Rd, S of San Ysidro Dr
		Harlan's ground sloths	*Paramylodon harlani*	FT-9	E side Bor Sprs Rd, N of Big Horn Rd
		Camelops	*Camelops* sp.	"	E side Bor Sprs Rd, N of Big Horn Rd
		Camelops	*Camelops* sp.	FT-10	E side Bor Sprs Rd, S of Big Horn Rd
		gomphotheres	*Gomphotherium*	"	E side Bor Sprs Rd, S of Big Horn Rd
Farm Workers	23	Di Giorgio Fruit Corp farm workers		H/N-5	(11/21/09 some units removed & replaced in January) SW corner Big Horn Rd & Di Giorgio Rd
Juan Bautista de Anza	2	Anza on horse		H/N-6	in front of BS Chamber of Commerce, Palm Cyn Dr
S3 Highway Grp	26	sabertooth cats	*Smilodon gracilis*	FT-11	3.8m S of Xmas Circle on S3, S side
		extinct horses	*Equus* sp.	"	3.8m S of Xmas Circle on S3, S side
		Aiolornis in nest	*Aiolornis incredibilis*	FT-12	on S3, N of horses & sabertooth cats
		extinct horses	*Equus* sp.	FT-13	N side S3, E of *Aiolornis*, W of mammoths
		mammoth family	*mammuthus columbi*	FT-14	N side S3, E of horses, NW Anzio Dr
Aiolornis	2	*Aiolornis* with prey	*Aiolornis incredibilis*	FT-15	.2m S on Anzio Dr off S3
		prey-peccary	*Platygonus* sp.	"	.2m S on Anzio Dr off S3
Jurassic Park Dinosaurs*	13	*Spinosaurus*	*Spinosaurus*	D-2	S of S3 on dirt rd between Anzio extension & Glorietta Cyn Rd
		fighting dinosaurs	*Carnotaurus & Allosaurus*	D-3	S of S3 on dirt rd between Anzio extension & Glorietta Cyn Rd
		Utahraptor	*Utahraptor*	D-4	S of S3 on dirt rd between Anzio extension & Glorietta Cyn Rd
		Tyrannosaurus rex	*Tyrannosaurus rex*	D-5	S of S3 on dirt rd between Anzio extension & Glorietta Cyn Rd
					* S on Anzio to dirt + .5m, turn W; or S .8m on Glorietta Cyn Rd, turn E

Category 1 (FT) – Sky Art Inspired by Fossil Evidence

As Presented in *Fossil Treasures of the Anza-Borrego Desert*

The descriptions below are based on the text found in *Fossil Treasures of the Anza-Borrego Desert* [Jefferson and Lindsay 2006]. The Sky Art sculptures are numerically listed as they are generally found in a north to south order. See attached table for a list of combined Sky Art inspiration categories listed north to south

FT-1: Peccary – *Platygonus sp.*

Even-toed ungulates or hoofed animals belong to the Order Artiodactyla as opposed to Perissodactyla, the odd-toed ungulates. The artiodactyls include peccaries, llamas, camels, deer, sheep, goats, cattle, giraffes, and pronghorns. The perissodactyls are browsing and grazing animals that include horses, tapirs, and rhinoceroses. Peccaries are members of the Family Tayassuidae, endemic to North America from the Miocene to Holocene epochs. Fossils from the extinct genus *Platygonus* have been found throughout North America. In Anza-Borrego they date from 3 million to 1.7 million years ago. Although artiodactyls are basically herbivores, the peccaries were like their living pig relatives, eating leaves, seeds, roots, fruit, worms, larvae, small vertebrates, and eggs. They were probably gregarious and hunted in packs. Their bodies were larger than modern peccaries and they had long legs and carnivore-like tusks.

The Sky Art peccary metal sculptures are located on the southwest corner of Galleta Parkway and Stagecoach Way within Indian Head Ranch. Four piglets are nursing a sow as the boar observes.

FT-2: Giant Tortoise – *Hesperotestudo sp.*

Hesperotestudo is an extinct species of the Family Testudinidae which are the tortoises or land turtles. The presence of this tropically-related fossil in Anza-Borrego indicates warmer winters, cooler summers and enough precipitation to create permanent bodies of water during the Pliocene and early to middle Pleistocene. Two species of the giant tortoises have been identified based on their size. The largest measures almost 4 feet long, 3 feet wide, and 2 feet tall [Gensler, Roeder, and Jefferson in Jefferson and Lindsay 2006]. They first appear in the fossil record in Anza-Borrego about 3 million years ago and are found in various strata through to 1 million years ago. Since these animals did not burrow, they could only survive in a frost-free area that had pools of water where they could cool themselves. Fossils from *Hesperotestudo* have been found from North America to Central America.

Two Sky Art metal tortoise sculptures are located on the east side of Galleta Parkway at the junction of Stagecoach Way.

FT-3: Merriam's Tapir – *Tapirus merriami*

Members of the Tapiridae family are perissodactyls (see FT-1) who have changed very little evolutionarily since they first appeared some 40 million to 30 million years ago. The minor changes that have occurred include a general increase in size, pre-molar teeth becoming more molar-like, and refinement of the proboscis. Both the North American Pleistocene fossil tapirs and the extant relatives all belong to the same genus, Tapirus. Pleistocene tapirs came in two sizes – large and small. In the southwest, Tapirus merriami was the larger form, and its fossil remains in Anza-Borrego date from a little over 2 million years ago. The most complete fossil specimen of this species was found in Anza-Borrego. Their closest relatives are the odd-toed ungulates – horses and rhinoceroses.

Seven Sky Art tapir sculptures are found on the east side of Galleta Parkway inside of Indian Head Ranch, midway between the entrance gate and Stagecoach Way.

FT-4: Gracile Sabertooth Cat – *Smilodon gracilis*

The felids are the most represented fossils of large carnivores found in Anza-Borrego. They fall into the following subfamilies – the extinct Machairodontinae (the sabertooth cat), the Pantherinae (the jaguar), and the Felinae (cheetah-like cat). Of the three, the most commonly recovered species is *Smilodon gracilis*, the gracile sabertooth cat. Anza-Borrego holds the only fossil record for this species in western North America [Shaw and Cox in Jefferson and Lindsay 2006], and it dates from 2.1 million to less than 1 million years ago. It is a direct ancestor to *Smilodon fatalis*, the California state fossil. It is the smallest of the Smilodon species. Powerful legs and a short tail indicate that the gracile sabertooth cat used stealth and ambush rather than speed to capture its prey. It could open its mouth 120 degrees, as compared to a lion, who can open its mouth 65 degrees. In size, they were comparable to the extant jaguar.

The Sky Art metal *Smilodon* sculptures are found just within the entrance gate to Indian Head Ranch on the east side on Galleta Parkway.

FT-5: Giant Tortoise – *Hesperotestudo sp.*

See FT-2 for a description. There are five giant tortoise sculptures positioned on the south side of Henderson Canyon Road across from the entrance gate to Indian Head Ranch and one to the west of the entrance on the north side of the road.

FT-6: African Elephant – *Loxodonta Africana*

The name of the Order Proboscidea refers to the elongated nose or proboscis (trunk) of family members that include the mastodons, gomphotheres, and elephants. This order arose out of Africa. The elephant family includes mammoths and the Asian and African elephants which have not been found in the North American fossil record. The elephant is the largest land mammal in the world, weighing about 10,000 pounds. Fossil remains of proboscideans found in Anza-Borrego include gomphotheres and mammoths. Mastodon fossils have not been positively identified here [McDaniel in Jefferson and Lindsay 2006]. See FT-10 for a discussion on gomphotheres and FT-14 for information about the Columbian mammoth.

Two African elephant metal sculptures are found on the east side of Borrego Springs Road, north of Santa Rosa, at the Galleta Meadows Estate sign. Also at the same location is a metal plaque commemorating the Anza expeditions to Alta California.

FT-7: Camelids – (Llamas) *Hemiauchenia sp.* and Camels – *Camelops sp.*

The family Camelidae originated in North America about 44 million years ago. The two sub-families include Tribe Lamini, represented today by llamas and alpacas of South America, and Tribe Camelini, represented today by the Bactrians of Asia and the dromedaries of Africa. *Hemiauchenia* sp. and *Camelops* sp. are in the Tribe Lamini. No Sky Art sculpture represents Tribe Camelini, although fossil remains of one genus – *Gigantocamelus* – have been found in Anza-Borrego. Fossils of the camelid family are the second most commonly found fossils of Anza-Borrego after horses and first in diversity of species. The various species of camel are found in deposits that date from 5 million to 0.5 million years ago. Camelids are distinguished by ipsilateral limb pairs, that is, the fore and hind limbs on the same side move forward and back at the same time as the animal moves. They also have very distinct foot bones – the foot toes were reduced to two – which allowed them to thrive in open country and later dryer lands.

Hemiauchenia was probably ancestral to all other llamas in North and South America. Based on characteristics of modern llamas, it is believed that it was an open plains animal that fed on grasses [Webb, Randall, and Jefferson in Jefferson and Lindsay 2006]. Although Camelops closely resembled modern day camels, morphologically they were closer to llamas. The largest Camelops sp. was seven feet tall, almost 20 percent larger than today's dromedary camels.

The Sky Art Camelids found at the southeast corner of Catarina Drive and San Ysidro Drive represent three *Hemiauchenia* sp. and two *Camelops* sp.

FT-8: Shasta Ground Sloth – *Nothrotheriops shastensis*

Animals in the Order Xenarthra are usual for their dentition, which lacks enamel, and for the presence of extra articulations between the vertebrae of the lower back. This order evolved in South America and dispersed into North America in three invasions in the late Cenozoic. Included in this order are tree sloths, anteaters, and armadillos, which are still living, and ground sloths, which are extinct. Fossil finds of ground sloths in Anza-Borrego are from all three invasions which are represented by different sloths who all utilized different types of habitats. The earliest xenarthrans entered North America in the late Miocene, about 9 million years ago, while the last ones arrived during the Pleistocene. *Nothrotheriops shastensis* arrived during the last invasion and was the smallest of the North American ground sloths, said to be about the size of a small calf. The skull of the Shasta ground sloth is longer and narrower than the other sloth species. It may have been a browser that was better adapted to arid desert conditions than the other ground sloths. The earliest fossils of the Shasta ground sloth found in Anza-Borrego date from 2 million years ago.

The two metal sculptures of the Shasta ground sloth are found on the southwest corner of San Ysidro Drive and Borrego Springs Road.

FT-9: Harlan's Ground Sloth – *Paramylodon harlani* and Camels – *Camelops sp.*

See FT-8 for evolutionary history of ground sloths. Paramylodon harlani arrived in North America during the second invasion and first appears in the fossil record in Anza-Borrego about 2.3 million years ago. It was the largest of the Anza-Borrego ground sloths. The muzzle of this ground sloth is much wider than that of the Shasta ground sloth. Harlan's ground sloth is thought to have been a mixed feeder that lived in a more open countryside, such as a savanna. The skin contained dermal ossicles – pieces of imbedded bone – which is not found in the other ground sloths. These bony nodules on the back of

the animal provided protection from predators. These animals also had very strong forearms and curved claws that suggest they could dig.

A large upright, 800-pound, metal Harlan's ground sloth is found on the east side of Borrego Springs Road north of Big Horn Road. It stands 17 feet tall. Just to the south of this sloth is another with a baby on its back.

Two large *Camelops sp*. are found to the south of the ground sloths. The unique toe structure of these animals is clearly visible. See FT-7 for a description.

FT-10: Gomphothere – *Gomphotherium* and Camels -- *Camelops sp.*

The gomphotheres are one of the distinct families in the Order Proboscidea. See FT-6. Gomphotheres differed from elephants in their tooth structure and tusks. Two members of this family are found in Anza-Borrego – *Gomphotherium* and *Stegomastodon*. *Gomphotherium* crossed the Bering land bridge to North America about 15 million years ago. It was a hippopotamus-sized animal with short legs and four tusks. A distinguishing characteristic was its elongated chin that caused the tips of the lower tusks to extend almost to the tips of the larger upper tusks. *Gomphotherium* lived in marshy areas. The oldest *Gomphotherium* fossils found in the Park date back to 9 million years.

The *Gomphotherium* Sky Art sculptures found at the southeast corner of Borrego Springs Road and Big Horn Road depict a family. The larger units weigh 1,000 pounds and stand 12 feet tall. They are 20 feet long. Oddly enough, the Greek translation for *Gomphotherium* is "welded beast." Directly to the north of the three sculptures are a mother *Camelops* and its calf. See FT-7 for a description of *Camelops*.

FT-11: Gracile Sabertooth Cat – *Smilodon gracilis* and Extinct Horse – *Equus sp.*

See FT-4 for a description of the gracile sabertooth cat. The six sabertooth cats are located on the south side of Highway S3, 3.8 miles south of Christmas Circle. They are posed in active stance, attacking prey, lying in ambush, and fighting.

Horses are perissodactyls (see FT-1 and FT-3) or odd-toes ungulates that often bear hooves. In the case of the horse, this is extreme, whereby the central digit is huge and the other lateral toes have become accessory splint bones – an evolutionary adaptation to running. They are members of the family Equidae which includes true horses, zebras, and asses (donkeys). Horses are native to North America, originating on this continent about 57 million years ago [Scott in Jefferson and Lindsay 2006]. There were several successful emigrations to the Old World, crossing the Bering land bridge, throughout their history. They went extinct in the Pleistocene Epoch in North America about 11,000 years ago. They were later reintroduced to North America when the Spaniards conquered Mexico. Fossil remains in Anza-Borrego capture the more recent evolutionary history of the horse. These horses were adapted to eating coarse, gritty plants rather than leaves. Dental patterns are often used in identifying horse species. The first fossil record for the subgenus that includes the modern domestic horse may have been recorded in Anza-Borrego. It is still not confirmed [Scott in Jefferson and Lindsay]. The oldest fossils are from the ancestors of *Equus* which date to just over 4 million years ago, and they may possibly be the youngest occurrence of *Dinohippus* in North America.

Four Sky Art sculptures depict the extinct horse as it is being pursued by hunting carnivores – chased, attacked, and stalked by the gracile sabertooth cats.

FT-12: Incredible Wind God Bird – *Aiolornis incredibilis* in Its Nest

The largest flight-capable bird in North America was the *Aiolornis incredibilis* with a wingspan of 16 to 17 feet. Only six specimens of this four-foot tall bird have been found, and three of those come from Anza-Borrego, with the oldest fossil specimens dating about 1 million years and the most recent about 0.5 million years. The fossil specimens indicate that the area was much wetter, with streams, lakes, and ponds. The name *Aiolornis* translates from Greek as "wind god bird." It had previous been called *Teratornis incredibilis*, and was a predator more closely related to Old World storks.

The metal sculpture located to the north of Highway S3, almost 4 miles south of Christmas Circle, depicts *Aiolornis incredibilis* in its nest with two fledglings who have been presented a snake for their dinner. The entire sculpture weighs more than 1,400 pounds.

FT-13: Extinct Horse – *Equus sp.*

See FT-11, FT-3, and FT-1 for information about horses and perissodactyls. The nine Sky Art sculptures of *Equus sp.* found on the north side of Highway S3, between *Aiolornis* and the mammoths, are found in various poses as they might have appeared in Anza-Borrego during the Pleistocene.

FT-14: Columbian Mammoth – *Mammuthus columbi*

Mammoths (*Mammuthus*) are medium to large-sized elephants that originated in southern and eastern Africa about 4 million years ago, subsequently spreading through Europe, Asia, and North America. Four species of mammoth originally crossed the Bering land bridge to North America, and only two of the species are found in Anza-Borrego – the southern mammoth and the Columbian mammoth. The southern mammoth, *Mammuthus meridionalis*, was a medium-sized elephant that was here at least 1.4 million years ago. The Columbian mammoth was the largest North American elephant and its skeletal remains date from 1.1 million years ago. For a long time the imperial mammoth was thought to have been a separate species, but it is now considered an early evolutionary stage of the Columbian mammoth. All of the Columbian mammoth species found in Anza-Borrego belong to this early evolutionary stage. A specimen from the later Columbian evolutionary stage was found east of the Park near the Salton Sea.

Sky Art metal sculptures of a *Mammuthus columbi* family are found on the north side of Highway S3, northwest of Anzio Drive.

FT-15: Incredible Wind God Bird – *Aiolornis incredibilis* with Prey – *Platygonus sp.*

The 1,400-pound metal sculpture found on the west side of Anzio Drive, south of Highway S3, depicts Aiolornis incredibilis as it has just captured a Platygonus sp. The wing span of the sculpture is 16 feet, which was the actual size of Aiolornis incredibilis. The sculpture is 24 feet long from beak to tail. See FT-12 for information about Aiolornis incredibilis and FT-1 for a description of the Platygonus sp.

Category 2 (HN) – Sky Art Inspired by Historical Events and Natural Features of the Anza-Borrego Desert

By pure serendipity, the subjects selected to create Sky Art sculptures in this category happen to be significantly important to the area's history and natural features and would have been the ones selected had there been an original plan for this category. Breceda has taken artistic license in some of the representations that don't accurately portray fact, such as in the Aztec-style Indian head. The sculptures should be viewed as symbolic representations.

The descriptions below are based largely on *Anza-Borrego A to Z: People, Places, and Things* [Lindsay 2001]. The Sky Art sculptures are numerically listed as they are generally found in a north to south order. See attached table for a list of combined Sky Art inspiration categories listed north to south.

HN-1: (1) Peninsular Bighorn Sheep – *Ovis canadensis cremnobates*

One of the last refuges of the endangered Peninsular bighorn sheep, *Ovis canadensis cremnobates*, is Anza-Borrego Desert State Park. The special relationship to this preserve is seen in the Park's very name – borrego is Spanish for lamb or sheep. The very survival of this animal is dependent on having open wilderness areas in which it can roam. The Park contains 90 percent of California's designated wilderness areas. "Peninsular" refers to the Peninsular mountain ranges where this subspecies lives. They are currently considered endangered only north of the Mexico border. They were added to the federal list of endangered species in March 1998. They are fully protected by law. It is illegal to hunt sheep. Drought, disease, and mountain lion and coyote predation are a threat to their existence. The Park monitors the bighorn through an annual sheep count held on the 4th of July weekend. The 2010 sheep count tallied 255 sheep of which 109 were ewes and 88 were rams [Bier 2010]. The rest were lambs and yearlings. Many of the sheep are also monitored by radio telemetry by wearing radio-collars. The Peninsular bighorn is also San Diego County's official animal.

The first to note the presence of bighorn in the Anza-Borrego area was Fr. Pedro Font. In his diary of the second Anza expedition, he mentions seeing the horns of wild sheep in Coyote Canyon after leaving Santa Catarina Spring on December 24, 1775.

Bighorn sheep are very elusive and difficult to see. The Sky Art sculptures make it possible for all to see the sheep in their native habitat. The sculptures are found on the south side of Stagecoach Way, 0.2 mile west of Galleta Parkway in Indian Head Ranch.

HN-1: (2) Gold Miner and His Mule

It was the siren call of gold that first brought emigrants to California after James W. Marshall's discovery in 1848. The rush was on, and the Southern Emigrant Trail, which crosses through the southern half of the Anza-Borrego desert, became the all weather route whereby thousands of emigrants passed en route to the gold fields.

The earliest claim for actually finding gold in the Anza-Borrego area goes to mountain man Thomas Long "Pegleg" Smith who spread tales about his 1829 discovery in San

(above) the artist:
Ricardo Arroyo Breceda,
with *camelops* sculpture
(below) African Elephant
& Galleta Meadows sign

FT-1: Peccary

FT-2 & FT-5: Giant Tortoise

FT-3: Merriam's Tapir

FT-4:
Gracile Sabertooth Cat

FT-7: *Hemiauchenia*

FT-8: Shasta Ground Sloth

FT-10: Gomphothere

FT-11:
Gracile Sabertooth Cat

HN-1:
Peninsular Bighorn Sheep

FT-14: Columbian Mammoth

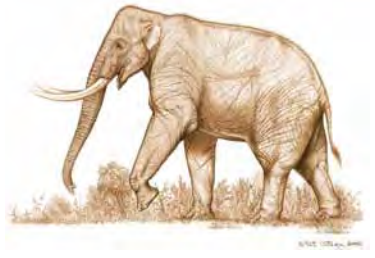

FT-15: Incredibile Wind God Bird

HN-1 (2):
Gold Miner and His Mule

HN-2: Indian Head

HN-3:
Spanish Padre

Francisco saloons, years after California's gold rush. His stories, combined with the actual discovery of gold in the Julian area, were enough to keep prospectors looking for gold in the Anza-Borrego area for years to come. The many stories eventually led to the creation of the Pegleg Smith Liar's Contest in 1948, an annual event celebrated at Pegleg Smith Monument on the first Saturday night in April.

Gold was discovered in Julian in 1869 and then in Banner and Chariot canyons. The only significant gold mine in the Park was the Oriflamme Mine. Primarily worked from 1870 to 1885, it yielded less than $25,000. There were other diggings in Mine Canyon, Grapevine Canyon, Blair Valley, and in the Santa Rosa Mountains.

The Sky Art sculptures of the gold miner and his mule are found on Stagecoach Way, 0.2 mile west of Galleta Parkway in Indian Head Ranch.

HN-2: Indian Head – Representing Sebastián Tarabal and/or Salvador Palma

The Indian head, located appropriately across from the entrance gate to Indian Head Ranch on Henderson Canyon Road, faces toward the sculpture of the padre and the entrance to Coyote Canyon. The sculpture represents the two Indians who played a significant role in the Anza expeditions. Or, it could represent just one of them.

Sebastián Tarabal:

Sebastián Tarabal was a Cochimi Indian born at Mission Santa Gertrudis, north of San Ignacio, in Baja California. He married Maria Dolores Kinajan at Mission Santa Gertrudis on November 5, 1764. Five years later, he was recruited to accompany Captain Gaspar de Portolá and Fr. Junípero Serra on the overland expedition to establish the first mission in Alta California in 1769. He and his wife later became residents of San Gabriel Mission.

In the fall of 1773, Tarabal, his wife, and a companion fled from the virtual enslavement suffered by all Mission Indians and attempted to cross the desert to Arizona. Only Tarabal survived the rigors of the crossing. He arrived at Tubac in January 1774, just as Juan Bautista de Anza was ready to leave on his first exploratory expedition to find a route to California. Immediately, Anza recruited him as a guide.

Anza named the campsite near the marsh at San Sebastian for Tarabal who could clearly identify the route from there to Mission San Gabriel. After they arrived at the mission, Tarabal did not stay. In 1776 he and Fr. Francisco Garcés explored a wide area that included the Mojave Desert, the San Bernardino Valley, the San Fernando Valley, and the San Joaquin Valley. What happened to him afterwards is unknown. Tarabal is also called the *Peregrino* or the "Wanderer," which is sometimes a title used in referring to Garcés (see HN-3).

Salvador Palma:

Olleyquotequiebe, whose name meant "wheezy one" and who may have been asthmatic, was chief of the Yuma (Quechan) Indians when Juan Bautista de Anza arrived at the Colorado River in 1774 while exploring for a road to California. Anza named him Chief Salvador Carlos Antonio Palma. The crossing of the Colorado River was a vital link for a road to California. Knowing this, Anza viewed friendship with Chief Palma as indispensable. Palma was treated with every courtesy and was presented a medal in the likeness of the Spanish king. The Yumas, in turn, offered protection and a base of operations for crossing the river.

Palma warmly received Anza and the colonists when they arrived at Yuma on the second expedition in 1775-6. Anza left Fr. Francisco Garcés and another priest with the Yumas to establish mission outposts at the crossing. On his return from the second expedition, Anza took Palma with him to Mexico City to report the success of the journey, and while they were there, Palma was baptized in the cathedral.

Despite the proffered friendship, the relationship with the Yumas gradually deteriorated over the next five years. In July 1781, the Yumas rose up and destroyed the missions. Palma had joined in the attack. After the destruction of the missions, the Anza trail fell into disuse.

HN-3: Spanish Padre – Representing Fr. Francisco Garcés and/or Fr. Pedro Font with an Arizona Sonoran Desert Saguaro

A Galleta Meadows memorial plaque commemorates the Anza expeditions of 1774 and 1775-6, which together constitute one of the most important events in the history of California after its discovery by Juan Cabrillo and the establishment of the first mission in California by Gaspar de Portolá and Fr. Junípero Serra. The first expedition in 1774 opened the overland road to California, while the second expedition the following year brought the first colonists to California who settled in the San Francisco Bay area. There are two identical plaques – one is found on the gate entrance to Indian Head Ranch, and the other is found at the entrance to Galleta Meadows Estate where the Sky Art elephants are found. The padre represents one or the other or both of the padres who accompanied the

Anza expeditions. The padre is located north beyond the pavement of Borrego Springs Road, west of the entrance to Indian Head Ranch.

Fr. Francisco Garcés:

Franciscan missionary Francisco Hermenegildo Garcés served as the padre on the first Anza expedition. He was born in Aragon, Spain, and after he was ordained, he was assigned to Mission San Javier del Bac, near present-day Tucson, Arizona. He was known as the "wandering priest" because of his explorations of the southwest. In 1771 he explored west down the Gila River to the Colorado River and followed it south into the delta country of Sonora and Baja California. Turning northwest, Garcés wandered within sight of Signal Mountain, just below the present international border near Calexico. Looking across the Anza-Borrego desert, he saw a break in the Peninsular Ranges at Coyote Canyon, which suggested a pass or a river course through the mountains that might lead to the coast and the California settlements. He shared this information with Juan Bautista de Anza, presidial captain at Tubac, and was later recruited as guide and spiritual advisor on Anza's first expedition to California. He also accompanied the second expedition as far as the Colorado River, where he remained with a fellow priest to establish two missions among the Yuma Indians near present day Yuma.

Garcés is also noted for his exploration of the San Joaquin Valley, the Mojave Desert, the San Bernardino Valley, and the Colorado River to Grand Canyon. On July 17, 1781, the Yumas rose up and destroyed the Colorado River missions, killing Fr. Garcés, another priest, and the soldiers who were stationed there.

Fr. Pedro Font:

Franciscan friar Pedro Font was the chaplain and navigator on the second Anza expedition to California in 1775-76. He was born in Gerona, Spain, and assigned to Mission San José de los Pimas when he was recruited for the second expedition. Font had the training and ability to determine latitudes. He was chosen as diarist and spiritual guide for the expedition, while his other skills would prove valuable for navigation.

Font is remembered for his negativity toward almost everything on the expedition. He was sick most of the time and found fault with almost everything that Anza did. He did not approve of celebrations that Anza allowed on the expedition involving drinking, singing, and dancing. He could see no beauty in Coyote Canyon and saw it only as a worthless wasteland. His comments about the Indians are degrading. And yet, he is honored in name for one of the most picturesque areas of the Park – Fonts Point. Font was, however, very observant. He was the first to surmise about the age of some of the marine fossils that he observed, and he was also the first to make note of the wild bighorn sheep of the area. He was assigned to the mission at Caborca in 1780 and died there the following year.

Saguaro:

The saguaro Sky Art sculpture found to the west of the padre sculpture does not represent a plant found in this desert. It is a native of the Sonoran Desert found to the east of the Colorado River. It can symbolically represent the Tubac/Tucson area where Anza launched his expeditions.

HN-4: 1951 Willys Jeep (CJ-3A)

The iconic World War II military Jeep, manufactured from 1941 to 1945, was a small four-wheel drive utility vehicle that had its counterpart in the later-developed civilian Jeep (CJ). Ford, who was a competitor with Willys-Overland producing Jeeps for the Army during WWII, unsuccessfully sued Willys-Overland for the rights to the name. With the rights battle out of the way, Willys-Overland took its Jeep public with its first full production of the civilian version – the CJ series – beginning in 1945. The classic CJ-3A had improvements over the first CJ, and 132,000 were produced between 1946 and 1953.

After WWII, surplus military jeeps also became available to the public. The Jeep literally opened up desert exploration and forever changed the Park (then known as Anza Desert State Park). It created a crisis in Park management. Between 1952 and 1957 Park visitation grew by almost 500 percent [Lindsay 1973]. To better handle the increased visitation and Park exploration, the Park was split into two units in 1952: Anza Desert State Park in the north and Borrego State Park to the south of Highway 78. Despite creating two smaller Parks with more staff, the situation did not improve. In 1957 the two Parks were recombined to form Anza-Borrego Desert State Park and eight patrol districts were established to better control use of the Park. The patrol districts continue to this day with a ranger assigned to each area with a four-wheel drive vehicle.

Uncontrolled off-road use, which was in direct conflict with Park resource protection and preservation, was a major problem for the Park until a portion of the Park was combined with federal and private lands to form the 14,000-acre Ocotillo Wells State Vehicular Recreation Area in 1976 – an open area for vehicular use and

exploration that is generally unrestricted. The focus there is conservation vs. preservation. Today this off-road area is over 80,000-acres in size – the second largest unit within the State Park system after Anza-Borrego Desert State Park. Intrusions by off-roaders who do not obey State Park regulations continue to be a problem for Anza-Borrego Desert State Park, especially in areas bordering Ocotillo Wells State Vehicular Recreation Area.

This "ode to the off-roaders," as Dennis Avery calls it, is the "last" in the series of Sky Art sculptures on Galleta Meadows Estate. This sculpture was inspired by a group of off-roaders who respect Park rules and regulations and enjoy "poking around the desert" at their own pace. This informal group calls itself the "Herd of Turtles" and emphasizes that they are "careful to leave everything" as they find it and to "stick to the trail and 'pick up' where others before us haven't," according to their spokesperson Myrna Horn [Horn e-mail 9/11/10]. To honor the off-road philosophy of the Herd of Turtles, Avery granted them the right to select the final resting place for the CJ-3A, which is on the west side of the north end of Borrego Springs Road just before the junction of Henderson Canyon Road, west of the Indian head sculpture.

HN-5: Farm Workers in Di Giorgio Fruit Corporation Grape Fields

Borrego Valley's grape fields played an important role in the five-year grape strike (September 1965-July 1970) and national grape boycott by drawing attention to the plight of the farm workers when key leaders were arrested on June 29, 1966, at the Di Giorgio Ranch in Borrego Valley. Their inhumane treatment by local police units may have gone unnoticed had not the arrested included Cesar Chavez, president of United Farm Workers Union (UFWU), Rev. Wayne Hartmire, Jr., head of the California Migrant Ministry, and Fr. Victor Salandini. The three had been asked to peacefully accompany 10 field workers who had walked off their job that day and were afraid to go back to the labor camp on the ranch to pick up their checks and their personal belongings because of past harassments and the presence of Di Giorgio security guards and their police dogs. As soon as the group entered ranch property, they were arrested for trespassing, "stripped and chained together in groups of three" by sheriff's deputies who first took them to the Borrego Valley Sheriff's substation, according to testimony by Rev. Hartmire [Hartmire 1966]. They were then transported to the San Diego County jail and placed in a cell block. The next day they were released on bail and returned to Borrego Springs where the strike was still in progress. All of the 279 farm workers from Mexicali, of which one-third were women, had voted to strike and left their $1.20 per hour paying jobs.

The purpose of the strikes at the various Di Giorgio ranches located in Borrego Valley, Lamont, Delano, Marysville, and Yuba City was to draw attention to the plight of the farm workers which included unfair labor practices. The 1966 strikes began in Borrego Valley because that is where the first grapes were ready to be harvested at Di Giorgio ranches. Other growers were targeted in 1965 and after 1966 [Padilla interview 2011]. The various strikes and heated court battles that followed eventually brought the resolution that the UFWU sought. It also brought to a close the 20-year history of harvesting grapes in the Borrego Valley.

The Di Giorgio Fruit Corporation originally purchased land in Borrego Valley so that they could harvest grapes well ahead of the later maturing grapes of northern California and be first to the eastern markets. By the mid-1950s, the corporation was cultivating grapes on over 2,500 acres. Typically it took more than 600 seasonal field workers to harvest, pack, and ship the grapes. By the 1960s, however, Di Giorgio began scaling back their farming interests in favor of housing and development of the Borrego Valley. By the time that Cesar Chavez was elected the head of the UFWU in 1965, the Borrego farming operation was slowly coming to an end. The ensuing strike in the Borrego fields the following year precipitated the complete shutdown of all grape growing activity in the valley soon thereafter.

HN-4: Farm Workers

An interesting side note is the role played by the Park. When members of the UFWU came to Borrego Springs to lead the strike, they soon found themselves without a place to stay and went to Borrego Palm Canyon and camped at a large ramada in the campground. Di Giorgio interests asked the State Park to evict them from the campground. Supervisor Wesley Cater refused stating that the members of the UFWU had the right to stay in the campground

Galleta Meadows Sky Art Sites

Map Legend

FT ●: Sky Art Inspired by Fossil Evidence as Presented in *Fossil Treasures of the Anza-Borrego Desert*

HN ▼: Sky Art Inspired by Historical Events and Natural Features of the Anza-Borrego Desert

D ■: Sky Art Inspired by the Whim and Imagination of Artist Ricardo B receda, Not Based on any Fossil Evidence Found in the Anza-Borrego Desert

FT-1: Peccary – *Platygonus* sp.
FT-2: Giant Tortoise – *Hesperotestudo* sp.
FT-3: Merriam's Tapir – *Tapirus merriami*
FT-4: Gracile Sabertooth Cat – *Smilodon gracilis*
FT-5: Giant Tortoise – *Hesperotestudo* sp.
FT-6: African Elephant – *Loxodonta Africana*
FT-7: Camelids – (Llamas) *Hemiauchenia* sp. and (*Camelops*) *Camelops* sp.
FT-8: Shasta Ground Sloth – *Nothrotheriops shastensis*
FT-9: Harlan's Ground Sloth – *Paramylodon harlani* and (*Camelops*) *Camelops* sp.
FT-10: Gomphothere – *Gomphotherium* and (*Camelops*) *Camelops* sp.
FT-11: Gracile Sabertooth Cat – *Smilodon gracilis* and Extinct Horse – *Equus* sp.
FT-12: Incredible Wind God Bird – *Aiolornis incredibilis* in Its Nest
FT-13: Extinct Horse – *Equus* sp.
FT-14: Columbian Mammoth – *Mammuthus columbi*
FT-15: Incredible Wind God Bird – *Aiolornis incredibilis* with Prey – *Platygonus* sp.

HN-1: Peninsular Bighorn Sheep – *Ovis canadensis cremnobates*
Gold Miner and His Mule
HN-2: Indian Head – Representing Sebastián Tarabal and/or Salvador Palma
HN-3: Spanish Padre – Representing Fr. Francisco Garcés and/or Fr. Pedro Font with an Arizona Sonoran Desert Saguaro
HN-4: 1951 Willys Jeep (CJ-3A)
HN-5: Farm Workers in Di Giorgio Fruit Corporation Grape Fields
HN-6: Capt. Juan Bautista de Anza on His Horse

D-1: *Velociraptor* – found in Mongolia
D-2: *Spinosaurus* – found in Egypt & Morocco
D-3: *Carnotaurus* – found in Argentina
Allosaurus – found in North America
D-4: *Utahraptor* – found in the U.S.A.
D-5: *Tyrannosaurus rex* – found in North America

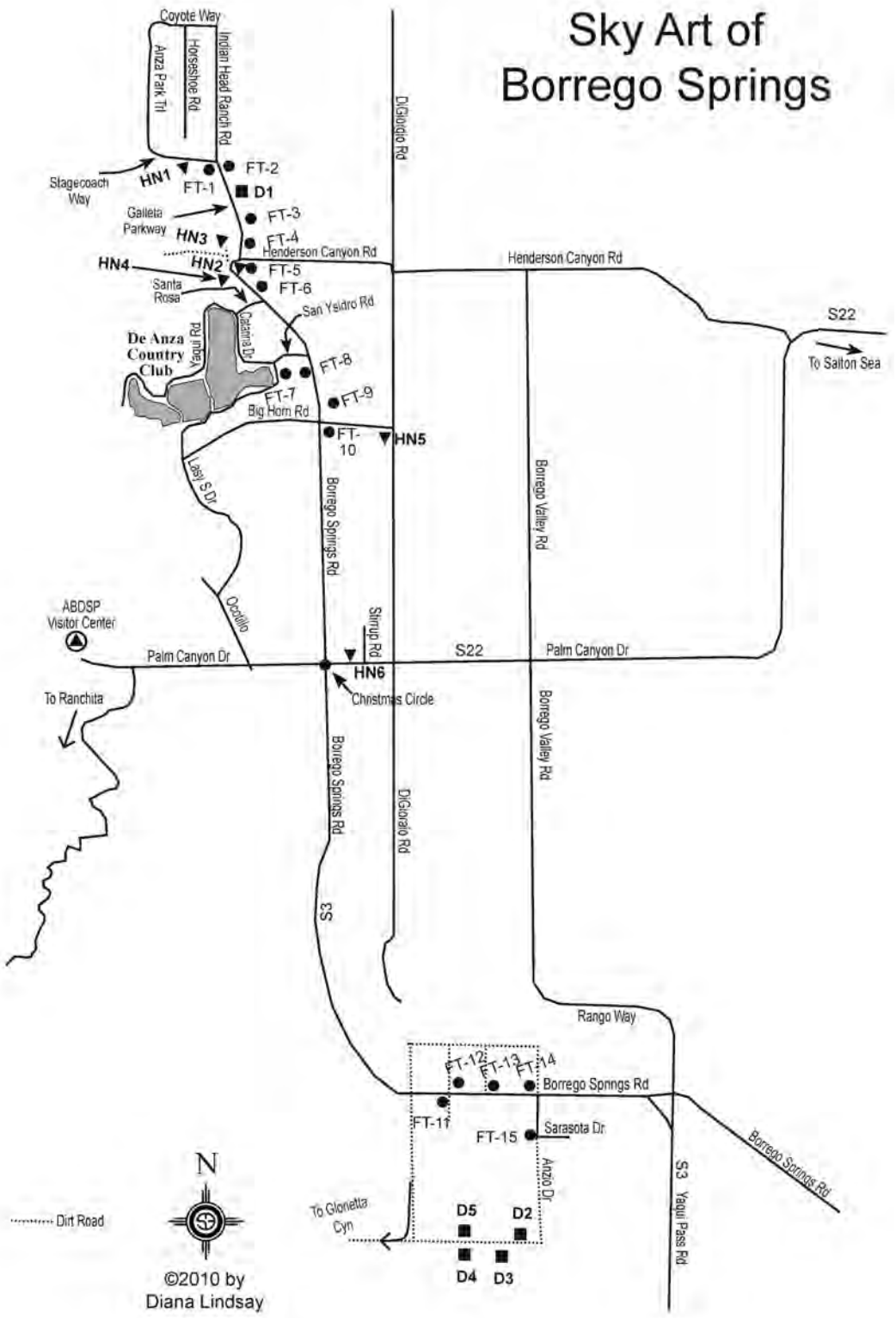
Sky Art of
Borrego Springs
Coyote Way
Anza Park Trl
Horseshoe Rd
Indian Head Ranch Rd
Di Giorgio Rd
Stagecoach Way
HN1
FT-1
FT-2
D1
Galleta Parkway
HN3
FT-3
FT-4
Henderson Canyon Rd
HN4
HN2
FT-5
FT-6
Santa Rosa
San Ysidro Rd
Henderson Canyon Rd
S22
To Salton Sea
De Anza Country Club
Yaqui Rd
Cahuma Dr
FT-8
FT-7
FT-9
Big Horn Rd
FT-10
HN5
Borrego Valley Rd
Borrego Springs Rd
Ocotillo
Stirrup Rd
ABDSP Visitor Center
Palm Canyon Dr
S22
Palm Canyon Dr
HN6
Christmas Circle
To Ranchita
Borrego Springs Rd
Di Giorgio Rd
Borrego Valley Rd
S3
Rango Way
FT-12
FT-13
FT-14
Borrego Spnngs Rd
FT-11
FT-15
Sarasota Dr
Borrego Springs Rd
Anzio Dr
S3 Yaqui Pass Rd
N
Dirt Road
To Glorietta Cyn
D5
D2
D4
D3
©2010 by
Diana Lindsay

just like anyone else who paid their fees [Cater interview 2008].

There are 23 individual sculptures on the southwest corner of Big Horn Road and Di Giorgio Road on the site of a former grape field once owned by Di Giorgio. Sky Art sculptures include farm workers, grape arbors, and stacked boxes of grapes in life-like poses. Half of the original sculptures were replaced when some members of the community complained about the lack of authenticity. Ironically, one of the complaints had to do with women in the fields. As it turns out, women did work in the fields.

HN-6: Capt. Juan Bautista de Anza on His Horse

Juan Bautista Agustín de Anza, for whom Anza-Borrego Desert State Park is named, was an Indian fighter, soldier, explorer, colonizer, and an administrator. He was born on July 7, 1736, in Fronteras, Sonora, and was the son of Capt. Juan Bautista de Anssa. He became a presidial captain at the most northern frontier outpost of Mexico, outside of California, just as his father had been before him.

In 1737, Anza's father had proposed mounting an expedition to search for a land route to Alta California at his own expense, but it never materialized due to his untimely death in 1740 at the hands of marauding Apaches. At his father's death, Anza was barely four years of age. As he grew up, he spelled his name with a "z" instead of using the original Basque spelling of the family name. He also kept the "de" which was added to the family name when the Basques made a pact with the Spaniards. "De" denotes nobility and was essential in Anza's day for holding land or a better job. Anza included it in his name even though his name was simply "Juan Anza." It clearly indicated his status and was used as his official name.

Anza followed in his father's footsteps becoming the presidial captain of the Fronteras outpost. He also proposed to look for a land route to California, as his father had done, and was granted permission to do so in 1774. The success of the first expedition led to his promotion to Lieutenant Colonel and his orders to recruit settlers and lead a second expedition of colonists to California to establish a presidio, mission, and village on San Francisco Bay. A new promotion followed the second expedition. He was appointed the political and military governor of the Province of New Mexico and held this post until his death on December 19, 1788.

The Sky Art sculpture of Anza sits prominently in front of the Borrego Springs Chamber of Commerce on the northwest corner of Palm Canyon Drive and Stirrup Road.

Category 3 (D) – Sky Art Inspired by the Whim and Imagination of Artist Ricardo Breceda,

Not Based on any Fossil Evidence Found in the Anza-Borrego Area

No dinosaur ("terrifying or powerful lizard") fossils have been found in the Anza-Borrego area. All of the Sky Art dinosaurs selected for placement in Galleta Meadows by artist Ricardo Breceda represent various families of carnivorous theropods, bipedal dinosaurs whose front legs were not intended for locomotion. Several of these were featured in the best-selling book and film Jurassic Park. All had large, powerful jaws and sharp teeth and were most active in the early to middle Cretaceous Period, beginning some 144 million years ago, following the older Jurassic Period of the Mesozoic Era. Perris Jurassic Park is the name of Breceda's metal sculpturing business in Perris, California.

The descriptions below are based on the general descriptions found on the Wikipedia website. The Sky Art sculptures are numerically listed as they are generally found in a north to south and east to west order. See attached table for a list of combined Sky Art inspiration categories listed north to south.

D-1: *Velociraptor* – found in Mongolia

The "Speedy Raider" was a dromaeosaurid ("running or swift lizards"), which are small to medium-sized carnivorous, bird-like theropod dinosaurs with feathers, commonly referred to as raptors. The *Velociraptor* was the smartest of the dromaeosaurids and was equipped with a large sickle-shaped foot claw and three strongly-curved hand-claws. It had slender legs and an S-shaped neck and spine. The *Velociraptor* stood 2- to 3-feet tall, weighed 15to 30 pounds, and was about 5 to 6 feet long. They lived during the late Cretaceous Period, about 85 million to 80 million years ago. Several fossil specimens have been found in Mongolia, where Anza-Borrego has a sister park. They may have run up to 40 miles per hour and also may have hunted in packs.

When the movie "Jurassic Park" was made, the actual size of the *Velociraptors* was exaggerated for dramatic purposes. At that time, no dromaeosaurid was thought to have existed that was so large. However, soon after the film was released, the first *Utahraptor* specimen was found, and it more than matched the size of that portrayed in the film. See D-4.

Sky Art at Sunrise. On this page and the next, are some photos I snapped one beautiful Borrego Springs morning in January of 2011. Here's the silhouette of a Columbian Mammoth.

Three of the examples of extinct horse at location FT-13.

Gomphotherium at location FT-10.

Camelids at location FT-7.

Harlan Ground Sloth at location FT-9.

Columbian Mammoths at location FT-14.

This was the first Sky Art dinosaur installation. It is located on the east side of Galleta Parkway in Indian Head Ranch, south of Stagecoach Way and the giant tortoises.

D-2: *Spinosaurus* – found in Egypt and Morocco

The "Spiny Lizard" was a carnivorous theropod that lived in Africa (specimens found in Egypt and Morocco) during the late Cretaceous Period, about 98 million to 95 million years ago, and had a 6-foot long sail-like structure protruding from its back vertebrae that may have had some use in thermo-regulation, defense or display threat, or sexual attraction. It weighed more than 4 tons and was 40 to 50 feet long. It had a large crocodile-like skull and jaws with long sharp teeth. Only incomplete fossils have been found, including the neural spines.

A Sky Art sculpture of a *Spinosaurus* with three juveniles is found by following a dirt road south 0.5 mile past the end of the payment of Anzio Drive, and then turning west and proceeding 0.1 mile. They are found on the north side of the road.

D-3: *Carnotaurus* – found in Argentina

This "Flesh-eating Bull" from Argentina lived in the Cretaceous Period about 113 million to 91 million years ago and had two horn-like protrusions above its eyebrows. Its arms were even smaller than those of *Tyrannosaurus* rex, and the fingers were fused, immobile, and lacked claws. It weighed about 1 ton, stood about 6 feet tall, and was about 25 feet long. Only a single fossil specimen was found in Patagonia. It had a long neck, a small head and a slender lower jaw. Its eyes were close together and it may have had binocular vision, which was unusual for a dinosaur. Impressions of skin found with skeletal remains show that *Carnotaurus* lacked feathers [Wikipedia]. It also had a row of bumps along the spine that became larger toward the tail.

Allosaurus – found in North America

The "Different Lizard" had a vertebra that was lighter in weight than other dinosaurs. This huge carnivorous theropod weighed about 2 to 3 tons, stood 10 to 15 feet tall, and was about 30 to 40 feet long. It lived during the late Jurassic Period, about 150 million to 140 million years ago. Fossil have been found in North America, Europe, Africa, and Australia. *Allosaurus* had a large head with sharp serrated teeth, short arms and three-fingered hands. It was at the top of the food chain and may have had some cooperative behavior.

The Sky Art "fighting" dinosaurs are found by following a dirt road south 0.5 mile past the end of the payment of Anzio Drive and then turning west and proceeding 0.2 mile. They are found on the south side of the road. The sculptures weigh about 1,000 pounds each.

D-4: *Utahraptor* – found in the U.S.A.

"Utah's Raider" was a carnivorous theropod who lived in the early Cretaceous Period, about 125 million years ago, and was in the same family as that of the *Velociraptor*. It has only been found in the U.S.A. It was the largest member of the dromaeosaurids at about 6 feet tall, 23 feet long, and 1 ton in weight. It resembled a giant roadrunner with about a 9-inch middle-toe claw and three fingers on each hand that had large curved claws. It was a light, fast, agile, highly intelligent bird-like dinosaur with large, sharp, serrated teeth, powerful jaws, and a long, stiff, rod-like tail that allowed it to keep its balance. Like other dromaeosaurids, it may have hunted in packs. See D-1.

The two *Utahraptor* metal sculptures and nest are found by following a dirt road south 0.5 mile past the end of the payment of Anzio Drive and then turning west and proceeding 0.3 mile. They are found on the south side of the road.

D-5: *Tyrannosaurus rex* – found in North America and Mongolia

The "Tyrant Lizard King" was a massive carnivorous theropod that lived during the late Cretaceous period, about 85 million to 65 million years ago. It stood about 13 feet tall, weighed up to 7 tons, and was about 40 feet long. It was a smart and fast-running predator with hollow bones and small arms about 3 feet long. Its jaw was larger than its arm at about 4 feet, and it had about 50 to 60 long, conical teeth that were serrated and continually replaced. It is estimated that it could eat up to 500 pounds of meat in one bite. *Tyrannosaurus* had a stiff pointed tail that acted as a counterbalance for its enormous head. Fossilized skin specimens show that the skin was similar to that of an alligator. It was one of the last non-avian dinosaurs to exist before the Cretaceous-Tertiary extinction. About 30 incomplete fossils have been found in North America as well as Mongolia.

The Sky Art *Tyrannosaurus rex* and her four juveniles are found by following a dirt road south 0.5 mile past the end of the payment of Anzio Drive and then turning west and proceeding 0.3 mile. They are found on the north side of the road. The large 13-foot sculpture weighs about 1,000 pounds.

REFERENCES AND ACKNOWLEGMENTS

Allen, Beth. 2006. "Stanley Marsh 3: A Texas Revolutionary." Associated Content, 11 July.

http://www.associatedcontent.com/article/43322/stanley_marsh_3_a_texas_revolutionary.html

Avery, Dennis. 2010. E-mail correspondence with the author, 23 August and 25 August.

Bier, Steve. 2010. "The 40th Anniversary Sheep Count." California: The Resources Agency, Department of Parks and Recreation, Anza-Borrego Desert State Park. 4 July.

Bonincontro, Aldo. "Exitinct mega-predators : Utahraptor." 2010.

Borrego Sun. 2008. "Sky Art" – paid advertising, 17 April, 16.

Brancheau, Maris. 2008. "At last, fossil bird sculpture takes wing." Borrego Sun, 27 November, 17, 37.

--------. 2008. "Prehistoric gomphotheres return to Borrego Valley." Borrego Sun, 17 April, 1, 26.

--------. 2008. "Prehistoric horses, sabertooth cats bring interactive quality to Galleta Meadows." Borrego Sun, 16 October, 13, 24.

--------. 2009. "Galleta Meadows becomes home for eight new dinosaur sculptures." Borrego Sun, 11 June, 13.

--------. 2010. "Revised sculptures of grape workers placed in fields." Borrego Sun, 4 February, 19.

De Wyze, Jeannette. 2010. "Ricardo Loves Dinosaurs." San Diego Reader, 5 May.

http://www.sandiegoreader.com/news/2010/may/05/feature-ricardo-loves-dinosaurs/

Gerwen, Rob Van, ed. 2001. Richard Wollheim on the Art of Painting: Art ad Representation and Expression. Cambridge: Cambridge University Press.

Hartmire, Jr., Wayne C. 1966. Letter to Forrest Weir, Paul Shelford, Bob Stellar, and Carroll Shuster. "Arrest in Borrego Springs, June 29, 1966." 5 July. Copy of letter at

http://www.unionoftheirdreams.com/PDF/Borrego_Springs_arrest.pdf

Hartwell, Dickson. "The Mighty Jeep." American Heritage Magazine, December 1960, Vol. 12.

http://www.americanheritage.com/articles/magazine/ah/1960/1/1960_1_38.shtml

Holtz Jr., Thomas R. 2006. Dinosaurs: The Most Complete, Up-to-Date Encyclopedia for Dinosaur Lovers of All Ages. New York: Random House.

Horn, Myrna. 2010. E-mail correspondence with the author, 11 September.

Jefferson, George T. and Lowell Lindsay, eds. 2006. Fossil Treasures of the Anza-Borrego Desert. San Diego: Sunbelt Publications, 2006.

Jones, J. Harry. 2008. "Beauty and the beasts." Sign on San Diego, 26 April.

http://legacy.signonsandiego.com/news/northcounty/20080426-9999-1m26beasts.html

Lindsay, Diana. 1973. Our Historic Desert: The Story of the Anza-Borrego Desert – The Largest State Park in the United States of America. San Diego: Copley Books.

--------. 2001. Anza-Borrego A to Z: People, Places, and Events. San Diego: Sunbelt Publications.

McKinnon, Julissa. 2008. "Perris sculptor populates Anza-Borrego 'creature desert' with dinosaurs, extinct mammals, more." The Press Enterprise, 30 June.

http://www.pe.com/localnews/rivcounty/stories/PE_News_Local_S_dinosaur30.4310b60.html

Padilla, Gilbert. 2011. Author telephone interview with the former Secretary/Treasurer of the United Farm Workers, 11 September. Copy of interview transcript at ABDSP.

-------- and Wesley Cater. 2008. Frank Padilla and Leslie Bellah interview with the former Secretary/Treasurer of the United Farm Workers and the Superintendent of ABDSP 1965-1968. ABDSP, 13 January. Copy of transcript at ABDSP.

Wollheim, Richard. 1980. "Art and evaluation," Essay VI in Art and Its Objectives: with six supplementary essays. Cambridge: Cambridge University Press.

WEBSITES:

http://www.christojeanneclaude.net/

http://latimesblogs.latimes.com/culturemonster/2009/03/watts-towers.html

http://www.willysoverland.com/index.php/WO/history/

http://4wheeldrive.about.com/od/willyshistory/Willys_Overland_History_and_Facts_About_Willys_Jeeps.htm

http://www.enchantedlearning.com/subjects/dinosaurs/

http://www.helium.com/items/1937945-extinct-mega-predators-utahraptor

http://www.wordiq.com/definition/Utahraptor_ostrommaysorum

http://www.enchantedlearning.com/subjects/dinosaurs/dinos/Utahraptor.shtml

ACKNOWLEDGMENTS FOR TEXT REVIEW: Linda Gilbert, George T. Jefferson, Dave Bloom, Lowell Lindsay and Carole L. Ziegler

PHOTO AND ART CREDITS: All photos and charts by Diana Lindsay; sketches by Pat Ortega; paleontology illustrations by John Francis; Anza illustration from *Anza Conquers the Desert* (San Diego: Copley Books, 1971).

HN-5: Capt. Juan Bautista de Anza

D-1: *Velociraptor*

D-2: *Spinosaurus*

D-3: *Allosaurus*

D-4: *Utahraptor*

D-5: *Tyrannosaurus rex*

THE YAQUI RIDGE ANTIFORM AND DETACHMENT FAULT: MID-CENOZOIC EXTENSIONAL TERRANE WEST OF THE SAN ANDREAS FAULT

Patricia A. Schultejann
Scripps Institution of Oceanography,
University of California, San Diego,
La Jolla, California

ABSTRACT

The narrow zone of mid-Cenozoic detachment terrane in the southwestern United States can be widened and traced across the southern strands of the San Andreas fault zone into the eastern margin of the Peninsular Ranges Batholith. The Yaqui Ridge core complex and detachment fault, in southern Borrego Valley, California, exemplifies the nature of detached terranes in south-central California. The detachment fault dips 10°-40° to the northeast, and separates a lower core of gneissic Late Cretaceous granodiorite from an unconsolidated, unmetamorphosed megabreccia of Eocene to Miocene age. Foliations in the lower plate generally conform to the strike and dip of the overlying detachment fault, and become less distinct away from the fault. The megabreccia which forms the upper plate is composed of unsorted, fairly well rounded clasts characteristic of batholithic and metasedimentary rocks of the region. Plio-Pleistocene lacus trine sediments unconformably overlie the megabreccia in some areas. The detachment fault and upper plate are expressed as a series of klippen which parallel Yaqui Ridge along the northeast and southeast flanks. The fault is marked by a typically narrow (~6-10 cm) band of intensely sheared cataclasite. A chlorite-breccia zone occurs below the cataclasite, and gradually grades into the less deformed, regionally foliated gneissic granodiorite. On the southeast flank, what appears to be an extension of the cataclasite and detached upper plate is exposed only locally, near the southeast nose of the antiform. Here, the upper plate consists of blocks of pale gray to tan, aphanitic fault gouge. Superimposed upon and cutting through the detachment-related features is a broad zone of left-oblique-slip faulting termed the Yaqui Ridge shear zone. This fault zone trends WNW-ESE, parallel to Yaqui Ridge, and separates the detachment fault from the ridge, merging with the detachment fault near the eastern margin. Further east, the shear zone widens into a massive zone of gouge > 400 m wide and disappears under the sediments of Borrego Valley and the Salton Trough. To the west, the shear zone slices into the eastern margin of the Peninsular Ranges Batholith and extends the marginal plutons in an E-W direction. Four dominant tectonic episodes can be recognized from exposures at and adjacent to Yaqui Ridge: (1) A Late Cretaceous synkinematic cataclasis and metamorphism accompanying and following emplacement of the Yaqui Ridge and related plutons, and forming a pervasive regional NW- trending foliation and NE-trending lineation. (2) A subsequent mid-Cenozoic, shallow, low temperature event of detachment faulting and folding which produces localized brittle cataclasis which overprints the earlier NW-trending fabrics. (3) The Late Miocene- Early Pliocene development of Yaqui Ridge shear zone along the northeast margin of Yaqui Ridge, shearing, rotating and overprinting the fabrics formed during the Late Cretaceous plutonism and regional deformation. (4) A Pleistocene of high-angle and episode faulting folding which produce a series of E-W-trending anti-clines and synclines in Upper Pliocene to Pleistocene sediments. Linear elements which have formed throughout the several Late Cretaceous to Cenozoic deformations are concordant.

TECTONICS, VOL. 3, NO. 6, PAGES 677-691, NOVEMBER 1984

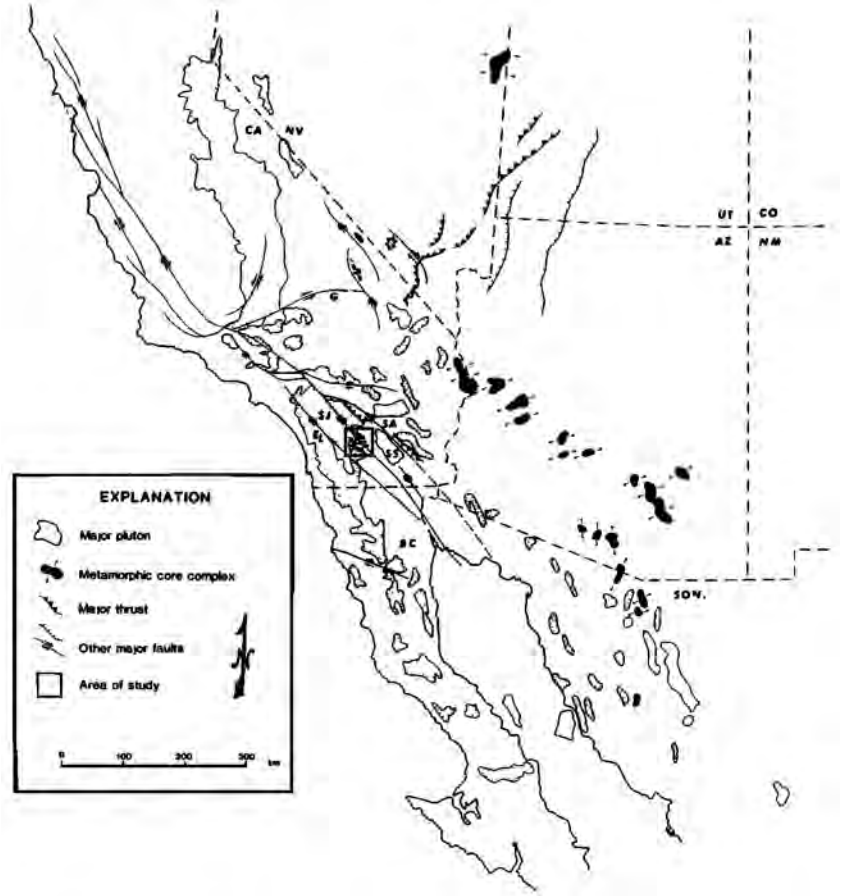

Fig. 1. Regional map, modified from Coney [1980] and Armstrong [1982] showing the distribution of major faults, major plutons, and postulated "metamorphic core complexes" in southwestern United States and northern Mexico. The box indicates the location of Yaqui Ridge along the eastern margin of the Peninsular Ranges Batholith. The occurrence and dominant lineations within the core complexes are shown by arrows. Faults: G-Garlock, E-Elsinore, SA-San Andreas, SJ-San Jacinto. SS--Salton Sea.

INTRODUCTION

The nature, distribution, and origins of mid-Cenozoic and late Mesozoic detachment faults and related "core complexes" in the western United States are the subject of extensive investigation and discussion (Davis [1983]; Miller et al. [1983]; Stewart [1983]; Frost and Martin [1982]; Armstrong [1982]; Wernicke [1981]; Crittenden et al. [1980]; Davis et al. [1979]; Davis and Coney [1979]; Coney [1974]; Armstrong [1972]; Anderson[1971]; and many others) (Figure 1). Despite the intensive study, clear distinctions between the several ages of detachment faults, their specific features, and distribution remains obscure. In the southwestern U.S., major questions include (1) the western extent and forms of the mid-Cenozoic detachments that project into and across the San Andreas fault system, (2) the relationship of these detachments to the extensional tectonics involved in the development of the Basin and Range Province, Salton Trough, and Gulf of California, (3) the extent to which the Peninsular Ranges Batholith is cut and distended by mid-Cenozoic detachment features, and (4) relations of detachment faults and cataclasis to older metamorphic and deformational events. This report concerns the occurrence and features of the mid-Cenozoic Yaqui Ridge detachment fault and related antiform and its northwest prolongation into the main block of the Peninsular Ranges Batholith, which has been folded, faulted, and extended during the mid-Cenozoic detachment kinematics.

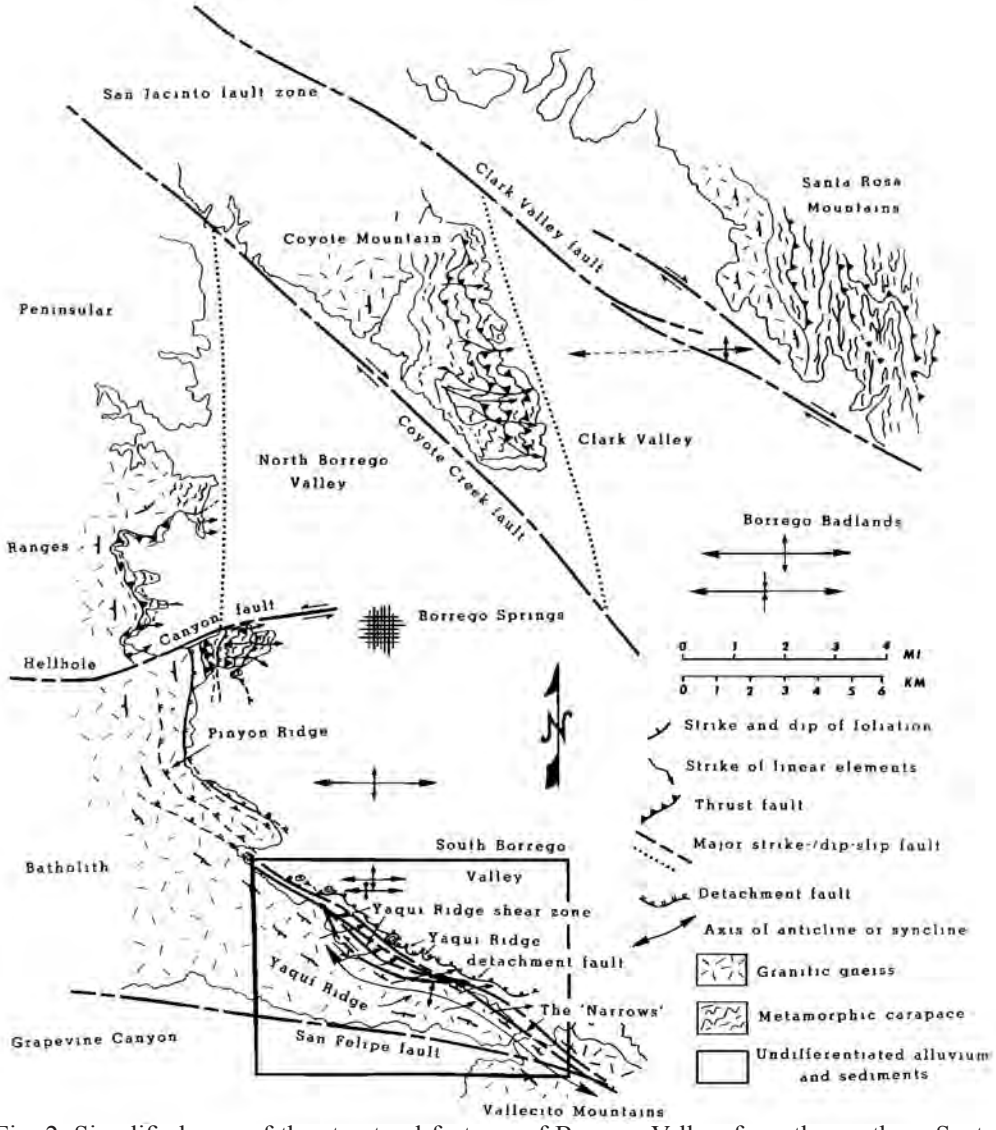

Fig. 2. Simplified map of the structural features of Borrego Valley, from the southern Santa Rosa Mountains southward to Yaqui Ridge. Major features include Late Cretaceous thrusting and folding in the metamorphic carapace, mid-Cenozoic detachment faulting and development of a folded plutonic core, Late Miocene-Pliocene left-oblique slip faulting, and Pleistocene-Holocene antiform-synform formation.

LOCATION

Yaqui Ridge consists of a portion of one of the easternmost plutons of the Peninsular Ranges Batholith in south-central California, and forms a narrow elongate ridge which strikes WNW-ESE. It is bounded on the north and south by southern Borrego Valley and Grapevine Canyon, respectively, on the east by the Vallecito Mountains, and on the west by the main block of the Peninsular Ranges [see Engel and Schultejann, this issue, Figure 2].

The Yaqui Ridge pluton has been warped in the Tertiary into an asymmetrical antiform (core complex) that trends ESE. The steeply dipping (~50-80°) northeast flank of the antiform is breached by a series of mid-late Cenozoic left-oblique-slip faults, here referred to as the Yaqui Ridge shear zone. The southwest flank slopes gently southward into Grapevine Canyon. The antiform extends southeastward into the Vallecito Mountains and is breached by the San Felipe Creek at "the Narrows" (Figure 2). The San Felipe fault cuts the Yaqui Ridge antiform without appreciable lateral offset, suggesting largely dip-slip motion on this strand of the Elsinore fault system. This possible

Fig. 3. Photograph of the Yaqui Ridge chlorite-breccia zone, cataclasite, and detachment fault. The chlorite-breccia zone consists of sheared and chloritized gneiss with foliation often conformable or semi-conformable to the strike and dip of the overlying cataclasite and detachment fault.

restriction to dominantly vertical displacement was first noted by Lowman [1980; see, however, Clark, 1983].

The dominant topographic features of the region are the steep granitic mountain fronts of the Peninsular Ranges Batholith. The eastern marginal portions of the Peninsular Ranges are detached into a series of N-S trending blocks which are step-faulted downward to the east into the broad valley floors of the Salton Trough [see Engel and Schultejann, this issue, Figure 12].

GEOLOGIC FEATURES

Yaqui Ridge is most similar to the Whipple and related detachment fault structures in southeastern California. The lower plate "core" of the complex is composed entirely of gneissic granodiorite typical of the eastern plutons of the Peninsular Ranges Batholith [Todd and Shaw, 1979; Larsen, 1948]. The Ordovician metasedimentary section thrust over the eastern margin of the batholith in Late Cretaceous time is not present along the central and western portions of the ridge (Figure 2) [Engel and Schultejann, this issue]. Locally, small pockets of marble and quartzite are present as inclusions in the host gneissic granodiorite of Yaqui Ridge. However, the metasediments are present along the eastern margin in the Vallecito Mountains and as a screen or roof pendant in Grapevine Canyon to the south and southwest (Figure 2).

The gneissic granodiorite core of Yaqui Ridge has never been dated radiometrically, but lithologically similar plutons immediately to the south have yielded U-Pb zircon ages of ~95-110 Ma and K-Ar "cooling ages" that range from ~70-100 Ma [Todd and Shaw, 1979; Silver et al., 1979; Krummenacher et al., 1975]. Isotopic studies in the Peninsular Ranges Batholith have determined a general age and lithologic progression in the plutons comprising the batholith [Silver et al., 1975, 1979; Baird et al., 1979; Taylor and Silver, 1978; Early and Silver, 1973; Larsen, 1948]. Generally, older, more mafic plutons are concentrated in the western portions of the Peninsular Ranges, becoming younger and more granitic eastward. It is probable that Yaqui Ridge does not represent an anomalous pluton and generally conforms to this pattern. The close association in

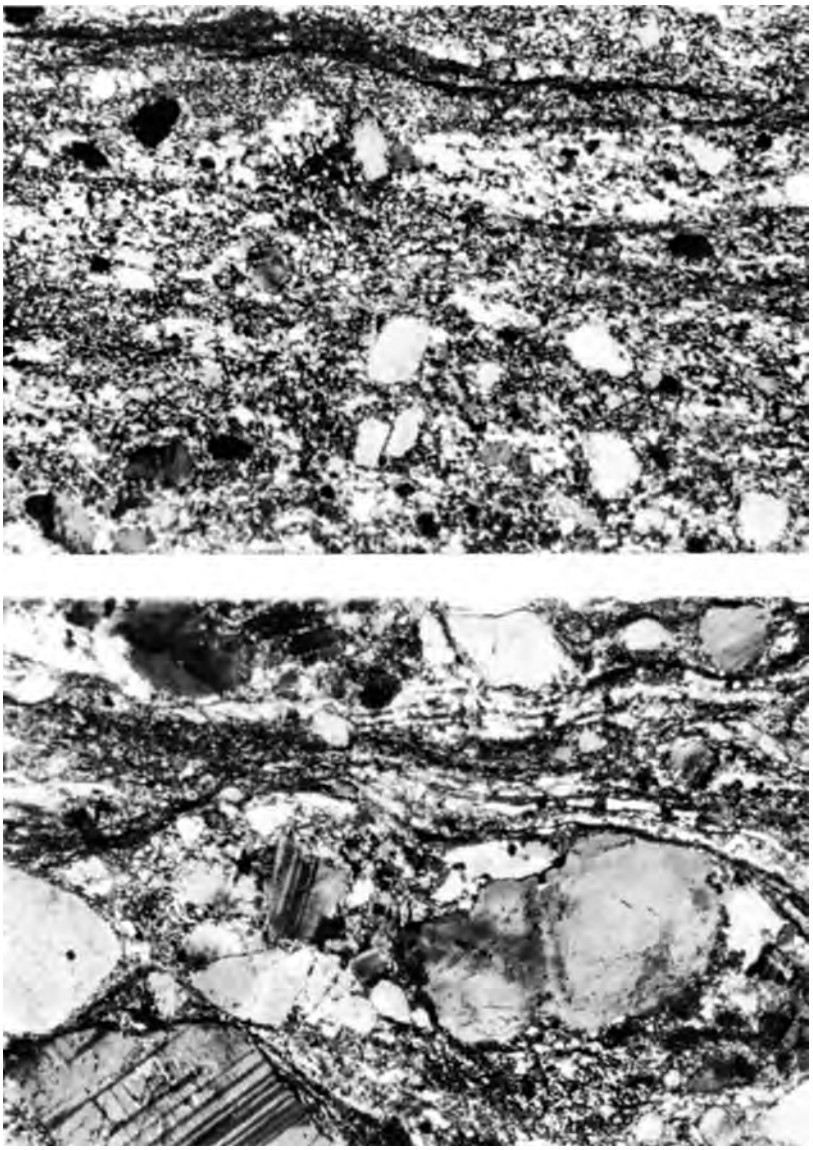

Fig. 4. Photomicrographs of the cataclasite showing limited flow banding, porphyroclasts of embayed quartz and feldspar, and recrystallized quartz veinlets. The mineralogy and fabric of the cataclasite suggests it was derived from extreme crushing of the gneiss.

space and lithologic similarity of the Yaqui Ridge pluton with dated plutons immediately to the southwest, strongly suggests a mid-Late Cretaceous age for Yaqui Ridge.

The less deformed, foliated gneissic granodiorite of Yaqui Ridge grades upwards into a zone of intensely sheared and chloritized, cataclastic gneiss characteristic of the "chlorite-breccia zone" widely described from similar detachment structures east of the San Andreas fault [Davis et al., 1982; Frost and Martin, 1982; Mueller et al., 1982; Phillips, 1982; Crittenden et al., 1980; Davis et al., 1980]. The chlorite-breccia zone is directly overlain by the microbreccia or cataclasite which marks the Yaqui Ridge detachment fault (Figure 3).

Steeply dipping pegmatite dikes associated with final stages of pluton emplacement are abundant at Yaqui Ridge and predominantly strike NE-SW to E-W. These Cretaceous pegmatites intrude the lower plate gneiss, but are always truncated by the detachment fault. Dikes are overprinted with the same distinctive, lower temperature, near surface mid-Tertiary cataclasis present in the gneiss. This mid-Tertiary granulation is, in turn, superimposed upon the

Fig. 5. Photograph of upper plate megabreccia at Yaqui Ridge. The upper plate is exposed in klippen which border the NE flank of the ridge. The upper plate is composed of unconsolidated and unsorted boulder to silt-size particles of gneissic granodiorite, quartzite, and amphibolite representative of the rocks occurring in the region. The megabreccia ranges in thickness from < 1 m to ~40 m, and may be related to the Miocene Anza Formation which is exposed just to the southeast.

Cretaceous amphibolite facies metamorphism and mylonitization widespread throughout the eastern portions of the Peninsular Ranges Batholith[Engel and Schultejann, this issue; Todd and Shaw, 1979].

The core of the complex is separated from unconsolidated, unmetamorphosed upper plate rocks by a zone of intense cataclasis which is capped by the detachment surface itself. The cataclasite is a dark brown to black aphanitic rock which forms a distinct ledge ~10-30 cm thick. In thin section, the cataclasite exhibits limited recrystallization and flow banding, porphyroclasts of embayed quartz and feldspar, and veinlets of crushed, partially recrystallized quartz in interlocking texture in a crushed, micro-crystalline matrix (Figure 4). The mineralogy and fabric of the cataclasite suggests it was derived from extreme communition of the gneiss.

The Yaqui Ridge detachment surface is polished, stained with iron and manganese oxides, and displays striae indicating upper plate motions parallel and subparallel to the northeast dip. All preexisting structures and fabrics present in the underlying gneiss have been obliterated within the cataclasite and detachment zone. The contact between the detachment surface and upper plate is sharp. There is little, if any, cataclasis above the detachment surface.

Upper plate rocks at Yaqui Ridge consist of an unconsolidated, unmetamorphosed megabreccia, or cobble-boulder fanglomerate, locally overlain unconformably by Plio-Pleistocene sediments of the Borrego Formation. The Yaqui Ridge megabreccia consists of boulder to silt-size particles in an unconsolidated mass that displays little or no sorting or sedimentary structures (Figure 5). It is devoid of any layering or bedding. The clasts range from subangular to well-rounded and are composed primarily of quartzite and amphibolite characteristic of the metasedimentary section present

to the north, west, and south, as well as plutonic rocks of the Peninsular Ranges Batholith. This megabreccia ranges in thickness from < 1 m to ~40 m.

The megabreccia appears to be a part of a series of

debris slides shed from the rising eastern margin of the Peninsular Ranges Batholith during Paleocene to mid-Cenozoic time. Younger debris slides occur locally in conjunction with extensive fanglomerates which are still evolving.

A very similar appearing cobble and boulder fanglomerate is exposed just to the southeast of Yaqui Ridge in the Vallecito and Fish Creek Mountains. This unit forms the upper section of the Miocene Anza Formation, and is interbedded with reddish-brown arkosic sandstone in the lower section [Woodard, 1974]. These beds are composed primarily of locally derived granodiorite, gneiss, pegmatite, quartzite, and amphibolitic schist, virtually identical to the constituents of the megabreccia at Yaqui Ridge. Although the Yaqui Ridge megabreccia and associated debris slides and fanglomerates along the western edge of Borrego Valley appear to be lithologically and temporally equivalent to the upper section of the Anza Formation, this correlation has not been substantiated.

The Yaqui Ridge megabreccia is overlain unconformably on the western and eastern edges of Yaqui Ridge by light-gray to buff colored, poorly cemented lacustrine claystones and interbedded sandstone of probable Upper Pliocene to Pleistocene age [Sharp and Clark, 1972; Dibblee, 1954].

STRUCTURAL FEATURES

Yaqui Ridge Detachment Fault

The structural geology of Yaqui Ridge is complex and the detachment fault is only one of the several distinct structural features in this region. The Yaqui Ridge detachment fault flanks Yaqui Ridge on the northeast side and is expressed as a series of klippen that trend parallel to the axis of the ridge, ~WNW-ESE (Figure 6). The fault surface dips 10°-40° to the north and northeast and defines the northeastern flank of the antiformal upwarp of Yaqui Ridge. The detachment fault has since been cut and partially destroyed by the younger Yaqui Ridge shear zone which is discussed in the following pages. This is especially evident at "the Ship," a conical erosional remnant, where the detachment fault slices through the hill at an angle of ~30° (Figure 6). Corresponding features of the detachment fault on the crest and southern flank of Yaqui Ridge, if present, have subsequently been destroyed by erosion and faulting, or buried by later deposition of Pliocene-Holocene sediments.

The detachment fault, where exposed, forms a smooth, planar surface. Striae are visible on some surfaces and indicate movement parallel and subparallel to the northeast dip of the fault. The fault surface forms a resistant cap over the band of intensely sheared cataclasite. Together, the detachment and cataclasite weather into a resistant ledge that is commonly exhumed at the base of the megabreccia and above the crushed and chloritized granitic gneiss of the core.

Chlorite-Breccia Zone

The mid-Cenozoic cataclastic deformation extends into the lower plate forming the chlorite-breccia zone of intense cataclasis and chloritization. The cataclastic foliation and lineation displayed in this zone are truncated by the cataclasite marking the detachment fault. Locally, the cataclastic fabric grades into and is dragged subparallel to the cataclasite. The lineation, as defined by the alignment of amphiboles and streaks of crushed biotite, feldspar, and quartz, remains at a constant N60°E ±10° throughout the chlorite-breccia zone, as well as in the entire "core complex" (Figure 6).

Within the chlorite-breccia zone are "secondary detachment surfaces": zones of intense crushing, similar to the cataclasite of the primary detachment surface but exhibiting no well defined differential movement (Figure 7). The secondary cataclasites occur within a few meters of the primary detachment. These low-angle features are parallel to the dip of the detachment fault and are limited in extent, usually dying out laterally within a few meters. Locally, two or three of these secondary zones can be observed, decreasing in thickness and occurrence with depth into the plutonic core.

Several similar appearing mid-Cenozoic cataclastic zones occur within the marginal plutons of the eastern batholith, west of Borrego Valley [see Engel and

Schultejann, this issue, Figure 12]. These zones have steep to vertical dips and are the loci of high-angle block faulting. The batholithic blocks are stepped progressively downward to the east and appear to extend the eastern margins of the Peninsular Ranges Batholith some 5-10 km.

Foliations

Two dominant gneissic foliations are present in the granodioritic core of Yaqui Ridge and in adjacent segments of the Peninsular Ranges Batholith. The late Mesozoic, more ductile, northwest-trending foliation characteristic of the batholithic margins occurs in regions of the complex where little mid-Cenozoic deformation was induced. This foliation is defined by elongated and flattened inclusions as well as aligned and recrystallized biotite, feldspar, and quartz. Thin section analysis reveals embayed, anhedral quartz and feldspar along with bent twins and undulatory extinction indicative of a strained rock. This earlier foliation is regional in extent and is the product of late Mesozoic NE-SW compression during final stages of pluton emplacement throughout the eastern margin of the Peninsular Ranges Batholith [Engel and Schultejann, 1984; Todd and Shaw, 1979; Theodore, 1970]. At Yaqui Ridge, this late Mesozoic foliation dips at a moderate to gentle angle, and is folded during the Cenozoic to define the Yaqui Ridge antiform. The more brittle and highly localized, mid-late Cenozoic cataclastic foliation, related to detachment and oblique-slip faulting, is superimposed upon the more ductile, higher temperature and pressure, late Mesozoic foliation. The cataclastic foliation found within the chlorite-breccia zone and imposed during, and perhaps shortly after, the mid-Tertiary detachment faulting, grades downward into conformity with the late Mesozoic foliation. Everywhere in the Yaqui Ridge detachment complex, both the late Mesozoic and the superimposed Tertiary mineral lineations are quasi-accordant, striking ~N60°E.

Pegmatite dikes related to Late Cretaceous plutonic activity intrude the gneissic granodiorite on Yaqui Ridge. They typically strike ENE-WSW to E-W. Dikes occurring in the lower plate beneath the detachment fault are always truncated by the mid-Cenozoic detachment surface and cataclasite. Both the older, late Mesozoic, and the mid-Tertiary rock fabrics imposed upon the host gneiss overprint the pegmatites, and in more intensely deformed areas diffuse the boundary between pegmatite and granodiorite. Pegmatites also display the constant northeast-striking mineral lineation so pervasive in the gneiss.

The upper plate is well exposed in klippen that border the northeast limb of the Yaqui Ridge antiform. Along the eastern margin of the Peninsular Ranges to the north, the upper plate consists of faulted and extended portions of the batholith as well as units comparable to those in the upper plate at Yaqui Ridge (Figure 2).

Upper plate structures involving listric faulting and extension have been reported for many mid-Cenozoic detachment fault complexes in the southwestern U.S. (Miller et al. [1983]; Mueller et al. [1982]; Frost and Martin [1982]; Crittenden et al. [1980]; Davis et al. [1980]; Davis [1980]; Rehrig and Reynolds [1980]; Coney [1974]; and many others). However, if such faulting did occur at Yaqui Ridge, the evidence for it has not been retained in the megabreccia.

Yaqui Ridge Shear Zone

Superimposed upon and cutting through the Yaqui Ridge detachment fault is a broad zone of intense left-oblique-slip faulting termed the Yaqui Ridge shear zone (Figure 6). This zone runs the length of Yaqui Ridge and is clearly younger than the antiform and associated detachment fault. It cuts through the northern flank of Yaqui Ridge just north of the axial trace of the antiform, and locally attains a width of > 800 meters.

The shear zone can be traced westward into the Peninsular Ranges Batholith where it slices into the eastern margin of the batholith and forms a series of narrow, almost vertical cataclastic zones. As noted above, these extend westward and northward along the eastern margin of the Peninsular Range in Borrego Valley and result in a step-faulted, E-W distension of some 5-10 km within the marginal plutons (Figure 2), and see Engel and Schultejann [this issue, Fig.

12]. This extension appears to be the most westerly known manifestation of the mid-Cenozoic regional detachment process in the southwestern United States.

The eastern segment of Yaqui Ridge shear zone cuts through the northern edge of the Vallecito Mountains. It continues eastward to the western margin of the Salton Trough, a distance of ~15 km, where it appears to be downfaulted beneath the thick sedimentary section of the trough.

The Yaqui Ridge shear zone separates and divides the main body of the antiform from the Yaqui Ridge detachment fault by a broad, intensely sheared zone of anastomosing faults which widen and narrow in an intricately braided pattern, breaking the intra-fault region into a series of rotated and sheared blocks (Figure 6). Many of the fault surfaces display striae which indicate a component of dip-slip motion as well as left-lateral motion. Pegmatites and foliations entering the shear zone are locally warped and dragged in a left-lateral sense (Figure 6). In general, the individual strands within the shear zone dip vertically, and cataclastic rocks of the lower plate gneiss have been both crushed and rotated as coherent blocks. Strikes of the cataclastic foliation vary, but the dominant direction is ~E-W. Dips of the foliation are predominantly steep to moderately steep and vary in direction, but predominantly dip north or south. Foliation is typically vertical at shear zone contacts. Throughout the Yaqui Ridge shear zone, regardless of foliation direction, the mineral lineation remains at N60°E + 10°, accordant with the strike of lineations found not only in the Yaqui Ridge detachment complex, but also throughout Late Cretaceous and post-Miocene structural features along the eastern portions of the Peninsular Ranges Batholith in Borrego V alley [Engel and Schultejann, this issue].

The Yaqui Ridge shear zone merges with the detachment fault near the eastern flank of Yaqui Ridge (Figure 6). Further east, the shear zone and detachment fault again diverge. The detachment fault attains a more easterly strike and disappears under the sediments of southern Borrego Valley. In contrast, the shear zone continues southeastward where it widens into a gouge zone > 400 m wide that is unconformably overlain to the north by Upper Pliocene to Holocene sediments adjacent o "the Narrows"(Figure 6). At "the Narrows," the zone consists of a mass of black cataclasite with isolated outcrops of extremely crushed gneiss. This cataclastic gneiss is aphanitic and structureless, possessing little or no foliation or lineation. Rare striae within the cataclasite range from vertical to horizontal, further suggesting both dip- and strike-slip motions.

The southern limb of Yaqui Ridge is relatively undeformed and disappears beneath the alluvium in San Felipe Canyon, presumably the trace of the San Felipe fault (Figure 6). Strands of the San Felipe fault splay and widen into an intense shear zone near the eastern terminus of the antiform.

What is inferred to be an extension of the upper plate with associated cataclasite is exposed north of this shear zone and along the southeast boundary of the San Felipe Canyon at "the Narrows" (Figure 6). It dips ~10° to the SSW and is parallel to Yaqui Ridge. A characteristic narrow band of black, aphanitic cataclasite separates the underlying brecciated and chloritized gneiss from the cover rocks of pale gray to tan, aphanitic fault gouge. Very faint and rare striae suggest dipslip motion. This fault may represent an extension of the Yaqui Ridge detachment fault along the southern limb of the antiform, and dating of the cataclasites is in progress.

Associated with the Yaqui Ridge shear zone is a series of E-W trending anticlines and synclines in folded Upper Pliocene to Pleistocene sediments. These features occur north and northwest of the shear zone, and along the eastern margin of the Peninsular Ranges Batholith (Figures 2 and 6).

Northwest of Yaqui Ridge, some of these folds are cored by steeply faulted gneiss with Plio-Pleistocene lacustrine sediments draped over the core. At least one faulted core is capped only by colluvial debris and is devoid of sedimentary deposits. It is not readily discernable if the folds to the north and east also contain faulted cores at depth.

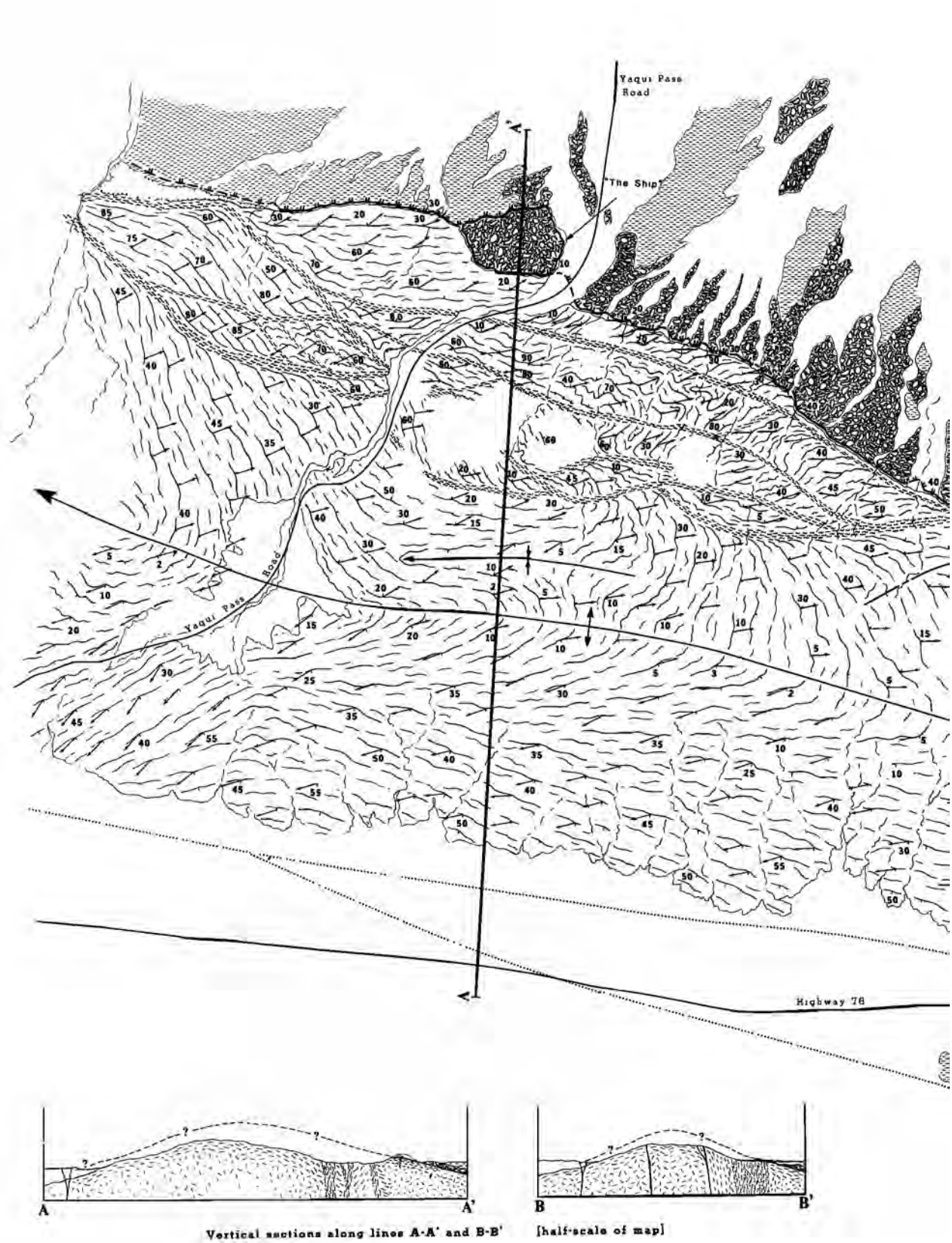

Fig. 6. Geologic map and cross sections of Yaqui Ridge core complex. The Yaqui Ridge detachment fault dips from 10-40 degrees to the NE and general transport direction of upper plate is down-dip to the NE. The axis of Yaqui Ridge antiform is cut by strands of the San Felipe fault without appreciable right-lateral offset.

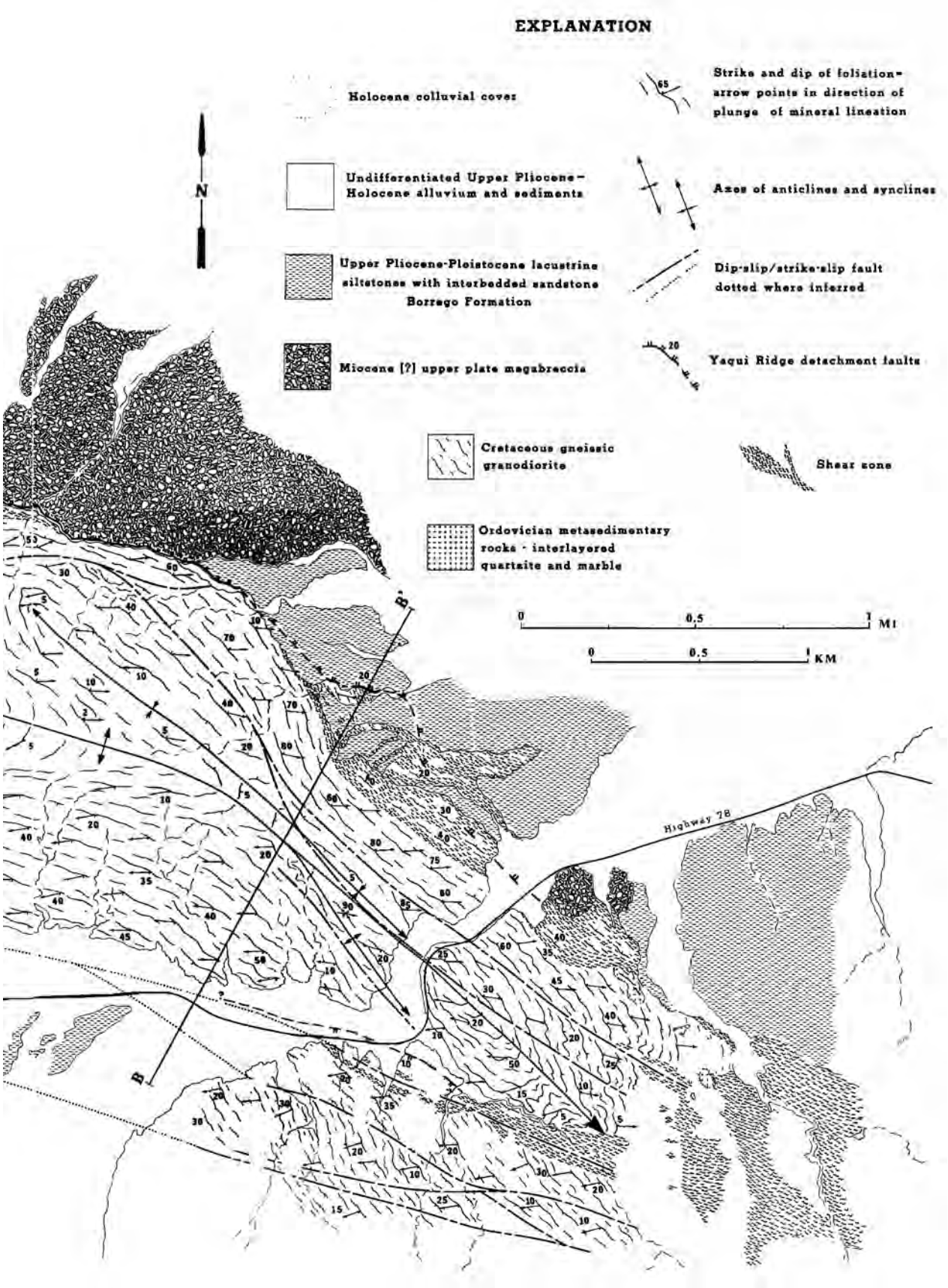
EXPLANATION
Holocene colluvial cover
Undifferentiated Upper Pliocene–Holocene alluvium and sediments
Upper Pliocene-Pleistocene lacustrine siltstones with interbedded sandstone Borrego Formation
Miocene [?] upper plate megabreccia
Cretaceous gneissic granodiorite
Ordovician metasedimentary rocks - interlayered quartzite and marble
Strike and dip of foliation- arrow points in direction of plunge of mineral lineation
Axes of anticlines and synclines
Dip-slip/strike-slip fault dotted where inferred
Yaqui Ridge detachment faults
Shear zone
N
0 0.5 1 MI
0 0.5 1 KM
Highway 78
B
B'

Fig. 7. Photograph of secondary cataclasites formed beneath and concordant with primary detachment and cataclasite. These secondary zones are limited in extent and die out laterally within a few meters.

DEFORMATIONAL HISTORY

Based on the structural features and relationships outlined in the preceding sections, a preliminary structural history of Yaqui Ridge antiform can be inferred which involves a series of magmatic, metamorphic, and deformational events ranging from Mid-Late Cretaceous through the Cenozoic (Table 1). These are presented in order from oldest to youngest:

1. A Mid-Late Cretaceous synkinematic mylonitization and deformation accompanying and following the emplacement of the Yaqui Ridge and associated plutons of the Peninsular Ranges Batholith. This dynamothermal metamorphism reached amphibolite facies throughout the eastern margins of the Peninsular Ranges [Todd and Shaw, 1979; Taylor and Silver, 1978; Theodore, 1970; Sharp, 1967]. To the north, late Mesozoic deformation and metamorphism was accompanied by westward thrusting of the Santa Rosa Cataclastic Zone over the Peninsular Ranges [Engel and Schultejann, this issue].

Immediately to the south of Yaqui Ridge, Todd and Shaw [1979] have emphasized the occurrence of

TABLE 1. Relative Ages and Relationships of Deformational Events at Yaqui Ridge

Age	Event	Stratigraphic Relationships
Pleistocene	Formation of E-W trending anticlines and synclines	Deformation of Upper Pliocene Borrego Fm. that unconformably overlies Yaqui Ridge shear zone
Late Miocene-Pliocene	Development of Yaqui Ridge shear zone	Dip-slip and left-lateral motions overprint earlier
Late Oligocene-Miocene	Development of Yaqui Ridge detachment fault and antiform	Chlorite-breccia zone and brittle metamorphic fabrics overprint pervasive NW-SE semi-ductile foliations formed in Late Cretaceous
Mid-Late Cretaceous	Yaqui Ridge pluton emplacement and synkinematic deformation	Regional NW-SE fabric imposed upon granodiorite and pegmatites at Yaqui Ridge

mylonites and related metamorphic textures within adjacent portions of the eastern Peninsular Ranges Batholith. These may include both Cretaceous and Tertiary cataclasites. Dating of these cataclasites and mylonites is in progress. At Yaqui Ridge, Cretaceous tectonism and metamorphism were accommodated by overprinting the igneous textures with a distinctive NNW-trending gneissic foliation, cataclasis, and pervasive northeast-trending mineral lineations.

E-W to ENE-WSW trending pegmatite dikes were emplaced in the final protoclastic stages of batholithic emplacement along the eastern margins of the Peninsular Ranges Batholith. The pegmatites are overprinted with the same Late Cretaceous mylonitic foliation and east to NE-trending mineral lineation characteristic of the granodiorite gneiss.

2. A mid-Cenozoic low temperature episode of ENE-WSW extension and detachment faulting accompanied by lower greenschist facies metamorphism and brittle deformation. This event is most probably a westward extension of the mid-Tertiary ENE-WSW detachment episodes recorded in core complexes extending from southeastern California to the Colorado Plateau [Frost and Martin, 1982; Crittenden et al., 1980]. Dating of the cataclasites associated with detachment faulting is now in progress. However, the age of this event is presently inferred to be Miocene by stratigraphic relationships and by analogy with very similar detachment structures in the Whipple Mountains and related detachment terrane east of the San Andreas fault (Table 1).

At Yaqui Ridge and along the eastern margin of the Peninsular Ranges Batholith in this region, the mid-Cenozoic detachment fault and formation of associated cataclasite and chlorite-breccia zone are clearly superimposed upon and much younger than the higher temperature, more ductile Cretaceous deformational structures.

Several models have been proposed recently for the origin of mid-Cenozoic detachment faults in what has been termed "metamorphic core complexes" of the southwestern U.S. It is rapidly becoming apparent that one single model cannot be applied to each and every "complex" [Armstrong, 1982; Davis et al., 1980]. Even among mid-Cenozoic "core complexes" and detachment terrane in the southwest, there is diversity in features and speculated modes of evolution.

The Yaqui Ridge detachment fault and antiform are most probably genetically related to the Whipple Mountains and related detachment complexes in

southeastern California. However, Yaqui Ridge possesses characteristics and structures which fit a number of models proposed in the literature for formation of detachment faults and associated structural and petrologic features. Unfortunately, the lack of diagnostic structural features in the upper plate constrains any attempt to formulate a kinematic model for the origin of the structures at Yaqui Ridge.

The most striking feature of Yaqui Ridge is the unequivocal low temperature-low pressure (lower greenschist facies) cataclastic nature of the deformation. Both upper plate and lower plate rocks behaved in a brittle manner, as manifested by the chloritized, brecciated nature of the lower plate adjacent to the crushed cataclasite. The upper plate most probably has been faulted and deformed, but the lack of cohesiveness inherent in the megabreccia precludes the formation and retention of fault surfaces and other structural features. Consequently, the amount and direction of extension in the upper plate cannot be determined. There is no evidence for the brittle-ductile boundary or transition zone observed at other "complexes" [Miller et al., 1983; Rehrig and Reynolds, 1980]. Perhaps this suggests that Yaqui Ridge has not been as deeply eroded, did not experience as much extension, or was not formed in the same temperature-pressure environment as other "complexes."

The megabreccia at Yaqui Ridge may be the remnants of a debris or gravity slide, similar to structures in models proposed b y Davis et al. [1980], Coney [1974], and Armstrong [1972]. Motion directions interpreted from striae on the detachment fault are certainly consistent with this interpretation; that is, the upper plate moved down the dip of the fault, parallel to lineation direction in the underlying gneiss and normal to the axis of the antiform. This would suggest upper plate extension to the northeast. It is difficult, however, considering the nature of the upper plate, to invoke this mechanism to form the band of cataclasite at the base and underlying brecciated, chloritic gneiss.

G. H. Davis' [1983] model of progressive simple shear describes more completely the structural relations at Yaqui Ridge and appears a more likely model for the origin of the Yaqui Ridge detachment fault and associated cataclasite. In this model, the detachment cataclasites are formed at deeper levels and are brought into contact with surficial rocks along shear zones. The locally moderate dip (30-40°) and brittle, cataclastic nature of the deformation at Yaqui Ridge would, according to this model, constraint he amount of displacement to the upper reaches of the shear zone. This model nicely accounts for the formation of the cataclasite at the base of the detachment fault.

It is clear that Yaqui Ridge and related core complexes in southeastern California include folding and faulting of epizonal and mesozonal segments of sialic crust. However, whether or not these complexes are associated with a regional decollement" rooting" into the crust as Wernicke [1981] has suggested is equivocal.

The temporal relations concerning arching of the Yaqui Ridge pluton and detachment faulting are still unclear. A plausible inference is that it may have occurred during the final stages of detachment and probably post-detachment. Essentially N-S compressive strain (E-W extension) is need to fold the antiform and is accordant with the Plio-Pleistocene to Holocene strain regime in Borrego Valley [Engel and Schultejann, this issue; Savage et al., 1978, 1979; Sharp and Clark, 1972]. The detachment surface appears to be warped conformably with the antiform, but subsequent faulting has obscured much of the fault surface. Additional mapping of other detachment features in this area will offer more compelling evidence for the kinematics of detachment faulting and related antiform evolution.

3. The development of the Yaqui Ridge left-oblique shear zone along the northeast margin of Yaqui Ridge and Vallecito Mountains in Late Miocene-Early Pliocene time. This shear zone developed northeast of and parallel to the axis of the Yaqui Ridge antiform, most likely following a preexisting zone of weakness along the axial trend. The shear zone cuts through the antiform and detachment fault, isolating the remaining detachment fault and upper plate as klippen. Preexisting pegmatites, and Late Cretaceous gneissic fabrics are dragged, folded,

and rotated, in places into conformity with the shear zone as it evolved. Plio-Pleistocene sediments are unconformably deposited on the shear zone and upper plate megabreccia. This relationship is well exposed on the northeast and northwest flanks of the antiform.

4. A Pleistocene episode of folding and high-angle faulting forming a series of E-W-trending anticlines and synclines in Upper Pliocene to Pleistocene sediments of the Borrego Valley.

CONCLUSIONS

The complex Cenozoic history at Yaqui Ridge indicates that the mid-Cenozoic ENE-WSW extensional terrane present throughout most of the southwestern United States persists west of the San Andreas fault in southcentral California, at least into the eastern margins of the Peninsular Ranges Batholith. Yaqui Ridge is one type of small antiformal "core complex" which developed in a mid-Cenozoic regional strain regime of ENE-WSW extension and ~N-S compression. Yaqui Ridge has structural features which conform to some previously proposed models. However, because of the brittle nature of the deformation, it appears to be constrained to a near surface, low temperature and pressure environment. Estimates on the amount of extension involved are difficult due to the eroded and subsequently faulted nature of the detachment fault and megabreccia upper plate.

The cataclastic fabrics and structures associated with mid-Cenozoic detachment faulting overprint an earlier, Late Cretaceous, NW-trending mylonitic foliation. These cataclastic fabrics are, in turn, overprinted and cut by left-oblique-slip faults of the Yaqui Ridge shear zone in Late Miocene-Early Pliocene time. These faults are unconformably overlain by Plio-Pleistocene sediments of the Borrego Formation. These sediments and related sedimentary units are folded into a series of E-W-trending antiforms and synforms throughout Borrego Valley, suggesting a continuation of the N-S compressive strain pattern and associated E-W extension to the present day. The remarkable accordance of linear elements ranging in age from Late Cretaceous to Pleistocene throughout the entire region seems difficult to rationalize for any one crustal strain pattern.

Superimposed upon these more localized tectonic patterns are the regional patterns represented by the formation of the Salton Trough and Gulf of California, Basin and Range Province, and right-lateral San Andreas fault system. The relationships between Cenozoic tectonics in southcentral California and the regional tectonics remains to be determined.

Acknowledgments. This work was made possible by funding from the National Science Foundation, grants EAR 81-10867 and EAR 76-80871. The Jet Propulsion Laboratory, U.S. Geological Survey, and Zonta International provided valuable assistance and support. Many thanks to George H. Davis, Peter J. Coney, and B.C. Burchfiel for their constructive reviews of the manuscript. I especially thank A . E. J. Engel for his helpful comments and advice.

REFERENCES

Anderson, J. L., Thin skin distension in Tertiary rocks of southeastern Nevada, Geol. Soc. Am. Bull., 82, 43-58, 1971.

Armstrong, R. L., Low-angle (denudation) faults, hinterland of the Sevier orogenic belt, eastern Nevada and western Utah, Geol. Soc. Am. Bull., 83, 1729-1754, 1972.

Armstrong, R. L., Cordilleran metamorphic core complexes--From Arizona to southern Canada, Annu. Rev. Earth Planet. Sci., 10, 129-154, 1982.

Baird, A. K., K. W. Baird, and E. E. Welday, Batholithic rocks of the northern Peninsular and Transverse Ranges, southern California: Chemical composition and variation, in Mesozoic Crystalline Rocks: Peninsular Ranges Batholith and Pegmatites, Point Sal Ophiolite, edited by P. L. Abbott and V. R. Todd, pp. 177-231, Geological Society of America, Boulder, Colo., 1979.

Clark, M. M., Map showing recently active breaks along the Elsinore and associated faults, California, between Lake Henshaw and Mexico,

scale 1:24,000, Misc. Invest. Ser., 1-1329, U.S. Geol. Surv., Reston, Va., 1983.

Coney, P. J., Structural analysis of the Snake Range "Decollement," east-central Nevada, Geol. Soc. Am. Bull., 85, 973-978, 1974.

Crittenden, M.D., Jr., P. J. Coney, and G. H. Davis (Eds.), Cordilleran metamorphic core complexes, Mem. Geol. Soc. Am., 153, 490 pp., 1980.

Davis, G. A., J. L. Anderson, E.G. Frost, and T. J. Shackelford, Regional Miocene detachment faulting and early Tertiary (?) mylonitization, Whipple-Buckskin-Rawhide Mountains, southeastern California and western Arizona, in Geologic Excursions in the Southern California Area, edited by P. L. Abbott, pp. 75-108, San Diego State University, San Diego, Calif., 1979.

Davis, G. A., J. L. Anderson, E.G. Frost, and T. J. Shackelford, Mylonitization and detachment faulting in the Whipple-Buckskin-Rawhide Mountains terrane, southeastern California and western Arizona, Cordilleran Metamorphic Core Complexes, edited by M. Crittenden, Jr. et al., Mem. Geol. Soc. Am., 153, 79-130, 1980.

Davis, G. A., J. L. Anderson, D. L. Martin, D. Krummenacher, E.G. Frost, and R. L. Armstrong, Geologic and geochronologic relations in the lower plate of the Whipple detachment fault, Whipple Mountains, southeastern California: A progress report, in Mesozoic-Cenozoic Tectonic Evolution of the Colorado River Region, California, Arizona, and Nevada, Anderson-Hamilton Symposium Volume, edited by E.G. Frost and D. L. Martin, pp. 409-432, Geological Society of America, Boulder, Colo., 1982.

Davis, G. H., Structural characteristics of metamorphic core complexes, southern Arizona, Cordilleran Metamorphic Core Complexes, edited by M.D. Crittenden, Jr. et al., Mem. Geol. Soc. Am., 153, 35-78, 1980.

Davis, G. H., Shear-zone model for the origin of metamorphic core complexes, Geology, 11,342-347, 1983.

Davis, G. H. and P. J. Coney, Geologic development of the Cordilleran metamorphic core complexes, Geology, 7, 120-124, 1979.

Dibblee, T. W., Jr., Geology of the Imperial Valley region, California, Geology of Southern California, edited by R. H. Jahns, Bull. Calif. Div. Mines Geol., 170, 22-28, 1954.

Early, T. O., and L. T. Silver, Rb-Sr isotopic systematics in the Peninsular Ranges batholith of southern and Baja California, Eos Trans. AGU, 54, 494, 1973.

Engel, A. E. J., and P. A. Schultejann, Late Mesozoic and Cenozoic tectonic history of south central California, Tectonics, this issue.

Frost, E.G., and D. L. Martin (Eds.), Mesozoic-Cenozoic Tectonic Evolution of the Colorado River Region, California, Arizona, and Nevada, Anderson-Hamilton Symposium Volume, 608 pp., Geological Society of America, Boulder, Colo., 1982.

Krummenacher, D., R. G. Gastil, J. Bushee, and J. Dupont, K-At apparent ages, Peninsular Ranges Batholith, southern California and Baja California, Geol. Soc. Am. Bull., 86, 760-768, 1975.

Larsen, E. S., Jr., Batholith and associated rocks of Corona, Elsinore, and San Luis Rey quadrangles, Southern California, Mem. Geol. Soc. Am., 29, 182 pp., 1948.

Lowman, P. D., Jr., Vertical displacement on the Elsinore fault of southern California: Evidence from orbital photographs, J. Geol., 88, 41 5-432, 1980.

Miller, E. L., P. B. Gans, and J. Garing, The Snake Range decollement: An exhumed mid-Tertiary ductile-brittle transition, Tectonics, 2, 239-263, 1983.

Mueller, K. J., E.G. Frost, and G. Haxel, Mid-Tertiary detachment faulting in the Mohawk Mountains of southwestern Arizona, in Mesozoic-Cenozoic Tectonic Evolution of the Colorado River Region, California, Arizona, and Nevada, Anderson-

Hamilton Symposium Volume, edited by E.G. Frost and D. L. Martin, pp. 449-457, Geological Society of America, Boulder, Colo., 1982.

Phillips, J. C., Character and origin of cataclasite developed along the low-angle Whipple detachment fault, Whipple Mountains, California, in Mesozoic-Cenozoic Tectonic Evolution of the Colorado River Region, California, Arizona, and Nevada, Anderson-Hamilton Symposium Volume, edited by E.G. Frost and D. L. Martin, pp. 109-116, Geological Society of America, Boulder, Colo., 1982.

Rehrig, W. A., and S. J. Reynolds, Geologic and geochronologic reconnaissance of a northwest-trending zone of metamorphic core complexes in southern and western Arizona, Cordilleran Metamorphic Core Complexes, edited by M.D. Crittenden et al., Mem. Geol. Soc. Am., 153, 131-157, 1980.

Savage, J. C., W. H. Prescott, M. Lisowski, and N. King, Measured uniaxial north-south regional contraction in southern California, Science, 202, 883-885, 1978.

Savage, J. C., W. H. Prescott, M. Lisowski, and N. King, Deformation across the Salton Trough, California, 1973-1977, J. Geophys. Res., 84, 3069-3079, 1979.

Sharp, R. V., The San Jacinto fault zone in the Peninsular Ranges of southern California, Geol. Soc. Am. Bull., 78, 705-730, 1967.

Sharp, R. V., and M. M. Clark, Geologic evidence of previous faulting near the 1968 rupture on the Coyote Creek fault, The Borrego Mountain Earthquake of April 9, 1968, edited by R. V. Sharp et al., U.S. Geol. Surv. Prof. Pap., 787, 131-140, 1972.

Silver, L. T., T. O. Early, and T. H. Anderson, Petrological, geochemical, and geochronological asymmetries of the Peninsular Ranges Batholith (abstract), Geol. Soc. Am. Abstr. Programs, 7, 375-376, 1975.

Silver, L. T., H. P. Taylor, and B. Chappell, Some petrological, geochemical, and geochronological observations of the Peninsular Ranges Batholith near the international border of the U.S.A. and Mexico, in Mesozoic Crystalline Rocks: Peninsular Ranges Batholith and Pegmatites, Point Sal Ophiolite, edited by P. L. Abbott and V. R. Todd, pp. 83-110, Geological Society of America, Boulder, Colo., 1979.

Stewart, J. H., Extensional tectonics in the Death Valley area, California: Transport of the Panamint Range structural block 80 km northwestward, Geology1, 1, 153-157, 1983.

Taylor, H. P., and L. T. Silver, Oxygen isotope relationships in plutonic igneous rocks of the Peninsular Ranges Batholith, southern and Baja California, Short Papers of the Fourth International Conference on Geochronology, Cosmochronology, and Isotope Geology, edited by R. E. Zartman, U.S. Geol. Surv. Open File Rep., 78- 701, 423-426, 1978.

Theodore, T. G., Petrogenesis of mylonites of high metamorphic grade in the Peninsular Ranges of southern California, Geol. Soc. Am. Bull., 81, 435-450, 1970.

Todd, V. R., and S. E. Shaw, Structural, metamorphic, and intrusive framework of the Peninsular Ranges Batholith in southern San Diego County, California, in Mesozoic Crystalline Rocks: Peninsular Ranges Batholith and Pegmatites, Point Sal Ophiolite, edited by P. L. Abbott and V. R. Todd, pp. 177-231, Geological Society of America, Boulder, Colo., 1979.

Wernicke, B., Low angle normal faults in the Basin and Range Province: Nappe tectonics in an extending orogen, Nature, 291,645-647, 1981.

Woodard, G. D., Redefinition of the Cenozoic stratigraphic column in Split Mountain Gorge, Imperial Valley, California, Am. Assoc. Pet. Geol. Bull., 58, 521-525, 1974.

Stratigraphic record of Pleistocene initiation and slip on the Coyote Creek fault, Lower Coyote Creek, southern California

Rebecca J. Dorsey*
Department of Geological Sciences, 1272 University of Oregon, Eugene, Oregon 97403-1272, USA

ABSTRACT

The Coyote Creek fault is a major strand of the San Jacinto fault zone in southern California. Pleistocene sediments and sedimentary rocks exposed in the lower Coyote Creek area preserve a record of surface deformation, stream reorganization, and erosion that resulted from initiation and slip on the Coyote Badlands strand of the Coyote Creek fault. A well-exposed section of conglomerate and sandstone contains the 760 ka Bishop Ash and reveals (1) complete reversal of paleocurrents from northwest-directed (opposed to modern drainages) to southeast-directed (consistent with modern drainages); (2) fanning dips and a progressive unconformity bounded by the Coyote Creek and Box Canyon faults; (3) a thick gravel unit (Qg) that caps the fanning-dip section and accumulated between ca. 700 and 600 ka; and (4) post-Qg offset and deep erosion of the entire section. The fanning dips and reversal of paleocurrents are interpreted to record initiation of the Box Canyon and Coyote Creek faults by dip-slip (normal) displacement beginning at 750 ka. Strike-slip offset of Qg is equal to total offset on the Coyote Creek fault in the study area (~6 km), indicating that strike-slip motion on the fault began after deposition of Qg, after ca. 600 ± 100 ka. This gives a time-averaged slip rate in Coyote Creek of ~10 mm/yr. Two alternative models for Pleistocene fault evolution are considered: (1) prior to ca. 600 ka, the Clark and southern Coyote Creek faults were connected via a releasing bend that produced a pull-apart basin in the Borrego Badlands, and initiation of the Coyote Badlands strand at 600 ka represents northwestward propagation of the Coyote Creek fault; or (2) the Coyote Creek fault was initiated along most or all of its length at ca. 600 ka, establishing the modern link to plate-boundary faults in the Imperial Valley. Existing data are equivocal on this question.

INTRODUCTION

The San Jacinto fault zone is a seismically active system of strike-slip fault segments, segment-bounding discontinuities, and related zones of contractional and extensional deformation in southern California (Sharp, 1967; Wesnousky, 1986, 1988; Sanders, 1989; Sanders and Magistrale, 1997). The San Jacinto splays off from the San Andreas fault in a complex zone of diffuse strike-slip faults northwest of San Bernardino (Fig. 1; Matti et al., 1992; Morton and Matti, 1993), and southeast of there the two fault zones accommodate most of the motion on the Pacific-North American plate boundary (Fig. 1; DeMets et al., 1994; DeMets, 1995). Although recent studies of historical seismicity provide insights into modern fault behavior and interactions, relatively little is known about the Pleistocene history of fault slip, sedimentation, and deformation in the San Jacinto fault zone. The evolution of the fault zone at geologic time scales of 0.5–2.0 Ma has been largely overlooked in

*E-mail: rdorsey@darkwing.uoregon.edu

Dorsey, R.J., 2002, Stratigraphic record of Pleistocene initiation and slip on the Coyote Creek fault, Lower Coyote Creek, southern California, *in* Barth, A., ed., Contributions to Crustal Evolution of the Southwestern United States: Boulder, Colorado, Geological Society of America Special Paper 365, p. 251–269.

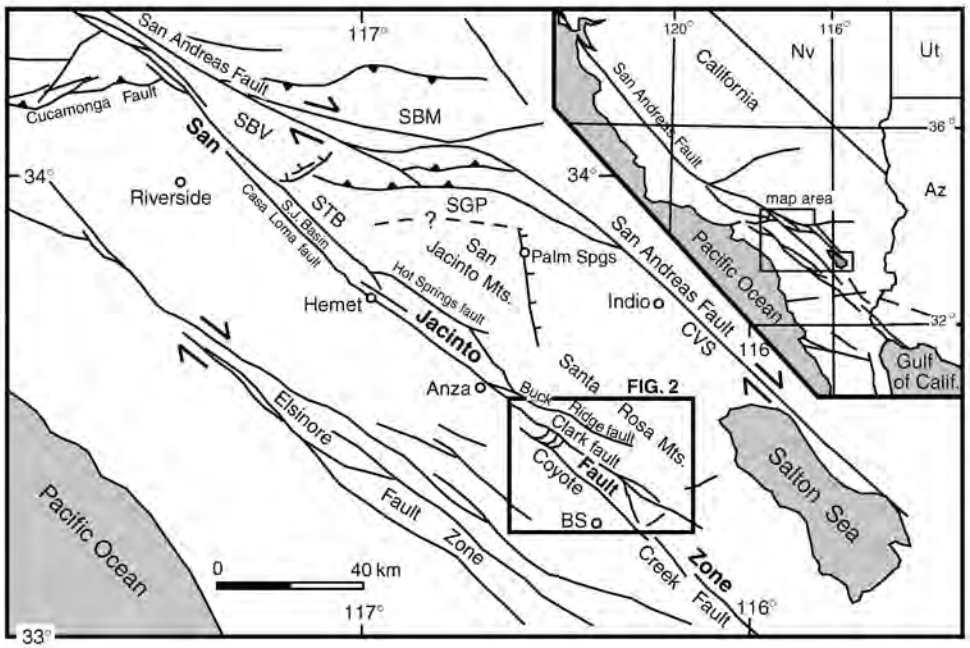

Figure 1. Map showing the San Andreas, San Jacinto, and Elsinore strike-slip fault zones in southern California, and location of Figure 2. BS—Borrego Springs, CVS—Coachella Valley strand of San Andreas fault, SBM—San Bernardino Mountains, SBV—San Bernardino Valley, SGP—San Gorgonio Pass, S.J. Basin—San Jacinto basin, STB—San Timoteo Badlands. Modified from Sharp (1967).

previous studies, in spite of its significance for understanding the fault kinematics, strain partitioning, and regional slip budget of the San Andreas fault system.

One poorly understood aspect of the San Jacinto fault zone is its age of initiation, which is directly related to long-term slip rate. Based on velocities determined from GPS measurements and offset of late Quaternary deposits, it is generally believed that slip on the San Jacinto fault is ~10–12 mm/yr and slip on the San Andreas fault southeast of the Transverse Ranges (Coachella Valley strand) is ~25 mm/yr (Sharp, 1981; Rockwell et al., 1990; Bennett et al., 1996; Kendrick et al., 1994). Northwest of Cajon Pass, slip on the San Jacinto and San Andreas faults merge to produce ~35 mm/yr slip on the Mojave segment of the San Andreas fault (Weldon and Sieh, 1985; Weldon and Humphreys, 1986; Humphreys and Weldon, 1994). If one assumes a rate of 10 mm/yr and total offset of 24 km (Sharp, 1967), the age of inception for the San Jacinto fault zone is inferred to be ca. 2.4 Ma. However, geologic and stratigraphic relationships in the northern part of the fault zone provide evidence for initiation between ca. 1.5 and 1.0 Ma (Morton and Matti, 1993; Albright, 1999), which would imply a slip rate of ~16–24 mm/yr. These discrepancies reflect existing limits in our understanding of the fault zone, and indicate a need for detailed studies of fault initiation and evolution in areas where stratigraphic controls exist.

This paper presents a stratigraphic analysis of middle Pleistocene sediments and sedimentary rocks exposed in the central San Jacinto fault zone north of Borrego Springs, California (Figs. 1, 2). Internal stratigraphy, lithofacies, paleocurrent data, and growth structures in these strata provide a record of sedimentation and surface deformation that resulted from initiation and slip on the Coyote Badlands strand of the Coyote Creek fault, a major strand of the San Jacinto fault zone. The deposits are well exposed in steep gullies and badlands erosional topography, and their age (early to middle Pleistocene) is known from the presence of dated volcanic ashes. Following accumulation of the thick section (~400 m), the sediments have been offset by younger faults and deeply dissected by vigorous erosion. Thus, the area has experienced profound changes in topography over the past 700,000 yr that are clearly related to active strike-slip faulting. In this paper, stratigraphic data are integrated with structural and geomorphic analyses to reconstruct the Pleistocene history of initiation and slip on the Coyote Creek fault in the lower Coyote Creek area.

STRUCTURAL AND GEOMORPHIC SETTING

The two active segments of the San Jacinto fault zone in the study area are the Coyote Creek and Clark faults (Figs. 1, 2). The Clark fault displays abundant geomorphic features characteristic of active strike-slip faulting, such as offset stream channels, beheaded alluvial fans, shutter ridges, and fresh fault scarps cut through late Pleistocene deposits. The Clark fault terminates to the southeast in a zone of diffuse faulting and strongly folded Pleistocene sedimentary rocks at the south end of the Santa Rosa Mountains (Fig. 2; Dibblee, 1954). This is the site of a 1954 M 6.2 earthquake that initiated at the southeast end of the fault and propagated southeastward into the zone of diffuse brittle deformation (Sanders, 1989). Active fault features are extremely well developed along the Clark fault and are also present, but less pronounced, along the trace of the Coyote Creek fault.

This study focuses on a segment of the Coyote Creek fault located between the Borrego Badlands and Fig Tree Valley

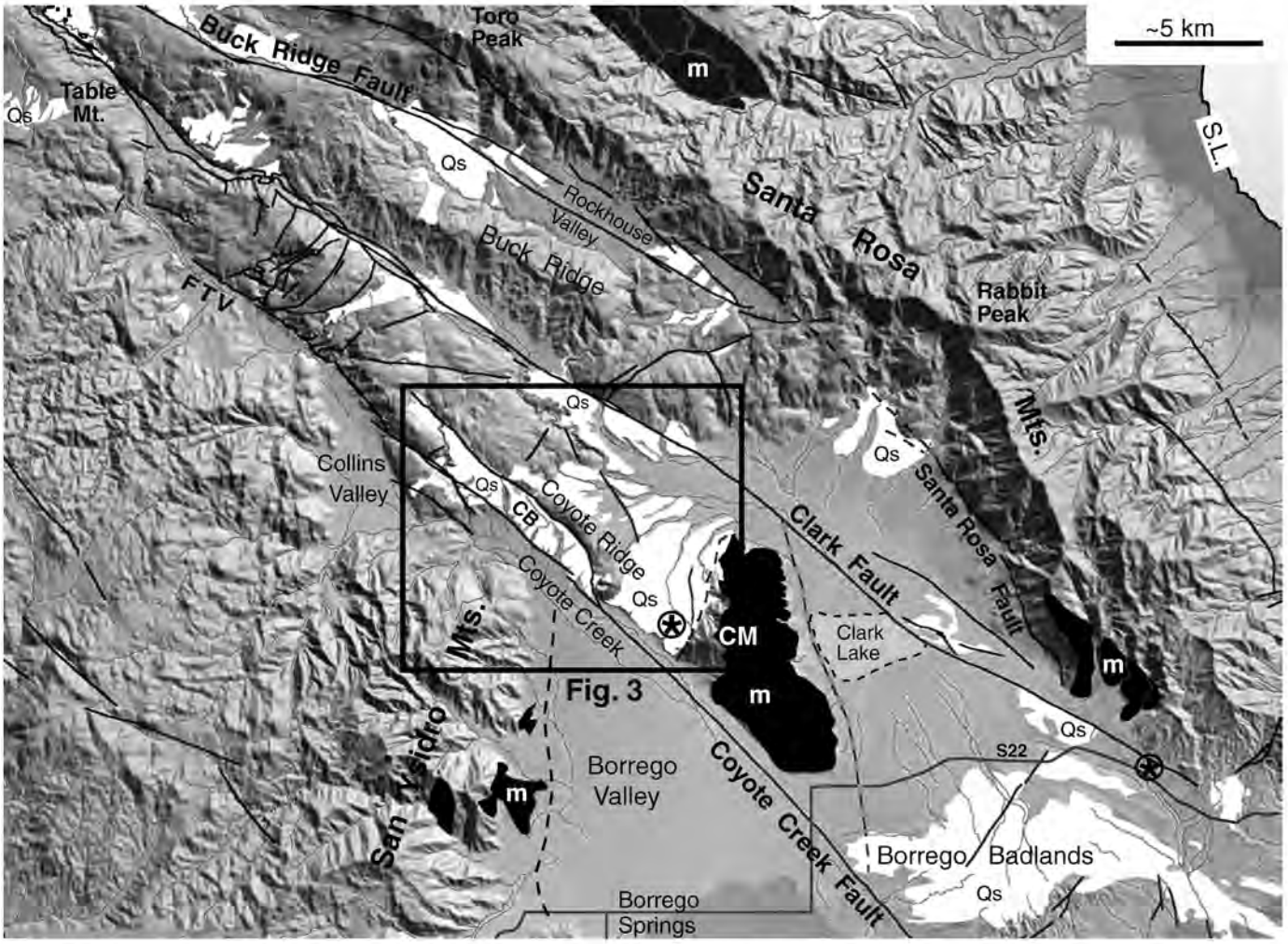

Figure 2. Shaded relief map showing major faults and fault-related topography in the central San Jacinto fault zone. White areas (Qs) are Quaternary sediments and sedimentary rocks; dark areas (m) are Cretaceous Santa Rosa mylonite. Unlabeled areas are mostly nonmylonitic crystalline rocks (rough topography) or late Pleistocene to Quaternary alluvium (low smooth topography); area south of Qs in Borrego Badlands is underlain by sedimentary rocks. Faults are indicated by solid lines, dashed where buried or inferred (except line around Clark Lake). Circled asterisk near southeast end of Clark fault shows location of 1954 M_L-6.2 Arroyo Salada earthquake; asterisk west of Coyote Mountain is the 1969 M_L-5.8 Coyote Mountain earthquake (Sanders, 1989). CB—Coyote Badlands, CM—Coyote Mountain, FTV—Fig Tree Valley, S22—State Highway 22, S.L.—sea level.

(Figs. 2, 3), informally named the Coyote Badlands strand. Displacement on the Coyote Creek fault decreases to the northwest through Fig Tree Valley, and slip is transferred from there to the northeast through a series of normal faults to the Clark fault (Fig. 2; Sharp, 1975). The Buck Ridge fault has measurable offset near Anza (Fig. 1; Sharp, 1967), but observations made during this study show that it has no geologic offset or geomorphic expression where it has been mapped in southeastern Rockhouse Valley (Fig. 2). Thus, it appears that slip on the northwestern part of the Buck Ridge fault either steps south to the Clark fault or is transferred southeast to the Santa Rosa fault south of Toro Peak, or both.

The Santa Rosa fault is a large normal fault that forms a steep topographic escarpment separating the high Santa Rosa Mountains from Clark Valley (Fig. 2). This fault was originally recognized by Dibblee (1954), but Sharp (1967) stated that there is no evidence for a large-offset fault at this location. In fact, numerous features reveal the presence of a large normal fault, including well-preserved high triangular facets defining a linear range front, intense brittle fracture and cataclasis in a steeply southwest-dipping fault zone, short steep drainages and wineglass canyons in the footwall, and asymmetric topography in the Santa Rosa Mountains that reflects tilting to the northeast (Fig. 2). Correlation of bedrock mylonite across the Santa Rosa fault suggests ~400 m of dip-slip separation near its south end, with vertical displacement probably increasing to the north. The largest well-preserved facets along the Santa Rosa range front are 400–500 m high, which can be inferred to represent a

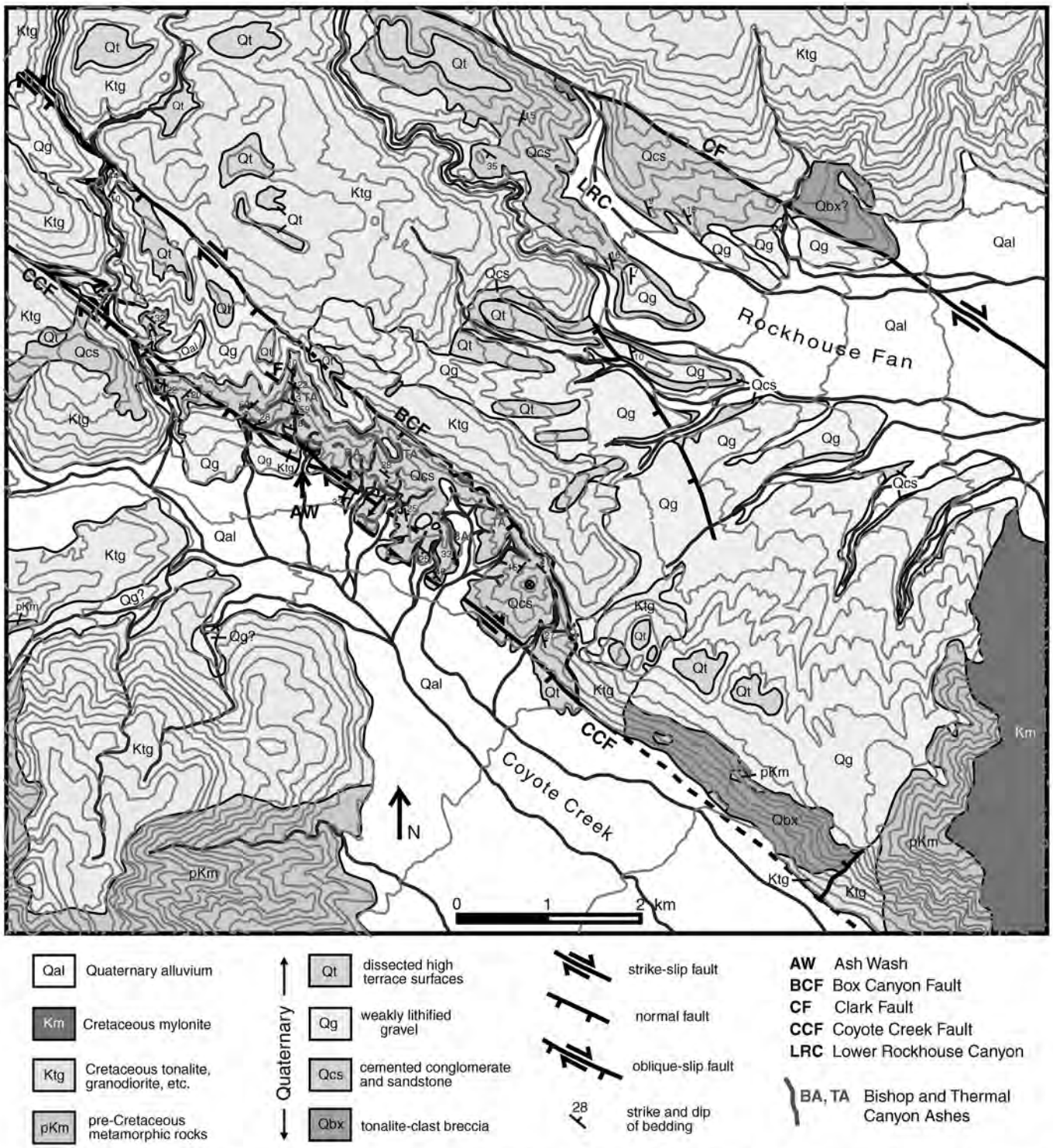

Figure 3. Geologic map of the lower Coyote Creek area. Coyote Badlands is the area of eroding Qcs (sedimentary rocks) and Qg (gravel) bounded by the Box Canyon and Coyote Creek faults. Thin gray lines are topographic contours, contour interval 40 m. Line "F" shows position and orientation of fulcrum of tilting (neutral line) as determined for fanning-dip growth structure in Figure 9. Most contacts within crystalline rocks (pKm, Ktg, Km) are from Sharp (1967).

vertical slip rate of ~1.0 mm/yr (dePolo and Anderson, 2000). Despite these well-developed large-scale features, modern fan channels do not show observable offset on the Santa Rosa fault, and late Pleistocene alluvial fans in the hanging wall (southwest side) of the fault are currently being bypassed and eroded. These observations suggest that the Santa Rosa fault recently has become inactive and that slip ended sometime in late Pleistocene time. The Santa Rosa fault loses its expression in a zone of hummocky topography west of Rabbit Peak, and reappears as a well-defined fault scarp with triangular facets on the northeast margin of Rockhouse Valley (Fig. 2). The discontinuous aspect of the fault is not well understood; it may strike north and then cut west in the area of Rabbit Peak, or it may continue on a northwesterly trend and be buried beneath a large mass of footwall-derived landslide material.

Offset on the Clark and Coyote Creek faults is constrained by the presence of laterally continuous, moderately to steeply dipping Cretaceous mylonite in the bedrock (Fig. 2; Sharp, 1967). Sharp (1967) measured 15 km of dextral offset on the Clark fault across Clark Valley, and 5 km on the Coyote Creek fault across Borrego Valley. Remeasurement of these offsets using Sharp's map yields general agreement with minor revision: About 15 km on the Clark fault and 6 km on the Coyote Creek fault, for a total of ~21 km on the two faults. Between Anza and Hemet (Fig. 1), offset of the Thomas Mountain sill on the San Jacinto and Thomas Mountain faults is ~22–24 km (Sharp, 1967). Other studies have proposed greater amounts of total offset on the San Jacinto fault zone, ranging up to ~29–30 km (Bartholomew, 1970; Hill, 1984; Revenaugh, 1998). Measurements of offset across Borrego and Clark Valleys is considered here to be reliable because the mylonite zone is a continuous bedrock unit that provides a good strain marker. Thus, there appears to be a discrepancy between total offset measured in the study area (~21 km) versus the Anza area (~22–24 km) and farther north. This may be due to a displacement gradient on the San Jacinto fault in which slip decreases to the southeast, or distributed shear on small faults that transfer slip outside of the shear zone from northwest to southeast. West-side-down normal displacement on the Santa Rosa and Coyote Creek faults would have the effect of decreasing the amount of strike-slip offset and increasing the mismatch in offset between the different parts of the fault zone.

Restoration of offset on the Clark fault results in alignment of the Santa Rosa fault with a north-northeast-striking inactive normal fault on the west side of Coyote Mountain (Fig. 2). Mapping of crystalline rocks across the fault (Fig. 3) indicates less than ~300 m of normal offset. Correlation of this fault with the Santa Rosa fault suggests that they may once have been a single normal fault prior to offset on the Clark fault, and that slip on the older fault was terminated by initiation of the Clark fault. However, the age of this fault and its relation to older stratigraphy in this area are not well understood. Two other, old faults of uncertain age are located on the east side of Coyote Mountain and east side of the San Ysidro Mountains (west side of Borrego Valley) (Fig. 2). The east Coyote Mountain fault was inferred on the basis of gravity data by Sharp (1967), and was interpreted by Bartholomew (1970) to be an oblique-slip fault that linked the Clark and southern Coyote Creek faults during middle to late Pleistocene slip. This interpretation seems unlikely because the geomorphology on the east side of Coyote Mountain is irregular and subdued, and does not display any features diagnostic of recent fault slip, such as are seen on the Santa Rosa fault. Instead, the morphology on the east side of Coyote Mountain is similar to that of the east side of the San Ysidro Mountains; both faults display an irregular and embayed mountain range front, which suggests that the two faults are correlative and predate slip on the Coyote Creek fault. This interpretation is supported by the presence of large negative gravity anomalies in Borrego and Clark Valleys that have similar magnitude (−75 to −80 Mgal) and are oriented parallel to the inactive north-trending range fronts (Fig. 2; Bartholomew, 1970).

The Coyote Creek, Clark, and Box Canyon faults cut all Pleistocene units in the study area (Fig. 3), and therefore have a history of late Pleistocene to Holocene slip. In contrast, the normal fault on the west side of Coyote Mountain cuts older breccia (Qbx) but is overlapped by Qg gravel, indicating that this fault is older than the others. Kinematic data from the Box Canyon fault reveal slip directions clustered into strike-slip (right lateral) and dip-slip (normal) motion (Fig. 4). This reflects a complex history of movement that includes both horizontal and vertical displacement. Although it is not possible to determine the relative ages of striations in the fault zone, the stratigraphic history described below suggests that the fault initially experienced dip-slip motion during growth of a fanning-dip section in Ash Wash, and later was dominated by strike-slip motion associated with horizontal displacement on the Coyote Creek fault.

PLEISTOCENE STRATIGRAPHY OVERVIEW

Pleistocene sediments and sedimentary rocks in the study area belong to a regionally extensive sequence of sandstone, mudstone, conglomerate and breccia known informally as Bautista Beds (Frick, 1921; Sharp, 1967). These deposits are preserved in patches throughout the San Jacinto fault zone and are especially abundant and well exposed in the study area (Fig. 3). The Coyote Badlands is an area of deep canyons and vigorous erosion located between the Coyote Creek and Box Canyon faults, which provides exceptional exposures of fault-bounded Bautista beds stratigraphy (Fig. 5A). The stratigraphy is subdivided into four units (from oldest to youngest): (1) tonalite-clast breccia (Qbx; Fig. 5B), (2) bedded conglomerate and sandstone (Qcs; Fig. 5C), (3) weakly consolidated gravel (Qg; Fig. 5D), and (4) late Quaternary terrace gravels (Qt) and Holocene alluvium (Qal). This study focuses on the deposition and deformation of units 2 and 3.

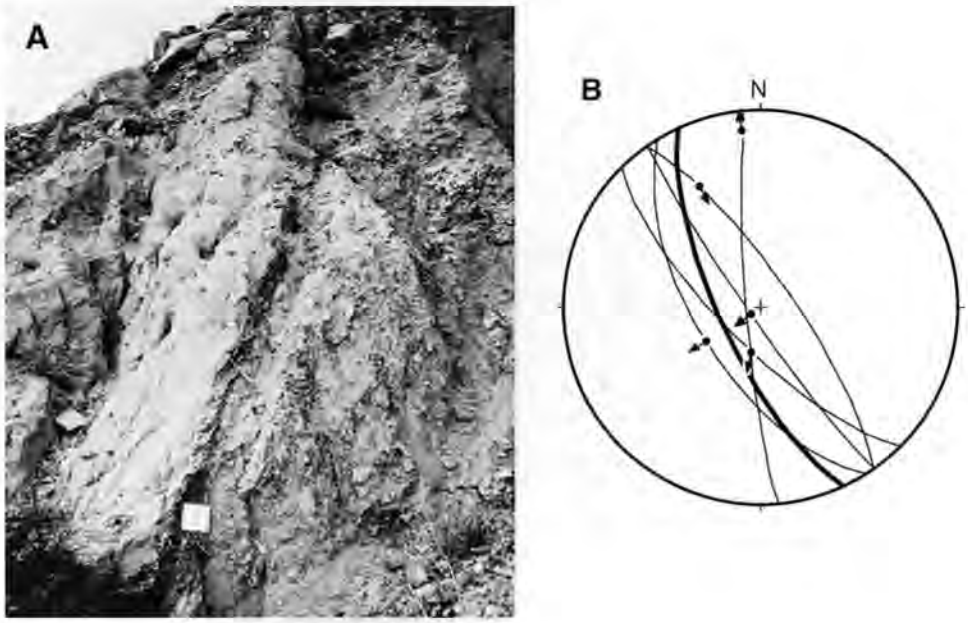

Figure 4. A: Exposure of Box Canyon fault in the Coyote Badlands near center of Figure 3, view looking northwest. Map board is 30 cm long and sits in master fault zone with well-developed clay gouge. Pleistocene sandstone and conglomerate are on left (southwest) side of fault, and brecciated Cretaceous granodiorite is on right (northeast). Fault is capped by colluvium. B: Equal area projection of fault-kinematic data from locality shown in A. Thick line is the master fault zone; thin lines are microfault planes within the fault zone and adjacent brecciated footwall. Dots with small arrows show fault striations and direction of movement of hanging wall block for each microfault. Note large variation in orientation of fault lineations, which vary from dip-slip (normal) to strike-slip (right lateral). Plot produced using Fault-Kin program by R. Allmendinger.

Tonalite-clast breccia is exposed northwest of Coyote Mountain and in a small area in lower Rockhouse Canyon (Fig. 3). At Rockhouse Canyon, Qcs depositionally overlies Qbx along a sharp uneven contact that probably is either an unconformity or the irregular upper surface of a rock avalanche deposit (Fig. 5B). This implies that Qbx is older than Qcs northwest of Coyote Mountain, and that an unconformity separates Qbx and Qg at that location. Bedded conglomerate and sandstone (Qcs) are cemented with calcite in the Coyote Badlands but are only weakly lithified in the area around lower Rockhouse Canyon. This probably reflects a difference in diagenetic history between the two areas, with deeper burial and more subsurface fluid flow inferred for well-lithified sedimentary rocks in the Coyote Badlands. The Qcs unit shows a systematic lateral facies change in the Coyote Badlands, from dominantly conglomerate in southeast to dominantly sandstone in the northwest, consistent with northwest-directed paleocurrents measured in the older part of that unit (data presented in following sections).

The Qg gravel unit is widespread in the study area. It occupies a large northeast-dipping surface northwest of Coyote Mountain, where it is located ~200 m above Coyote Creek on the northeast side of the Coyote Creek fault (Fig. 3). In this area Qg contains abundant plutonic and metamorphic clasts, with no mylonite, and imbricated clasts record transport to the northeast. It therefore is interpreted to be a beheaded gravel deposit that was derived from nonmylonitic rocks in the northern San Ysidro Mountains, on the southwest side of the Coyote Creek fault (Figs. 2, 3). It was later displaced to the southeast away from its source by strike-slip offset and at least 100–150 m of uplift due to the dip-slip component of oblique slip on the Coyote Creek fault.

ASH WASH STRATIGRAPHIC SECTION

A thick section of Pleistocene strata unconformably overlies Cretaceous plutonic rocks and is well exposed in Ash Wash in the Coyote Badlands (Figs. 3, 6). The section is 400 m thick and displays a systematic up-section increase in grain size from sandstone and pebbly sandstone (Qcs) to interbedded conglomerate and sandstone (also Qcs) to weakly lithified gravel (Qg) at the top. No tonalite-clast breccia is exposed in this section or anywhere in the structural block bounded by the Box Canyon and Coyote Creek faults. The Ash Wash section was measured at a vertical scale of ~1:200, and data were collected for sedimentary lithofacies (grain size, bed thickness, sorting, sedimentary structures, etc.), ash stratigraphy, paleocurrents, synsedimentary growth structures, and samples for paleomagnetic analyses.

Sedimentary lithofacies and depositional environments

Sedimentary rocks exposed in Ash Wash are representative of most lithologic variations (excluding tonalite breccia) observed in Pleistocene deposits in the study area. The Qcs unit (conglomerate and sandstone) makes up the lower 310 m of the measured section (Fig. 6) and consists of three main lithofacies associations: (1) sandstone and pebbly sandstone (2) conglomerate and sandstone, and (3) fine-grained sandstone with minor mudstone and claystone. The Qg unit (gravel) occupies the upper 90 m of the section. The transition from well-cemented sedimentary rocks to weakly consolidated gravel occurs in the upper ~50 m of Qcs in the transition to Qg. In the following section, lithofacies of Qcs and Qg are described and interpreted

in terms of their dominant depositional processes and paleoenvironments.

Sandstone and pebbly sandstone. The lower part of the Ash Wash section is dominated by weakly bedded, poorly sorted, arkosic fine- to coarse-grained sandstone and pebbly (grussic) sandstone. These deposits contain interbedded and discontinuous thin lenses, stringers, and beds of granule to small pebble conglomerate. They are massive and structureless or display weak low-angle trough cross-bedding and planar stratification. Rare beds of siltstone and nodular calcitic sandstone are also present, some with slight admixtures of reworked ash, typically ranging up to ~50 cm thick. Some parts of the section contain 5- to 10-meter thick intervals that display weak fining-upward from thin conglomerate to sandstone and pebbly sandstone to fine-grained sandstone or siltstone (e.g., 65–80 m; Fig. 6).

Sandstone and pebbly sandstone are interpreted as the record of deposition in a sand-rich braided stream system (e.g., Walker and Cant, 1984; Miall, 1996). Trough cross-bedding was produced by deposition from sandy bars in active stream channels, and fining-up intervals resulted from lateral channel migration and abandonment. Nodular calcitic beds represent weakly developed paleosols that formed in short-lived overbank subenvironments (e.g., Retallack, 1990). The relative paucity of silt and clay rules out a meandering stream model for these facies.

Conglomerate and sandstone. This facies association displays large variations in relative abundance of conglomerate, varying from rare interbeds of conglomerate in sandstone to amalgamated thick beds of conglomerate in intervals >10 m thick (Fig. 6). Conglomerate beds are moderately sorted, clast-supported, and contain mainly pebble to cobble size clasts in a pebbly sandstone matrix. Low- to moderate-angle trough cross-bedding, lenticular discontinuous bedding, clast imbrications, and basal scour-and-fill geometries are common in pebble-cobble conglomerate where it is interbedded with sandstone (Fig. 5C). Where sandstone is present it tends to form the upper parts of fining-up intervals (e.g., 210–250 m; Fig. 6). Some beds include small boulder-size clasts (~25–40 cm diameter), with the maximum clast size ranging up to ~70 cm in the coarsest deposits. Boulder-bearing beds are internally structureless, channelized at their base, and clast-supported. Clast compositions include tonalite, granodiorite, biotite schist, quartzite, and gneiss (in roughly subequal amounts), with lesser amounts of mafic plutonic rocks.

The conglomerate and sandstone facies records deposition in a gravelly braided stream system. A fluvial origin is indicated by the presence of trough cross-bedding, which records deposition by migrating gravelly bedforms, and by weakly developed fining-up intervals (e.g., Miall, 1996). Boulder-bearing beds represent channel fill deposits that formed during large floods. An alluvial fan environment (narrowly defined; cf. Blair and McPherson, 1994) is ruled out due to the abundance of fluvial features and the lack of evidence for deposition by debris flows, sheet floods or rock avalanches. Clast compositions reflect derivation from Cretaceous plutonic rocks and pre-Cretaceous metamorphic rocks in the surrounding areas, and notably lack mylonite.

Fine-grained sandstone, mudstone, claystone. This facies association is found only between ~140 and 180 m in the section (Fig. 6), and comprises two interbedded facies. The first consists of well-sorted fine to very fine-grained sandstone and minor siltstone with abundant planar low-angle cross-bedding. Internal stratification is often difficult to see due to uniform grain size and weathering, but very fresh exposures show that it is abundant. Detrital biotite is common. One interval of sandstone contains well-developed high-angle cross-bedding in 1-m-thick bed sets. The second facies is massive, pale green to reddish claystone and mudstone seen in two 2- to 3-m-thick intervals between 150 and 180 m in the section (Fig. 6).

Fine-grained sandstone is interpreted as the deposits of eolian sand dunes. Claystone records suspension settling in standing water, probably in a small lake, fluvial floodplain, or mudflat. The close association of claystone and fine-grained sandstone implies a sediment-starved depocenter that was isolated for a short time from the input of coarse-grained sediment, allowing eolian sand dunes to form around the margins of a shallow pluvial lake or river floodplain. The tectonic significance of fine-grained sediments in this part of the section is discussed below.

Boulder-bearing gravel (Qg). Qg is a thick unit of weakly consolidated pebble-cobble to boulder-grade gravel that typically forms rubbly covered slopes in the study area, but fresh exposures in upper Ash Wash permit direct observation of the sedimentologic character of this unit. It typically contains few or no sandstone interbeds, and is characterized by broadly lenticular beds of pebble-cobble gravel that alternate with cobble-boulder beds (Fig. 5D). The deposits are moderately to poorly sorted and clast-supported, with common clast imbrication. Bedding contacts tend to be diffuse and irregular, but sharp and channelized basal contacts are also observed. Boulder-bearing beds are typically 0.5–1.5 m thick, and some show weak inverse grading and/or large boulders protruding above the top of the bed. The maximum measured clast size is ~1.5 m (long axis). Matrix-supported texture is present but rare.

Inversely graded boulder-bearing gravel beds are interpreted as the deposits of debris flows that formed on a large alluvial fan, similar to the modern Rockhouse fan in the northwest corner of Clark Valley (Fig. 3). Finer-grained, pebble-cobble conglomerate beds may also record debris-flow deposition, or they may have formed by traction transport during large flood flows.

Ash stratigraphy and paleomagnetism

The Bishop Ash is well dated at 760 ka (Sarna-Wojcicki et al., 2000), and is interbedded with sedimentary rocks at three localities in the San Jacinto fault zone: North of Anza (Sharp,

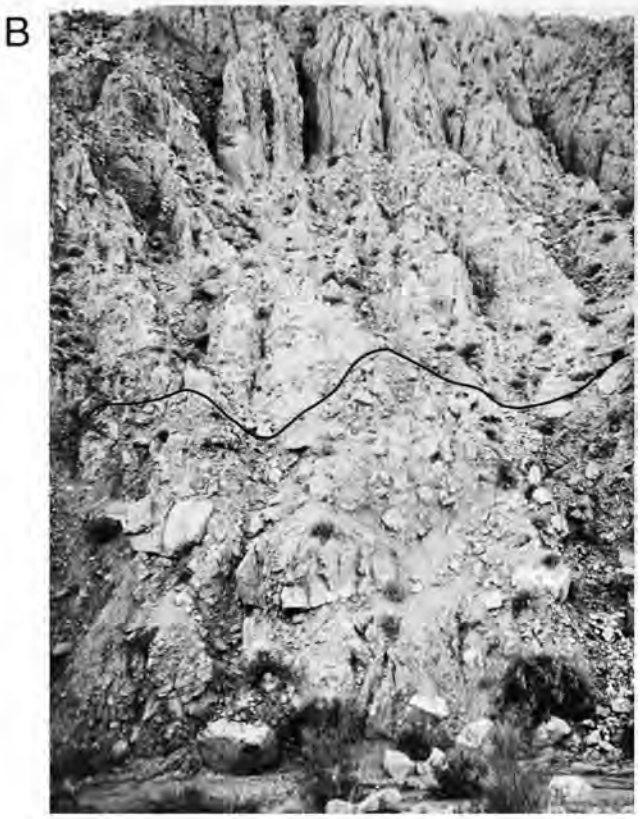

Figure 5. A: View looking southeast at deeply eroded Pleistocene deposits (mainly Qcs) in the Coyote Badlands. Box Canyon fault (BCF) on the northeast and Coyote Creek fault (CCF; two strands shown) on the southwest. Area in foreground is Ash Wash. B: Tonalite-clast breccia (Qbx) and overlying conglomerate and sandstone (Qcs) in lower Rockhouse Canyon. Irregular depositional contact (solid line) is a possible unconformity. Large block in lower middle is ~4 m long (horizontal axis). (*Continued on facing page.*)

1981), the Borrego Badlands southeast of the study area (Remeika and Beske-Diehl, 1996), and Ash Wash in the Coyote Badlands (this study; Sarna-Wojcicki et al., 1980). In Ash Wash the Bishop Ash is 1.6 m thick and consists of a 35-cm basal air-fall deposit overlain by stratified and reworked ash that is mixed with minor amounts of detrital arkosic sand and biotite. The 100 m of section above the Bishop Ash contains a series of thinner ashes, including two ash beds located 25 and 80 m above the Bishop Ash that are possible equivalents of the 740 ka ash of Thermal Canyon (Fig. 6). The Thermal Canyon ash

Figure 5. C: Example of interbedded conglomerate and sandstone in upper part of Qcs, Ash Wash. Hammer (circled) is 32.5 cm long. D: Example of Qg gravel exposed in upper Ash Wash. Measuring staff (indicated by arrow, near center) is 1.8 m long.

is recognized in the Mecca Hills where it occurs 40 m above the Bishop Ash, and in the Borrego Badlands 15 km southeast of the Coyote Badlands (Fig. 2) (Sarna-Wojcicki et al., 1997). The bed 80 m above the Bishop ash is a composite 1.4-m-thick ash unit with a very white (relatively pure) 50-cm-thick upper subunit that is easily traced for up to 3 km along strike to the northwest and southeast from Ash Wash. It was collected for geochemical analysis but was found to lack isotropic glass, making it unsuitable for trace element geochemistry (A. Sarna-Wojcicki, 2001, personal commun.). However, because of its relatively pure and laterally persistent character, unlike all other ashes in the section except the Bishop Ash, this unit is assigned to the Thermal Canyon Ash with a high degree of confidence.

The results of a reconnaissance paleomagnetic study in Ash Wash show that six stations collected at or above the Bishop Ash have normal polarity, and two stations located 28 and 36 m

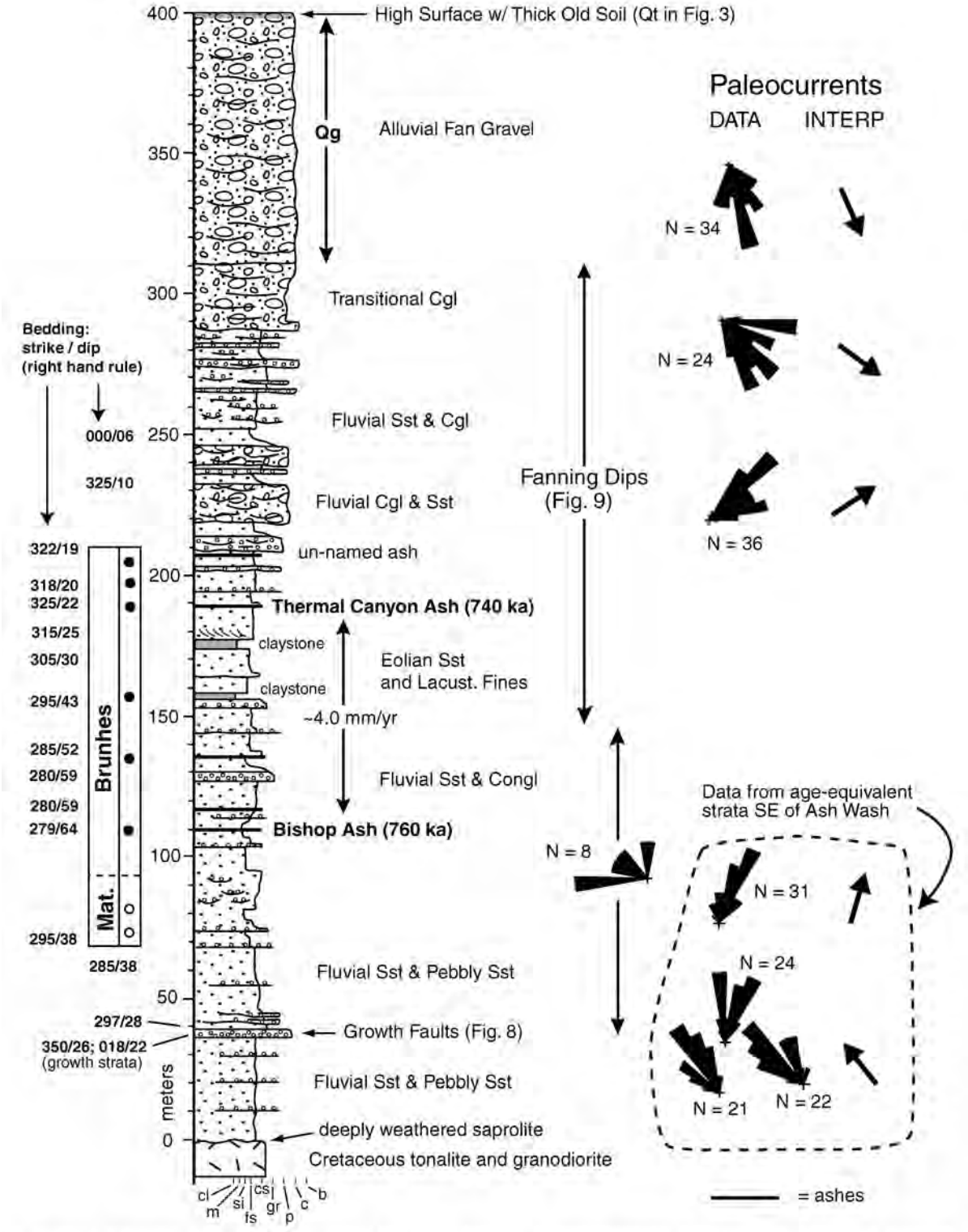

Figure 6. Measured section in Ash Wash. Dots show position of paleomagnetic samples; open circles are reversed polarity and filled circles are normal polarity. Cgl—conglomerate, sst—sandstone. Grain-size scale: cl—clay, m—mud, si—silt, fs—fine sand, cs—coarse sand, gr—granule, p—pebble, c—cobble, b—boulder. See Figure 3 for location, and text for discussion.

below the ash have reversed polarity (Fig. 6; J. Stimack, 1999, personal commun.). This is consistent with the known position of the Bishop Ash in the paleomagnetic time scale, and indicates that the Matayama-Bruhnes boundary (780 ka) is <28 m below the Bishop Ash. More detailed sampling would be needed to accurately place this polarity reversal in the section.

Sedimentation rates are constrained by stratigraphic thicknesses and ages of the magnetic polarity reversal and two ashes (Fig. 6). The Matuyama-Brunhes reversal (780 ka) is <28 m below the Bishop Ash (760 ka), giving a maximum sedimentation rate of 1.4 mm/yr in this part of the section. The actual rate is probably less than this, and is uncertain due to large sample spacing. Assuming ~0.5–1.0 mm/yr sedimentation rate for the lower part of the section in Ash Wash, the base of the section is inferred to be ca. 0.9–1.0 Ma. The Thermal Canyon ash is 80 m above the Bishop ash, which records an increase in sedimentation rate to ~4 mm/yr. This rate is rapid but not unreasonable for an area of active fault controls on subsidence and sedimentation.

Age of Qg gravel

In most places the basal contact of Qg is an angular unconformity where it overlies older dipping Pleistocene sediments (Qbx and Qcs), or it is a nonconformity where it rests on crystalline basement rocks. One important exception to this is found in Ash Wash (Fig. 3) where Qg conformably overlies Qcs sandstone and conglomerate in the down-tilted part of a Pleistocene growth structure (described below). The age of Qg is not known from direct dating, but it can be inferred using the age of older deposits and the stratigraphic thickness from dated older deposits to the top of Qg. The conformable base of Qg is 120 m above the 740 ka Thermal Canyon Ash (Fig. 6), and its thickness ranges up to ~120–140 m in areas northwest and southeast of Ash Wash (Fig. 3). This gives a total thickness of ~250 m from the Thermal Canyon Ash to the top of Qg. Assuming a range of likely sedimentation rates (1–4 mm/yr), the possible duration of time represented by this thickness is ~60–250 k.y. The top of Qg is thus bracketed between 490 and 680 ka (rounded to ca. 600 ± 100 ka). Although Pleistocene climate variations are not well known in this area, it is likely that bracketing the sedimentation rate between 1 and 4 mm/yr encompasses the variations that might have occurred due to variations in rainfall and erosion rate.

Paleocurrents

Paleocurrent data were collected from Qcs and Qg units in the Coyote Badlands and lower Rockhouse Canyon (Figs. 6, 7). The data were obtained from imbricated clasts, crossbedding, current lineations, and channel axes, with the majority of measurements obtained from clast imbrications. Paleocurrents in Ash Wash and elsewhere in the Coyote Badlands (Fig. 6) show a systematic reversal through the section, from north-

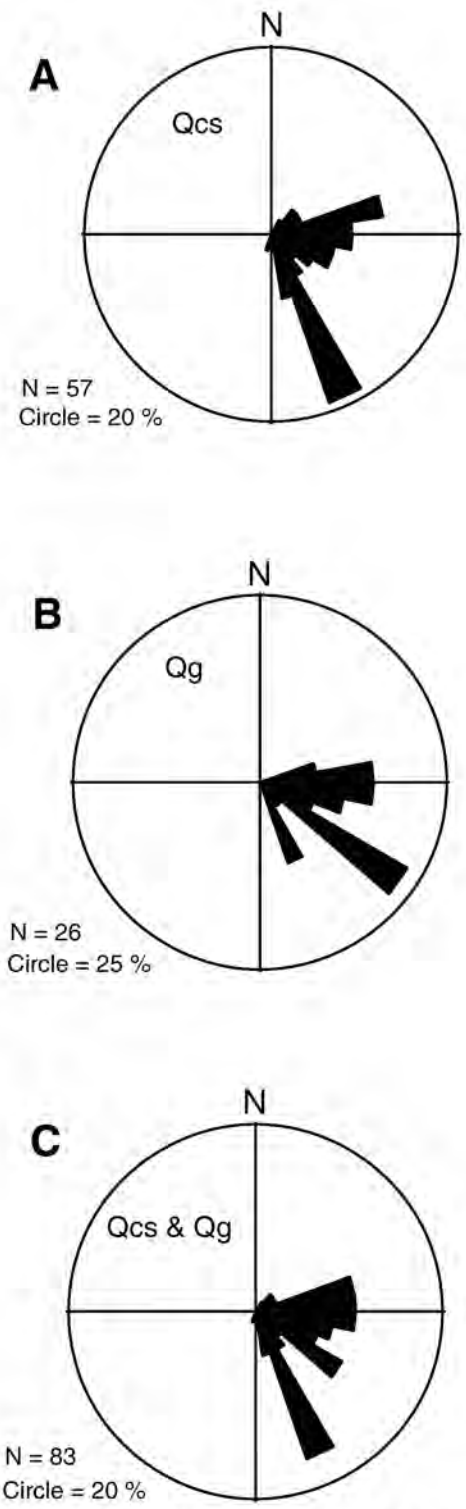

Figure 7. Paleocurrent data collected from clast imbrications in Qcs (A), Qg (B), and both units combined (C) in the lower Rockhouse Canyon area (LRC, Figure 3). The data show overall transport toward the east and southeast, with a bimodal distribution in the Qcs-only data. Paleocurrents record sediment dispersal to the southeast along the Clark fault valley, and to the east-northeast due to a component of northeastward tilting toward the Clark fault.

west-directed in lower Qcs to northeast- and then southeast-directed in upper Qcs and Qg. This change begins gradually below the Bishop Ash, and the main change occurs across the interval of fine-grained eolian and lacustrine deposits between 150 and 180 m (Fig 6). Northwest-directed paleocurrents in the lower part of the section are opposed to the overall direction of stream flow in modern Coyote Creek and its tributaries, but they are consistent with observed lateral fining of facies in lower Qcs from mainly conglomerate in the southeast to mainly sandstone in the northwest. In contrast to the Coyote Badlands, lower Qcs deposits in and around lower Rockhouse Canyon near the Clark fault show transport dominantly to the east and southeast, consistent with modern drainages in that area (Figs. 3, 7). This indicates that the Clark fault was active and formed a fault valley during deposition of Qcs, and continued to influence drainage patterns during Qg deposition. A prominent component of transport toward the east-northeast in Qcs (Fig. 7A) probably is due to northeastward tilting toward the Clark fault during this time.

Growth structures

Two sets of growth structures with different orientations are exposed in Ash Wash: (1) small northeast-striking normal faults low in the section (Fig. 8), and (2) a large northwest-striking fanning-dip section and progressive unconformity higher in the section (Figs. 6, 9).

In the lower part of the section, several growth faults strike northeast, dip northwest, and cut sedimentary units that show pronounced thickness changes and up-section decrease in offset across the faults (Fig. 8). The strike of bedding is slightly different than that of the faults, suggesting a component of strike-slip displacement, but the displacement geometries indicate that the faults record dominantly small-scale dip-slip (normal) offset. These faults are overlapped by probable late Pleistocene terrace gravel deposits set into the modern Ash Wash. Farther up section a normal fault with the same orientation cuts the Bishop Ash, lacks brittle fault features, and is filled with a sand dike injected by liquefaction from the lower part of the faulted ash deposit. These features record extensional or transtensional deformation on northeast striking, northwest dipping faults during deposition of the lower part of Qcs in Ash Wash. This orientation is similar to the northeast-striking normal fault that cuts Qbx breccia on the northwest side of Coyote Mountain (Figs. 2, 3), and they are interpreted to be genetically related.

The second growth structure occupies the upper part of the Ash Wash section (Figs. 6, 9). Figure 9 shows a systematic up-section decrease in bedding dips, from 43° in the lower part through 20° to subhorizontal in Qg (Fig. 9). The fanning-dip interval is capped by a progressive unconformity in which the contact itself changes laterally from a well-defined angular unconformity on the left (southwest) to a completely conformable contact on the right (northeast) (Fig. 9). The lateral change from unconformity to conformable contact takes place through a zone of complex lateral interfingering and onlapping. The fanning dips and progressive unconformity preserve a record of northeastward tilting, erosion, and sedimentation during deposition of upper Qcs and transition to Qg gravel. The fulcrum of tilting (neutral line) is located about half way between the Coyote Creek and Box Canyon faults (Fig. 3), and it is inferred that slip on these faults controlled syn-depositional tilting.

Because strike-slip offset on the Qg unit is equal to total

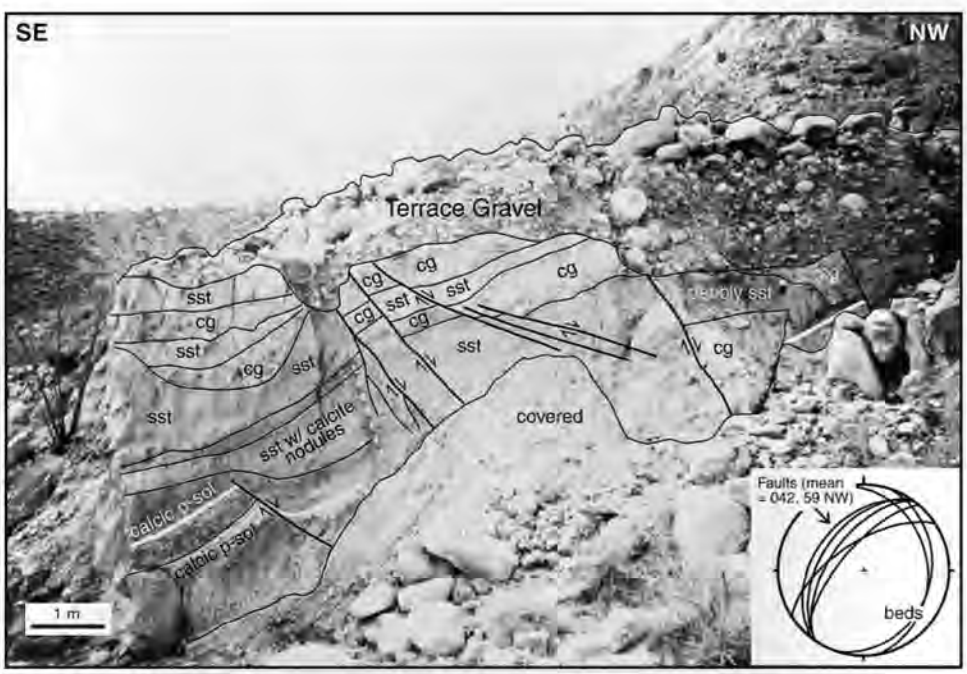

Figure 8. Close-up view of growth faults exposed in the lower part of Ash Wash section (Fig. 6), view looking southeast. Bold white line represents correlatable, offset calcic paleosol (p-sol) horizon. Note upward decrease in slip and draping of strata over fault on left side. Inset shows equal-area stereonet projection of faults and bedding planes in this exposure.

displacement on the Coyote Creek fault (Figs. 2, 10), the phase of tilting represented by fanning dips must predate the onset of strike-slip offset. This, combined with the lack of similarly oriented growth structures lower in the section and the position of the fulcrum of tilting, all support the interpretation that the fanning-dip structure records the earliest, initial phase of slip on the Coyote Creek and Box Canyon faults in the Coyote Badlands at 750 ka (Fig. 6). The derived sense of offset is dip-slip (normal), down on the southwest side of the bounding faults, with no evidence for strike-slip displacement during the initial phase of fault slip. A vertical component of displacement and northeastward tilting is further indicated for the Box Canyon fault by juxtaposition of thick sedimentary rocks southwest of the fault directly against Cretaceous plutonic rocks on the northeast side, progressive increase in thickness of Qcs to the northeast away from the fault (Fig. 3), and down-dip lineations in the fault zone (Fig. 4). Evidence for dip-slip offset on the Coyote Creek fault is seen in the large fault sliver of Cretaceous plutonic rock in lower Ash Wash, and the fact that the large area of stranded Qg gravel on the northeast side of the Coyote Creek fault sits ~120 m above the present elevation of its source valleys on the southwest side of the fault (Fig. 3).

INTERPRETATION OF VERTICAL TRENDS

The above information provides insights into the evolution of depositional environments, sediment-dispersal patterns, subsidence rates, and surface deformation during Pleistocene faulting and sedimentation. Deposition of Qbx may have resulted from movement on the Santa Rosa and west Coyote Mountain faults, prior to displacement on the Clark fault, but the timing and controls on this early phase of sedimentation are not well understood. The lower part of Qcs in lower Rockhouse Canyon was deposited in a southeast-flowing valley, providing evidence that the Clark fault was initiated sometime prior to Qcs deposition. The up-section reversal of paleocurrents in Ash Wash, from northwest- to southeast-directed, can be understood in the context of regional structural controls on geomorphology and stream evolution in the San Jacinto fault zone. Initiation of the Clark fault at ca. 1.5 Ma is believed to have breached the former Peninsular Ranges divide and created steep new drainages that flowed southeast to the Salton Sea, causing reorganization of the regional stream system and widespread drainage reversals that are still active today (Dorsey and Ryter, 2000; Dorsey, 2001). The reversal in paleocurrents at Ash Wash is believed to be part of these regional stream captures, and is related to the complex evolution of drainages as controlled by slip on the Clark and Coyote Creek faults (see below).

Figure 6 shows that very rapid sedimentation (~4 mm/yr) coincided with a reversal in paleocurrent directions, onset of northeastward tilting, and deposition of the finest-grained sediments in the section. The synchronous occurrence of these changes suggests that they are genetically related, and are interpreted to record initiation of dip-slip movement on the Coy-

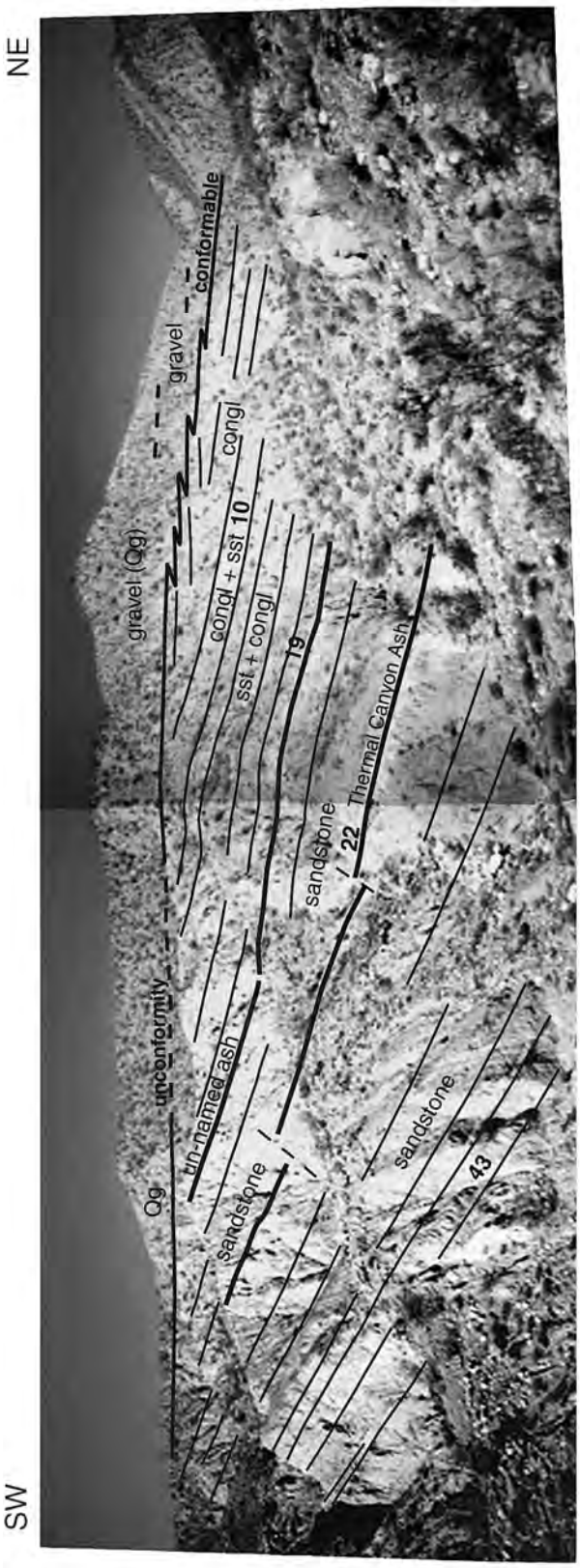

Figure 9. Photomosaic with interpretation of fanning-dip section and progressive unconformity in upper Ash Wash. This growth structure records initiation of the Coyote Creek and Box Canyon faults by dip-slip (normal) displacement and syndepositional tilting to the northeast. Congl—conglomerate, sst—sandstone. See Figure 3 for location and Figure 6 for stratigraphic position.

ote Creek and Box Canyon faults. Rapid production of accommodation space by fault slip temporarily trapped coarse detritus in a small area of subsidence close to the Box Canyon fault, causing development of a small lake basin with limited input of fine-grained eolian sand and silt. Northwest-flowing streams that formerly were connected to a larger, west flowing regional stream system were captured by streams flowing southeast along the Clark fault, probably due to this faulting episode. A new source area located to the northwest along the present-day Coyote Creek supplied a large volume of coarse gravel, possibly reworked from older deposits, which quickly filled the small lacustrine depocenter with a prograding boulder-rich alluvial fan. This situation probably resembled the modern advance of the bouldery Rockhouse fan into the northwest corner of Clark Valley (Fig. 3).

COYOTE CREEK FAULT RECONSTRUCTION

Restoration of strike-slip offset

In order to interpret the history of fault slip, it is useful to restore total strike-slip offset on the Coyote Creek fault. The reconstruction is produced by correlating the western contact of mylonite across the Coyote Creek fault, from Coyote Mountain on the northeast side to the eastern San Ysidro Mountains on the southwest (Figs. 2, 3, 10). The age of this reconstruction coincides with the end of Qg deposition, which is uncertain but is bracketed between ca. 500 and 700 ka (see above). There is some uncertainty in the amount of strike-slip offset because the mylonite contact with plutonic and metamorphic rocks is not exposed immediately adjacent to the Coyote Creek fault on the southwest side of the fault, and therefore is projected northward beneath alluvium in northern Borrego Valley (Figs. 2, 10). The mylonite contact trends approximately due north at Coyote Mountain and ~020° in the eastern San Ysidro Mountains, and it probably does not vary significantly from this trend where it is covered. Accounting for these uncertainties, ~6 km of right lateral offset is measured on the Coyote Creek fault. It is difficult to quantify the uncertainty in this measurement, but the error is probably ~0.5–1 km.

Because the mylonite dips to the east, any southwest-side-down offset on the Coyote Creek fault due to northeastward tilting would produce a component of apparent right-lateral separation that is not due to strike-slip offset. The importance of

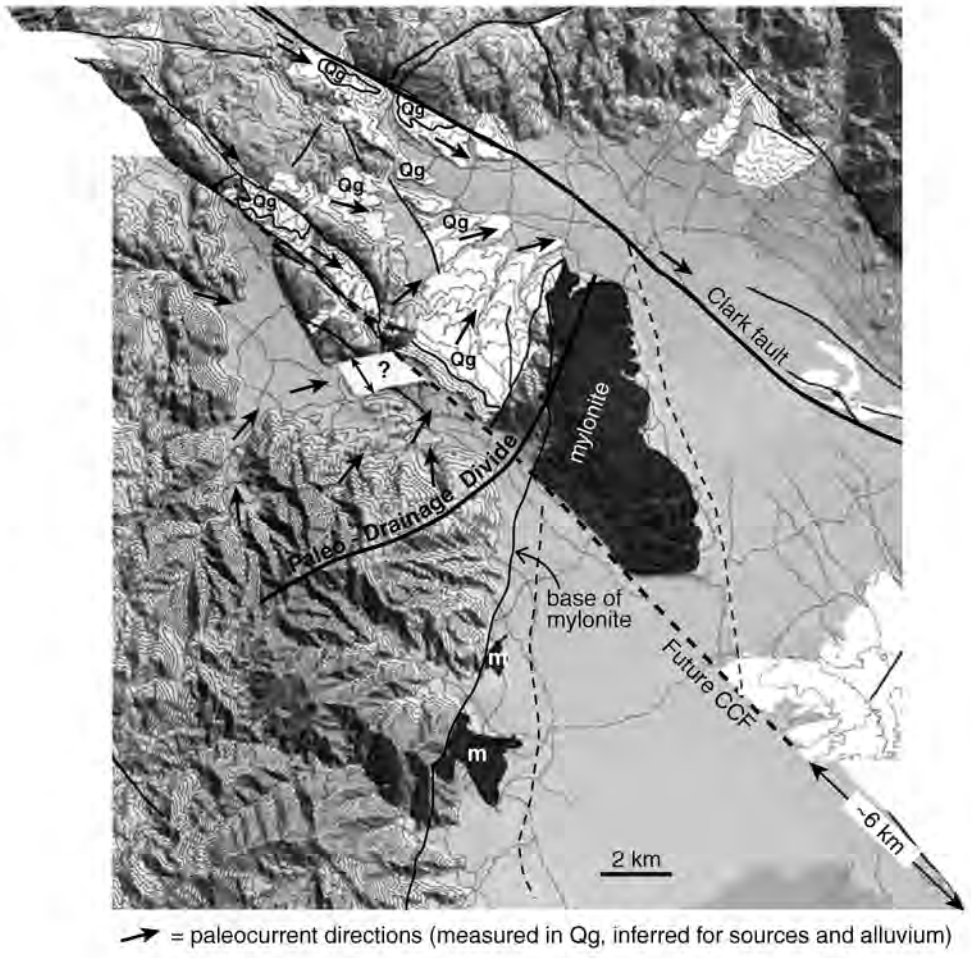

Figure 10. Reconstruction of Coyote Creek fault (CCF) during Qg deposition, prior to onset of strike-slip displacement on the fault. Restores strike-slip displacement only, and does not restore vertical fault offsets or surface erosion. Position of paleo-drainage divide is based on measured paleocurrent directions and inferred sources for Qg gravel.

this effect can be evaluated by comparing fault offset measured on the mylonite with that of displaced Quaternary deposits. Geomorphic and geologic maps, clast compositions, and paleocurrents all show that Qg gravel was derived from northeast-draining streams located in the northern San Ysidro Mountains (Figs. 2, 3, 10). Restoration of ~6 km of strike-slip offset on the Coyote Creek fault restores a wide area of Qg downstream from that source, with the southeast margin of Qg located slightly southeast of the easternmost feeder channel (Fig. 10). This pattern is consistent with downstream widening of the channel that is expected for catchments and alluvial fans. Thus, the total strike-slip offset on Qg is virtually the same as offset measured on the bedrock contact between mylonite and plutonic rocks. Although there is evidence for some dip-slip displacement of Qg on the Coyote Creek fault (~100–150 m), and probably somewhat more on older sediments and bedrock, it is not enough to produce a large artificial component of apparent strike-slip separation on the fault.

The timing and average rate of slip can be estimated from the above information. Strike-slip offset on the Coyote Creek fault began sometime after deposition of Qg. Thus, total offset of ~6.0 ± 1 km since 600 ± 100 ka gives a time-averaged slip rate of ~10 ± 3 mm/yr. The reconstruction in Figure 10 shows that, prior to strike-slip offset on the Coyote Creek fault, high topography in Coyote Mountain and the San Ysidro Mountains formed a drainage divide that controlled sediment transport. Qg gravel preserved on the gently northeast-dipping slope west of Coyote Mountain was derived from the northern San Ysidro Mountains and transported northeastward into Clark Valley. North and northwest of this slope of Qg, in the area of lower Rockhouse Canyon, paleocurrent data show that Qg sediment was transported toward the east and southeast (Figs. 7, 10) indicating that the Clark fault was active during this time.

Fault-slip and sedimentation history

Using data and explanations presented above, it is possible to reconstruct the history of sedimentation as controlled by faulting in the Coyote Badlands and surrounding areas (Fig. 11). Deposition of the oldest sediments in the Coyote Badlands (lower Qcs, pre–760 ka) took place prior to initiation of the Coyote Creek fault (Fig. 11A). Sediment derived from the northern San Ysidro Mountains was transported along two pathways: (1) northwest through what is now the Coyote Badlands, and (2) northeast into Clark Valley and then southeast along the Clark fault. The northwest-flowing streams are believed to be a remnant of a regional stream system that flowed to the west off the high Santa Rosa and San Jacinto Mountains prior to initiation of the San Jacinto fault zone (Dorsey and Ryter, 2000; Dorsey, 2001). By ca. 800 ka the former regional stream network had been partially disrupted by stream captures resulting from early slip on the Clark fault, producing the complex paleocurrent patterns shown in Figure 11A. Gravel was transported southeast along the Clark fault (Fig. 7) and into the Borrego Badlands where it is represented by the Ocotillo Formation. The Borrego Badlands may have been a subsiding pull-apart basin during this time, but the evidence for that hypothesis is inconclusive (see Discussion).

By ca. 600 ka several significant changes had occurred: (1) the Coyote Creek and Box Canyon faults were initiated by dip-slip normal offset, as recorded in the fanning dip section and progressive unconformity in Ash Wash, (2) streams in the Coyote Badlands had reversed direction and now flowed to the southeast, and (3) southeast-flowing streams in the Coyote Badlands turned and flowed northeast into Clark Valley where they joined the active Clark fault (Fig. 10, 11B).

By ca. 400 ka (Fig. 11C), early strike-slip offset on the Coyote Creek fault had breached the drainage divide that formerly connected Coyote Mountain to the San Ysidro Mountains. This created a new fault valley that flowed southeast into Borrego Valley and established the modern drainage pattern. Broad uplift and northeastward tilting of Qg on the northeast side of the fault, combined with strike-slip displacement away from its source in the San Ysidro Mountains, caused a large area of previous Qg deposition to be abandoned and eroded. Clark Valley had probably become a closed depression by this time, but the timing of that transition is not well known. Figure 11D shows the modern geomorphology and present stage of fault-zone development.

DISCUSSION

The data and reconstructions presented above provide new insights into the history of initiation and subsequent slip on the Coyote Creek fault in the lower Coyote Creek area, but the relationship of these events to evolution of the San Jacinto fault zone at the regional scale remains uncertain. This uncertainty is represented by two structural models that are mutually exclusive but appear to be equally supported and contradicted by existing data. In the first hypothesis, the southern Coyote Creek fault (southeast of the Borrego Badlands; Figs. 1, 2) is the same age as the Clark fault and was connected to the Clark fault via a normal fault on the east side of Coyote Mountain prior to ca. 600 ka (e.g., Bartholomew, 1970; Fig. 11A, B). In this model, Pleistocene sedimentary rocks exposed in the Borrego Badlands were deposited in a pull-apart basin, and initiation of the Coyote Badlands strand represents northwestward propagation of the Coyote Creek fault, transfer of slip from the Clark fault to the Coyote Creek fault, and straightening of the San Jacinto fault zone which continues today. In the second hypothesis, the whole Coyote Creek fault was initiated along most or all of its length at the same time as the Coyote Badlands strand, at ca. 600 ± 100 ka. In either case, I infer that the old normal faults on the east side of Coyote Mountain and the San Ysidro Mountains, and the associated linear gravity lows seen in the flanking modern valleys (Bartholomew, 1970), represent dissected remnants of the breakaway of a regional low-angle normal fault (detachment) system that was active in the western Salton

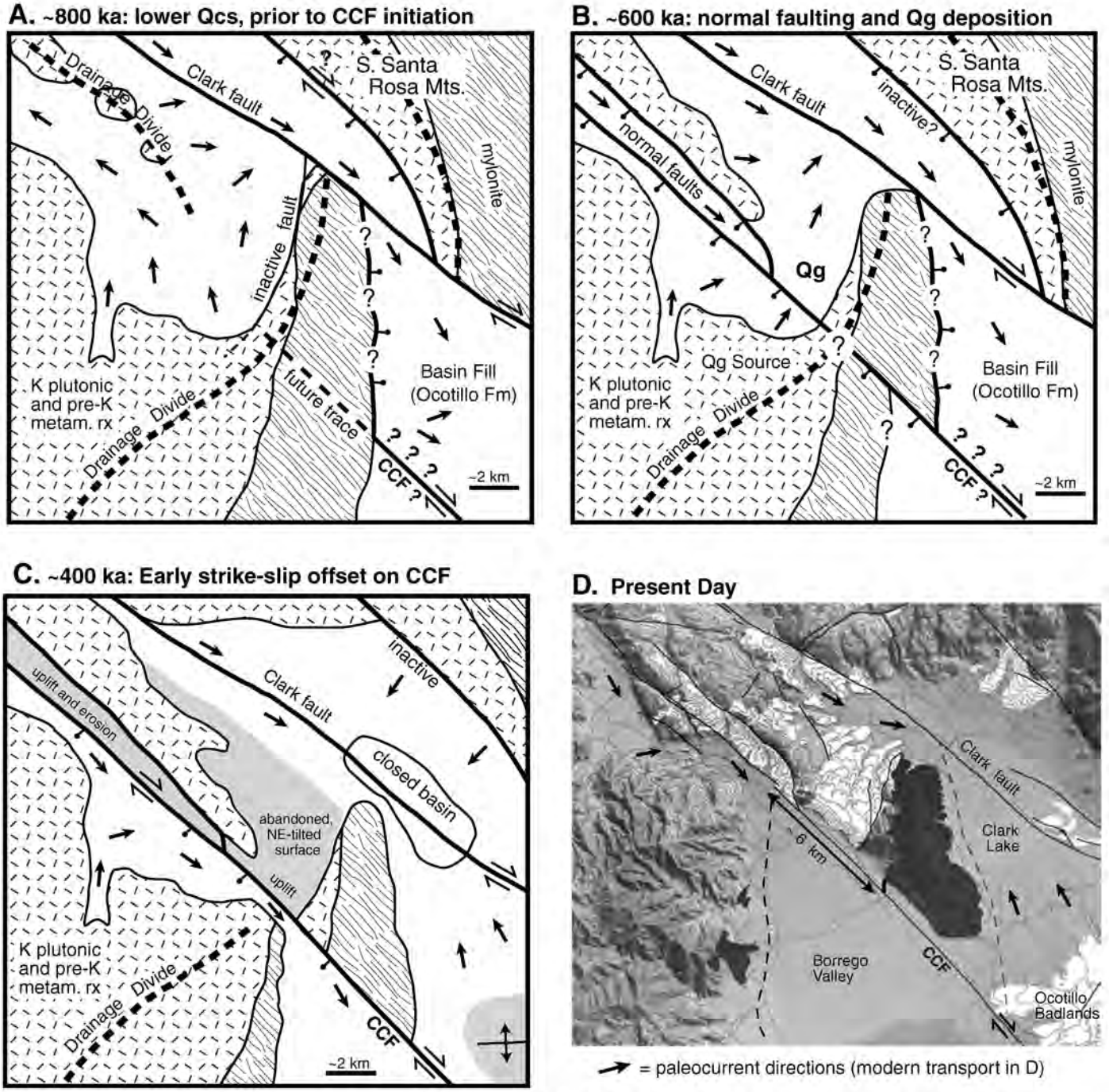

Figure 11. Four-stage reconstruction of the Coyote Creek fault (CCF) and adjacent areas since ca. 800 ka. A: Prior to initiation of the CCF (ca. 800 ka), lower Qcs sand and gravel were deposited in a complex setting that included both inherited (northwest-flowing) and young (southeast-flowing) streams. B: By 600 ka, prior to strike-slip displacement on the CCF, the Coyote Creek and Box Canyon faults had been initiated by dip-slip normal offset. Sediment transport in the Coyote Badlands had reversed, and Qg gravel accumulated in a large alluvial fan system that drained to the Clark fault valley. C: Early strike-slip offset on the CCF resulted in breaching of the former drainage divide and initiation of sediment transport to the southeast along the fault; northeastward tilting and abandonment of Qg gravel on Coyote Ridge; and onset of folding in the Ocotillo Badlands. D: Present-day setting shows active faulting controls on modern topography and streams. Paleocurrent data used to reconstruct sediment-dispersal patterns are shown in Figures 6 and 7.

Trough from late Miocene to early Pleistocene time (Axen and Fletcher, 1998). In the following section, I briefly summarize the evidence for and against these two hypotheses and discuss their regional tectonic implications.

The fault-jog (pull-apart basin) hypothesis is supported by (1) the large thickness of Pleistocene sedimentary rocks in the Borrego Badlands compared to areas southwest of the Coyote Creek fault (Dibblee, 1954, 1984), (2) the short distance over which the Clark fault dies out to the southeast into deformed Pleistocene strata (Fig. 2), and (3) the geometry of the Coyote Creek fault, which is favorably oriented to simplify and straighten the San Jacinto fault zone through time (Figs. 1, 2; cf. Wesnousky, 1988; Zhang et al., 1989). The fault-jog hypothesis is contradicted by (1) apparent lack of unconformities in the thick sedimentary section exposed in and south of the Borrego Badlands, which should form during creation of a pull-apart basin due to strike-slip faulting, (2) widespread regional distribution of the Ocotillo Formation, which should be restricted to the Borrego Badlands if it accumulated in a localized pull-apart basin, (3) subdued morphology and apparent old age of the normal fault on the east side of Coyote Mountain, and its likely correlation to the old fault on the west side of Borrego Valley (Fig. 2), (4) probable similarity of offset (~6 km) on the Coyote Creek fault northwest and southeast of the Borrego Badlands, although this is not well constrained, and (5) presence of abundant fresh fault scarps, shutter ridges, and offset stream channels along the Clark fault, suggesting that it has been at least as active as the Coyote Creek fault during late Pleistocene and Holocene time. If the fault-jog hypothesis is not correct, then the southern Coyote Creek fault does not share an older slip history with the Clark fault and instead was initiated along most or all of its length at ca. 600 ± 100 ka. It is beyond the scope of this paper to attempt a full presentation of data for and against the fault-jog hypothesis, but it appears from this summary that the question presently is unresolved.

The only widespread coarse-grained clastic unit in the western Salton Trough (Fig. 1) is the Ocotillo Formation, which ranges in age from 1.2 to ca. 0.6 Ma (Remeika and Beske-Diehl, 1996; Dibblee, 1954). The base of the Ocotillo (1.2 Ma) has recently been interpreted to represent a large pulse of sediment that prograded into the basin in response to initiation of the Clark fault and a related history of regional stream captures in the Peninsular Ranges (Dorsey and Ryter, 2000; Dorsey, 2001). The lag time between fault initiation and arrival of coarse sediment in the Borrego Badlands is difficult to determine and may plausibly range from ~100–500 k.y. Given the existing uncertainties, initiation of the Clark fault (and thus the San Jacinto fault zone) is tentatively estimated to be ca. 1.5 ± 0.2 Ma. Combining this age estimate with total slip of 22–24 km on the San Jacinto fault zone (Sharp, 1967) yields a time-averaged slip rate of ~13–18 mm/yr. This is only slightly faster than the late Pleistocene slip rate (13 mm/yr) favored by Rockwell et al. (1990) near Anza, where large uncertainties exist due to the difficulty of estimating absolute ages from soil chronology, and is consistent with an estimate of 15 ± 3 mm/yr determined from paleoseismology in the Anza area (Merifield et al., 1989).

The two hypotheses described above have different implications for the history of strike-slip faulting and basin evolution in the western Salton Trough. If the fault-jog hypothesis is correct, it implies that the southern Coyote Creek fault shares an older slip history with the Clark fault and that both were initiated ca. 1.5 Ma, or possibly earlier. In this case, initiation of the Coyote Badlands strand of the Coyote Creek fault would represent a relatively minor straightening and reorganization of the San Jacinto fault zone. Alternatively, if the Coyote Creek was initiated along most of its length at ca. 600 ka, early slip on the Clark fault may have been accommodated by growth of contractional folds and faults in the San Felipe Hills, southeast of the Borrego Badlands (Feragen, 1986; Wells, 1986). In this reconstruction, north-south shortening in the San Felipe Hills occurred in a large restraining step-over between the Clark and Imperial faults, and increasing resistance to transpressional deformation may have caused initiation of the Coyote Creek fault at ca. 600 ka (Ryter and Dorsey, 2002). In a possible hybrid of these hypotheses, pre–600 ka slip on the Clark fault may have been linked to now-inactive faults on the northeast margin of the Fish Creek and Vallecito Mountains (Dibblee, 1954) in a releasing-bend geometry that was terminated by initiation of the modern Coyote Creek, Superstition Mountain, and Superstition Hills faults. These models make a number of testable predictions about stratigraphic and structural relationships in the western Salton Trough, and highlight the need for future studies of the geologic evolution of the San Jacinto fault zone in this region.

CONCLUSIONS

The Pleistocene history of initiation and slip on the Coyote Badlands strand of the Coyote Creek fault, central San Jacinto fault zone, is recorded in thick sedimentary deposits, active faults, and geomorphology of the lower Coyote Creek area. Sedimentary units include tonalite-clast breccia (Qbx), conglomerate and sandstone (Qcs) and weakly consolidated boulder-bearing gravel (Qg). The age of the deposits is known from the presence of the Bishop Ash (760 ka) and Thermal Canyon Ash (740 ka) interbedded in the Qcs units. Qbx and Qg were deposited in alluvial fan environments, and Qcs accumulated in a sandy fluvial setting that was punctuated in the Coyote Badlands by formation of a short-lived shallow lake or mudflat with fringing eolian dunes.

The upper part of Qcs contains a large growth structure comprising a thick section of fanning dips and progressive unconformity, which records initiation of the Coyote Creek and Box Canyon faults by dip-slip (normal) displacement beginning at 750 ka. Qg gravel conformably overlies the growth structure, and its top (~250 m above the Thermal Canyon Ash) is inferred to be ca. 600 ± 100 ka. Offset of Qg is equal to the total strike-slip displacement (~6 km) on the Coyote Creek fault. There-

fore, all strike-slip motion on the Coyote Creek fault in the study area has occurred since ca. 600 ka, and the time-averaged slip rate is ~10 mm/yr. The relation of these events to the regional evolution of the San Jacinto fault zone remains uncertain.

ACKNOWLEDGMENTS

Funding for this study was provided by the National Science Foundation (EAR-9805794). The author gratefully acknowledges support and collecting permits from the Anza Borrego Desert State Park of California. George Jefferson is thanked for years of logistical and moral support. John Stimack and Ray Weldon assisted with the paleomagnetic study; Derek Ryter provided minor additions to the geologic map and assisted with GIS image analysis. Discussions with Derek Ryter, George Jefferson, Susanne Janecke, Tom Rockwell, and Ray Weldon provided valuable insights and motivation during the course of this study. Steve Graham, Karen Grove, George Jefferson, and Andy Barth are thanked for constructive reviews of the manuscript.

REFERENCES CITED

Albright, L.B., III, 1999, Magnetostratigraphy and biochronology of the San Timoteo Badlands, Southern California, with implications for local Pliocene-Pleistocene tectonic and depositional patterns: Geological Society of America Bulletin, v. 111, p. 1265–1293.

Axen, G.J., and Fletcher, J.M., 1998, late Miocene–Pleistocene extensional faulting, northern Gulf of California, Mexico and Salton Trough, California: International Geology Review, v. 40, p. 217–244.

Bartholomew, M.J., 1970, San Jacinto fault zone in the northern Imperial valley, California: Geological Society of America Bulletin, v. 81, p. 3161–3166.

Bennett, R.A., Rodi, W., Reilinger, R.E., 1996, Global Positioning System constraints on fault slip rates in Southern California and northern Baja, Mexico: Journal of Geophysical Research, v. 101, p. 21943–21960.

Blair, T.C., and McPherson, J.G., 1994, Alluvial fans and their natural distinction from rivers based on morphology, hydraulic processes, sedimentary processes, and facies assemblages: Journal of Sedimentary Research, v. 64, p. 450–489.

DeMets, C., 1995, Reappraisal of seafloor spreading lineations in the Gulf of California: Implications for the transfer of Baja California to the Pacific plate and estimates of Pacific-North America motion: Geophysical Research Letters, v. 22, p. 3545–3548.

DeMets, C., Gordon, R.G., Argus, D.F., Stein, S., 1994, Effect of recent revisions to the geomagnetic reversal time scale on estimates of current plate motions: Geophysical Research Letters, v. 21, p. 2191–2194.

dePolo, C.M., and Anderson, J.G., 2000, Estimating the slip rates of normal faults in the Great Basin, USA: Basin Research, v. 12, p. 227–240.

Dibblee, T.W., Jr., 1954, Geology of the Imperial Valley region, California, *in* Jahns, R.H., ed., Geology of southern California: California Division of Mines Bulletin 170, p. 21–28.

Dibblee, T.W., 1984, Stratigraphy and tectonics of the San Felipe Hills, Borrego Badlands, Superstition Hills and vicinity, *in* Rigsby, C.A., ed., The Imperial Basin: Tectonics, sedimentation and thermal aspects: Los Angeles, California, Pacific Section Society of Economic Paleontologists and Mineralogists Field Trip Guidebook, v. 40, p. 31–44.

Dorsey, R.J., 2001, Two-stage evolution of the San Jacinto fault zone: Crustal response to Pleistocene oblique collision along the San Andreas fault: Eos (Transactions, American Geophysical Union), v. 82, p. F933.

Dorsey, R.J., and Ryter, D.W., 2000, Stratigraphic and geomorphic evidence for Pleistocene initiation of the San Jacinto fault zone: Eos (Transactions, American Geophysical Union), v. 81, p. 1141–1142.

Feragen, E.S., 1986, Geology of the southeastern San Felipe Hills, Imperial Valley, California [M.Sc. thesis]: San Diego, California, San Diego State University, 144 p.

Frick, C., 1921, Extinct vertebrate faunas of the Badlands of Bautista Creek and San Timoteo Canyon, southern California: California University, Department of Geology Bulletin, v. 12, p. 277–424.

Hill, R.I., 1984, Petrology and petrogenesis of batholithic rocks, San Jacinto Mountains, Southern California [Ph.D. thesis]: Pasadena, California, California Institute of Technology, 731 p.

Humphreys, E.D., and Weldon, R.J., 1994, Deformation across the western United States: A local estimate of Pacific-North America transform deformation: Journal of Geophysical Research, v. 99, p. 19975–20010.

Kendrick, K., McFadden, L., Morton, D., 1994, Soils and slip rates along the northern San Jacinto fault, *in* McGill, S.F., and Ross, T.M., eds., Geological investigations of an active margin: Geological Society of America, Cordilleran Section Annual Meeting Field trip Guidebook., v. 27, p. 146–151.

Matti, J.C., Morton, D.M., and Cox, B.F., 1992, The San Andreas fault system in the vicinity of the central Transverse Ranges province, Southern California: U.S. Geological Survey Open-File Report OF 92-0354.

Merifield, P.M., Rockwell, T.K., Loughman, C.C., and Klinger, R.E., 1989, Study of seismic activity by selective trenching along the San Jacinto fault zone, southern California: U.S. Geological Survey, Final Technical Report 89-1, 24 p.

Miall, A.D., 1996, The geology of fluvial deposits: Sedimentary facies, basin analysis, and petroleum geology: Berlin, New York, Springer-Verlag, 582 p.

Morton, D.M., and Matti, J.C., 1993, Extension and contraction within an evolving divergent strike-slip fault complex: The San Andreas and San Jacinto fault zones at their convergence in Southern California, *in* Powell, R.E., et al., eds., The San Andreas fault system: Displacement, palinspastic reconstruction, and geologic evolution: Boulder, Colorado, Geological Society of America Memoir 178, p. 217–230.

Remeika, P., and Beske-Diehl, S., 1996, Magnetostratigraphy of the western Borrego Badlands, Anza-Borrego Desert State Park, California: Implications for stratigraphic age control, *in* Abbott, P.L., and Seymour, D.C., eds., Sturzstroms and detachment faults, Anza-Borrego Desert State Park, California: South Coast Geological Society Annual Field Trip Guidebook, no. 24, p. 209–220.

Retallack, G.J., 1990, Soils of the past: Boston, Massachusetts, Unwin Hyman, 520 p.

Revenaugh, J., 1998, Seismic estimation of cumulative offset on the San Jacinto fault zone: Eos (Transactions, American Geophysical Union), v. 79, p. F593.

Rockwell, T., Loughman, C., Merifield, P., 1990, late Quaternary rate of slip along the San Jacinto fault zone near Anza, Southern California: Journal of Geophysical Research, v. 95, p. 8593–8605.

Ryter, D.W., and Dorsey, R.J., 2000, Quaternary tectonic evolution of the central San Jacinto fault zone, southern California: Geological Society of America Abstracts with Programs, v. 34, no. 5, p. 86.

Sanders, C., and Magistrale, H., 1997, Segmentation of the northern San Jacinto fault zone, Southern California: Journal of Geophysical Research, v. 102, p. 27453–27467.

Sanders, C.O., 1989, Fault segmentation and earthquake occurrence in the strike-slip San Jacinto fault zone, California, *in* Schwartz, D.P., and Sibson, R.H., eds., Proceedings of Conference XLV, Workshop on fault segmentation and controls of rupture initiation and termination: U.S. Geological Survey Open-File Report, OF 89-0315, p. 324–349.

Sarna-Wojcicki, A.M., Bowman, H.W., Meyer, C.E., Russell, P.C., Asaro, F.,

Michael, H., Rowe, J.J., Baedecker, P.A., and McCoy, G., 1980, Chemical analyses, correlations, and ages of late Cenozoic tephra units of East-central and southern California: U.S. Geological Survey Open File Report, OF 80-231, 57 p.

Sarna-Wojcicki, A.M., Meyer, C.E., and Wan, E., 1997, Age and correlation of tephra layers, position of the Matuyama-Brunhes chron boundary, and effects of Bishop Ash eruption on Owens Lake, as determined from drill hole OL-92, southeast California, *in* Smith, G.I., and Bischoff, J.L., eds., An 800,000-year paleoclimatic record from core OL-92, Owens Lake, southeast California: Boulder, Colorado, Geological Society of America Special Paper, v. 317, p. 79–90.

Sarna-Wojcicki, A.M., Pringle, M.S., and Wijbrans, J., 2000, New $^{40}Ar/^{39}Ar$ age of the Bishop Tuff from multiple sites and sediment rate calibration for the Matuyama-Brunhes boundary: Journal of Geophysical Research, v. 105, p. 21431–21443.

Sharp, R.V., 1967, San Jacinto fault zone in the Peninsular Ranges of Southern California: Geological Society of America Bulletin, v. 78, p. 705–729.

Sharp, R.V., 1975, En echelon fault patterns of the San Jacinto fault zone, *in* Crowell, J.C., ed., San Andreas fault in southern California: A guide to San Andreas fault from Mexico to Carrizo Plain: Sacramento, California, Special Report, California Division of Mines and Geology, v. 118, p. 147–152.

Sharp, R.V., 1981, Variable rates of late Quaternary strike slip on the San Jacinto fault zone, Southern California, Journal of Geophysical Research, v. 86, p. 1754–1762.

Walker, R.G., and Cant, D.J., 1984, Sandy fluvial systems, *in* Walker, R.G., ed., Facies models: Waterloo, Geoscience Canada Reprint Series (2nd Edition), p. 71–89.

Weldon, R.J., and Humphreys, E., 1986, A kinematic model of southern California: Tectonics, v. 5, p. 33–48.

Weldon, R.J., and Sieh, K.E., 1985, Holocene rate of slip and tentative recurrence interval for large earthquakes on the San Andreas fault, Cajon Pass, southern California: Geological Society of America Bulletin, v. 96, p. 793–812.

Wells, D.L., 1987, Geology of the eastern San Felipe Hills, Imperial Valley, California: Implications for wrench faulting in the southern San Jacinto fault zone [M.Sc. thesis]: San Diego, California, San Diego State University, 140 p.

Wesnousky, S.G., 1986, Earthquakes, Quaternary faults, and seismic hazard in California: Journal of Geophysical Research, v. 91, p. 12587–12631.

Wesnousky, S.G., 1988, Seismological and structural evolution of strike-slip faults: Nature, v. 335, p. 340–343.

Zhang, P., Burchfiel, B.C., Chen S., Deng Q., 1989, Extinction of pull-apart basins: Geology, v. 17, p. 814–817.

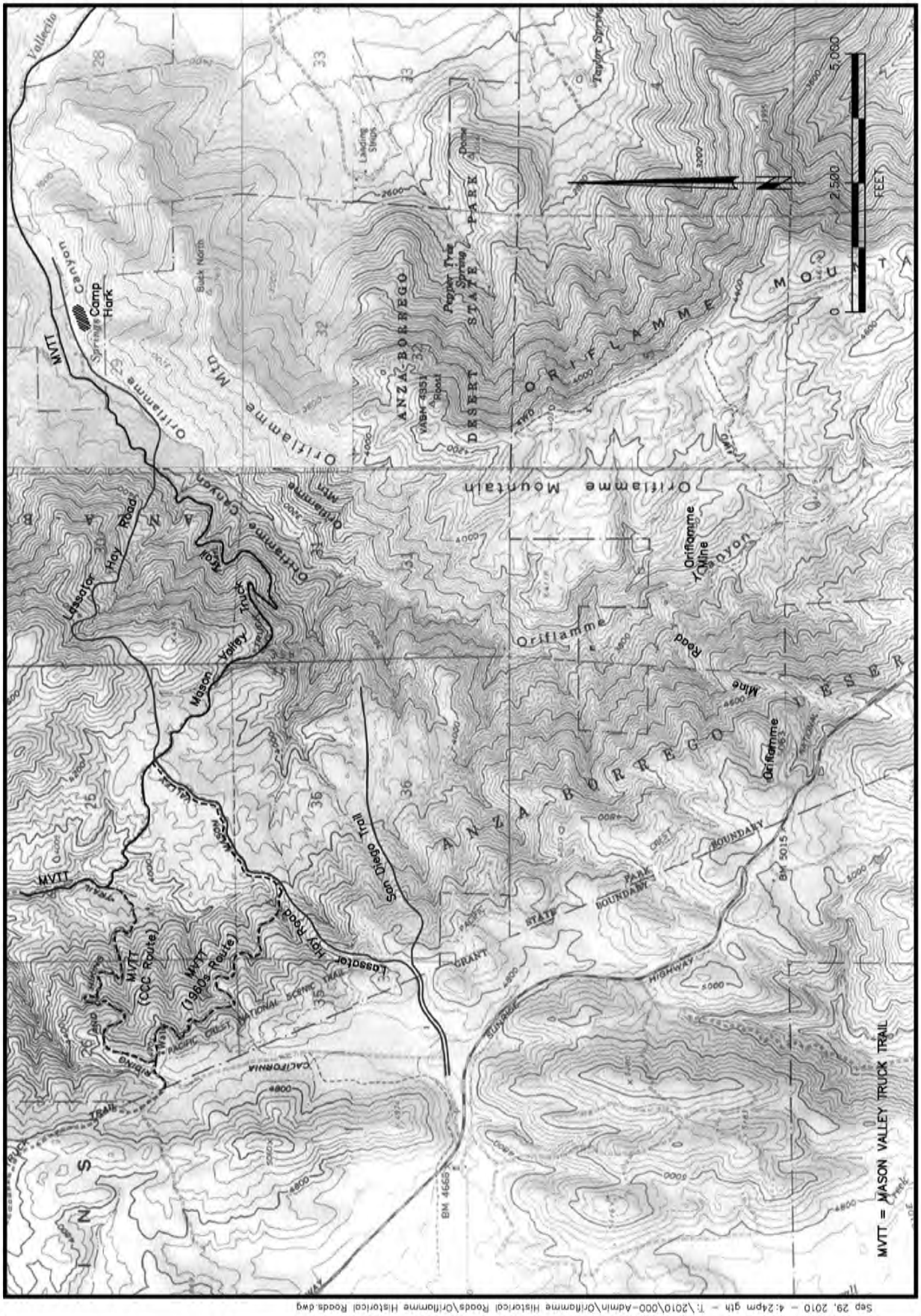

HISTORIC ROADS OF ORIFLAMME CANYON

The Oriflamme Canyon Travel Route and Lassator Hay Road

Chris Wray
Terra Blanca Books
TerraBlancaBooks.com

Author's note: I spell James Lassator's name with the two "A's" because he signed it that way. Most historians spell it Lassitor, which does not date from his time.

The level valley at the head of Chariot Canyon offers a geographic stair step in the steep slopes leading from the edge of the Cuyamaca meadows down into the desert below. Most routes between mountains and desert require a steep climb in a few miles with no natural breaks to lengthen the route and lessen the steepness. The appealing Oriflamme Canyon Route was used for centuries by Native Americans traveling between seasonal camps in the mountains and desert. It was their heavily worn trail that no doubt was seen by the first European explorers and became an important travel route during later years.

The first European to report using the trail was Pedro Fages, probably in his 1772 expeditions, and certainly by his 1782 trip, when he writes in his journal of the route. Fages was exploring the backcountry rounding up deserters from the San Diego Mission—both local natives who had fled to the hills, and his own men who sought relief from his notoriously dominant ways. Fages traveled from the desert to Cuyamaca using the Indian trail several times and became quite familiar with the region.

After Fages departed the scene, the local natives used the trail continuously through the 1800s. During the Gold Rush years of 1849-1850 some travelers left the main Southern Overland Trail in Mason Valley and used Rodriguez Canyon, the next canyon to the north of Oriflamme, a shortcut to Banner is and over the mountains to Santa Ysabel. The Rodriguez Route was also only a horse or mule trail until a much later date.

During the first American years in California, the military in San Diego needed to communicate with Fort Yuma, established at an important crossing on the Colorado River. Pioneering backcountry ranchers Joe Swycaffer and Sam Warnock held the mail contract to Fort Yuma. Although the men used various routes through the mountains from 1854-1857, they liked the Oriflamme Canyon Route because it led quickly down to the main Southern Overland Trail in Mason Valley. The name San Diego Trail was used for this mule and horse route up Oriflamme and through Cuyamaca. The winding route was never improved for wheeled vehicles, however.

Also in the year 1854, while Warnock and Swycaffer were carrying the military mail to Fort Yuma, James Lassator appeared on the scene and began operating the stage station at Vallecito. Lassator and his family settled in Cuyamaca's Green Valley where they built a small house, raised barley and feed for animal teams, and cut firewood. Initially, Lassator had a tough haul getting his feed and wood from Cuyamaca down to Vallecito, which although not a long straight line distance, required driving a wagon all the way to the Warner's Ranch area and following the main emigrant trail into the desert.

In 1857 Lassator's supply business took on new importance. James Birch was granted the first overland mail contract which designated a route from San Antonio, Texas to San Diego. The Birch Mail had two ways to reach the coast from the desert. Stage coaches required the typical journey up the Southern Overland Trail to Warner's and through Santa Ysabel toward San Diego. To shorten the route, and hasten the mail delivery, Birch and his field superintendant Isaiah Woods chose to use the Oriflamme Canyon Route to Lassator's ranch in Green Valley. This required both the mail, and any passengers willing to make the journey, to change from stages at Vallecito and use mules to cross to the mountains to Green Valley. Once at Lassator's the passengers and mail were again returned to a stage to complete their journey. This mule-bound leg of the journey caused one San Francisco journalist to dub the line the "Jackass Mail," a name that has stuck ever since, even though a mule is not a jackass.

Lassator decided to build a road to Vallecito since he now had a steady customer at Vallecito and needed to get his feed and wood down the hill in a faster way. The overland mail company hoped his new road would be suitable for stages as well, and offer them a wonderful shortcut across the mountains. Once Lassator began building his road, however, any plans for stage travel were quickly put to rest. To make the road feasible Lassator had to build it with such an excessive slope that traveling down it with his loaded freight wagon meant driving the wagon onto skids and sliding down the hills. The road Lassator built was incredibly steep; in fact, it is difficult to even walk up it in many places. The empty wagon was drawn

back up the slope by his plodding oxen to be refilled in Cuyamaca.

After dropping down the initial slope from the Cuyamaca meadows level into Chariot Canyon, Lassator's road climbed over the shoulder of Chariot Mountain and curved down the slopes high on the mountainside above Oriflamme Canyon. The road does not cross the modern truck trail until almost at the bottom of its descent. The road became somewhat of a legend in the history of the backcountry and is commonly called the "hay Road," or the "sled Road." Lassator used his road to haul supplies from the winter of 1857-1858 until the early 1860s.

The prosperity of the Birch Overland Mail did not last for long, since the Butterfield Overland Mail Company had been granted the larger and longer mail contract from near St. Louis to San Francisco, which almost immediately replaced Birch's line. Butterfield did not want mules, however, and chose to stick to the main overland trail through the desert. The Butterfield Mail did not turn toward San Diego anyway, continuing on toward Los Angeles and San Francisco. Lassator still had the business to supply the Butterfield Line at Vallecito, along with what remained of the Birch operation, and used his road to supply his station there.

James Lassator was killed in Arizona in 1863 and his stepsons took over the business for a few years. By the late 1860s, however, they did not use the road much and it fell into disrepair. A few prospectors and miners used different routes in the Oriflamme Canyon region, but they mostly led from the mountain rim down a short distance to the mines. The largest mine was the Oriflamme Mine itself, which eventually consisted of several adits and related equipment. This mine had its own road built down from the ridge, but the road did not extend farther into the depths of the canyon. The Oriflamme Canyon/Chariot Canyon route between desert and mountains was used lightly during the 1880s, but never again as heavily as in the busy overland mail years. During the early 1900s some cattlemen again used the Lassator Road to drive herds of cattle to seasonal pasture, but this use was slight and no new routes were opened during that time.

In the 1930s, in an effort to reopen the old route to vehicular traffic and to assist in fire protection, the Civilian Conservation Corps (CCC) was tasked with the job of building a new truck trail basically following the old Oriflamme Canyon Route. The CCC built a small camp at the base of the mountains at the lower end of Oriflamme Canyon called Camp Hark. Camp Hark probably consisted only of small tent cabins. The road built by the CCC crews was a huge undertaking at the time. The road was blasted and graded into the side of Chariot Mountain to make the climb. The road required a switchback near where it climbed from Oriflamme Canyon into the upper end of Chariot Canyon. The CCC road is basically what is still used as the Mason Valley Truck Trail. From Chariot Canyon, the original CCC road led up the final slope to the ridge farther north than did the later 1960s route which is still in use.

At the bottom of Oriflamme Canyon one can still see the flat terraces and stone steps from the CCC Camp Hark across the creek. Just a few curves up the truck trail from the bottom of the hill the Lassator Hay Road comes steeply down a small ridge from high above on Chariot Mountain. From the flat valley at the head of Chariot Canyon, the Lassator Hay Road led across the valley west to east and crossed the Mason Valley Truck Trail about where the branch leading to the west is located. Today, the scar of the "hay road" can be seen coming straight down the hill to the west (it is the older of two parallel scars on the slope close beside each other). The earlier San Diego Trail, the mule route of the military mail carriers and overland mail days, follows the point of a ridge a short distance south of the "hay road" scar. As one travels down into Chariot Canyon numerous old mine roads appear from the 1870s mining boom era.

Driving the Mason Valley Truck Trail offers glimpses of the hardships and triumphs of those who traveled the canyons a century and a half ago.

Chris Wray is a native of San Diego's East County. His love of the historic places, people, and stories of the region has grown as he combines his exploration and research with writing and publishing. Moving from mountains to desert with the seasons, Chris has immersed himself in historical records, old maps, books, photographs, and his own on-site observation to piece together the fabric of the San Diego backcountry.

Chris founded Tierra Blanca Books to provide local interest publications with in-depth research and accurate geographic information. He believes that every historic place can be identified on the ground today, often with some type of existing trace--that no place needs to be left in the past, lost in the haze of historic obscurity. Chris Wray resides in La Mesa, California.

Mineral Prospecting Near Banner, California

Excerpt from Chapter VII: Exploring and Mining Gems and Gold in the West
Fred Rynerson
Courtesy of Naturegraph Publishers, © 1967
Happy Camp, California
Contact: Barbara Brown, nature@sisqtel.net

It was while I was in Mesa Grande looking over a prospect called the Burro Claim, that Verd Angel told me Jose Rodrigues visited him to show some fine yellow and pink crystals of tourmaline which came out of a prospect he had near his ranch. I knew Verd recognized quality tourmaline so I decided to have a look-see. Verd couldn't get away to go with me, so I got his brother Fred to go, for he knew where Jose lived. We each got a horse, some provisions to last us two or three days, and left Angel Ranch for the old mining town of Banner, San Diego County. From there, we took off in a southeast direction several miles to Jose Rodrigues's ranch house.

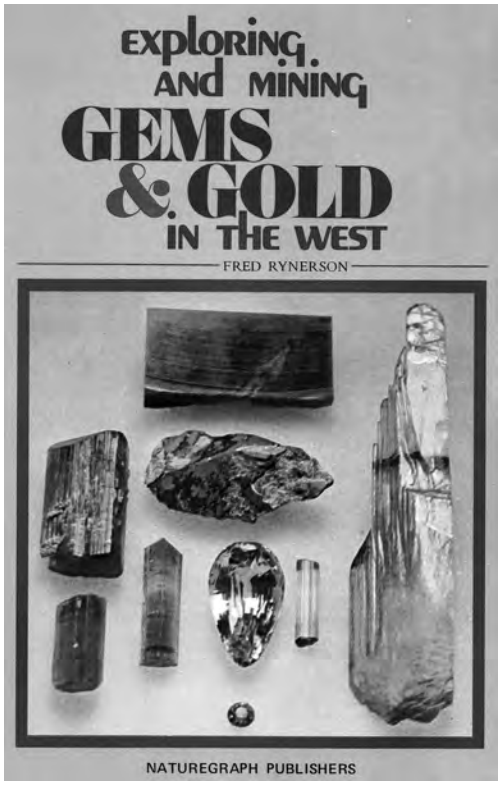

We arrived just about dark. As I dismounted, Jose came out of the house, for he had been informed by his good dog that someone was coming. I asked him if he had found some tourmalines; saying I would Iike to look over the prospect, if he would let me. He said he'd be glad to show us his mine in the morning. We were tired, so I asked him if he could tell us a good place to bed down for the night, and said we'd turn in. He asked, "Have you had supper?"

I told him "No," but that we had plenty of food. He said his daughter, his son-in-law and he himself had just left the table and there was plenty left for us, and wouldn't have it otherwise but we sit down and eat. I don't believe I ever had a meal go down with such satisfaction. We had tortillas and beans. The beans were cooked with beef and wheat, seasoned with "just a little chili to make them good", as the Mexicans say. While we were eating, we talked of Jose's mine and he showed us some specimens, which weren't so good, and said he would take us to his claim in the morning.

When we started to leave, Jose said his daughter had fixed a room for us to stay overnight and, and as it was late, we had better sleep in the house rather than the stumble around in the dark fixing our beds. So we turned in and slept on an old-fashioned feather bed. It was morning, it seemed, before we realized it. We had another swell feed (breakfast), then saddled the horses in about the soupiest fog I was ever in.

Which way we started out, I am not sure, but I think we came back a short way, the way we had come in, then turned to the right on a trail leading through high brush, high as my head, when I was on my horse, and as wet as it could be. We wound in and out of small canyons, and over ridges; ending up at the end of a small ridge. There was a hole about four feet wide, six feet long, and six feet deep. I could see that work had been done on a small pegmatite vein about two feet wide. I don't remember tracing out the strike of the vein. On the dump, which was all around the hole, there were a few small golden beryl crystals, the largest not over a quarter-inch in diameter. Some of them were of good color, but badly flawed. I did not see any tourmalines around the hole or in it.

When we got ready to leave, we asked Jose where we were and he told us if we went out “that way”, we’d come to a road, to follow that road to the right until we came to another road, then turn to the left, and then we’d be on the way to the Warner Ranch. After we rode over small hills and washes, “out that way”, we did come to a road, but the fog was so thick we could hardly see across it. We turned to the right at about a forty-five degree angle and followed the way until we came to the other road. This junction we recognized as “scissors Crossing” where the old Butterfield Stage Road crosses the Julian-Borrego Road. I never went back to that place again.

SkyArt sculpture HN-1: “Gold Miner and His Mule” - see Diana Lindsay’s article in this volume for more information.

Geochemistry of the Alverson Andesite, Volcanic Hills, San Diego County, California

**A Senior Thesis Presented to the Department of Geological Sciences,
San Diego State University San Diego, California
Briana Emily Johnson
briana.e.johnson@gmail.com**

Dr. David Kimbrough, Advisor

ABSTRACT

Miocene volcanic and sedimentary rocks are preserved in scattered locations along the eastern edge of the Peninsular Ranges Batholith and western Salton Trough in eastern San Diego County. These rocks include the Alverson Andesite (Dibblee, 1954) and Jacumba Volcanics (Minch & Abbott, 1973). The purpose of this study is to contribute geochemical data for the Alverson Andesite, to attempt a correlation to the Jacumba Volcanics, and to relate the chemistry of the area with the tectonic setting during deposition. The focus of the study is the Alverson Andesite outcrops in the Volcanic Hills, which are located within Anza-Borrego Desert State Park®, approximately 11 km northwest of Ocotillo, California, along State Highway S2. The Volcanic Hills were studied by Fourt (1979), whose mapping and stratigraphic analysis provided the geologic framework for this study. Thirteen samples were collected from the Alverson Andesite in the Volcanic Hills from the three main volcanic stratigraphic units defined by Fourt (1979): the lower flows, volcanic mudflows, and the upper flows. The samples were analyzed for the major and trace element abundances by X-ray fluorescence. All of the rocks analyzed are sub-alkaline and span a composition range in SiO2 from ~49 to 62% SiO2 corresponding to basalt, basaltic-andesite, and andesite. Basalt is entirely restricted to the lower flows, which in hand sample are fine-grained with small olivine phenocrysts. Clasts from the volcanic mudflows are andesite. The upper flows are both basaltic-andesite and andesite. All of these rocks plot as tholeiites on an AFM Diagram. An important conclusion of this study is that basalt erupted first, and as time progressed, the lavas became more differentiated basaltic-andesite and andesite. The nearby Jacumba Volcanics also have upper and lower flow units with basaltic lavas that were deposited first, followed by more differentiated rocks (Moses, 2007). However the similarities seem to end there, because the Jacumba Volcanics have a distinct calc-alkaline affinity compared to the Alverson Andesite. The Alverson Andesite analyses from the Volcanic Hills are also distinctly different from the Alverson Andesite outcrops in the nearby Coyote Mountains and Superstition Mountains (Gjerde, 1982). Correlating all of the different volcanic sections discussed here is difficult because of the lack of good radiometric ages. Further work is needed.

INTRODUCTION

Volcanic Hills are located within Anza-Borrego Desert State Park®, approximately 11 km northwest of Ocotillo, California along State Highway S2 (Figures 11 and 12). The Volcanic Hills contain a suite of Miocene basalts and andesite flows, interflow sediments, and volcanic mudflows volcanic rocks named the Alverson Andesite by Thomas Dibblee in 1954; however, it has been referred to as the Alverson Formation (Gjerde, 1982), and the Alverson Canyon Formation (Fourt, 1979). For the purposes of this project, I will refer to this suite of rocks as the Alverson Andesite.

PREVIOUS WORK

Robert Fourt (1979) was the first to map in detail the Volcanic Hills of San Diego County. He divided the rocks into five distinct map units: 1) upper flows; 2) lower flows; 3) interflow sediments; 4) volcanic mudflows; and 5) plugs, dikes, and cinder deposits. The stratigraphy of these map units can be seen in Figure 1, and the location of the upper and lower flows, as well as the volcanic mudflows can be seen in Figure 11. He also defined intrusive dikes and related flows that ranged in composition from olivine-bearing basalts to hypersthene-bearing andesites (Fourt, 1979).

Fourt believed that the Volcanic Hills represented the extension of the proto-Gulf of California during the Miocene. He characterized the Alverson Andesite lava flows as ranging in composition from basalt to andesite, and described the lower and upper flows as olivine basalts. The presence of large olivine phenocrysts suggests that the magma partly crystallized prior to eruption.

Ruisaard (1979) made a big contribution by documenting the stratigraphy of the Miocene Alverson Andesite in the Coyote Mountains and Fish Creek Wash. His work shows

that the Alverson Andesite stratigraphic sequence in these areas represents up to three phases of volcanism during the Miocene. He also suggests that the magma sources of the three phases are different and changed over time. Ruisaard (1979) presented K-Ar ages on samples from Fossil Canyon, Painted Gorge, Red Rock Canyon, and the Superstition Mountain (Table 1). His analysis shows that the Alverson Andesite ranges in age from 24.8±7.4 to 14.9±0.5 million years (Ruisaard, 1979).

Michael Gjerde (1982) completed a Master's Thesis on the Alverson Andesite, which focused on petrology and geochemistry. He used the Ruisaard's 1979 stratigraphic framework for his collection of samples. He concluded that the geochemistry of the rocks is variable. The volcanics in Superstition Mountains and in Fossil and Butaca Canyons are composed of alkali olivine basalts that erupted more than 16 million years ago (Ruisaard, 1979). In Painted Gorge and northern Red Rock Canyon, the volcanic flows are olivine tholeiites less than 16 million years in age. Gjerde (1982) believed that the volcanics outcropping in his field area were representative of the initiation of basaltic volcanism that accompanied the extension of the Miocene in Southern California (Gjerde, 1982).

The Alverson Andesite is thought to be associated with the Jacumba Volcanics of Jacumba, California by Dibblee (1954). These rocks were mapped and named by Minch and Abbott (1959) and were subdivided into lower basalts, andesite, and upper basalts. Hawkins (1970) reported a K-Ar age of 18.7±1.3 million years for the Jacumba Volcanics.

The geochemistry of the Jacumba Volcanics was studied by Maureen Moses (2007). She found that the rocks were calc-alkaline in nature with compositions ranging from basaltic-andesite to dacite (Moses, 2007). Variable incompatible trace element ratios (Nb, Zr) led Moses to suggest the possibility of different sources for the volcanics.

TECTONIC SETTING

The tectonic history of southern California is complicated. The region was the site of subduction of the Farallon Plate which began about 32 million years ago. At this time, the Farallon-Pacific spreading center, more commonly known as the "East Pacific Rise", came into contact with the trench. This configuration started the transition from a subduction regime to a transform and tensional regime. This was followed by the opening of the proto-Gulf of California. At about 5 million years ago, Baja California was transferred from the North American plate to the Pacific Plate which is moving in a northwesterly direction (Atwater, 2008). The mid-Miocene volcanism in San Diego and Imperial Counties appears to correlate with an extensional basin-and-range type environment as part of this process (Hawkins, 1970). Since the mid-Miocene, the San Jacinto and Elsinore fault zones have played an integral part of southern California tectonics, which have affected the Volcanic Hills, Coyote Mountains, and Jacumba. The Miocene volcanics and associated sedimentary rocks have been uplifted and eroded, leaving the isolated patches that we see today.

PROBLEM

In San Diego and Imperial Counties, there are several eroded Miocene volcanic outcrops. The main outcrops are located in Jacumba, California, and the Volcanic Hills of eastern San Diego County. The Miocene Volcanics are also found in the Superstition Mountains and Coyote Mountains in areas such as: Fossil Canyon, Butaca Canyon, Red Rock Canyon, and Fish Creek Wash (Gjerde, 1982). For a comparison, the stratigraphic sections for the Volcanic Hills, Fossil Canyon, and the Jacumba Volcanics can be seen in Figures 1 and 2.

The age of the Alverson Andesite corresponds to the tectonic reorganization of southern California from a subduction environment to the San Andreas strike-slip system (Gjerde, 1982).

Although the Alverson Andesite of the Volcanic Hills is thought to be Miocene in age based on the K-Ar ages from the Coyote Mountains and elsewhere, little geochemistry, and no age dating has been done in the Volcanic Hills.

INTENT

The objectives of this thesis is: 1) to contribute geochemical data that will give a more accurate picture of the Miocene geology of San Diego County and the Volcanic Hills, 2) to determine whether the Miocene lavas of San Diego and Imperial County are chemically related, 3) to find out whether or not the tectonic environment during deposition can be determined and if the data supports or refutes the hypotheses that the tectonic environment changed from subduction to a rift-zone environment, 4) to attempt to make a correlation with the Alverson Andesite of the Volcanic Hills with other Miocene volcanic exposures in San Diego and Imperial Counties, especially with the Jacumba Volcanics.

METHODS

Using the 2006 SDAG Field Trip Road Log (Figure 12) and the Master's Thesis by Fourt (1979), 13 samples were collected by the author from the upper flow (Tafu), the lower basalt flow (Tafu), and the volcanic mudflows (Tal). These samples were analyzed for their major and trace elements by XRF. Plots were then made using the Igpet plotting program of Carr (2006). The sample names, units, and locations are summarized in Table 4, and the major and minor element concentrations are presented in Tables 2 and 3.

The data collected from the Volcanic Hills (2010) was compared to the geochemical data of the Jacumba Volcanics studied by (Moses 2007). The Jacumba Volcanics outlined earlier were studied by Minch and Abbott (1959), Hawkins (1970), and Moses (2007).

UNITS SAMPLED IN THIS STUDY

Three map units defined by Fourth (1979) were sampled.

The Upper Flows (Tafu) are characterized by dark gray platey basalt flows that contained weathered and non-weathered olivine phenocrysts.

The Volcanic Mudflows (Tal) are lahars that contain red volcanic clasts. In hand sample, the clasts are dark gray olivine basalts.

The Lower Flows (Tafl) are characterized by light gray olivine basalt flows. Within these lower flows there were vesicular and non-vesicular lava clasts. A flow-front breccia was visible in Montero Canyon where the bulk of the lower flow samples were collected.

GEOCHEMISTRY

In Figure 3 the Volcanic Hills samples were plotted on a TAS diagram (LeBas et al., 1986). The Alverson Andesite of the Volcanic Hills shows a distinct trend in increasing silica and total alkalis with time. The lower flows are basaltic in nature and the volcanic mudflow clasts and upper flows differentiate into basaltic-andesites and andesite.

In Figure 2 the samples were plotted on an AFM diagram (Irvine and Baragar, 1971). The Volcanic Hills samples show a definite tholeiitic trend with iron enrichment.

Trace element concentrations of the Alverson Andesite samples are plotted in Figure 4. This is a standard "spider diagram" plot with concentrations normalized to primitive mantle (Sun and McDonald, 1989) and organized in order of decreasing incompatibility from left to right. On this plot there is a distinct trough in Nb which is characteristic of arc-related magmatism.

In Figure 4, the Volcanic Hills Alverson Andesite samples and the Jacumba Volcanics samples (Moses, 2007) are plotted together on a K2O vs SiO2 diagram. Both groups plot in a relatively linear trend within the calc-alkaline series, with increasing silica and potassium. However, the Jacumba basalt samples have slightly higher K2O content relative to the Alverson Andesite.

The two groups were then plotted on an AFM diagram (Figure 5). The Jacumba samples are distinctly calc-alkaline, whereas the Volcanic Hills samples are tholeiitic.

Figure 6 shows Mg# (molecular MgO/MgO+FeO) plotted vs. SiO2 for the two areas. The Jacumba samples exhibited a high degree of scatter in comparison to the Volcanic Hills samples. The Volcanic Hills samples showed a relatively linear increase in silica with a decrease in Mg#. A unique feature of this graph is that three of the Jacumba samples have Mg# values at approximately 70. These samples may be high Mg andesites. The FeO/MgO vs SiO2 plot (Miyashiro, 1974) displayed in Figure 7 shows that the Volcanic Hills samples have a higher FeO/MgO ratio than the Jacumba samples and they are tholeiitic. The Jacumba Volcanics samples plot again as calc-alkaline.

A Harker Diagram (Figure 8) shows the relationship between the two incompatible elements Zr and Ba. This plot shows that the Jacumba Volcanics and the Volcanic Hills samples both trend relatively linear; however, they deviate from the origin of the graph. These basalts, therefore, were not derived directly from the mantle. Another interesting feature shown in this graph is that there are two clusters in which several of the Jacumba samples plot together in small groups away from the general trend, possibly implying different source region compositions.

POSSIBLE INTERPRETATIONS

The K-Ar ages for the Alverson Andesite and Jacumba Volcanics (Table 1), and the available geochemical data suggest that there are significant differences in the geochemistry and age between the two areas. The Miocene Volcanics of eastern San Diego County and western Imperial County studied by Gjerde (1982) and Hawkins (1970) range in age from 21.5±3.9 and 14.9±0.5 million years. One possible explanation for the variable differences in the ages is that, at the same time, there could be different magma sources for the Miocene Volcanics. Another possibility is that there could be different sources due to the differences in age. The age of the volcanics in

both areas post-date subduction along this section of the margin by ~10 million years, yet the Nb depletion and other features of the chemistry are consistent with a "subduction-related" origin for the volcanics. Maybe this means that the mantle has a sort of chemical memory that is held over a period of time and is shown at a later date.

CONCLUSION

The Alverson Andesite in the Volcanic Hills is a tholeiitic suite of rocks that exhibit a definite pattern in terms of their volcanic composition. Basalts were erupted first, and then the rocks became more differentiated basaltic-andesite and andesite. The trace elements show that the rocks have a tholeiitic-transitional calc-alkaline affinity. In comparison to the Jacumba Volcanics, the Jacumba Lavas are compositionally distinct from the Volcanic Hills, which is well illustrated by the high magnesium andesites of the Jacumba rocks. Overall, correlating the Volcanic Hills to the other Miocene volcanic localities throughout eastern San Diego and Imperial Counties is difficult because existing geochronology is inadequate. This project requires further study.

Acknowledgements

I would like to thank Dave and Joan Kimbrough for their supervision and guidance while learning the research process. I would also like to thank J.R. Morgan for his opinions and help in the field. I would like to thank Wesley Rubio for his encouragement and support. Lastly, I would like to thank the SDSU Department of Geological Sciences for their financial assistance during this project.

REFERENCES

Atwater, Tanya, 2008, N.E. Pacific and W. North America Plate History, 38 Ma to Present, Animation, UCSB. http://emvc.geol.ucsb.edu/download/nepac.php.

Bloom, D.M., 2006, Where the Pavement Ends: A Geologic Excursion in Canyon Sin Nombre and the Volcanic Hills, SDAG Field Trip Road Log, p. 27-42.

Dibblee Jr., T.W., 1954, Geology of the Imperial Valley Region, California, CDMG Part I, v. 170, p. 21-28.

Fourt, Robert, 1979, Post-Batholithic Geology of the Volcanic Hills and Vicinity, San Diego County, California: Masters of Science Thesis, San Diego State University, 66p.

Gastil, G., Krummenacher, D., Minch, J., 1979, The Record of Cenozoic Volcanism around the Gulf of California, GSA Bulletin Part I, v. 90, p. 839-857.

Gjerde, M.W., 1982, Petrography and Geochemistry of the Alverson Formation, Imperial County, California: Masters of Science Thesis, San Diego State University, 85p.

Hawkins, J.W., 1970, Petrology and Possible Tectonic Significance of Late Cenozoic Volcanic Rocks, Southern California and Baja California, GSA Bulletin, v. 81, p.3323-3338.

Minch, J.A., Abbott, P.L., 1973, Post-Batholithic Geology of the Jacumba Area in Southeastern San Diego County, California, Transactions of the Society of Natural History, v. 17(11), p. 129-136.

Moses, M.N., 2007, The Geochemistry and Petrogenesis of the Jacumba Volcanics, Jacumba, California: Senior Thesis, San Diego State University, 24p.

Ruisaard, C.I., 1979, Stratigraphy of the Miocene Alverson Formation, Imperial County, California: Masters of Science Thesis, San Diego State University, 125p.

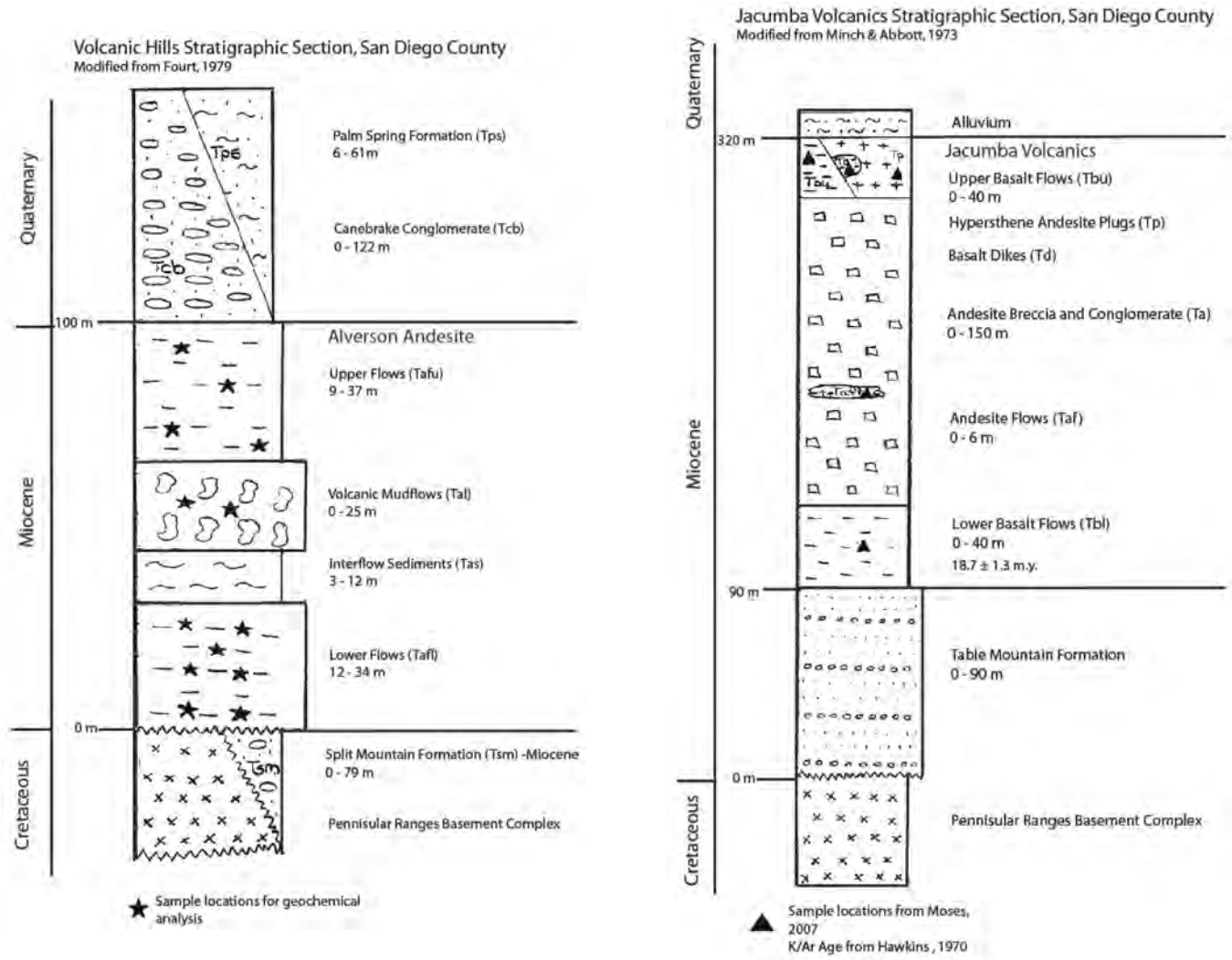

Figure 1: Comparison of the Alverson Andesite and Stratigraphy of the Volcanic Hills with the Jacumba Volcanics. Both areas contain lower basalt flows, with interflow layers, followed by upper basalt flows.

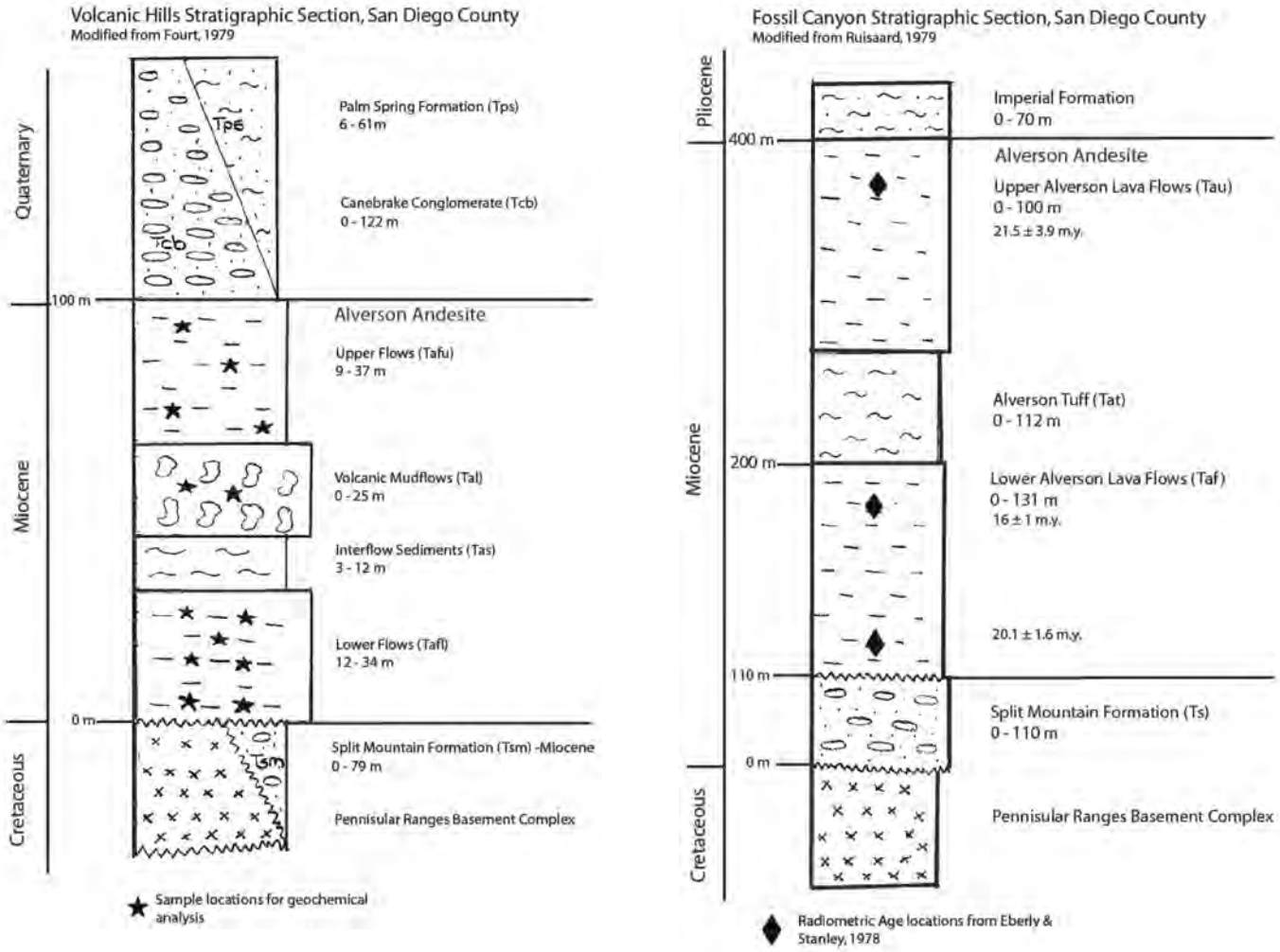

Figure 2: Comparison of the Alverson Andesite and Stratigraphy of the Volcanic Hills and Fossil Canyon. Both areas contain lower basalt flows, with interflow layers, followed by upper basalt flows.

. **For Figures 3 through 5: diamonds = lower flows, triangles = upper flows, squares = volcanic mudflow clasts.

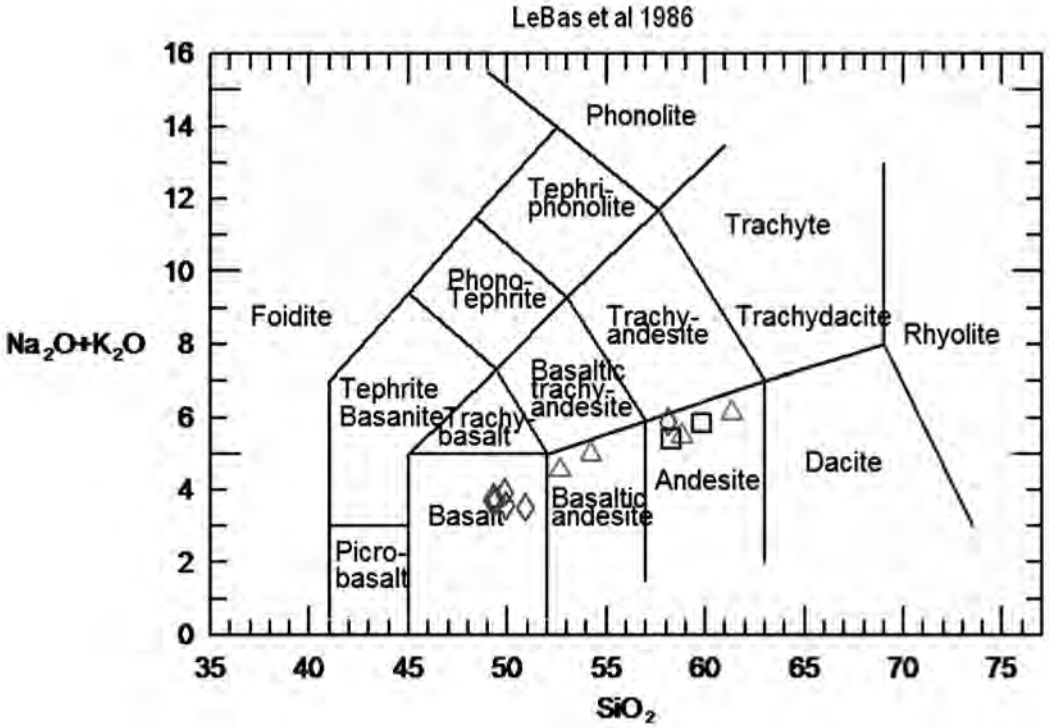

Figure 3: Total Alkali Silica Diagram for the Alverson Andesite of the Volcanic Hills. The samples range in composition from basalt to andesite.

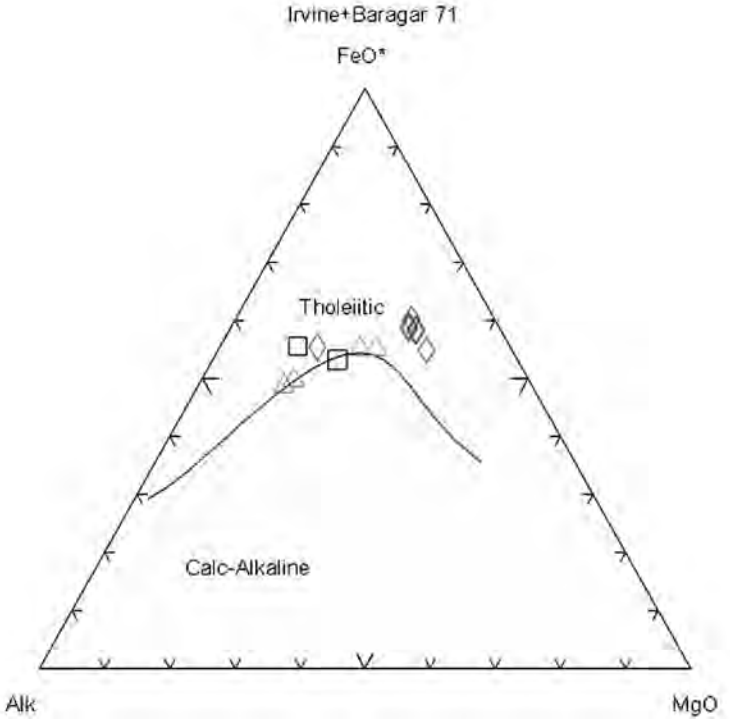

Figure 4: AFM Diagram of the Volcanic Hills. The Alverson Andesite exhibits a tholeiitic nature.

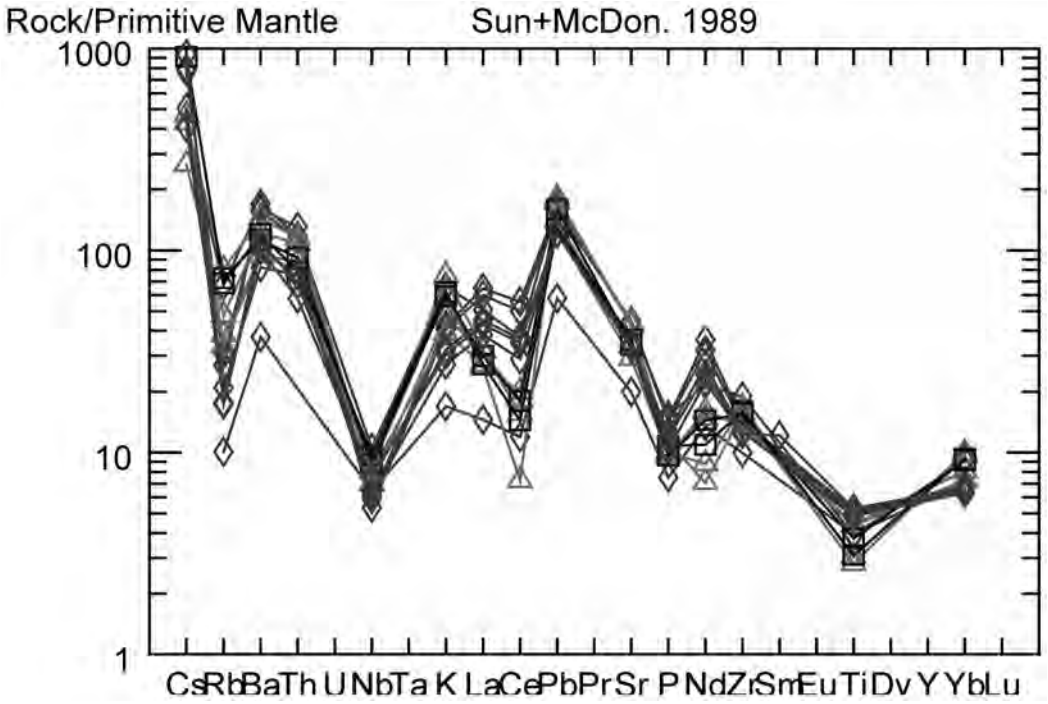

Figure 5: Spider Diagram of the Alverson Andesite Lavas of the Volcanic Hills. There are two distinct troughs in Nb and P, and peaks in Pb and Zr. Together, these are characteristics of calc-alkaline magmatism.

**For Figures 6 through 9: diamonds = Alverson Andesite, stars = Jacumba Volcanics.

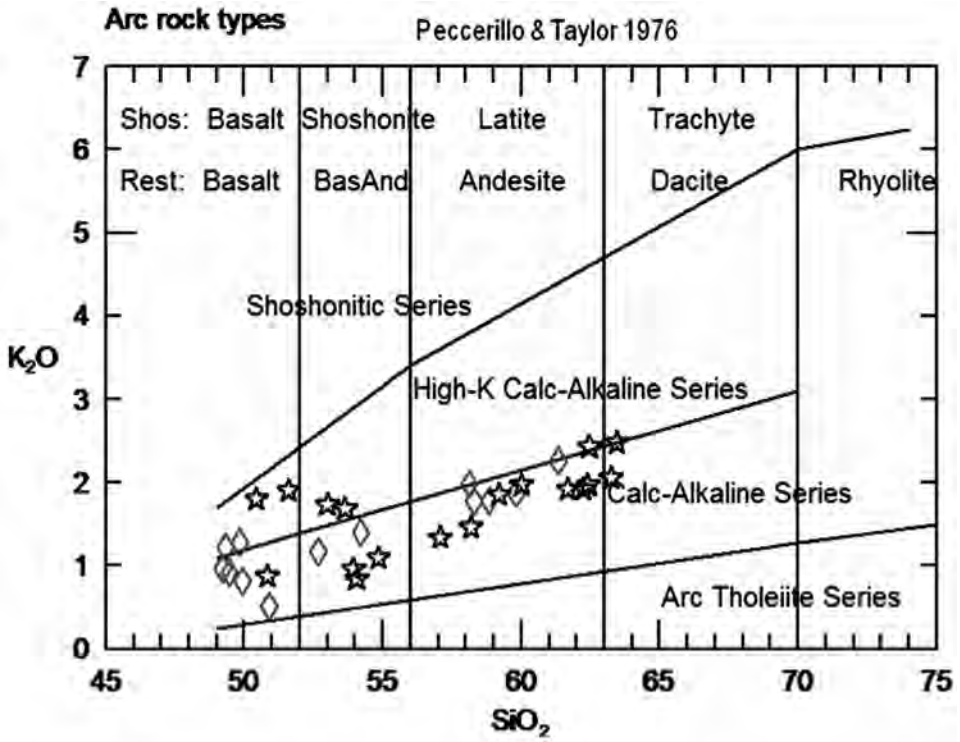

Figure 6: The Jacumba Volcanics Samples (Moses, 2007) and the Volcanic Hills Samples on a K vs. Si Diagram. Both areas have a calc-alkaline affinity and some of the Jacumba Volcanics plot in the high-K Calc-Alkaline Series.

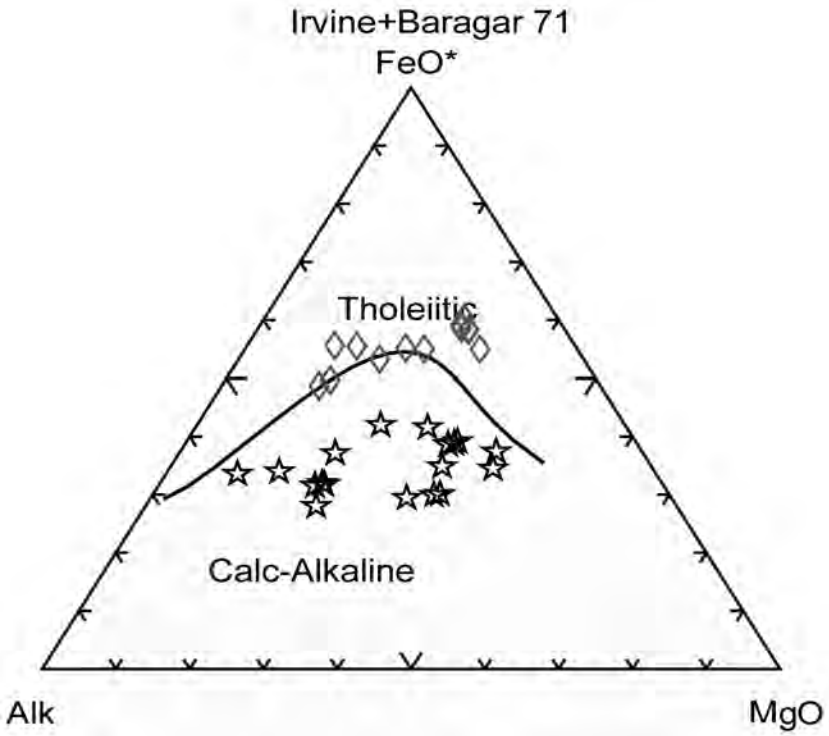

Figure 7: The Jacumba Volcanics Samples (Moses, 2007) and the Alverson Andesite Samples of the Volcanic Hills on an AFM Diagram. The Jacumba Volcanics are clearly calc-alkaline.

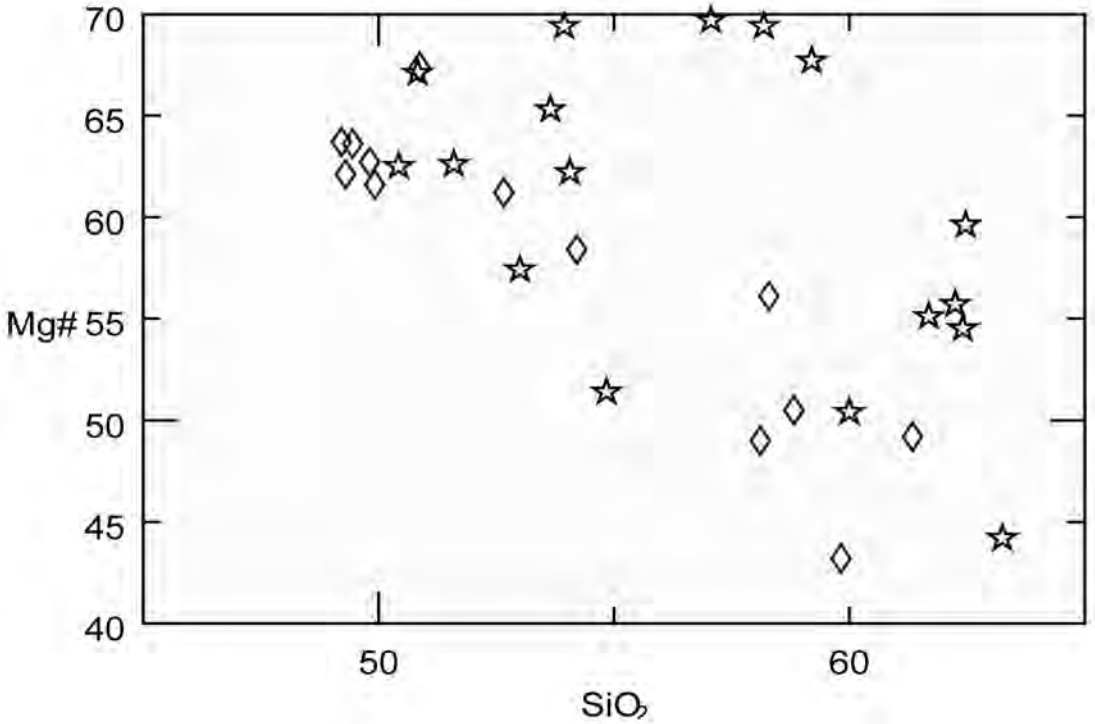

Figure 8: Jacumba Volcanics and Volcanic Hills Sample Scatter Plot. The Jacumba samples exhibit a high degree of scatter in comparison to the Volcanic Hills samples. The Volcanic Hills samples showed a relatively linear increase in silica with a decrease in Mg#. Three of the Jacumba samples are high Mg andesites, (shown with black arrow).

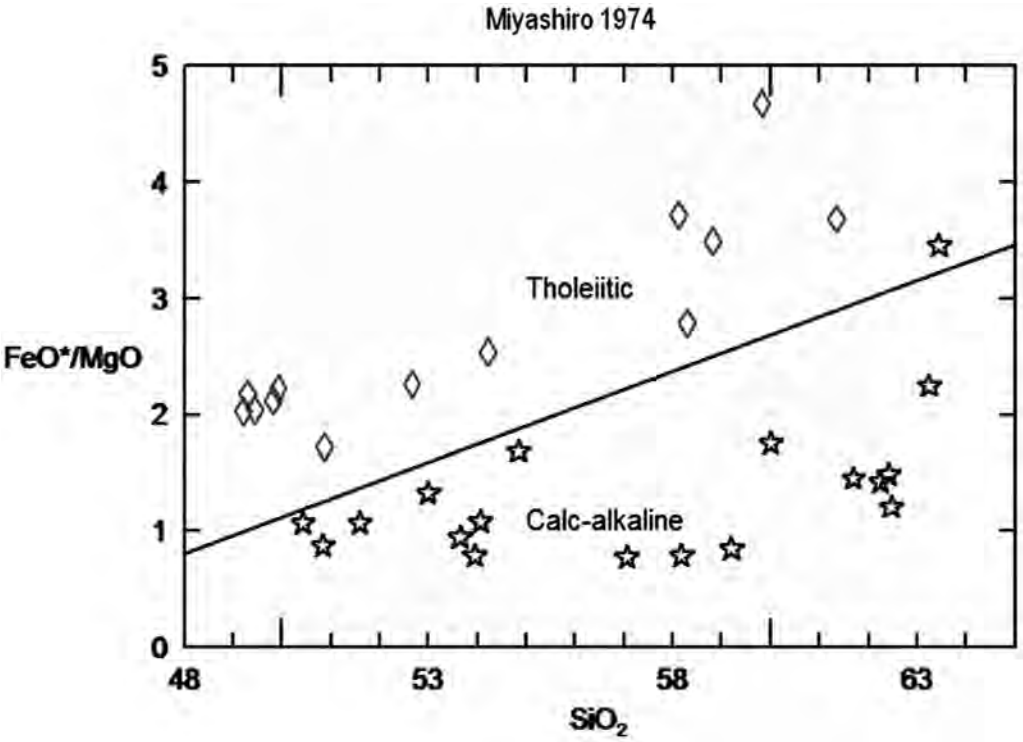

Figure 9: The Volcanic Hills samples have a higher FeO/MgO ratio than the Jacumba samples and they are tholeiitic in nature. The Jacumba samples plot consistently as calc-alkaline.

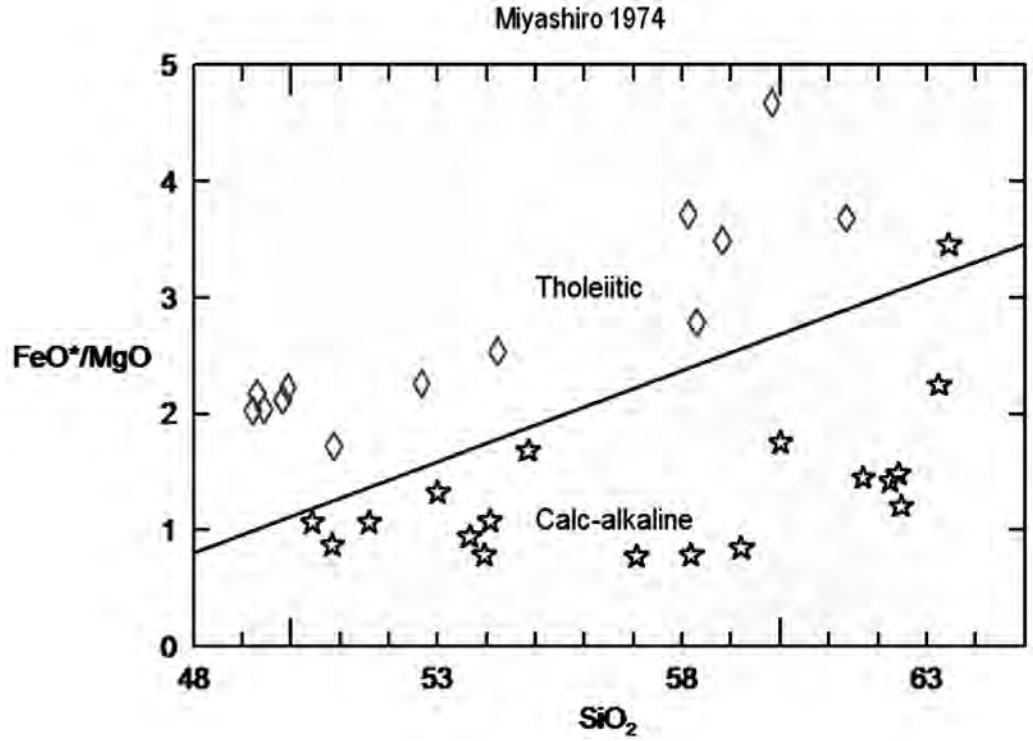

Figure 10: A Harker Diagram of the Two Incompatible Elements Ba and Zr for the Jacumba Volcanics and the Alverson Andesite of the Volcanic Hills. This suggests that neither of the lavas are in ratio with their source mantle.

Formation Name	Sample	Age (m.y.)	Source	Location	Rock Type	SiO_2
Alverson Andesite	FC-A1	18.6±0.8	Gjerde 1982	Southern/Central Fossil Canyon	Alkali Basalt	49.21
Alverson Andesite	FC-N4	21.5±3.9	Gjerde 1982	Northern Fossil Canyon	Alkali Basalt	50.35
Alverson Andesite	FC-NA	20.1±1.6	Gjerde 1982	Northern Fossil Canyon	Transitional Basalt	53.21
Alverson Andesite	BC-6	17.1±0.5	Gjerde 1982	Butaca Canyon	Alkali Basalt	52.55
Alverson Andesite	SM-2	16.1±0.5	Gjerde 1982	Superstition Mtn	Alkali Basalt	52.2
Alverson Andesite	PG-4D	15.8±1.3	Gjerde 1982	Painted Gorge	Tholeitic Basalt	53.77
Alverson Andesite	PG-2D	15.8±1.3	Gjerde 1982	Painted Gorge	Tholeitic Basalt	53.74
Alverson Andesite	PG-1A	14.9±0.5	Gjerde 1982	Painted Gorge	Tholeitic Basalt	52.81
Alverson Andesite	RR-2	20.0±0.9	Gjerde 1982	Red Rock Canyon	Tholeitic Basalt	52.23
Jacumba Volcanics	J-1	18.7±1.3	Hawkins 1970	Jacumba Peak	Basaltic Andesite	53.16
Rosarito Beach Formation	Baja 7	14.7±1.3	Hawkins 1970	Tijuana-Ensenada Toll Rd Marker 15	High-Alumina Tholeiite	47.6
Santa Rosa Basalts	SR-61a	8.3±0.5	Hawkins 1970	Mesa de la Burro, Murietta, CA	Alkali Basalt	45.93
Santa Rosa Basalts	SR-74d	8.3±0.5	Hawkins 1970	Murietta, CA	Tholeitic Basalt	51.69

Table 1: Available K-Ar Age Dates of Miocene Volcanics in Southern California and Northern Baja California.

Sample Name	SiO_2	Al_2O_3	Fe_2O_3	CaO	MgO	K_2O	Na_2O	MnO	TiO_2	P_2O_5
VH-1	54.21	17.37	6.59	8.71	4.67	1.4	3.58	0.115	0.957	0.219
VH-2	52.66	16.76	6.70	9.22	5.33	1.17	3.37	0.107	0.946	0.210
VH-3	61.34	17.80	4.34	5.29	2.12	2.26	3.85	0.074	0.663	0.218
VH-4	58.82	17.28	4.19	7.34	2.16	1.78	3.70	0.074	0.612	0.245
VH-5	59.82	17.92	5.54	5.64	2.13	1.87	3.97	0.076	0.672	0.235
VH-6	58.29	17.45	5.79	6.61	3.74	1.78	3.63	0.096	0.816	0.210
VH-7	49.45	15.84	9.18	9.43	8.09	0.92	2.80	0.143	1.049	0.258
VH-8	49.21	15.76	9.29	9.40	8.24	0.97	2.75	0.145	1.055	0.275
VH-9	49.92	16.10	9.45	10.09	7.64	0.82	2.75	0.145	1.145	0.226
VH-10	49.30	15.59	9.08	9.95	7.52	1.22	2.56	0.149	1.090	0.312
VH-12	49.81	15.56	9.18	10.10	7.78	1.28	2.65	0.147	1.132	0.324
VH-13	50.87	16.06	8.12	9.16	8.49	0.51	3.00	0.133	0.856	0.164
VH-14	58.11	18.42	6.11	6.40	2.96	1.98	3.89	0.101	0.847	0.333

Table 2: Volcanic Hills-Alverson Andesite Major Element Concentrations (%).

Sample Name	Sc	V	Cr	Co	Ni	Cu	Zn	Rb	Sr	Y
VH-1	24.4	159.7	169.4	28.7	62.5	25.3	77.7	24.2	712.1	15.2
VH-2	26.2	164.6	340.5	46.8	129.2	34.8	75.9	21.2	619.3	15.7
VH-3	11.1	79.3	2.6	34.0	6.3	9.0	70.7	51.2	926.0	8.4
VH-4	12.7	67.0	3.4	6.6	8.1	9.9	68.8	30.3	894.3	7.4
VH-5	11.2	73.6	2.6	34.7	6.9	10.3	72.6	43.6	764.5	11.9
VH-6	17.7	119.3	48.3	21.9	30.4	26.7	76.0	46.1	718.1	12.8
VH-7	29.2	180.0	362.4	64.5	130.4	32.2	86.5	11.0	693.4	18.3
VH-8	30.1	183.6	368.0	51.3	144.4	33.7	88.3	11.2	703.5	18.0
VH-9	30.1	187.9	320.8	45.3	66.5	24.2	89.9	13.3	718.1	17.2
VH-10	29.0	195.4	364.4	42.5	110.4	20.6	91.5	19.4	942.3	15.7
VH-12	30.7	199.2	353.2	44.1	105.1	37.0	89.2	17.1	931.8	15.7
VH-13	28.8	169.9	519.3	45.9	166.8	37.9	76.6	6.4	421.4	16.0
VH-14	16.7	127.4	6.5	24.2	10.4	12.7	83.1	42.6	900.5	13.2

Table 3a: Volcanic Hills-Alverson Andesite Minor Element Concentrations (ppm).

Sample Name	Zr	Nb	Mo	Ba	La	Ce	Nd	Yb	Pb
VH-1	164.4	5.0	1.1	662.7	21.7	32.4	20.0	4.0	10.0
VH-2	151.2	5.7	1.0	660.2	18.7	35.6	21.7	3.6	8.9
VH-3	187.6	5.8	1.1	1006.1	22.0	27.7	11.9	4.9	12.3
VH-4	174.4	6.0	1.4	854.0	18.1	12.9	9.6	4.8	12.9
VH-5	179.0	6.9	1.5	840.9	18.8	25.6	14.8	4.6	9.2
VH-6	174.2	6.3	1.9	788.2	20.6	32.0	19.6	4.5	11.3
VH-7	141.7	5.4	1.2	704.3	29.4	61.9	32.9	3.1	8.6
VH-8	141.9	5.3	1.1	770.5	30.9	64.6	36.6	3.2	8.7
VH-9	138.7	4.4	0.7	577.3	26.2	51.4	30.3	3.3	8.7
VH-10	154.0	3.8	0.6	1094.3	41.2	88.7	43.2	3.3	11.2
VH-12	160.2	4.2	0.6	1114.8	44.5	98.9	48.6	3.2	11.6
VH-13	111.6	4.6	1.4	259.4	10.0	21.2	18.3	3.5	4.1
VH-14	212.0	7.5	1.3	1185.0	34.8	66.0	29.5	4.5	12.1

Table 3b: Volcanic Hills-Alverson Andesite Minor Element Concentrations (ppm) Continued.

Sample	Map Unit	Latitude	Longitude	Sample Description
VH-1	Tafu	32.79679	-116.10970	Sample taken from base of flow; platy gray lava with orange and green olivine phenocrysts
VH-2	Tafu	32.79540	-116.11096	Sample taken from base of red agglomerate lava flow; platy dark gray lava with orange olivine phenocrysts
VH-3	Tafu	32.80675	-116.13050	Float sample at base of hill; dark gray with small red olivine phenocrysts
VH-4	Tafu	32.80680	-116.13050	Float sample at vase of hill; light gray with black phenocrysts
VH-5	Tal	32.77834	-116.11344	Sample was a volcanic block from a breccia; dark gray with large orange and green olivine phenocrysts
VH-6	Tal	32.77724	-116.11574	Sample was a volcanic block from a breccia; ~20 cm in size; dark gray with few orange olivine phenocrysts
VH-7	Tafl	32.77074	-116.12395	Sample taken from lava flow; light grayish-red with large orange olivine phenocrysts
VH-8	Tafl	32.77109	-116.12404	Sample taken from lava flow; light gray with large orange olivine phenocrysts
VH-9	Tafl	32.77180	-116.12342	Sample taken from porphyritic flow unit; grayish-red microcrystalline basalt with black phenocrysts
VH-10	Tafl	32.77241	-116.12236	Sample taken near flow front breccia; vesicular olivine-bearning basalt
VH-12	Tafl	32.77317	-116.12110	Sample taken had stretched vesicles; dark gray with calcite omigules
VH-13	Tafl	32.79660	-116.15790	Sample taken from basal flow above contact with gneiss; dark gray with few orange phenocrysts
VH-14	Tafl	32.79660	-116.15766	Sample taken from basal flow above contact with gneiss; dark gray with few shiny black phenocrysts

Table 4: Volcanic Hills-Alverson Andesite Sample Descriptions (Johnson, 2007).

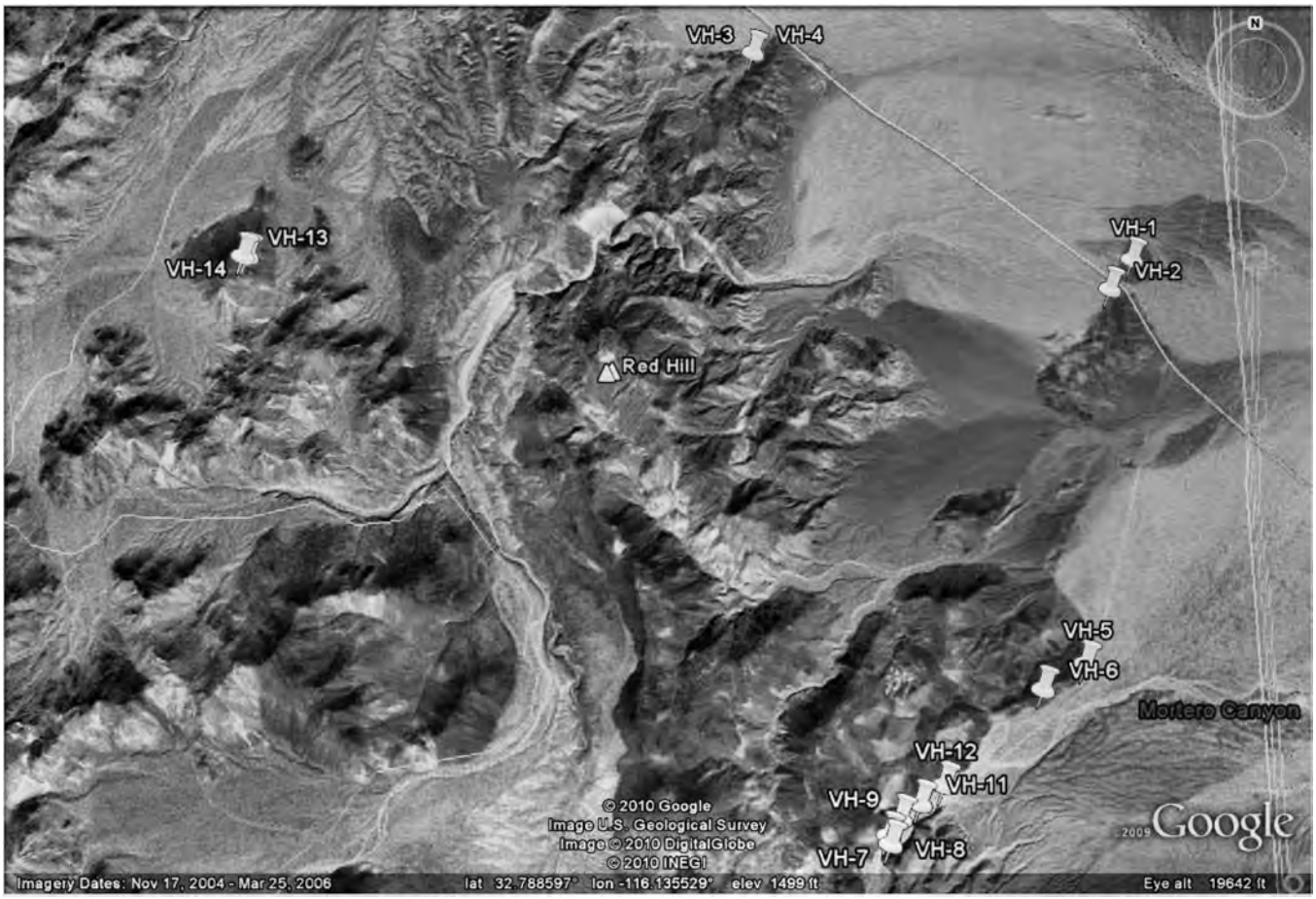

Figure 11: Sample Locations of the Alverson Andesite in the Volcanic Hills

Figure 12 (facing page): Geologic Map of Part of the Volcanic Hills by Fourt (1979), in San Diego Association of Geologists 2005/2006 Guidebook: Geology and History of Southeastern San Diego County.

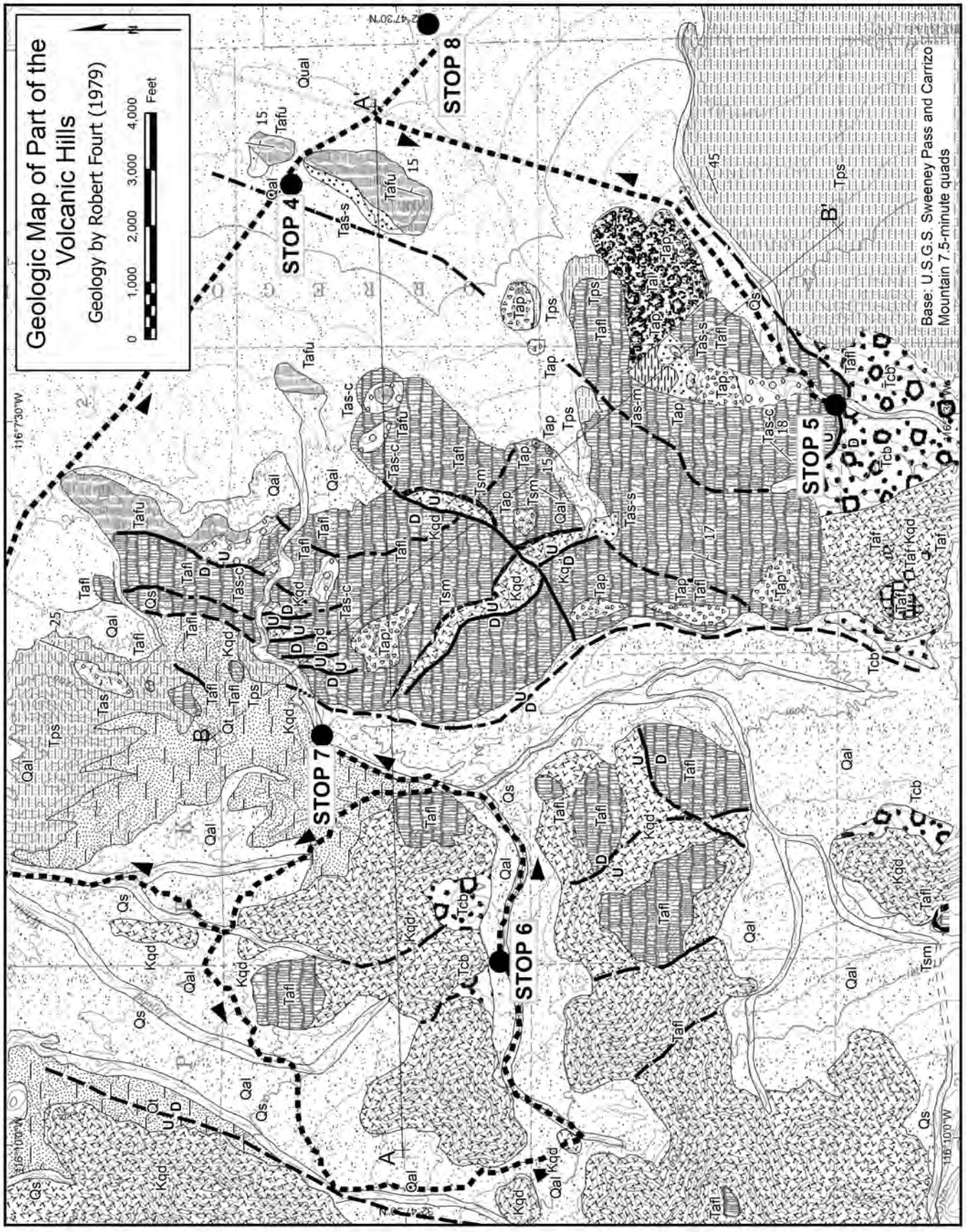
Geologic Map of Part of the Volcanic Hills
Geology by Robert Fourt (1979)
0 1,000 2,000 3,000 4,000 Feet
Base: U.S.G.S. Sweeney Pass and Carrizo Mountain 7.5-minute quads
STOP 4
STOP 5
STOP 6
STOP 7
STOP 8
A
A'
B
B'
Qal
Qs
Qt
Tafl
Tafu
Tap
Tas
Tas-c
Tas-m
Tas-s
Tcb
Tps
Tsm
Kqd
Qual

Santa Rosa Ridge “Sky Island”. An isolated 7000 to 8800 foot ponderosa pine forest above the Anza-Borrego Desert region, similar to the “Sky Island” of the Sierra San Pedro Martir. Photo: David M. Bloom

THE LITTLE-KNOWN "SKY ISLAND"

SIERRA SAN PEDRO MÁRTIR, BAJA CALIFORNIA

Robert C. Coates, Judge, California Superior Court
Founding President, SDSU Geology Alumni

Donald E. Albright, San Diego Natural History Museum
First Graduate, San Diego State College Geology Department

A stiff breeze sings through the trees, and is heard retreating into the woods, then another long gust comes. The aspens advertise their health with plentiful, light green leaves glittering. Behind the wind and the chirp of the morning birds, there lies a profound silence. This jutting range is steep to the west, with a flattish ladle-shaped plateau tilted upward to the north, and on the east side, a steep escarpment of schist, harder than the range's main rock, granodiorite. The plateau is heaven in the spring and summertime and exciting in late summer and fall when the monsoons roar up the Gulf of California to hit the plateau with lashing rains and lightning.

This description of Baja California's largest and highest mountain range could apply to many others of Peninsular California, that long, narrow slice of the earth's crust , a batholith, that extends from the San Jacinto Mountains in Riverside County hundreds of miles southeast through Baja California. The Peninsular Ranges Batholith is composed of hundreds of granitic plutons that collectively form over a dozen major mountain ranges in its southerly course along a great crustal rift, named for and mostly occupied by the Gulf of California and its northern offspring, the Salton Sea. Related ranges in the Anza-Borrego Desert Region and crossing the international border include the Santa Rosas, San Ysidros, Lagunas, Cuyamacas, Sierra Juarez, and the Sierra San Pedro Mártir. The following discussion of the latter range can give a broader perspective on its cousins to the north, including the Laguna Mountains of east-central San Diego County with their common gentle ascending western slopes and abruptly plunging eastern escarpments. This provides another look at "the lows and highs" of our dynamic region.

Donald Albright first explored the Sierra San Pedro Mártir, Baja California in the early 1950s as a Boy Scout on a Sierra Club pack mule trip led by the legendary Becky McScheehee. In 1960, Albright and Robert Coates made an early ascent from the desert floor up to the 10,100 foot summit of Picacho Del Diablo, and have been on many trips to the plateau, since. In 2004, they took a group of five The Nature Conservancy scientists there, intending to get the "Mártir" on to The Conservancy's Radar. This small mountain range has been protected by an oval-shaped National Park since 1946, yet civilization is squeezing the peninsula's wild areas from all sides. The aquifers on the desert side, for example, invite agriculture, although there has been only one now-discontinued, irrigated Ejido.

There are several threats currently visible. These include efforts by the peninsula's largest grower, Los Pinos Company, to build a dam on Rio San Antonio to facilitate tomato growing on the coast; the "Escalera Nautica" a Mexican government project to construct a ring of yachting harbors around and into the gulf, with a new road for yachts to be trucked across to Bahia de Los Angeles: the recent development of a new mountain resort near the Park's south boundary, with 2,000 one- to five-acre lots, a golf course, horse corrals, and a ski facility; and finally, a proposal for a string of giant windmills across the crests of two National Parks. The precipitants involved in the wind farms are Sempra Energy (for the Sierra Juarez National Park to the north) and the State government of Baja California, for the Mártir.

The Sierra San Pedro Mártir is the second mountain range south in Baja California, some 250 miles from the border and east of San Quintin Bay. The Mártir rises abruptly on all sides. There is a just-completed, paved road up from the west, running from San Telmo past the now well-run and famous Meling Guest Ranch ($40/night, or camp on the lawn.) The eastern, desert side features faulting like one sees to the east of the California Peninsula Ranges as well as the Sierra Nevada and in fact, the granitics which form the eastern spine of all these ranges are the same geologic age: some 92 million years. The granites are capped and fringed by older metamorphic rocks (Jurassic and Triassic schists and quartzites, with pegmatites-and no known gemstones!) and the range tilts from its western "hinge" so the eastern scarp peaks are tallest and steepest. *Reconnaissance Geology of the State of Baja California* (1975, with map) GSA Memoir, #140 by Gastil, Phillips

and Allison is the classic source (in the work of which, a generation of SDSU students participated.)

The Mártir and its lower, northern cousin range, the Sierra Juarez, are typical representatives of the entire Peninsular Ranges Batholith geomorphic province from Riverside County south to central Baja California (its southernmost mountain expression is the gorgeous, boulder-strewn Catavina). Granitic rock pops up all along the peninsula's spine, south to the emblematic, granite arches at Cabo San Lucas. All of these, the theory runs, were formed as sequelae of the subduction of the Pacific Plate.

Since Gastil et.al, there have been several SDSU Master's Theses regarding the geology, especially its petrology. Susan Helen Gunn, 1984 SDSU Master's Thesis is a 203 page tour de force titled *The geology, petrography, and geochemistry of the Laguna Juarez pluton, Baja California, Mexico*. There is a focus on the mineralogy and geochronology of the pluton, by William Vincent McCormick, III, in 1986; and another of the same year on the petrography and geochemistry, by Benjamin Gordon Eastman. Ms. Gunn's article explicitly concerns the mountain range immediately north of the Sierra San Pedro Mártir. It is included here, however, because its detailed examination of the mineralogy and petrology, as well as its conclusions, are likely quite congruent with the rocks found in the Sierra San Pedro Mártir. Since the Mártir has a higher elevation (3 to 4,000 feet higher than Sierra Juarez) the Mártir's petrology suggests a later-crystallizing of its pluton(s).

From Gunn's conclusions:

> *"The Laguna Juarez Pluton can best be compared to the Tuolomne Intrusive series...*
>
> *This study of the Laguna Juarez Pluton in the eastern Peninsular Ranges Batholith has shown that individual zoned plutons can exhibit both I-type and S-type characteristics. This variation is best explained by the increasing assimilation of either a lower crustal or sedimentary component by a mantle or oceanic-derived melt…*
>
> *The process of crystal fractionation concentrated SiO2 and K2O in the core of the pluton which was most likely emplaced at 7.6 to 11 kilometers of depth. The geometry of the body suggests that it was emplaced syntectonically as a cohesive diapir. Migration of the thermal regime to the east resulted in the asymmetric displacement of the core of the pluton to the southeast."*

The renowned Professor Gordon Gastil has a long-unpublished work on the geology of the Sierra San Pedro Mártir. This manuscript includes substantial geochemistry. To see that this manuscript is published and made publicly available would be an important, scientific project.

A summary of the plate tectonics affecting Baja, California may be read in the 1991 guidebook for an Ensenada Conference of the National Association of Geology Teachers: *Geologic Adventures in Northern Baja California*. We note that although at least four such geologic guidebooks have focused on Baja California over the past two decades, none went into the Mártir with their participant tours.

A pioneering "reconnaissance" study of the Sierra San Pedro Mártir, Baja California, was done in 1938, by Alfred Woodford, *Geological Reconnaissance Across Sierra San Pedro Mártir, Baja California*.

The high plateau starts at 6,200 feet at its south end and rises over its 25 miles to 8,200 feet at the north end. Its east side is fringed by peaks, including one at 9,200 feet topped by the Mexican National Astronomical Observatory's 100 inch telescope. The precipitous, granodiorite spire of Picacho Del Diablo (noted as La Providencia or La Encantada on Mexican topographic maps) looms 10,100 feet to the east, separated from the plateau by mile-deep Diablo Canyon.

What is spectacular about the Mártir derives from its elevation—and the resulting "sky island" ecosystem. Isolated in northern Baja California, one feels, here, as though one is in the high country of the Santa Rosa Mountains and San Jacinto National Monument—but that would be three hundred miles to the north! The woods are spectacular, featuring the southernmost aspen stands in North America, the San Pedro Martir cypress, incense cedar, sugar and lodgepole pines, white fir, as well as the Sierra Mártir mint, a species unique to the Mártir.

The desert canyons host the usual North American chaparral and California fan palm (*Washingtonian filifera*); plus the ubiquitous blue fan palm and throughout the range one finds bighorn sheep, mountain lions, and coyotes as well as small mammals. Grizzlies and Mexican gray wolves once roamed the plateau. Condors soar here, and there is a unique jay species, the piñon jay. Nelson's rainbow trout is also unique to the range. It is a close cousin to the golden rainbow found in the High Sierras.

Global warming may already have had its effects. There is today less winter rain, and the less dependable and torrential summer rains are eroding the meadows. Some

high-elevation species may be endangered. Lodgepole, a higher-elevation pine (usually found at 10,000 feet in the Sierras) may disappear. More big fires will be seen in the future; worse, perhaps, than the two-week fire which burned for 20 miles in June 2006, before it was stopped, just inside the southwest corner of the Park.

Our 2004 Nature Conservancy expedition was intended to insert this mountain jewel into the Conservancy's consciousness, before it is too late. Thus, also, this small article aims to alert caring geologists and Baja California enthusiasts to the lush environmental values of Mexico's Parque Nacional Sierra de San Pedro Mártir.

The Nature Conservancy, which recently boasted a net worth of $1.6 billion, places emphasis on the Baja California Peninsula, and staffs an office in Ensenada. It is looking at real estate deals to protect critical spots in the Sierra Juarez and on the flyway including San Quintin Bay and the Sierra San Pedro Mártir is on the focus list.

Robert C. Coates submission dated 9/3/2010

Final edit by SDAG Editorial Committee

Devil's Peak in Sierra San Pedro Mártir, Baja California, Mexico. Highest point in Baja, measuring 3078m, as seen from the Mexican National Astronomical Observatory.
Photo by Jaime Sanchez Diaz..
Downloaded from http://en.wikipedia.org/wiki/Sierra_de_San_Pedro_Mártir

"Whoa Nellybelle!" is what the passenger in the Jeep seems to be saying, now that boulders have been added to the sculpture at location HN-4. Photo by Diana Lindsay. (see pages 114 and 126)

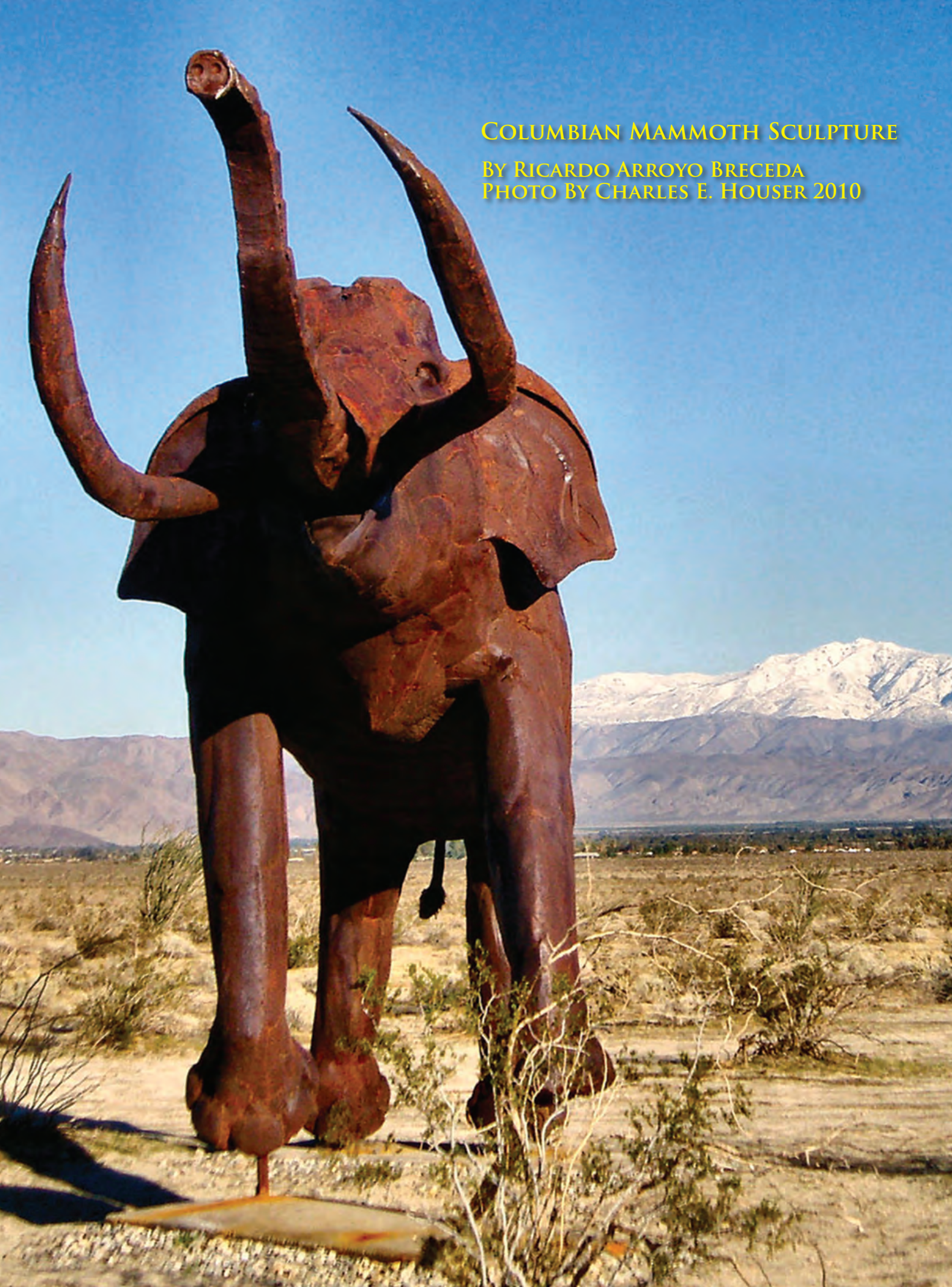

Columbian Mammoth Sculpture

By Ricardo Arroyo Breceda
Photo By Charles E. Houser 2010

Geology and Lore of Northern Anza-Borrego Desert Region, SDAG/SCGS Vol. 37 - 2010
Includes the field trip "The Lows to Highs of Anza-Borrego Desert State Park®"

This publication covers the geology of the northern portion of Anza-Borrego Desert Region, and includes the 2010 joint field trip for the South Coast Geological Society (SCGS) and the San Diego Association of Geologists (SDAG). It is useful for anyone interested in geology, mines, history, groundwater, geologic structures, particularly faulting - all of this between the lowest elevations of near sea level to the highest elevations of over 6,000 feet, all within the Anza-Borrego Desert Region! Newly published and classic papers by local geologists and scientists explore the region which includes the Borrego Valley, Coyote Mountain, Fonts Point, Clark Lake, regional tectonics and structural geology.

The self-guided tour first covers the lower elevation portion of the region with spectacular view stops including Fonts Point and Lute Ridge. The tour includes visits to large animal sculptures placed throughout Borrego Valley. Then the tour continues upward to Yaqui Pass to look at detachment faulting and then heads toward Banner Grade where you veer off toward Chariot Canyon to look at faulting and mine works. The tour continues up Banner Grade toward the historic mining town of Julian. Enjoy spectacular views of the Elsinore Fault trace on the east wall of Banner Canyon. One of the final stops is at Kwaaymii Point, a 6,000 foot elevation viewpoint which overlooks Shelter Valley, Borrego Valley, the Salton Sea and numerous mountains.

ISBN 978-0-916251-16-1
90000 >
9 780916 251161

Distributed by Sunbelt Publications